6D

PNL-4976
UC-46

Criticality Experiments with Low Enriched UO_2 Fuel Rods in Water Containing Dissolved Gadolinium

S. R. Bierman
E. S. Murphy
E. D. Clayton
R. T. Keay

February 1984

Prepared for
British Nuclear Fuels, Ltd.
under contract with
the U.S. Department of Energy

Pacific Northwest Laboratory
Operated for the U.S. Department of Energy
by Battelle Memorial Institute

Battelle

PNL-4976

DISCLAIMER

PACIFIC NORTHWEST LABORATORY
operated by
BATTELLE
for the
UNITED STATES DEPARTMENT OF ENERGY
under Contract DE-AC06-76RLO 1830

Printed in the United States of America
Available from
National Technical Information Service
United States Department of Commerce
5285 Port Royal Road
Springfield, Virginia 22161

NTIS Price Codes
Microfiche A01

Printed Copy

Pages	Price Codes
001-025	A02
026-050	A03
051-075	A04
076-100	A05
101-125	A06
126-150	A07
151-175	A08
176-200	A09
201-225	A010
226-250	A011
251-275	A012
276-300	A013

PNL-4976
UC-46

CRITICALITY EXPERIMENTS WITH LOW ENRICHED UO_2 FUEL RODS IN WATER CONTAINING DISSOLVED GADOLINIUM

S. R. Bierman
E. S. Murphy
E. D. Clayton
R. T. Keay[a]

February 1984

Prepared for British Nuclear Fuels, Ltd.
Risley, Warrington, Chesire
United Kingdom
Under Contract DE-SC06-82RL 10371
Through the U.S. Department of Energy
(BNFL Contract Number L88502)

Pacific Northwest Laboratory
Richland, Washington 99352

[a]British Nuclear Fuels, Ltd.

PREFACE

Early in 1981, the Technical Services staff of British Nuclear Fuels, Ltd. (BNFL) contacted personnel of the United States Department of Energy (USDOE) Pacific Northwest Laboratory (PNL) concerning the possibility of PNL performing some criticality experiments for BNFL. BNFL was interested in obtaining basic experimental data on light water reactor type fuel rods in water and uranyl nitrate solution poisoned with a soluble compound of gadolinium. They wished to obtain this data over a very wide range of gadolinium concentrations and moderator-to-fuel ratios. The data would be used primarily for validating calculational techniques that are used in criticality safety evaluations.

With considerable assistance from Alan C. Rither (PNL-Contract Services), M. J. Plahuta (USDOE - Richland Operations) and Clint Bastin (USDOE - Office of Nuclear Fuel Cycle), a contractural agreement between BNFL and the United States Department of Energy, Richland Operations Office, was reached in February 1982 for a series of criticality and related experiments involving low enriched UO_2 fuel rods in water and in water containing dissolved gadolinium. Since these types of fuels are less reactive in nitrate solutions than in water and since measurements in uranyl nitrate solutions would have involved a much greater effort, a decision was reached to limit the program to experiments with fuel rods in gadolinium - water solutions only.

A major aspect of these measurements was that some of the experiments involved the simultaneous irradiation of reaction rate foils in the experimental assembly and in the well defined thermal neutron flux of the United Kingdom Atomic Energy Authority Nestor Reactor followed by transport of the irradiated foils to the U. K. Atomic Energy Establishment Winfrith for analyses within twenty-four hours. The authors would like to especially acknowledge the co-operation and diligence of the following people in successively carrying out the considerable logistics associated with these reaction rate measurements:

Dale Hansen	Rockwell Hanford Operations Rockwell International
A. S. Gregory	Atomic Energy Establishment Winfrith
John M. Taylor	Pacific Northwest Laboratory
Patrick H. Burke	Pacific Northwest Laboratory
C. Andrews	Lep Air Ltd., Heathrow Airport

Also the co-operation and patience of the Nestor Reactor Operations staff is appreciated as well as that of J. H. Smith, Senior Reactor Operator at the USDOE Critical Mass Laboratory, in the performance of the simultaneous irradiations. The very professional and thorough preparation and analyses of the foil packs by M. F. Murphy of the Reactor Physics Division, AEEW, is also acknowledged.

The authors would also like to acknowledge the assistance and typing of L. N. Terry in the preparation of this report.

SUMMARY

The results obtained in a criticality experiments program performed for British Nuclear Fuels, Ltd. (BNFL) under contract with the United States Department of Energy (USDOE) are presented in this report along with a complete description of the experiments. The experiments involved low enriched UO_2 and PuO_2-UO_2 fuel rods in water containing dissolved gadolinium, and are in direct support of BNFL plans to use soluble compounds of the neutron poison gadolinium as a primary criticality safeguard in the reprocessing of low enriched nuclear fuels.

The experiments were designed primarily to provide data for validating a calculation method being developed for BNFL design and safety assessments, and to obtain data for the use of gadolinium as a neutron poison in nuclear chemical plant operations - particularly fuel dissolution. However, there are significant cost incentives to optimize the amount of gadolinium used per ton of fuel reprocessed, and thus to reduce the uncertainties present in the calculations upon which plant design and operations are based. Therefore, to the extent compatable with the primary objectives, the experiments were also designed to provide more general type information for use in improving neutronic calculations on low ^{235}U enriched uranium systems.

Very little operating experience or experimental data exists upon which to base the use of gadolinium as a soluble neutron poison for criticality control in plant operations. Consequently the experiments program covers a wide range of neutron moderation (near optimum to very undermoderated) and a wide range of gadolinium concentration (zero to about 2.5 g Gd/ℓ). Aslo the measurements presented herein provide critical and subcritcal k_{eff} data ($1 \geq k_{eff} \geq 0.87$) on fuel-water assemblies of UO_2 rods at two enrichments (2.35 wt% and 4.31 wt% ^{235}U) and on mixed fuel-water assemblies of UO_2 and PuO_2-UO_2 rods containing 4.31 wt% ^{235}U and 2 wt% PuO_2 in natural UO_2 respectively. Fission rate and fission-to-capture ratio measurement data were obtained on some of the experimental assemblies and are also presented herein. Specifically, the experiments involved the following:

- 4.31 wt% ^{235}U enriched UO_2 aluminum clad rods in water at three uniform center-to-center rod spacings
- 2.35 wt% ^{235}U enriched UO_2 aluminum clad rods in water at two uniform center-to-center rod spacings
- 4.31 wt% ^{235}U enriched UO_2 aluminum clad rods mixed with PuO_2-UO_2 zirconium clad rods to achieve fuel-water lattices, at one uniform center-to-center rod spacing, characteristic of irradiated fuel compositions specified by BNFL.

The critical size of these lattices were determined with water containing no gadolinium and with water containing dissolved gadolinium nitrate. Pulsed neutron source measurements were performed to determine subcritical k_{eff} values as additional amounts of gadolinium were successively dissolved in the water of each critical assembly.

Fission rate measurements in ^{235}U using solid state track recorders were made in each of the three unpoisoned critical assemblies of 4.31 wt% ^{235}U enriched UO_2 fuel rods and in the near-optimum moderated and the close-packed poisoned assemblies of this fuel. Foils of 4.31 wt% ^{235}U enriched UO_2 and depleted U metal (0.04 wt% ^{235}U) were also irradiated in these same five critical assemblies simultaneously with irradiations in the NESTOR reactor at the Atomic Energy Establishment-Winfrith to obtain data on neutron capture and fission in ^{238}U relative to fission in ^{235}U.

CONTENTS

FIGURES

TABLES

CRITICALITY EXPERIMENTS WITH LOW ENRICHED UO_2 FUEL RODS IN WATER CONTAINING DISSOLVED GADOLINIUM

1.0 INTRODUCTION

British Nuclear Fuels Limited (BNFL) is planning to use soluble compounds of the neutron poison gadolinium as a primary criticality safeguard in the reprocessing of nuclear fuels. Although effective in terms of plant capacity, such practices result in a cost penalty, both in the cost of the gadolinium itself and in the increased aqueous raffinate waste from solvent extraction. Consequently a cost incentive exists to control the gadolinum concentrations to a minimum conducive to criticality safety. Achieving this minimum concentration in actual plant operations is dependent on the uncertainties in calculations used to assess the criticality safety of the process in question. To reduce these uncertainties in the area of low enriched oxide fuel reprocessing, BNFL entered in a Contract (DE-SC06-82RL10371) with the United States Department of Energy for a series of criticality, and related, experiments. Primarily the experiments were to provide data for use in validating a calculation method being developed for BNFL design and safety assessments, and to derive data for the use of gadolinium as a neutron poison in nuclear chemical plant operations. To the extent compatable with this objective, however, the experiments were also to be designed to provide more general type information for use in improving neutronic calculations on low ^{235}U enriched uranium systems.

To provide data in support of plant design and operations, criticality data were needed, over a wide range of neutron moderation, on the poisoning effectiveness of gadolinium dissolved in aqueous solutions containing low enriched UO_2 fuel rods. Specifically data were needed on the variation in critical mass (critical size) with gadolinium concentration for neutron moderation ranging from near optimum down to that of tight packed fuel rods in solution. Such data were needed to firmly establish and to reduce costly uncertainties existing in computational methods used in criticality assessments.

Further, data were needed to establish uncertainties in the calculations as the gadolinium concentration was increased from the delayed criticality condition.

The experiments to provide the above data were performed at the USDOE Critical Mass Laboratory operated by Battelle Memorial Institute near Richland, Washington. A photograph of this facility is shown in Figure 1.1. A floor plan of the facility is shown in Figure 1.2. The experiments were performed in the large shielded area identified in Figure 1.2 as the critical assembly room. Existing experimental facilities within the critical assembly room were modified slightly for the experiments as described in the section entitled Experiments. The experiments performed and the results obtained are covered in detail in the sections of this report that follow.

Briefly, however, the experiments involved measurements with lattices of 2.35 wt% and 4.31 wt% ^{235}U enriched UO_2 fuel rods and PuO_2-UO_2 fuel rods in water containing up to about 2.5 g Gd/ℓ. The PuO_2-UO_2 fuel rods consisted of 2 wt% PuO_2 in natural UO_2 and were used with the 4.31 wt% ^{235}U enriched UO_2 rods to construct simulated "burn-up" fueled assemblies. Critical sizes were determined as a function of gadolinium concentration and neutron moderation. Reaction rate measurements were made on selected assemblies to determine fission rates in ^{235}U, and to determine the Relative Conversion Ratio (RCR) and the Fast Fission Ratio (FFR) of ^{238}U and ^{235}U for use in improving neutronic data. Also measurements were made, using the pulse neutron source technique, to determine the effect of gadolinium concentration on the effective neutron multiplication constant (k_{eff}) of assemblies simulating dissolver conditions.

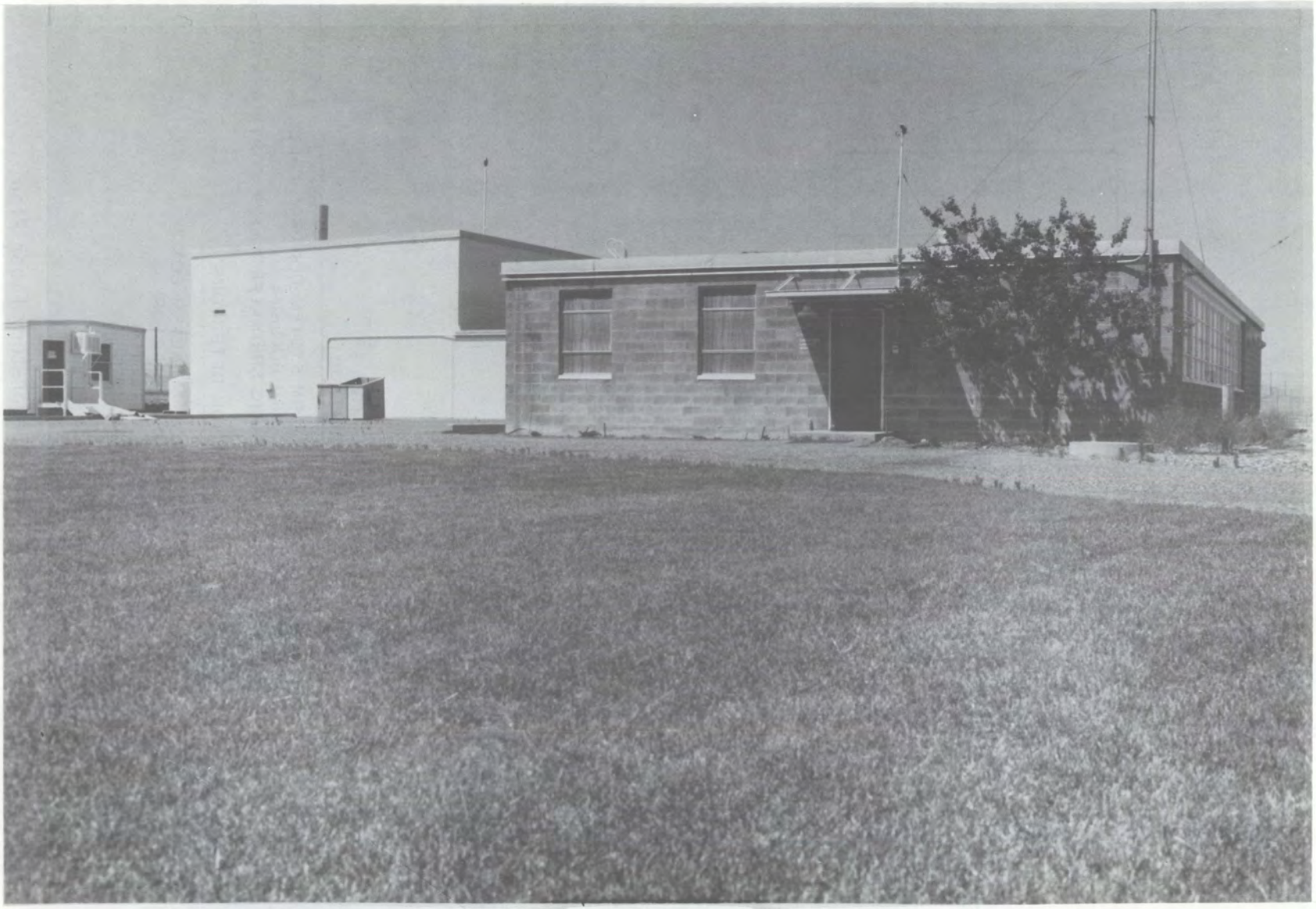

Figure 1.1 USDOE Critical Mass Laboratory near Richland, Washington

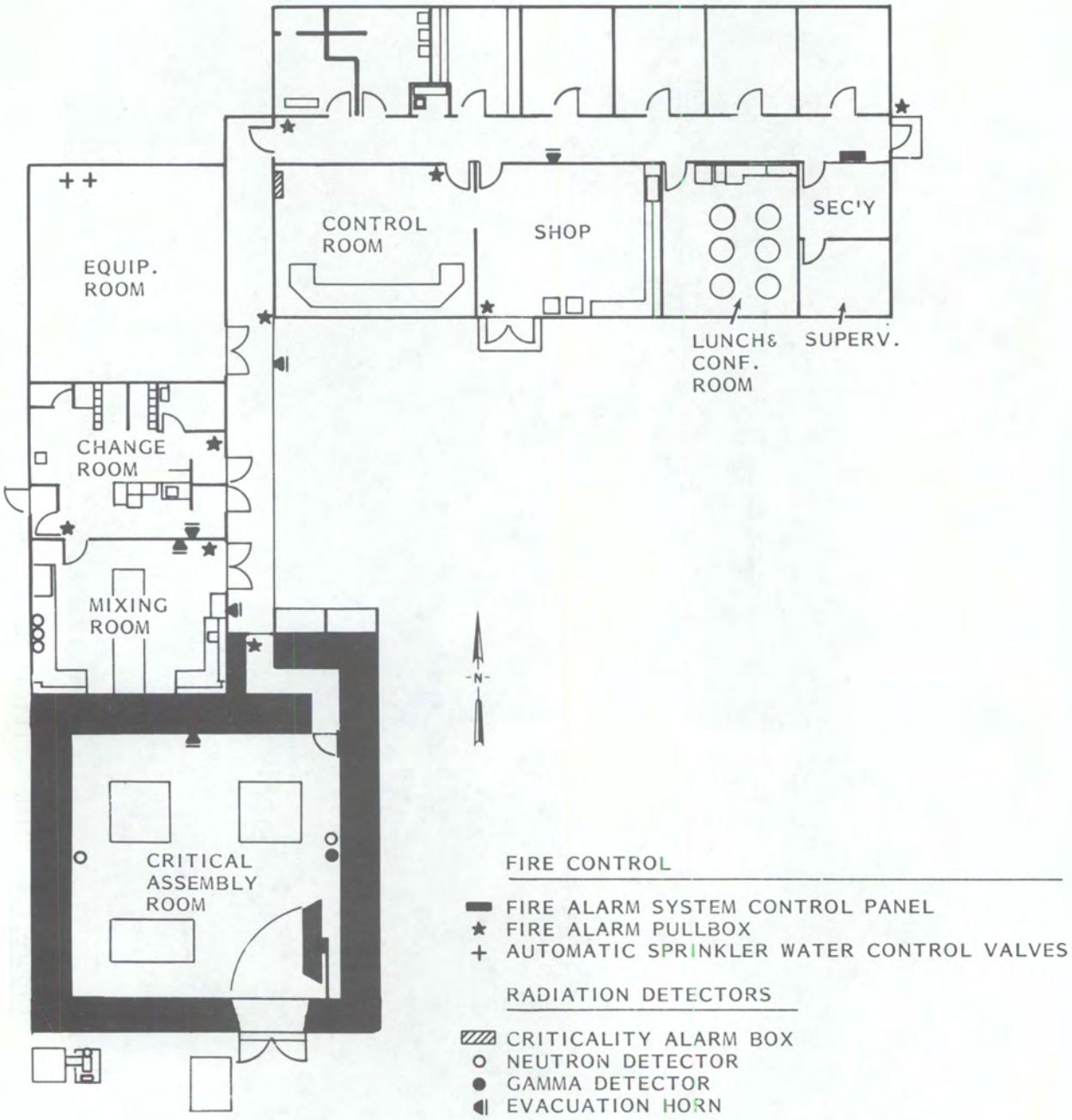

Figure 1.2 Critical Mass Laboratory Floor Plan

2.0 EXPERIMENTS

The types of measurements performed under this program are identified in this section. Also, the experimental system used in making these measurements is described in this section.

2.1 TYPE OF EXPERIMENTAL MEASUREMENTS

Measurements were performed on three types of uniform lattices of oxide fuel rods in water. These three fuel-water lattices were:

- 4.31 wt% ^{235}U enriched UO_2 aluminum clad rods in water at three uniform center-to-center rod spacings
- 2.35 wt% ^{235}U enriched UO_2 aluminum clad rods in water at two uniform center-to-center rod spacings
- 4.31 wt% ^{235}U enriched UO_2 aluminum clad rods mixed with PuO_2-UO_2 zirconium clad rods to achieve fuel-water lattices, at one uniform center-to-center rod spacing, characteristic of irradiated fuel compositions as specified by BNFL.

The critical size of these lattices were determined, as indicated in Table 2.1, with water containing no gadolinium and with water containing dissolved gadolinium nitrate. Also as indicated in Table 2.1, pulsed neutron source measurements were performed to determine subcritical k_{eff} values as additional amounts of gadolinium were successively dissolved in the water of each critical assembly.

Fission rate measurements in ^{235}U using solid state track recorders were made in each of the three unpoisoned critical assemblies of 4.31 wt% ^{235}U enriched UO_2 fuel rods and in the near-optimum and close-packed poisoned assemblies of this fuel. Foils of 4.31 wt% ^{235}U enriched UO_2 and depleted U metal (0.04 wt% ^{235}U) were also irradiated in these same five critical assemblies simultaneously with irraditions in the NESTOR reactor at the Atomic Energy Establishment-Winfrith (AEEW) to obtain data on neutron capture and fission in ^{238}U relative to fission in ^{235}U.

TABLE 2.1 Experimental Program - Identification and Summary Listing of Measurements Performed with Lattices of Fuel Rods in Water Containing Dissolved Gadolinium[a]

NOMINAL LATTICE SPACING	UO_2 FUEL RODS 4.31 wt% ^{235}U ENRICHED				UO_2 FUEL RODS 2.35 wt% ^{235}U ENRICHED				PuO_2-UO_2 FUEL RODS 2.00 wt% PuO_2 IN NATURAL UO_2			
	CRITICAL APPROACH (k_{eff} = 1)	PULSE NEUTRON ($1>k_{eff}\geq0.87$)	REACTION RATES (SSTR)[b]	REACTION RATES (FOILS)[c]	CRITICAL APPROACH (k_{eff} = 1)	PULSE NEUTRON ($1>k_{eff}\geq0.87$)	REACTION RATES (SSTR)[b]	REACTION RATES (FOILS)[c]	CRITICAL APPROACH (k_{eff} = 1)	PULSE NEUTRON ($1>k_{eff}\geq0.87$)	REACTION RATES (SSTR)[b]	REACTION RATES (FOILS)[c]
NEAR-OPTIMUM												
WITH NO GADOLINIUM	1	–	1	1	1	–	–	–	–	–	–	–
WITH GADOLINIUM	3	9	1	1	1	9	–	–	–	–	–	–
INTERMEDIATE												
WITH NO GADOLINIUM	1	–	1	1	–	–	–	–	–	–	–	–
WITH GADOLINIUM	6	8	–	–	–	–	–	–	–	–	–	–
CLOSE-PACK												
WITH NO GADOLINIUM	1	–	1	1	1	–	–	–	1	–	–	–
WITH GADOLINIUM	1	6	1	1	1	3	–	–	3	7	–	–

[a] NUMBERS SHOWN FOR EACH FUEL LATTICE INDICATE THE NUMBER AND TYPE OF MEASUREMENT PERFORMED ON THAT LATTICE
[b] EACH MEASUREMENT WITH SOLID STATE TRACK RECORDERS INVOLVES A SINGLE BARE ^{235}U SSTR LOCATED IN ONE OF THE FOIL POSITIONS IN THE LATTICE
[c] EACH MEASUREMENT WITH FOILS INVOLVES 4.31% ^{235}U ENRICHED UO_2 AND DEPLETED (0.04 wt% ^{235}U) U FOILS LOCATED IN THREE IDENTICAL POSITIONS IN THE LATTICE

Specific details of all the measurements identified in Table 2.1 are provided in the section that follows on experimental results.

2.2 DESCRIPTION OF EXPERIMENTAL ASSEMBLIES

An existing experimental system used previously in fuel element array studies at the Critical Mass Laboratory was used in carrying out the experiments summarized in Table 2.1. The system, consisting of a 1.8 m x 3 m x 2.1 m deep carbon steel tank provided with a water dump valve, a water deionizer system, a control blade drive, a safety blade drive and associated electronic detection and interlock devices, was modified by positioning a 152 cm diameter open top fiberglass tank beneath the control and safety blade drives to reduce the volume of water and quantity of gadolinium used in the experiments. This open top tank was connected to the water dump valve and deionizing system in addition to two 2600 ℓ covered polyethylene tanks for mixing and storing gadolinium solution. Also the control and safety blade drive systems were modified to permit replacing the blades with rod type devices. An overall photograph of the modified system, not including the mix-storage tanks is shown in Figure 2.1. A flow diagram of the system including the mix-storage tanks is shown in Figure 2.2.

Each experimental assembly consisted of a single array of fuel rods fully submerged in, and reflected by, either water or water containing dissolved gadolinium nitrate. A photograph of an experimental assembly in place is shown in Figure 2.3. The photograph has been annotated to identify the location of the neutron detectors used in determining neutron multiplication (data channels), the neutron detectors associated with the safety shutdown system (control channels), the pulse neutron source, the safety and control rods, the location of the temperature probe, and the fuel-lattice. All instrumentation inside the experimental vessel is shown in Figure 2.3. In all of the experimental measurements, the instrument thimbles were at least 15 cm from the fuel region (data channel 3 was moved radially on occasion to achieve this 15 cm minimum separation). Not discernible, and therefore not identified, in Figure 2.3 is a small ($\sim$ 0.6 microgram) ^{252}Cf source which was located in the center region of each experimental assembly.

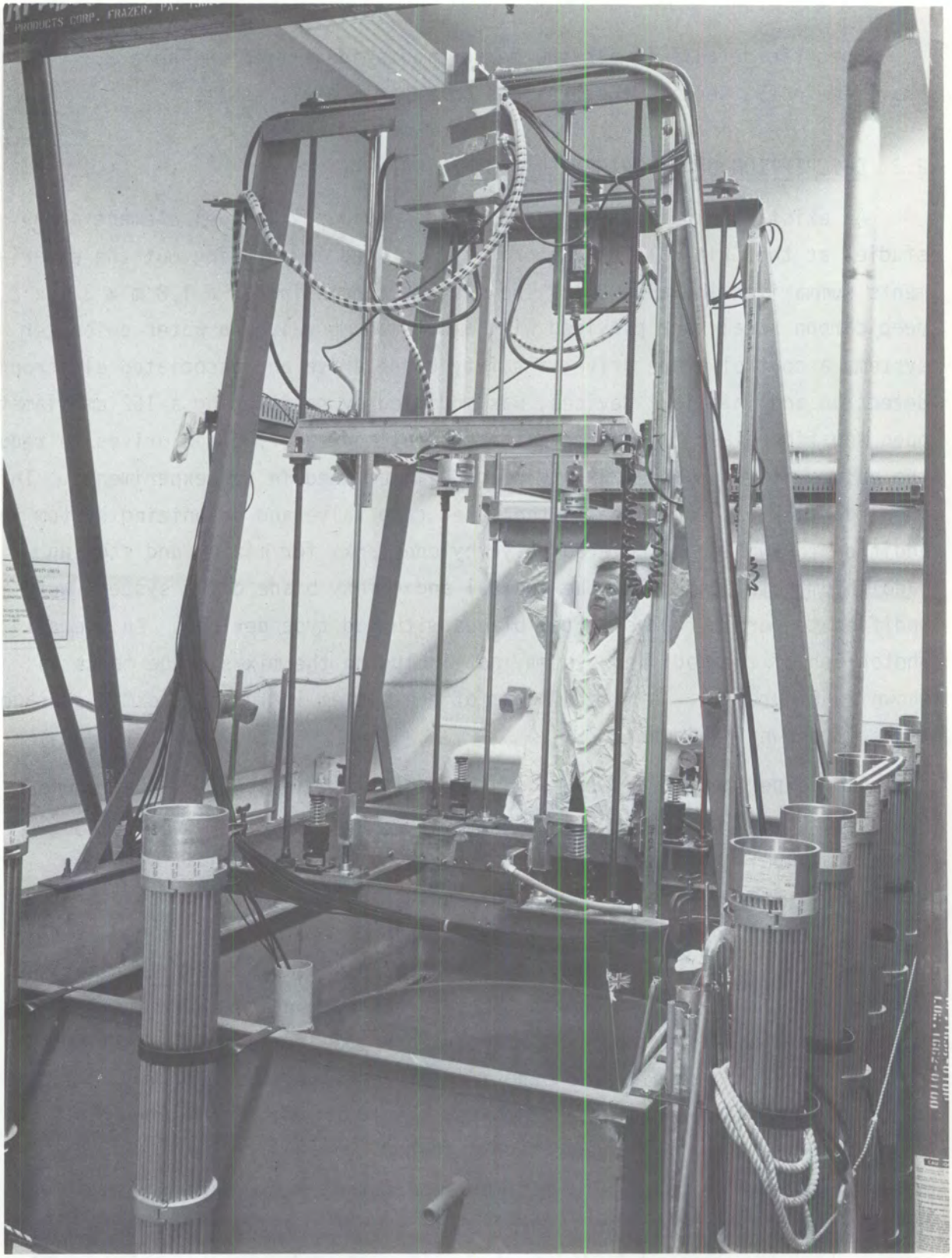

Figure 2.1 Experimental System Modified for Use in Experiments

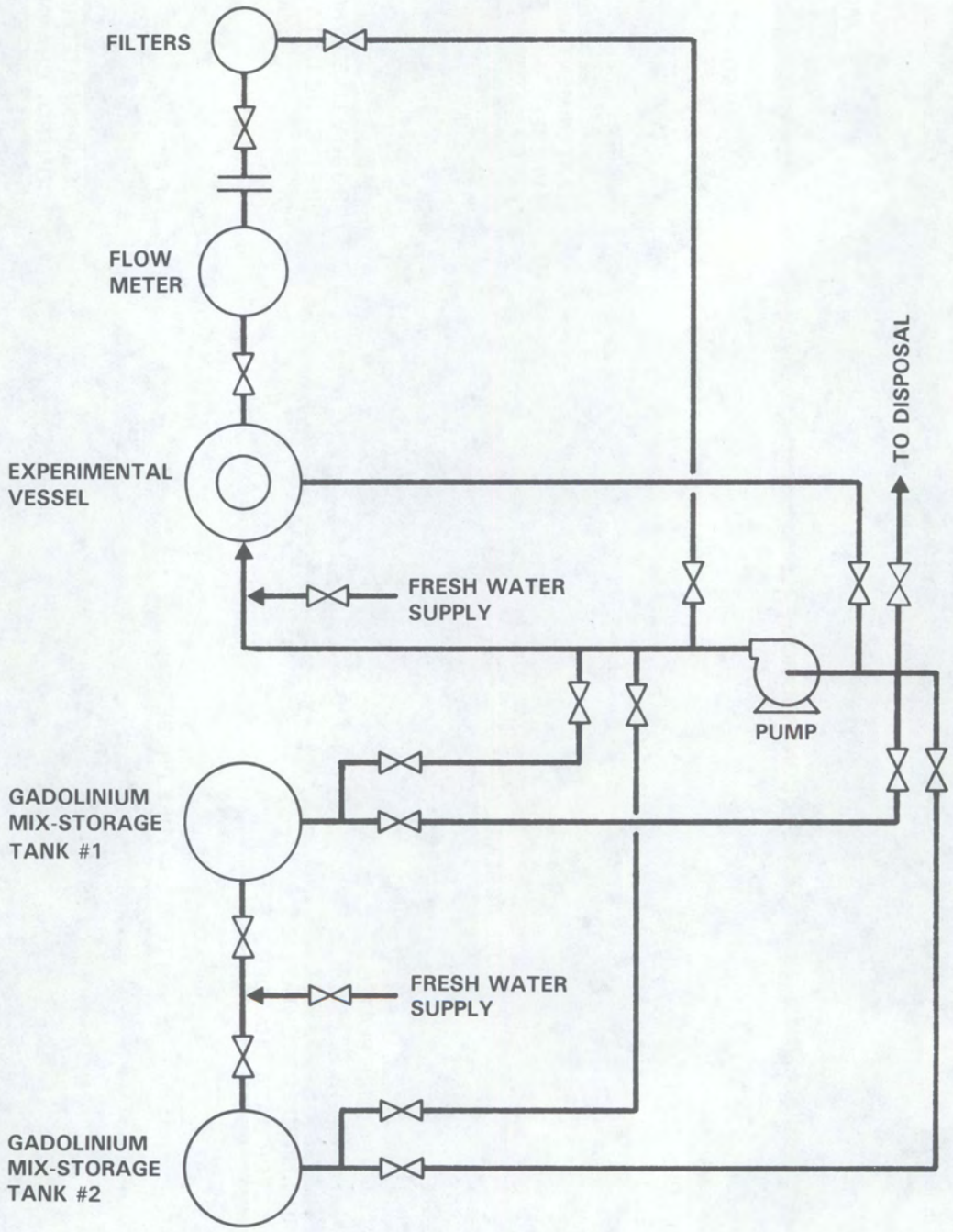

Figure 2.2 Flow Diagram of Experimental System

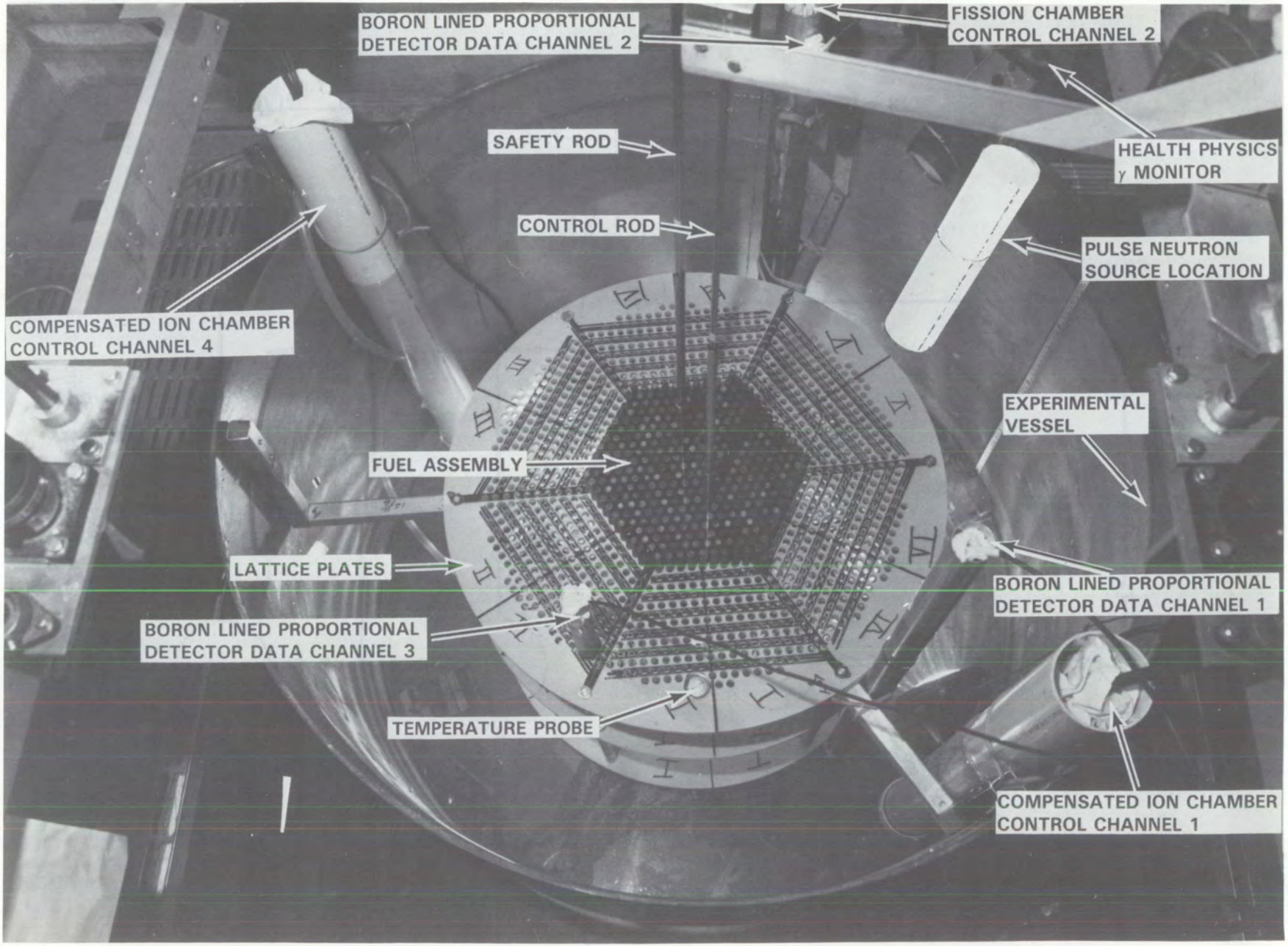

Figure 2.3 Annotated Photograph of Experimental Vessel and Fuel Assembly

The source was mounted in an open 0.6 cm diameter acrylic tube to minimize voiding effects in the gadolinium-water assemblies.

As indicated earlier, the fuel rods used in the experiments consisted of 4.31 wt% ^{235}U enriched UO_2 rods, 2.35 wt% ^{235}U enriched UO_2 rods and PuO_2-UO_2 rods containing 2.0 wt% PuO_2 in natural UO_2. A complete description of these rods is given in Figures 2.4, 2.5 and 2.6. The 4.31 wt% ^{235}U enriched UO_2 fuel rods, described in Figure 2.5, were obtained by downloading stainless steel clad rods, originally fabricated for Core II of the N.S. Savannah (Kaiz 1969), and reloading the pellets into Type 6061 aluminum tubes (see Appendix A for American Society for Testing Materials, ASTM, Specifications). The uranium assay (1059.64 ± 4.80 g/rod) and the ^{235}U enrichment (4.306 ± 0.013%) shown in Figure 2.5 for these rods are the average of six assay and six spectrographic analyses made on fuel pellets chosen at random during this reloading. The oxide density (10.40 ± 0.006 g UO_2/cm^3) given in Figure 2.5 is based on individual volume displacement measurements with 20 pellets selected at random during the reloading operations. The mass of UO_2 per rod (1203.38 ± 4.13 g) is the average mass of the 1865 rods of this type available for use in the experiments. The fuel diameter (1.265 ± 0.003 cm) given in Figure 2.5 was checked repeatable during the reloading operation and found to agree with that quoted in the document characterizing Core II of the N. S. Savannah (Kaiz 1969). The rubber end cap density (1.321 g/cm^3) quoted in Figure 2.5 for the 4.35 wt% ^{235}U enriched fuel is the result of a single mass-volume measurement with six end caps selected at random. The composition of the end caps is the result of four analyses on randomly selected end caps.

The 2.35 wt% ^{235}U enriched UO_2 fuel rods, described in Figure 2.4, are vibrationally compacted oxide rods that have been used in low power and subcritical measurements repeatable in previous years. The physical description and chemical composition given in Figure 2.4 are those defined during some of these previous measurements (Smith and Konzek 1976) and verified in latter measurements (Smith and Konzek 1978). Additional reanalyses of the fuel rods were not considered warranted since such analyses would require destroying several rods. ASTM chemical specifications for the cladding materials are given in Appendix A.

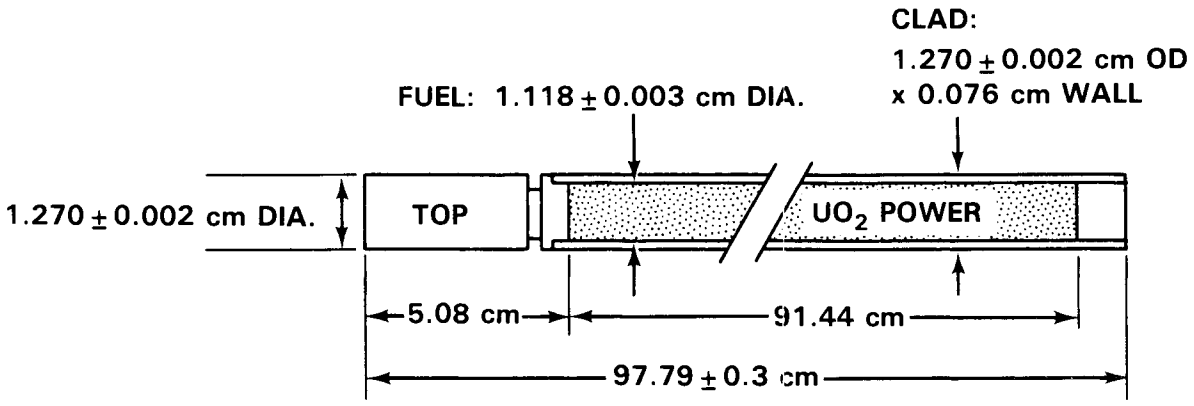

CLADDING: 6061 ALUMINUM TUBING SEAL WELDED WITH A LOWER END PLUG OF 5052-H32 ALUMINUM AND A TOP PLUG OF 1100 ALUMINUM

LOADING:

ENRICHMENT - 2.350 ± 0.003 WT% ^{235}U
OXIDE DENSITY - 9.20 g/cm^3
UO_2 - 825 g/ROD
U - 726 g/ROD

URANIUM COMPOSITION:

^{234}U - 0.0137 ± 0.0003 WT%
^{235}U - 2.350 ± 0.003 WT%
^{236}U - 0.0171 ± 0.0003 WT%
^{238}U - 97.62 ± 0.003 WT%

NOTES:

1. ERROR LIMITS ARE ONE STANDARD DEVIATION

Figure 2.4. Description of 2.35 Wt% ^{235}U Enriched UO_2 Fuel Rods

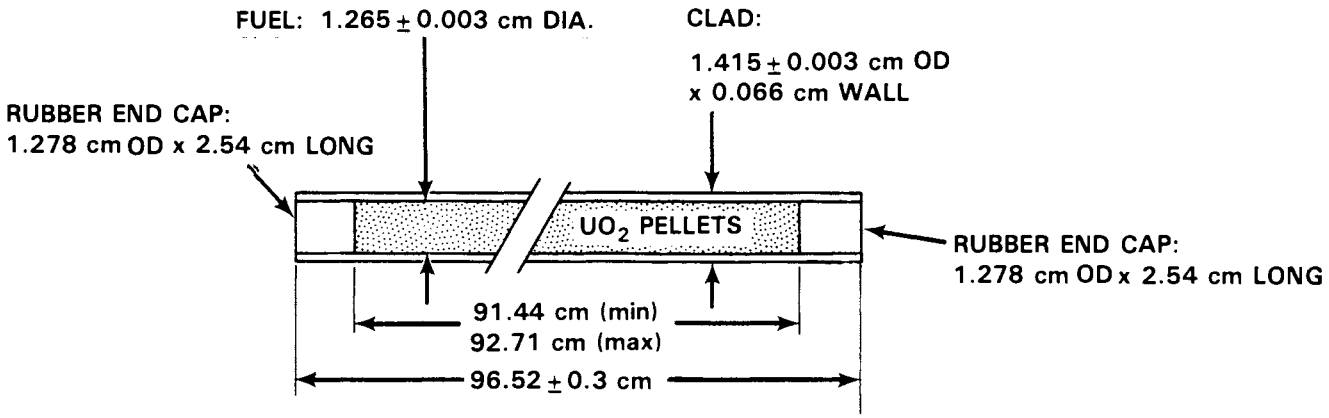

CLADDING: 6061 ALUMINUM TUBING

LOADING

ENRICHMENT - 4.306 ± 0.013% ^{235}U
OXIDE DENSITY - 10.40 ± 0.06 g/cm^3
UO_2 - 1203.38 ± 4.12 g/ROD
U - 1059.64 ± 4.80 g/ROD

URANIUM COMPOSITION:

^{234}U - 0.022 ± 0.002
^{235}U - 4.306 ± 0.013
^{236}U - 0.022 ± 0.002
^{238}U - 95.650 ± 0.017

END CAP:

C-58 ± 1 WT%	S-1.7 ± 0.2 WT%
H-6.5 ± 0.3 WT%	0-22.1 WT% (BALANCE)
Ca-11.4 ± 1.8 WT%	Si-0.3 ± 0.1 WT%

NOTES:

1. ERROR LIMITS ARE ONE STANDARD DEVIATION
2. END CAP DENSITY IS 1.321 g/cm^3

Figure 2.5 Description of 4.31 wt% ^{235}U Enriched UO_2 Fuel Rods

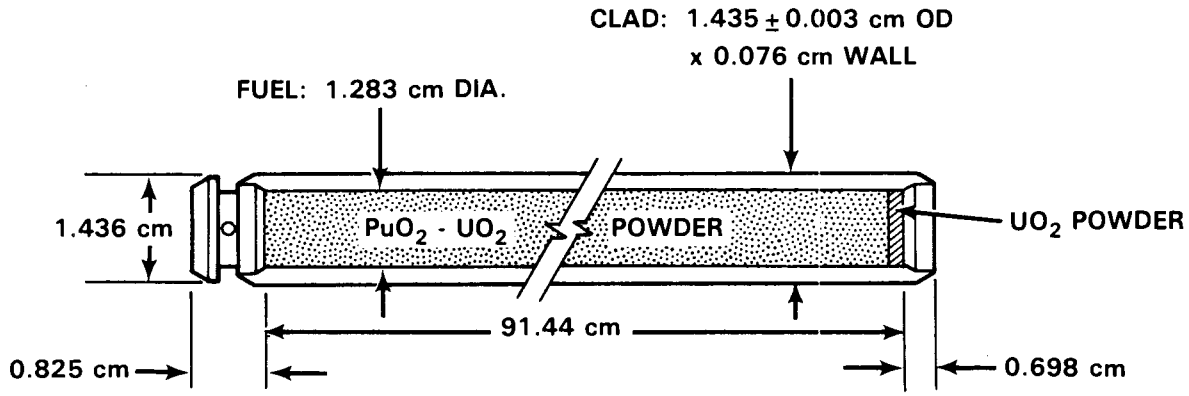

CLADDING: ZIRCALOY-2 TUBING WITH PLUGS SEAL WELDED AT BOTH ENDS

LOADING:

ENRICHMENT - 2.00 WT% PuO_2 IN NATURAL UO_2
OXIDE DENSITY - 9.54 g/cm^3
$PuO_2 + UO_2$ - 1128g/ROD
Pu - 20.169 ± 0.004 g/ROD
U - 970.306 ± 0.225 g/ROD
UO_2 POWDER - NATURAL URANIUM (SEE NOTE 4)

PLUTONIUM COMPOSITION:

^{238}Pu - 0.009 ± 0.001
^{239}Pu - 91.836 ± 0.006
^{240}Pu - 7.760 ± 0.006
^{241}Pu - 0.367 ± 0.001
^{242}Pu - 0.028 ± 0.001

AMERICIUM: 64.6 ± 0.1 PARTS ^{241}Am PER MILLION PARTS $PuO_2 + UO_2$ MIXTURE BY WEIGHT

NOTES:

1. EFFECTIVE AVERAGE CHEMICAL SEPARATION DATE FOR PLUTONIUM IS APRIL 1962
2. PLUTONIUM COMPOSITION AND AMERICIUM FROM ANALYSES MADE IN AUGUST 1976. SEE TEXT FOR JANUARY 1983 ANALYSIS BY GAMMA SPECTRUM ANALYSES.
3. DECEMBER 1965 CALCULATED $^{241}Pu/^{241}Am$ ATOM RATIO IS 5.22 (STINSON, 1971)
4. UO_2 POWDER IS AN END FILLER AND BARRIER ABOUT 0.2 cm THICK
5. ERROR LIMITS ARE ONE STANDARD DEVIATION

Figure 2.6 Description of Mixed Oxide Fuel Rods

The mixed oxide rods, described in Figure 2.6, are also vibrationally compacted oxide rods that have been used in previous experiments. The ASTM specifications for the zircalloy cladding is given in Appendix A. The physical description and oxide chemical composition given in Figure 2.6 are those defined (Uotinen 1967) and later verified (Smith and Konzek 1978) during these earlier measurements. The plutonium composition and americium concentration given in Figure 2.6 were determined from the analyses of samples taken from five randomly selected rods (Smith and Konzek 1978). The isotopic weight percent given in Figure 2.6 for the ^{241}Pu is in very good agreement with that obtained (0.366 wt%) by assuming a 14.5 year half life and calculating the decay of the ^{241}Pu concentration (0.726 wt%) used in the fabrication of these rods (March 1962).

Non-destructive gamma spectrum analyses were performed in January, 1983 using six randomly selected mixed oxide rods to obtain additional verification of the plutonium isotopic distribution in these rods. The results of this latest analyses is given below:

^{238}Pu - 0.010 ± 0.001 wt%
^{239}Pu - 91.806 ± 0.551 wt%
^{240}Pu - 7.876 ± 0.394 wt%
^{241}Pu - 0.277 ± 0.008 wt%
^{242}Pu - 0.031 ± ----- wt%

The amount of ^{241}Am in the fuel was determined from the gamma spectrum measurements to be 0.0043 g ^{241}Am/g Pu which agrees well with a value of 0.004 obtained by calculating the decay of the 1965 ^{241}Pu, given in Figure 2.6, to January 1983.

It was anticipated that the experimental results would be very sensitive to the amount of gadolinium dissolved in the water. Consequently several techniques, involving four laboratories, were investigated for analyzing the gadolinium-water samples taken from the experimental assemblies. The various analytical techniques were:

- flame emission spectroscopy
- DC argon plasma emission spectrocopy
- inductively coupled plasma emission spectroscopy
- mass spectrometry.

Each of these techniques, as performed by the various laboratories, are briefly described in Appendix B. The analytical results obtained by the respective laboratories are given in Table 2.2. As will be discussed in greater detail in the sections concerned with experimental results, a conclusion was reached that mass spectrometry provided results as good as could be reasonably achieved. Consequently the gadolinium concentrations referred to throughout this report are the average of the mass spectrometry results given in Table 2.2 for the respective experiments. In addition to analyzing the gadolinium water samples for gadolinium concentration, analyses were performed to determine the trace impurities present in the water and in the gadolinium nitrate dissolved in the water. The results of these analyses are given in Appendix C. Also densities were determined for each sample using a PAAR digital density meter in which the natural vibrational frequency of a hollow oscillator filled with sample is measured. The meter was calibrated using deaerated demineralized water and dry air. Each density result given in Table 2.2 is the average of two sample analyses, each by a different laboratory.

The analytical results in Table 2.2 and Appendix C were obtained on samples taken from larger one liter samples to which about one milliliter of 13 molar nitric acid had been added to improve gadolinium solubility. The large one liter samples were obtained immediately following each measurement by vertically traversing each experimental assembly at the edge of the lattice plates. One liter archival samples were identically obtained and treated following each measurement.

Three 91.44 cm diameter, 1.35 cm thick polypropylene lattice plates, positioned in the center of the open top fiberglass tank as indicated in Figure 2.3, were used in each experiment to obtain assemblies of equally spaced fuel rods at the desired neutron moderation. In all of the experimental assemblies, the lattice plates were positioned at the elevations indicated in Figure 2.7 to maintain a uniform spacing between fuel rods over the length of each assembly with minimum perturbation to the neutron flux. Polypropylene is a hydrocarbon having a C_3H_6 molecular structure with

TABLE 2.2 Results of Gadolinium-Water Samples Analyses

EXPERIMENT REFERENCE NUMBER	SAMPLE IDENTIFICATION NUMBER	GADOLINIUM CONCENTRATION[a] HEHF[b] (g Gd/liter)	PNL[c] (g Gd/liter)	AEEW[d] (g Gd/liter)	AEEW[e] (g Gd/liter)	BNFL[f] (g Gd/liter)	SOLUTION DENSITY[a][g] (g/cm^3)
4.3-000-182 & 185	1-1-2	0.094 ± 0.001	0.068 ± 0.007	0.069	0.069	0.068	0.9986 ± 0.0005
4.3-000-186	1-1-3	0.508 ± 0.011	0.427 ± 0.004	0.434	0.441	0.436	1.0062 ± 0.0011
4.3-000-188	1-1-4	0.575 ± 0.001	0.450 ± 0.005	0.479	0.482	0.483	1.0033 ± 0.0009
4.3-000-188	1-1-5	0.645 ± 0.021	0.522 ± 0.008	0.543	0.555	0.543	1.0025 ± 0.0006
4.3-000-188	1-1-6	0.755 ± 0.007	0.586 ± 0.006	0.617	0.627	0.651	1.0012 ± 0.0011
4.3-000-188	1-1-7	0.940 ± 0.001	0.753 ± 0.008	0.777	0.781	0.796	1.0032 ± 0.0011
4.3-000-192 & 201	1-2-5	–	0.110 ± 0.002	0.120	0.122	0.123	0.9983 ± 0.0009
4.3-000-202	1-2-6	–	0.355 ± 0.005	0.373	0.414	0.385	0.9985 ± 0.0007
4.3-000-203	1-2-7	–	0.880 ± 0.014	0.903	0.903	0.912	1.0000 ± 0.0013
4.3-000-204	1-2-8	–	1.275 ± 0.034	1.24	1.220	1.273	1.0008 ± 0.0016
4.3-000-204	1-2-9	–	1.354 ± 0.025	1.35	1.360	1.382	1.0010 ± 0.0013
4.3-000-204	1-2-10	–	1.434 ± 0.035	1.42	1.420	1.492	1.0013 ± 0.0010
4.3-000-204	1-2-11	–	1.752 ± 0.013	1.62	1.610	1.717	1.0022 ± 0.0011
4.3-000-204	1-2-12	–	2.343 ± 0.043	2.16	2.170	2.220	1.0040 ± 0.0014
4.3-000-205	1.2.13	–	1.457 ± 0.018	1.43	1.430	1.465	1.0014 ± 0.0008
4.3-000-206	1-2-14	–	1.527 ± 0.026	1.45	1.450	1.512	1.0015 ± 0.0006
4.3-000-194	1-3-3	–	0.763 ± 0.008	0.759	0.745	0.754	1.0025 ± 0.0006
4.3-000-194	1-3-4	–	0.633 ± 0.006	0.636	0.644	0.633	1.0026 ± 0.0005
4.3-000-194	1-3-6	–	0.442 ± 0.004	0.449	0.455	0.456	1.0030 ± 0.0056
4.3-000-194	1-3-5	–	0.124 ± 0.001	0.129	0.129	0.130	1.0003 ± 0.0024
4.3-000-198	1-3-7	–	0.118 ± 0.001	0.121	0.123	0.120	0.9996 ± 0.0006
2.35-000-160 & 165	2-1-2	0.146 ± 0.003	0.116 ± 0.001	0.120	0.120	0.121	0.9986 ± 0.0006
2.35-000-165	2-1-5	0.247 ± 0.004	0.207 ± 0.002	0.210	0.217	0.218	0.9992 ± 0.0011
2.35-000-165	2-1-3	0.306 ± 0.002	0.254 ± 0.003	0.258	0.260	0.264	0.9986 ± 0.0005
2.35-000-165	2-1-4	0.363 ± 0.003	0.302 ± 0.003	0.309	0.316	0.318	0.9986 ± 0.0006
2.35-000-170 & 172	2-2-2	–	0.044 ± 0.001	0.051	0.056	0 054	0 9988 ± 0 0005
2.35-000-170	2-2-1	–	0.071 ± 0.001	0.078	0.078	0 078	1 0004 ± 0 0005
2.35-000-170	2-2-3	–	0.236 ± 0.003	0.254	0.256	0 258	0 9990 ± 0 0005
4.3-002-196	3.2.5	0.275	0.191 ± 0.002	0.196	0.194	0.194	1.0014 ± 0.0023
4.3-002-196	3-2-4	–	0 371 ± 0 005	0 408	0 404	0 413	1 0014 ± 0 0008
4.3-002-196	3-2-2	0.685	0.606 ± 0.006	0.611	0.620	0.632	0.9986 ± 0.0006
4.3-002-196	3-2-3	1.060	0.910 ± 0.009	0.906	0.929	0.907	1.0054 ± 0.0009
4.3-002-207	3-2M-1	–	0.441 ± 0.008	0.467	0.465	0.467	0 9999 ± 0 0005
4.3-000-208	3-2M-2	–	0.556 ± 0.005	0.588	0.559	0.573	1 0004 ± 0 0005
4.3-000-209	3-2M-3	–	0.646 ± 0.006	0.670	0.673	0.673	1 0003 ± 0 0005
4.3-000-209	3-2M-4	–	0.740 ± 0.009	0.744	0.760	0.759	1 0022 ± 0 0005
4.3-000-209	3-2M-5	–	1.389 ± 0.029	1.39	1.370	1.372	1 0008 ± 0 0005
4.3-000-209	3-2M-6	–	2.374 ± 0.040	2.34	2.360	2.363	1 0013 ± 0 0005

[a] ERROR LIMITS GIVEN ARE ONE STANDARD DEVIATIONS
[b] FLAME EMISSION SPECTROSCOPY BY HANFORD ENVIRONMENTAL HEALTH FOUNDATION
[c] DC ARGON PLASMA EMISSION SPECTROSCOPY ANALYSIS BY PACIFIC NORTHWEST LABORATORY
[d] INDUCTIVELY COUPLED PLASMA EMISSION SPECTROSCOPY ANALYSIS BY ATOMIC ENERGY ESTABLISHMENT WINFRITH. ESTIMATED UNCERTAINTIES OF 0.75% AT THE ONE STANDARD DEVIATION LEVEL
[e] ISOTOPE DILUTION MASS SPECTROMETRY ANALYSIS BY ATOMIC ENERGY ESTABLISHMENT WINFRITH. ESTIMATED UNCERTAINTIES OF 0.5% AT THE ONE STANDARD DEVIATION LEVEL
[f] THERMAL IONIZATION MASS SPECTROMETRY ANALYSIS BY BRITISH NUCLEAR FUELS LTD - SELLAFIELD. ESTIMATED UNCERTAINTIES OF 0.5% AT THE ONE STANDARD DEVIATION LEVEL
[g] AVERAGE OF DENSITY MEASUREMENTS BY AEEW AND BNFL LABORATORIES

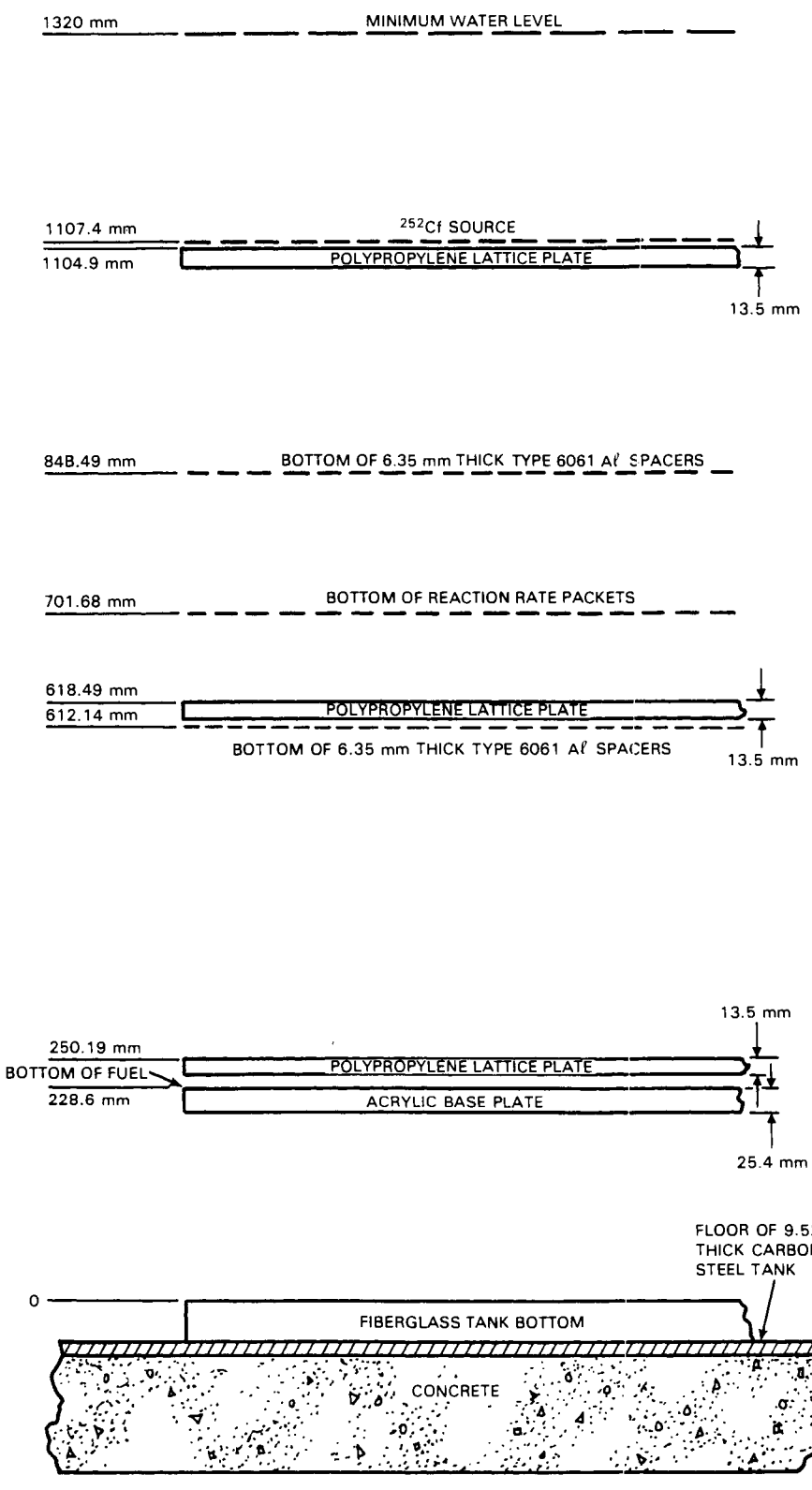

Figure 2.7 Experimental Assembly Elevations

neutron moderating properties similar to water and a density range of 0.902 g/cm^3 to 0.906 g/cm^3. The density of a sample taken at random from the polypropylene during fabrication of the lattice plates was determined, by volume displacement, to be 0.905 g/cm^3. Trace impurities present in the polypropylene are given in Appendix D. All of the experiments were performed with the fuel rods in a uniform triangular pattern and supported on a 2.54 cm thick acrylic plate (1.185 g/cm^3 containing 8 wt% H, 60 wt% C and 32 wt% O) mounted off the sides of the figerglass tank.

As stated previously, each experimental assembly was provided with a control rod and a safety rod. The rods were identical. Each rod consisted of three 0.48 cm diameter gadolinium metal rods banded together and mounted on the respective drive systems to move vertically into and out of the fuel region of the experimental assemblies. These rods and their associated Type 6061 aluminum sleeves were located near the center of each assembly as shown in the respective loading diagrams (see Appendix F). The control and safety rods are not defined since all of the criticality and subcriticality data reported herein are with these rods fully withdrawn from the experimental assemblies. ASTM specifications for the aluminum sleeves are given in Appendix A. The aluminum sleeves extended from the arcylic base plate shown in Figure 2.7 to above the top reflector level. The sleeves had a 1.283 $\pm$ 0.003 cm inside diameter and a wall thickness of 0.066 cm. A typical positioning of the control and safety rods is shown in Figure 2.3. A photograph showing the rod guide sleeves and a set of lattice plates assembled outside the experimental assembly is shown in Figure 2.8. Relative elevations present in each experimental assembly are given in Figure 2.7.

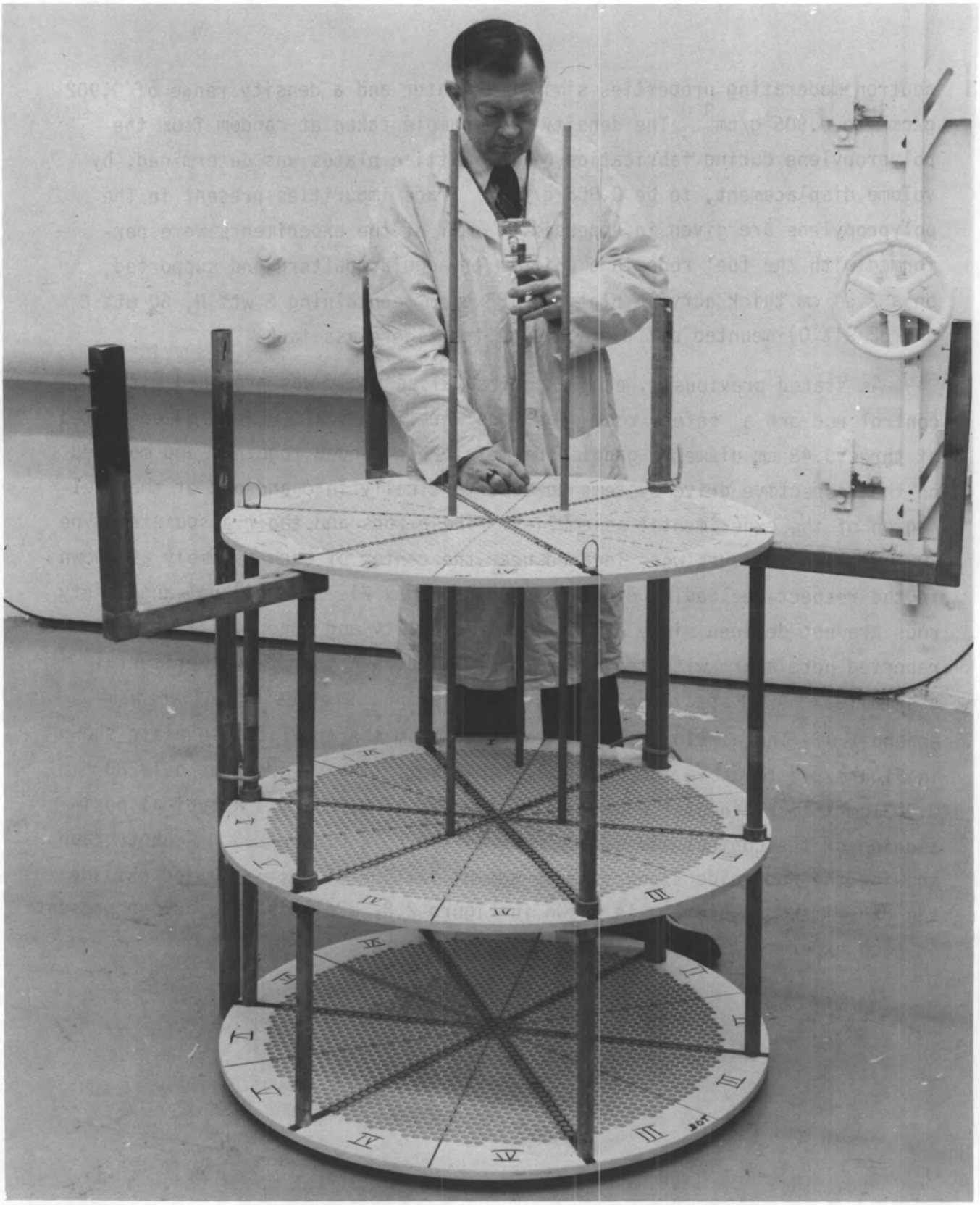

Figure 2.8. An Assembled Set of Lattice Plates Outside the Experimental Tank

3.0 EXPERIMENTAL RESULTS

The measurement techniques used to obtain the data discussed previously in the section on experiments are presented and discussed in this section along with the measurement results. The factors affecting the accuracy of the measurement results and sources of error are also covered in this section.

3.1 CRITICALITY EXPERIMENTS

To measure the effect of gadolinium concentration on the critical size of an assembly of fuel rods in water, the critical size was first determined for the condition of no gadolinium in the water. Gadolinium in the form of gadolinium nitrate was then dissolved into the water to achieve a critical assembly having a fuel region radius approximating that of the THORP fuel dissolver basket (about 30 - 33 cm). These two measurement determinations were made for each of the three fuel-water lattices as indicated in Table 2.1.

The objective of these measurements was to obtain data on fuel rods fully submerged in and reflected on all sides by water or water containing dissolved gadolinium. Direct experimental data was desired on fuel-water assemblies containing only perturbations that could be precisely and easily defined, or experimentally evaluated in terms of their effect on the critical size of the assembly. Consequently the experiments were performed with the assemblies constructed such that only the perturbation caused by the polypropylene lattice plates exist in the final experimental data. Although experimental assemblies were taken critical by partially withdrawing the control rod, the critical size of all the experimental assemblies covered herein were obtained by extrapolation of subcritical data with the rod fully withdrawn, as discussed in the section that follows.

3.1.1 Measurement Technique

In an approach-to-critical measurement to determine the critical conditions for a system, neutron multiplication measurements are made as the parameter of interest is varied such that the system "approaches" criticality. By extrapolating subcritical data very near critical, a precise definition of the critical conditions for that system can be obtained with the parameter of interest being the only perturbing variable. In each of the experiments covered by this report fuel was loaded into the lattice plates in increments that were neutronically symmetrical to each other. At each incremental loading, neutron count rates were obtained using the three boron lined proportional detectors identified as data channels in Figure 2.3.

Although these data channel detectors shown in Figure 2.3 are located to minimize spatial effects in the count rate data, far subcritical loadings will exhibit spatial dependencies between detector-fuel loading locations and result in different critical sizes being predicted by the count rate data from the three data channels. As the delayed critical condition is approached, however, the neutron flux becomes relatively large and the fuel loading increments, for safety reasons become smaller. Under these conditons spatial effects become negligible and the count rates from all three data channels tend to predict the same number of fuel rods for delayed critical. Near this delayed critical conditon the neutron count rate data will begin to vary linearly and a linear least squares fit of count rate data as a function of subcritical fuel loading can be made to obtain a very accurate determination of the delayed critical condition.

A plot of the approach-to-critical data for experiment 4.3-000-182 is shown in Figure 3.1 as an illustration of the measurements typically performed to determine the critical size for each of the experimental assemblies. A plot of the relative inverse neutron count rate observed by the three data channels for each of the assembly subcritical loadings is shown in Figure 3.1 (for clarity the initial data point at a fuel loading of 59 rods is not shown and some of data points for channel 3 have been deleted). At the delayed critical condition the neutron count rate approaches infinity.

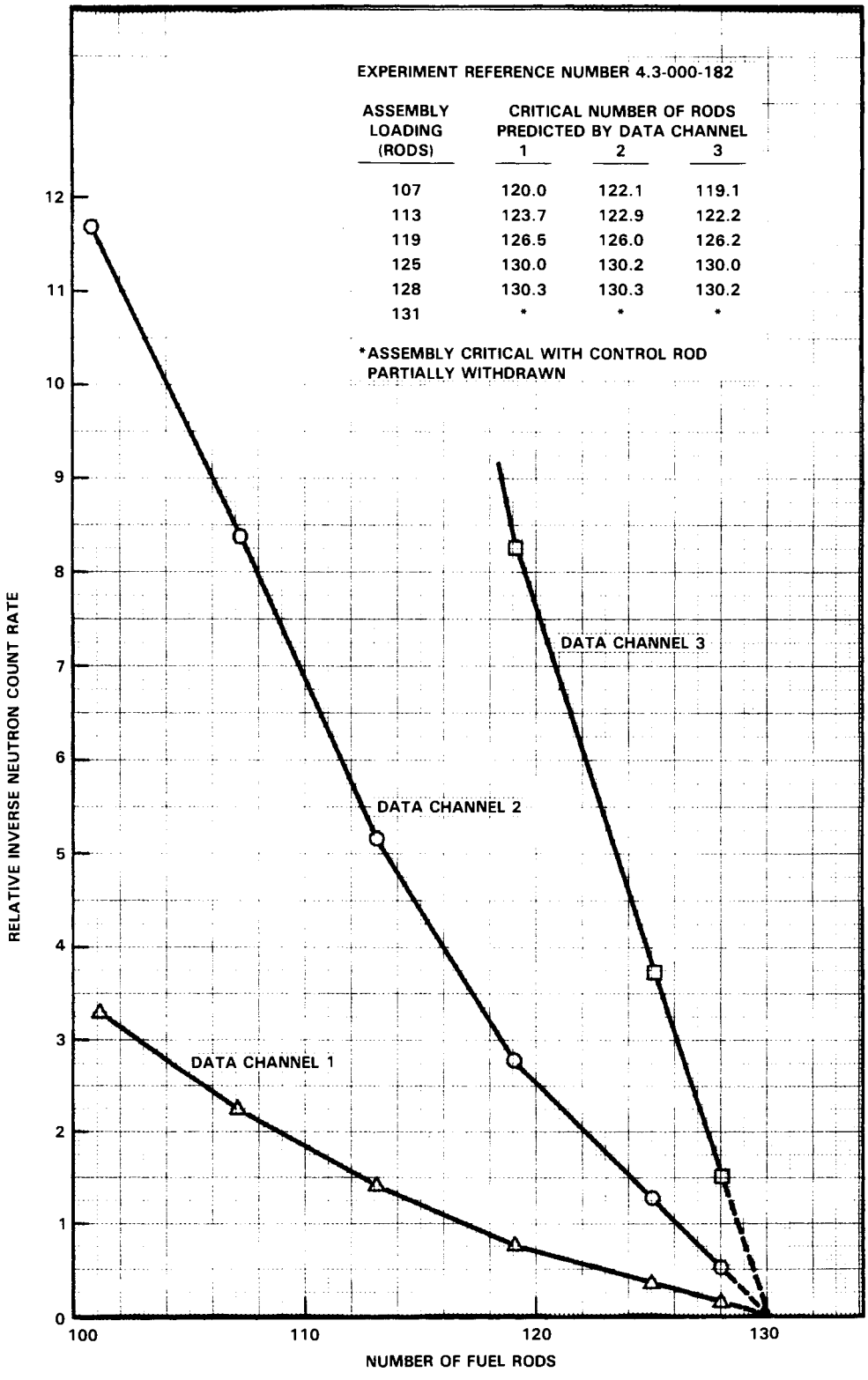

Figure 3.1 Typical Approach-to-Critical Plot

Consequently the number of fuel rods required for criticality can be predicted by extrapolating to an inverse count rate of zero. The critical number of fuel rods predicted by the data channels at each fuel loading is tabulated in Figure 3.1 for assembly 4.3-000-182 with the control and safety rods fully withdrawn. Note that in these triangular pitched assemblies the minimum number of rods that can be added symmetrically is three and that such an addition to 131 fuel rods in assembly 4.3-000-182 results, as would be expected from the subcritical predictions, in criticality with the control rod only partially withdrawn.

3.1.2 Criticality Experiments and Data

As indicated in Table 2.1, criticality experiments were performed with basically three types of fuel-water lattices. One of these consisted of 4.31 wt% ^{235}U enriched UO_2 fuel rods (see Figure 2.5 for rod description) arranged in a triangular pattern, in water, on center-to-center spacings of 2.398 ± 0.005 cm, 1.801 ± 0.005 and 1.598 ± 0.005. (See Appendix E for measurement of lattice spacings). These spacings (lattice pitches) result in water-to-fuel volume ratios of 2.726 ± 0.028, 0.973 ± 0.026 and 0.509 ± 0.019 respectively.

The experiments were performed at the 2.398 cm spacing to obtain data with the 4.31 wt% ^{235}U enriched fuel near optimum neutron moderation with no dissolved gadolinium in the water, and to determine the amount of dissolved gadolinium required to prevent criticality in such a fuel-water assembly approximately 30 cm in radius. Experiments were performed with fuel at the 1.801 cm spacing to obtain similar data in the intermediate region of neutron moderation (undermoderated) with no dissolved gadolinium in the water and at near optimum neutron moderation with sufficient gadolinium dissolved in the water to achieve criticality with an assembly approximately 30 cm in radius. The 1.598 cm lattice spacing was chosen to obtain data on this fuel at a neutron moderation as near as feasible to that of a tight packed assembly (0.91 fuel volume to total volume), fully sumberged and reflected on all sides with water. Although not originally planned, a sufficient amount of the 4.31 wt% ^{235}U enriched fuel was available to construct an over-sized assembly (over 30 cm in radius)

of this fuel in water containing dissolved gadolinium.

The second series of fuel-water lattices consisted of 2.35 wt% ^{235}U enriched UO_2 fuel rods (see Figure 2.4 for rod description) similarly arranged in a triangular pattern on center-to-center spacings of 1.895 ± 0.005 cm and 1.598 ± 0.005 cm resulting in water-to-fuel volume ratios of 1.853 ± 0.038 and 0.954 ± 0.025 respectively. Several experiments covering a wide range of neutron moderation had been previously performed (Smith and Konzek 1976, Bierman and Clayton 1981, Bierman, Durst and Clayton 1979) with this fuel in water only. Consequently the two lattice spacings of about 1.9 cm and 1.6 cm were chosen primarily to obtain data of interest on fuel-water assemblies containing dissolved gadolinium. As with the 4.31 wt% fuel, the 1.598 cm lattice spacing results in a neutron moderation as near to that of that packed fuel as is feasible in the experimental assembly. The 1.895 cm lattice spacing was chosen to obtain an approximately 30 cm radius critical assembly in water containing dissolved gadolinium. Also this spacing provides near optimum neutron moderation.

The third series of fuel-water lattices consisted of a mixture of the 4.31 wt% ^{235}U enriched UO_2 rods and PuO_2-UO_2 fuel rods containing 2.0 wt% PuO_2 and 98.0 wt% natural UO_2. These lattices of mixed fuel were performed at the close-pack triangular center-to-center spacing of 1.598 ± 0.005 cm with the PuO_2-UO_2 fuel rods uniformly distributed throughout the assembly to obtain a $Pu/^{235}U$ ratio approximating that characteristic of 20,000 MWD/Te fuel burn-up. Two region assemblies of the UO_2 and PuO_2-UO_2 fuel rods were also constructed at this lattice spacing to obtain data on large assemblies (35-40 cm radius) with high gadolinium concentrations ($\sim$2.5 g Gd/ℓ).

The experimental criticality data obtained on the three fuel-water lattice types are presented in Table 3.1, except for the easily defined lattice plates and base support plate, experimentally determined corrections were applied to the actual experimental data to obtain the critical sizes reported in Table 3.1 (except for the 2.35-000-172 data which was obtained in connection with the subcritical measurements). Replacement type experimental measurements were performed to determine in terms of fuel rods, the reactivity worth of:

TABLE 3.1 Experimental Results - Critical Lattices of Fuel Rods in a Uniform Pattern

EXPERIMENT REFERENCE NUMBER[a]	LATTICE IDENTIFICATION NUMBER	LATTICE PITCH[b,c] (cm)	WATER-TO-FUEL VOLUME RATIO[c]	FUEL RODS[d] TYPE	FUEL RODS[d] ENRICHMENT (wt%)	MODERATOR TEMPERATURE (°C)	GADOLINIUM CONCENTRATION (g Gd/liter)[c,e]	CRITICAL SIZE[c,f] (NUMBER OF FUEL RODS)
4.3-000-182	11	2.398 ± 0.005	2.711 ± 0.028	UO_2	4.31% ^{235}U	19	0	132 ± 1
4.3-000-185	11	2.398 ± 0.005	–	UO_2	4.31% ^{235}U	20	0.068 ± 0.001	167 ± 1
4.3-000-186	11	2.398 ± 0.005	–	UO_2	4.31% ^{235}U	21	0.438 ± 0.004	515 ± 2[g]
4.3-000-188	11	2.398 ± 0.005	–	UO_2	4.31% ^{235}U	18	0.482 ± 0.001	593 ± 1
4.3-000-192	12	1.801 ± 0.005	0.984 ± 0.026	UO_2	4.31% ^{235}U	14	0	378 ± 1
4.3-000-201	12	1.801 ± 0.005	–	UO_2	4.31% ^{235}U	18	0.122 ± 0.001	476 ± 1
4.3-000-202	12	1.801 ± 0.005	–	UO_2	4.31% ^{235}U	20	0.400 ± 0.021	630 ± 1
4.3-000-203	12	1.801 ± 0.005	–	UO_2	4.31% ^{235}U	20	0.908 ± 0.006	959 ± 1
4.3-000-204	12	1.801 ± 0.005	–	UO_2	4.31% ^{235}U	21	1.246 ± 0.038	1260 ± 1
4.3-000-205	12	1.801 ± 0.005	–	UO_2	4.31% ^{235}U	22	1.448 ± 0.025	1482 ± 2
4.3-000-206	12	1.801 ± 0.005	–	UO_2	4.31% ^{235}U	23	1.481 ± 0.044	1533 ± 2
4.3-000-194	13	1.598 ± 0.005	0.509 ± 0.019	UO_2	4.31% ^{235}U	14	0	1185 ± 3
4.3-000-198	13	1.598 ± 0.005	–	UO_2	4.31% ^{235}U	15	0.121 ± 0.002	1495 ± 1
2.35-000-160	21	1.895 ± 0.005	1.878 ± 0.038	UO_2	2.35% ^{235}U	30	0	431 ± 1
2.35-000-165	21	1.895 ± 0.005	–	UO_2	2.35% ^{235}U	22	0.120 ± 0.001	842 ± 1
2.35-000-170	22	1.598 ± 0.005	0.962 ± 0.025	UO_2	2.35% ^{235}U	19	0	1029 ± 2
2.35-000-172	22	1.598 ± 0.005	–	UO_2	2.35% ^{235}U	18	0.055 ± 0.001	1122 ± 2[h]
4.3-002-196	32[i]	1.598 ± 0.005	0.509 ± 0.019 0.460 ± 0.001[j]	MO_2 & UO_2	2.0% PuO_2 & 4.31% ^{235}U	24	0	1757 ± 6
4.3-002-207	32M[k]	1.598 ± 0.005	–	MO_2 & UO_2	2.0% PuO_2 & 4.31% ^{235}U	18	0.466 ± 0.001	1796 ± 1[l,m]
4.3-002-208	32M[k]	1.598 ± 0.005	–	MO_2 & UO_2	2.0% PuO_2 & 4.31% ^{235}U	20	0.566 ± 0.010	1913 ± 1[l,m]
4.3-002-209	32M[k]	1.598 ± 0.005	–	MO_2 & UO_2	2.0% PuO_2 & 4.31% ^{235}U	21	0.673 ± 0.001	2006 ± 1[m]

[a] SUPPORTING AND RELATED SETS OF MEASUREMENT DATA SIMILARLY IDENTIFIED ALPHA-NUMERICALLY
[b] CENTER-TO-CENTER SPACING BETWEEN FUEL RODS IN A TRIANGULAR PATTERN
[c] ERROR LIMITS ARE ONE STANDARD DEVIATION ESTIMATES. ERROR LIMITS ON CRITICAL SIZE ARE INTENDED TO INCLUDE THOSE ASSOCIATED WITH REPRODUCIBILITY
[d] FUEL RODS ARE FULLY DESCRIBED ELSEWHERE
[e] AVERAGE OF MASS SPECTROMETRY ANALYSES
[f] MEASURED CORRECTIONS APPLIED TO EXPERIMENTAL ASSEMBLIES TO OBTAIN LATTICES OF RODS IN WATER ONLY
[g] CORRECTED CRITICAL SIZE USING CORRECTIONS OBTAINED IN EXPERIMENT 4.3-000-188
[h] UNCORRECTED EXPERIMENTAL RESULTS. SEE TABLE IV.
[i] LATTICE OF PuO_2-UO_2 FUEL RODS AND UO_2 FUEL RODS IN A UNIFORM PATTERN OF ONE PuO_2-UO_2 ROD SURROUNDED BY SIX UO_2 RODS
[j] PuO_2-UO_2 LATTICE CELL WATER-TO-FUEL VOLUME RATIO
[k] LATTICE OF 1657 UO_2 RODS SURROUNDED BY PuO_2-UO_2 RODS
[l] CORRECTED CRITICAL SIZE USING CORRECTIONS OBTAINED IN EXPERIMENT 4.3-002-209
[m] ERROR LIMITS APPLY TO PuO_2-UO_2 FUEL RODS ONLY (SEE NOTE j)

- The aluminum clad water columns created in each assembly by the full withdrawal of the safety and control rods,
- the neutron source and source holder,
- the aluminum spacers used to achieve a higher degree of accuracy in positioning the reaction rate devices.

Of the above identified perturbations, only the water columns created by the withdrawal of the control and safety rod had a measurable effect on the critical size of the experimental assemblies. The reactivity worth of these water columns was determined to vary linearly over the range of interest (zero to three water columns) by varying the number of water columns present in an assembly and observing the changes in critical size as indicated in Figure 3.2.

As can be seen in Figure 3.2, the reactivity worth of the water columns is a linear function of the number of columns present over a sufficient range to permit linearly extrapolating to the critical assembly size with no water columns present. Also note in Figure 3.2 that to demonstrate this linearity between the critical size and number of water columns present, the assembly's safety rod was replaced in one measurement with a fuel rod leaving only the water column created by withdrawal of the control rod. Once linearity was demonstrated, however, the reactivity worth of the water columns caused by the control and safety rods being fully withdrawn was determined by increasing the number of columns from two to three and linearly extrapolating to zero as indicated in Figure 3.3. The experimental data for these extrapolations are presented in Table 3.2 for each experiment identified in Table 3.1. Fuel loading diagrams are presented in Appendix F for each experimental assembly identified in Tables 3.1 and 3.2.

As indicated in Table 3.1, each of the experimental measurements have been identified by an "experiment reference number" and a "lattice identification number." Measurements performed in support of, or in conjunction with, other experiments are identified by the same number with an alpha

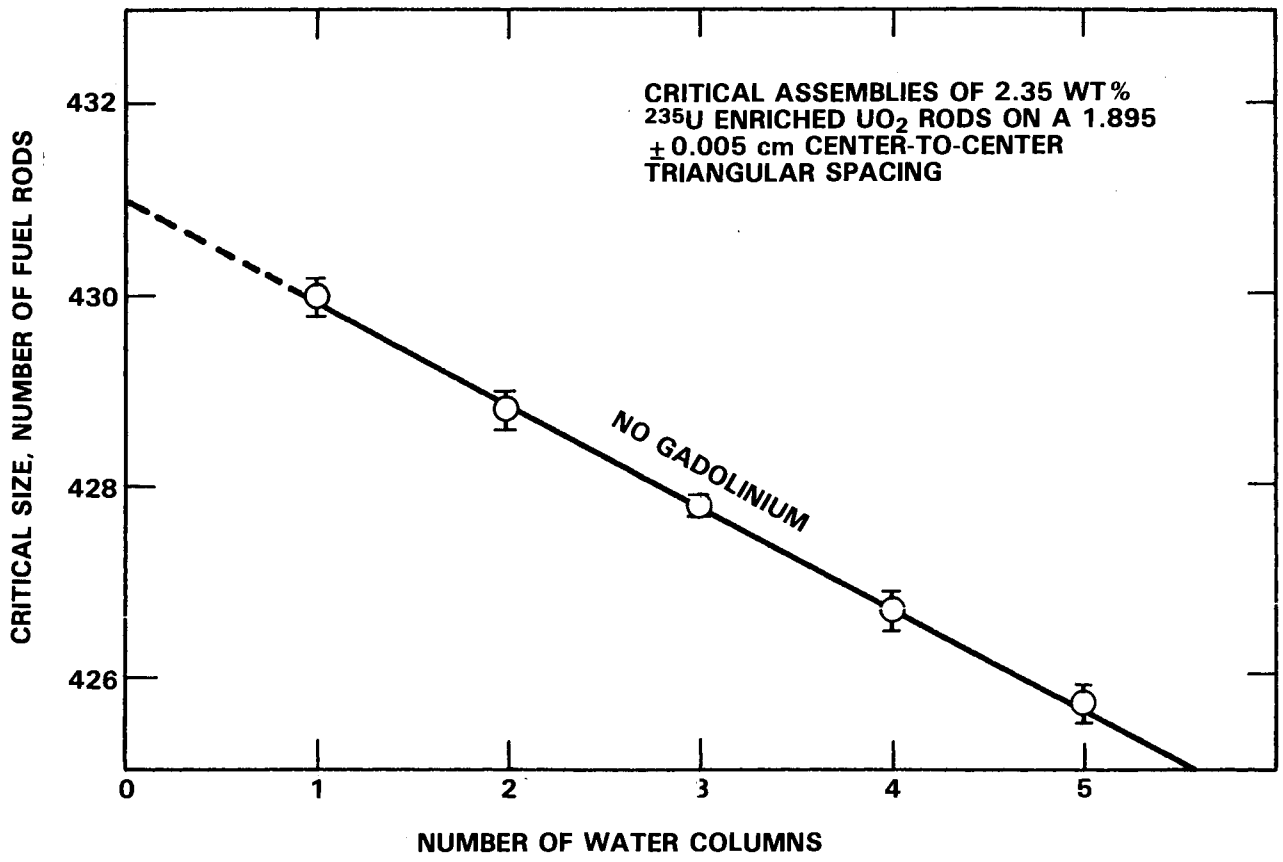

Figure 3.2 Measurement Data Showing Linearity and Effect of Aluminum Clad Water Columns in the Experimental Assembly

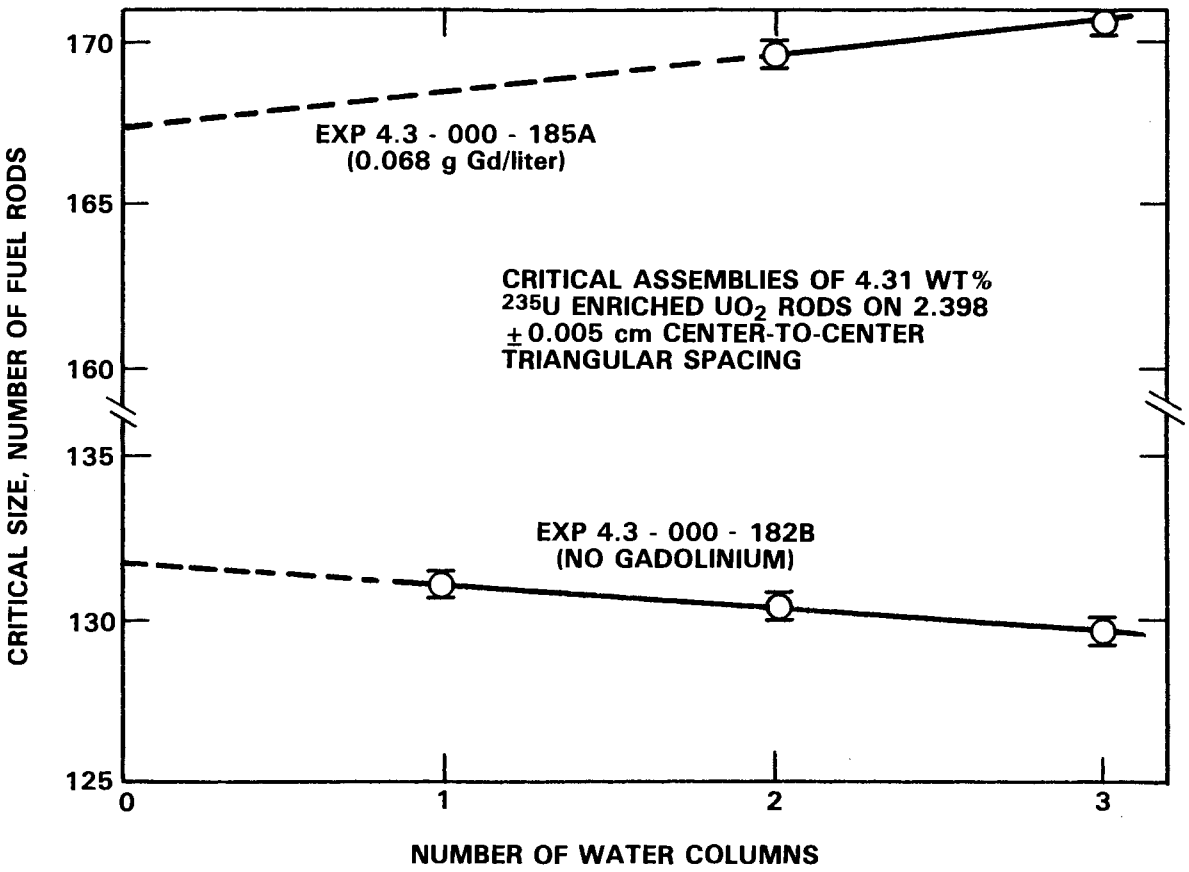

Figure 3.3 Typical Measurement Data Obtained in Evaluating the Reactivity of Aluminum Clad Water Columns Created by Withdrawal of the Safety and Control Rods

TABLE 3.2 Experimental Results - Critical Lattices of Fuel Rods with Irregular Features

EXPERIMENT REFERENCE NUMBER[a]	LATTICE IDENTIFICATION NUMBER	LATTICE PITCH[b,c] (cm)	WATER-TO-FUEL VOLUME RATIO[c]	FUEL RODS[e] TYPE	FUEL RODS[e] ENRICHMENT (wt%)	GADOLINIUM CONCENTRATION (g Gd/liter)[c,d]	CRITICAL SIZE[f] (NUMBER OF FUEL RODS)	IRREGULARITY
4.3-000-182A	11	2.398 ± 0.005	2.711 ± 0.028	UO_2	4.31% ^{235}U	0	130.3 ± 0.1	TWO WATER FILLED Al SLEEVES
4.3-000-182B	11	2.398 ± 0.005	2.711 ± 0.028	UO_2	4.31% ^{235}U	0	129.8 ± 0.1	THREE WATER FILLED Al SLEEVES
4.3-000-182C	11	2.398 ± 0.005	2.711 ± 0.028	UO_2	4.31% ^{235}U	0	131.1 ± 0.1	ONE WATER FILLED Al SLEEVE
4.3-000-185A	11	2.398 ± 0.005	–	UO_2	4.31% ^{235}U	0.068 ± 0.001	169.6 ± 0.1	TWO WATER FILLED Al SLEEVES
4.3-000-185B	11	2.398 ± 0.005	–	UO_2	4.31% ^{235}U	0.068 ± 0.001	170.7 ± 0.1	THREE WATER FILLED Al SLEEVES
4.3-000-186A	11	2.398 ± 0.005	–	UO_2	4.31% ^{235}U	0.438 ± 0.004	536.4 ± 0.2	TWO WATER FILLED Al SLEEVES
4.3-000-188A	11	2.398 ± 0.005	–	UO_2	4.31% ^{235}U	0.482 ± 0.001	614.6 ± 0.1	TWO WATER FILLED Al SLEEVES
4.3-000-188B	11	2.398 ± 0.005	–	UO_2	4.31% ^{235}U	0.482 ± 0.001	625.4 ± 0.1	THREE WATER FILLED Al SLEEVES
4.3-000-192A	12	1.801 ± 0.005	0.984 ± 0.026	UO_2	4.31% ^{235}U	0	369.9 ± 0.1	TWO WATER FILLED Al SLEEVES
4.3-000-192B	12	1.801 ± 0.005	0.984 ± 0.026	UO_2	4.31% ^{235}U	0	365.8 ± 0.2	THREE WATER FILLED Al SLEEVES
4.3-000-192C	12	1.801 ± 0.005	0.984 ± 0.026	UO_2	4.31% ^{235}U	0	344.7 ± 0.4	TWO WATER FILLED Al SLEEVES PLUS A SEVEN ROD WATER HOLE
4.3-000-201A	12	1.801 ± 0.005	–	UO_2	4.31% ^{235}U	0.122 ± 0.00	468.4 ± 0.1	TWO WATER FILLED Al SLEEVES
4.3-000-201B	12	1.801 ± 0.005	–	UO_2	4.31% ^{235}U	0.122 ± 0.00	464.5 ± 0.1	THREE WATER FILLED Al SLEEVES
4.3-000-202A	12	1.801 ± 0.005	–	UO_2	4.31% ^{235}U	0.400 ± 0.02	625.3 ± 0.2	TWO WATER FILLED Al SLEEVES
4.3-000-202B	12	1.801 ± 0.005	–	UO_2	4.31% ^{235}U	0.400 ± 0.02	622.9 ± 0.1	THREE WATER FILLED Al SLEEVES
4.3-000-203A	12	1.801 ± 0.005	–	UO_2	4.31% ^{235}U	0.908 ± 0.006	965.4 ± 0.2	TWO WATER FILLED Al SLEEVES
4.3-000-203B	12	1.801 ± 0.005	–	UO_2	4.31% ^{235}U	0.908 ± 0.006	968.4 ± 0.4	THREE WATER FILLED Al SLEEVES
4.3-000-204A	12	1.801 ± 0.005	–	UO_2	4.31% ^{235}U	1.246 ± 0.038	1269.9 ± 0.2	TWO WATER FILLED Al SLEEVES
4.3-000-204B	12	1.801 ± 0.005	–	UO_2	4.31% ^{235}U	1.246 ± 0.038	1274.9 ± 0.4	THREE WATER FILLED Al SLEEVES
4.3-000-205A	12	1.801 ± 0.005	–	UO_2	4.31% ^{235}U	1.448 ± 0.025	1493.9 ± 0.7	TWO WATER FILLED Al SLEEVES
4.3-000-205B	12	1.801 ± 0.005	–	UO_2	4.31% ^{235}U	1.448 ± 0.025	1500.0 ± 0.8	THREE WATER FILLED Al SLEEVES
4.3-000-206A	12	1.801 ± 0.005	–	UO_2	4.31% ^{235}U	1.481 ± 0.044	1548.5 ± 0.9	TWO WATER FILLED Al SLEEVES
4.3-000-206B	12	1.801 ± 0.005	–	UO_2	4.31% ^{235}U	1.481 ± 0.044	1555.4 ± 0.9	THREE WATER FILLED Al SLEEVES
4.3-000-194A	13	1.598 ± 0.005	0.509 ± 0.019	UO_2	4.31% ^{235}U	0	1147.3 ± 0.3	TWO WATER FILLED Al SLEEVES
4.3-000-194B	13	1.598 ± 0.005	0.509 ± 0.019	UO_2	4.31% ^{235}U	0	1134.7 ± 2.5	THREE WATER FILLED Al SLEEVES
4.3-000-194C	13	1.598 ± 0.005	0.509 ± 0.019	UO_2	4.31% ^{235}U	0	1116.0 ± 1.2	FOUR WATER FILLED Al SLEEVES
4.3-000-198A	13	1.598 ± 0.005	–	UO_2	4.31% ^{235}U	0.121 ± 0.002	1465.8 ± 0.3	TWO WATER FILLED Al SLEEVES
4.3-000-198B	13	1.598 ± 0.005	–	UO_2	4.31% ^{235}U	0.121 ± 0.002	1451.1 ± 0.1	THREE WATER FILLED Al SLEEVES
2.35-000-159A	21	1.895 ± 0.005	1.878 ± 0.038	UO_2	2.35% ^{235}U	0	427.8 ± 0.1	THREE WATER FILLED Al SLEEVES
2.35-000-159B	21	1.895 ± 0.005	1.878 ± 0.038	UO_2	2.35% ^{235}U	0	426.7 ± 0.2	FOUR WATER FILLED Al SLEEVES
2.35-000-159C	21	1.895 ± 0.005	1.878 ± 0.038	UO_2	2.35% ^{235}U	0	425.7 ± 0.2	FIVE WATER FILLED Al SLEEVES
2.35-000-160A	21	1.895 ± 0.005	1.878 ± 0.038	UO_2	2.35% ^{235}U	0	428.8 ± 0.2	TWO WATER FILLED Al SLEEVES
2.35-000-160B	21	1.895 ± 0.005	1.878 ± 0.038	UO_2	2.35% ^{235}U	0	430.0 ± 0.2	ONE WATER FILLED Al SLEEVES
2.35-000-165A	21	1.895 ± 0.005	–	UO_2	2.35% ^{235}U	0.120 ± 0.001	841.5 ± 0.3[g]	TWO WATER FILLED Al SLEEVES
2.35-000-165B	21	1.895 ± 0.005	–	UO_2	2.35% ^{235}U	0.120 ± 0.001	840.6 ± 0.2	THREE WATER FILLED Al SLEEVES
2.35-000-165C	21	1.895 ± 0.005	–	UO_2	2.35% ^{235}U	0.120 ± 0.001	842.7 ± 0.2	FOUR WATER FILLED Al SLEEVES
2.35-000-170A	22	1.598 ± 0.005	0.962 ± 0.025	UO_2	2.35% ^{235}U	0	1024.7 ± 0.9	TWO WATER FILLED Al SLEEVES
2.35-000-170B	22	1.598 ± 0.005	0.962 ± 0.025	UO_2	2.35% ^{235}U	0	1022.7 ± 0.9	THREE WATER FILLED Al SLEEVES
2.35-000-172	22	1.598 ± 0.005	–	UO_2	2.35% ^{235}U	0.055 ± 0.001	1122.2 ± 1.0	TWO WATER FILLED Al SLEEVES
4.3-002-196A	32[h]	1.598 ± 0.005	0.509 ± 0.019 0.460 ± 0.001[i]	MO_2 & UO_2	2.0% PuO_2 & 4.31% ^{235}U	0	1700.8 ± 1.2	TWO WATER FILLED Al SLEEVES AND FOUR FOIL CLUSTERS IN ASSEMBLY
4.3-002-196B	32[h]	1.598 ± 0.005	0.509 ± 0.019 0.460 ± 0.001[i]	MO_2 & UO_2	2.0% PuO_2 & 4.31% ^{235}U	0	1707.6 ± 1.8	TWO WATER FILLED Al SLEEVES AND THREE FOIL CLUSTERS IN ASSEMBLY
4.3-002-196C	32[h]	1.598 ± 0.005	0.509 ± 0.019 0.460 ± 0.001[i]	MO_2 & UO_2	2.0% PuO_2 & 4.31% ^{235}U	0	1693.0 ± 1.8	THREE WATER FILLED Al SLEEVES AND THREE FOIL CLUSTERS IN ASSEMBLY
4.3-002-207A	32M[j]	1.598 ± 0.005		MO_2 & UO_2	2.0% PuO_2 & 4.31% ^{235}U	0.466 ± 0.001	1775.2 ± 0.5	TWO WATER FILLED Al SLEEVES
4.3-002-208A	32M[j]	1.598 ± 0.005		MO_2 & UO_2	2.0% PuO_2 & 4.31% ^{235}U	0.566 ± 0.010	1891.8 ± 0.6	TWO WATER FILLED Al SLEEVES
4.3-002-209A	32M[j]	1.598 ± 0.005		MO_2 & UO_2	2.0% PuO_2 & 4.31% ^{235}U	0.673 ± 0.001	1985.1 ± 0.6	TWO WATER FILLED Al SLEEVES
4.3-002-209B	32M[k]	1.598 ± 0.005		MO_2 & UO_2	2.0% PuO_2 & 4.31% ^{235}U	0.673 ± 0.001	1974.7 ± 0.6	THREE WATER FILLED Al SLEEVES

[a] RELATED SETS OF MEASUREMENT DATA SIMILARLY IDENTIFIED
[b] CENTER-TO-CENTER SPACING BETWEEN FUEL RODS IN A TRIANGULAR PATTERN
[c] ERROR LIMITS ARE ONE STANDARD DEVIATION ESTIMATES
[d] AVERAGE OF MASS SPECTROMETRY ANALYSES
[e] FUEL RODS ARE FULLY DESCRIBED ELSEWHERE
[f] ERROR LIMITS ARE ONE STANDARD DEVIATION ON THE LEAST SQUARES FIT OF THE APPROACH TO CRITICAL DATA; HOWEVER, THE INDICATED ACCURACIES ARE RELATIVE ONLY BETWEEN THE PERTURBATIONS BEING EVALUATED
[g] BACK OFF WITH SOURCE REMOVED PREDICTS CRITICAL SIZE OF 841.8 ± 0.5 FUEL RODS
[h] LATTICE OF PuO_2-UO_2 FUEL RODS AND UO_2 FUEL RODS IN A UNIFORM PATTERN OF ONE PuO_2 UO_2 ROD SURROUNDED BY SIX UO_2 RODS
[i] PuO_2-UO_2 LATTICE CELL WATER-TO-FUEL VOLUME RATIO
[j] LATTICE OF 1655 UO_2 RODS SURROUNDED BY PuO_2-UO_2 RODS
[k] LATTICE OF 1654 UO_2 RODS SURROUNDED BY PuO_2-UO_2 RODS

notation. The experiment reference number refers to the experiment identification number assigned to the set of measurements and is tracable through the Critical Mass Laboratory operating records. The lattice identification number refers to the lattice type and degree of neutron moderation as described in Table 2.1. (For example, lattice 11 refers to the near-optimum moderated lattices of 4.31 wt% ^{235}U enriched fuel and lattice 12 refers to the intermediate moderated lattices of this same fuel).

As stated previously, the objective of the criticality experiments was, in general, to determine the critical size of each assembly with no gadolinium dissolved in the water and the amount of dissolved gadolinium required to achieve a critical assembly of fuel having a radius of about 30 cm or larger. However, the performance of some experiments resulted in additional data that may be useful in validating or developing calculational models. These additional data are included in Table 3.1 and 3.2 and primarily involve:

- Critical sizes for some experimental assemblies over a range of gadolinium concentrations,
- critical sizes for experimental assemblies containing irregular fuel loadings and multiple sized "water holes" at various locations in the assemblies,
- variation in the reactivity worth of aluminum clad water columns in an assembly as a function of gadolinium concentration.

The additional data available on variation in critical size with gadolinium is graphically presented in Figure 3.4 to permit making visual comparisons more easily.

Although each set of exprimental data presented in Table 3.2 provides information for at least two gadolinium concentrations on the reactivity worth of water columns created in each assembly by the withdrawal of the safety and controls rods, the 200 series provide a set of data over a wide range of gadolinium concentrations for a single lattice spacing. The variation observed in the reactivity worth of a water column with gadolinium concentration in this series of experiments is plotted in Figure 3.5. As can be seen in Figure 3.5, the water column with no gadolinium dissolved in

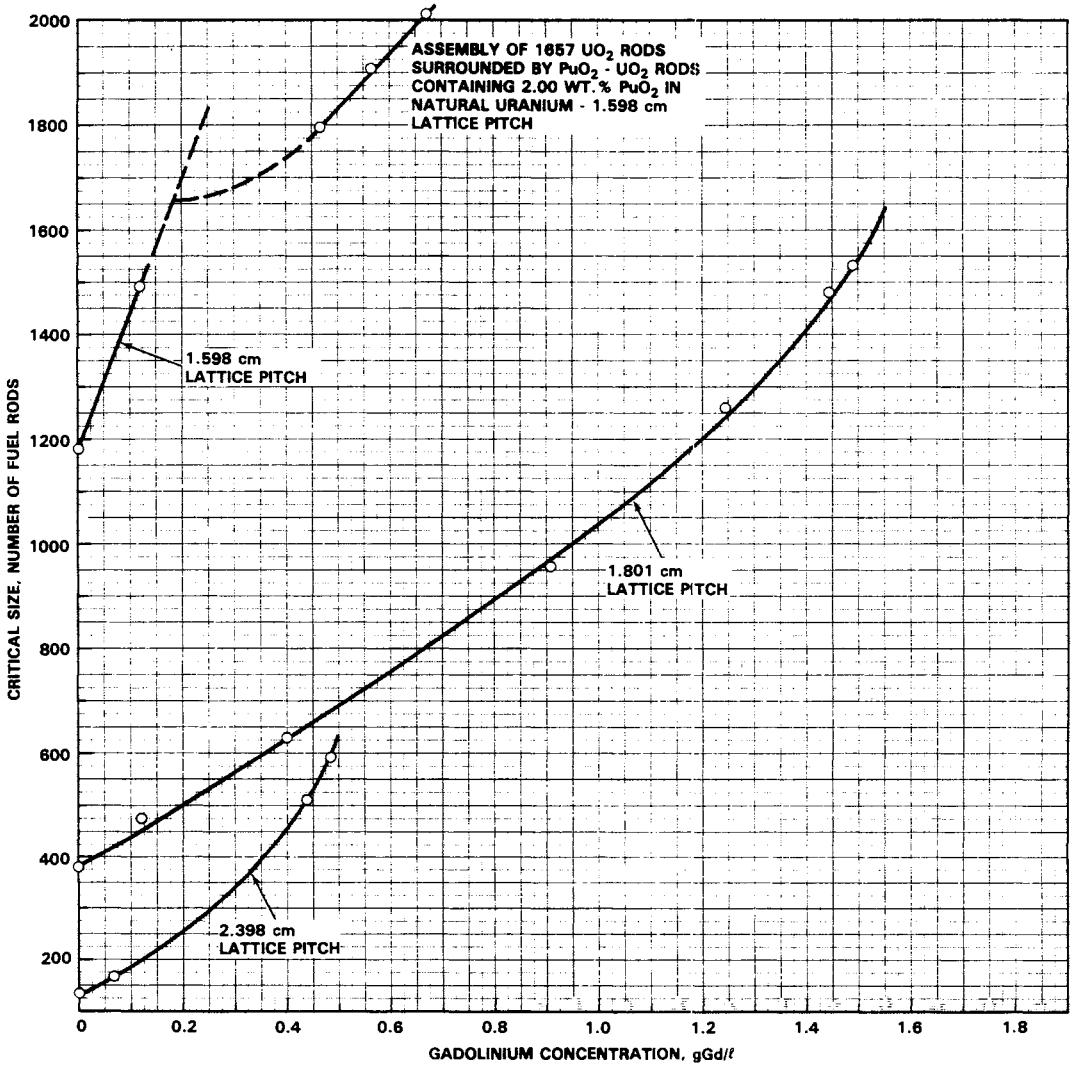

Figure 3.4 Critical Size of Lattices Using 4.31 wt% ^{235}U Enriched UO_2 Fuel as a Function of Gadolinium Concentration

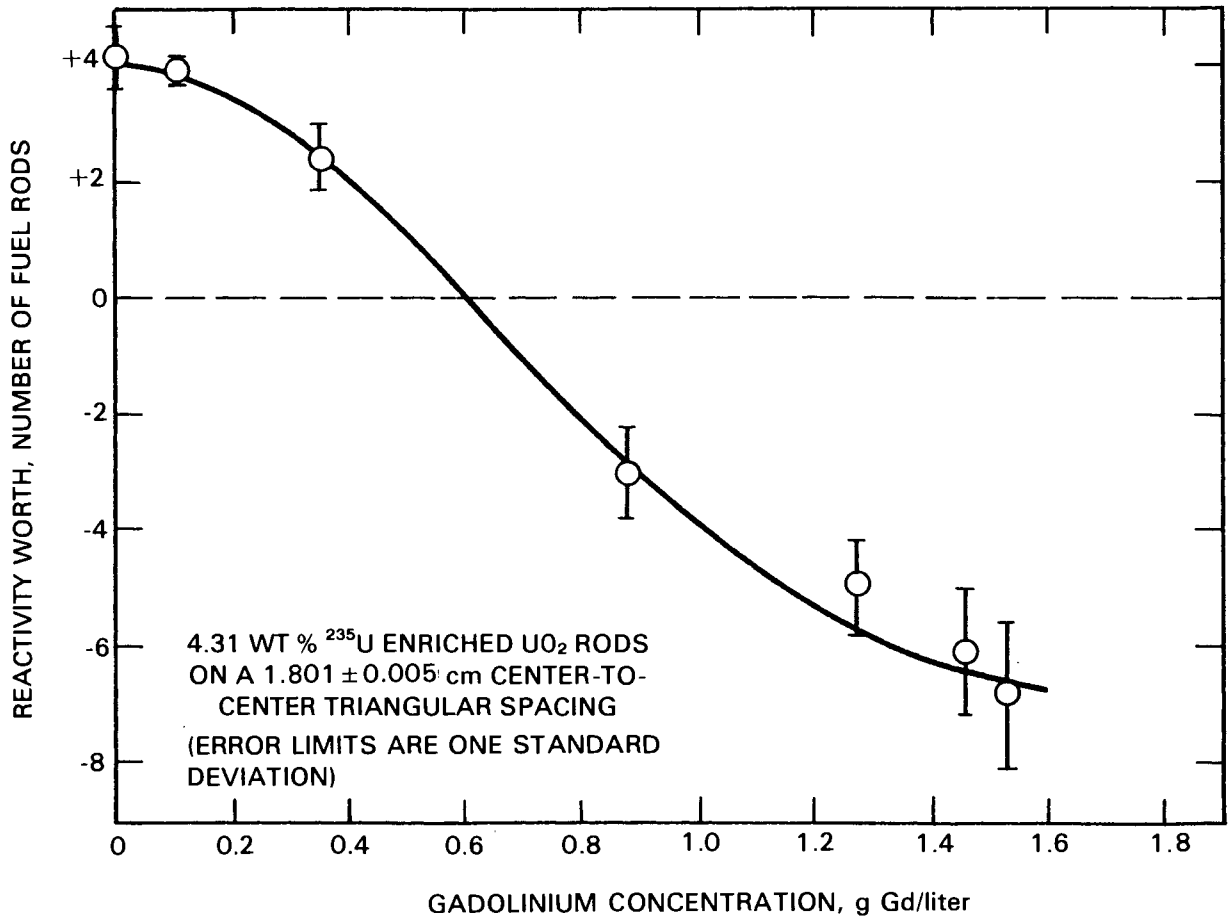

Figure 3.5 Effect of Gadolinium Concentrations on the Reactivity Worth of Aluminum Clad Water Columns Created by Withdrawal of the Safety and Control Rods

the water has a reactivity worth equivalent to four fuel rods in terms of critical size (that is, the assembly with no water column would require an additional four rods to achieve criticality). As the amount of gadolinium dissolved in the water increases at this lattice spacing (1.801 cm center-to-center triangular spacing), the worth of the water column decreases to a negative value approaching a limit of about seven rods. From the data plotted in Figure 3.5 it can be estimated that optimum neutron moderation for the 4.31 wt% ^{235}U enriched UO_2 fuel rods on a 1.801 cm triangular pitch occurs with about 0.6 g Gd/ℓ dissolved in the water. At gadolinium concentrations below this value the experimental assembly is undermoderated.

Of primary concern in performing the experiments summarized in Tables 3.1 and 3.2 was the sensitivity of the measurement data to errors or variations in the two primary parameters - lattice spacing and gadolinium concentration. The center-to-center spacing between fuel rods was measured along two diameters of each lattice plate to obtain an average lattice spacing for each experimental assembly and to verify uniformity of spacing across each assembly. These measurements are presented in Appendix E and resulted in lattice spacings quoted throughout this report with one standard deviation error limit. To assure that these stated spacings were not compromised by voiding due to air entrapped in the water and occluded in the fuel cladding, the final critical approach measurements on each assembly were not made until all voids had been removed and evidence obtained that gas evolution had ceased.

As discussed in Description of Experimental Assemblies, several analytical laboratories and methods were used to obtain values as good as could be reasonably achieved for the amount of gadolinium dissolved in the water of each experimental assembly. A discussion on the analytical methods and comparisons with prepared samples containing 0.25, 0.5 and 1.0 g Gd/ℓ is presented in Appendix B. The analytical results obtained by each method on samples taken from the experimental assemblies are given in Table 2.2. Although a great amount of effort was expended to obtain an adequate analyses of the amount of dissolved gadolinium in each gadolinium-water sample, a greater effort was made to assure the samples were representative of the respective experimental assembly.

Precautions were taken to assure:

- uniform distribution of gadolinium throughout the experimental assembly,
- no gadolinium carry-over contamination between experimental assemblies,
- samples were representative.

The gadolinium concentration in an experimental assembly was adjusted by adding either water or a gadolinium-water solution. To dilute the gadolinium concentration, a predetermined amount of experimental solution was either transferred to one of the mix-storage tanks shown in Figure 2.2 or discharged to ground and fresh water was added to the experimental vessel as the experimental solution was being recirculated. To increase the gadolinium concentration in the experimental solution, a predetermined amount of concentrated solution of gadolinium-water was added to the experimental solution instead of fresh water. This concentrated solution was either pumped from one of the mix-storage tanks (solution used in previous experiments) or obtained by dissolving a predetermined amount of gadolinium nitrate in a 20 to 30 liter quantity of water taken from the experimental vessel.

To assure that a gadolinium concentration adjustment was uniformly distributed throughout the experimental assembly, the experimental solution was recirculated at least twice through the pump if there were no fuel in the system. If the experimental assembly was partial loaded with fuel rods following a concentration change, the experimental solution was transferred to an empty, previously cleaned, mix-storage tank and then recirculated back into the experimental vessel. This routine was required to assure that the solution in the fuel region of the assembly was of the same gadolinium concentration as that in the reflector region - particularly for the closer spaced lattices.

To prevent gadolinium carry-over contamination between experimental assemblies each fuel rod was individually subjected to a hot soapy water wash followed by two cold water wash-rinses and a drying cycle. Initially

the lattice plates (lattice 21) and experimental vessel were subjected to a water wash and rinse only. However, reproducability measurements following the intial series of experiments involving gadolinium dissolved in the water (lattice 21) indicated a gadolinium retention in the experimental system of about 5 parts per million by weight. This carry-over was attributed to gadolinium retained on the lattice plates, support structures, detector thimbles, and the walls of the experimental vessel. Consequently, following a set of measurements involving gadolinium, the lattice plate assemby (typically shown in Figure 2.8) was removed from the experimental vessel, dismantled and subjected to the same wash, rinse and drying cycles as the fuel rods. The interior of the experimental vessel was also hand washed and rinsed following each series of measurements involving gadolinium.

Since it was necessary to completely remove and dismantle the experimental assemblies each time for hand washing to prevent gadolinium carry-over between experiments, the measurements were sequenced following those with lattices 11 and 21 such that all experiments without gadolinium were performed before those involving gadolinium. This procedure, although time consuming, eliminated any concern associated with the possible carry-over of slight amounts of gadolinium between experiments.

To assure samples were representative of the experimental solution, vertical traverse samples were taken on either side of the experimental assemblies with one liter bottles. Approximately one milliliter of 13 M nitric acid was added to each sample to minimize the possibilities of any gadolinium precipitation occurring during shipment to the various laboratories for analyses. The laboratory samples were taken from these one liter samples. An archival sample was retained. Except for the AEEW samples, all laboratory samples were shipped in polyethylene bottles. At the request of the AEEW laboratory, glass bottles were used for the samples analyzed by them.

It should be noted that about half way through the experimental program a white deposit was observed to be forming on top of some of the aluminum supports for the lattice plates. A DC Argon Plasma Emission Spectroscopy analyses of a deposit sample revealed the deposit to be about

60% gadolinium. To prevent this deposit formation, approximately 30 ml of 13 M nitric acid was added to the gadolinium-water solutions. (This is probably the cause of the step increase reported in Appendix C for the aluminum content of the water samples).

3.2 SUBCRITICALITY EXPERIMENTS

To measure the effect of gadolinium concentration on the reactivity of a critical assembly, incremental amounts of dissolved gadolinium nitrate were homogeneously added to the water, or water-gadolinium solution, of each critical assembly, as described in the previous section on Criticality Experiments. At each gadolinium concentration, pulse neutron source measurements were made to obtain k_{eff} values ranging down to about 0.87 as a function of gadolinium concentration.

3.2.1 Measurement Technique

In the pulse neutron source measurements, a burst of neutrons is injected into a system in a fraction of a microscecond and its effect on the neutron population at some point in the system is observed as a function of time following the burst. In actual practice, the measurements are made by repetively injecting bursts of neutrons into the system and accumulating the observed time behavior following each burst. The repetition rate and number of neutron bursts required depends on the statistics of the accumulated data, which, in turn, is dependent on the particular system. A proportional counter or a BF_3 tube is generally used for the detection of the neutrons, and a multi-channel analyzer is used as a series of sequentially gated scalers for the storage of the neutron counts as a function of time following each burst.

Since the pulse neutron source characteristically produces epi-thermal neutrons and since the neutron detector generally used is primarily sensitive to thermal neutrons, the count rate will reach a maximum and then begin to decrease exponentially as the epi-thermal neutrons slow down immediately following a neutron burst and become thermalized. Once an asymptotic distribution of neutrons is reached in the system, the count rate, as a function of time following the

neutron burst, can be described as the sum of two exponential terms:

$$n(t) = A_1 e^{-\alpha_1 t} + A_2 e^{-\alpha_2 t} \qquad (1)$$

One term describes the time behavior of the prompt neutrons and the other describes the time behavior of the delayed neutrons. Since the decay of the delayed neutrons is very slow compared to that of the prompt neutrons, Equation 1 is generally written as:

$$n(t) = A_1 e^{-\alpha_1 t} + N_D \qquad (2)$$

where N_D is a constant equal to the averaged delayed neutron contribution and

$$A_1 e^{-\alpha_1 t}$$

is the prompt neutron contribution decreasing exponentially with time at a rate α_1.

After a period of time, the prompt neutron portion of the total population, that is due to the neutron burst, will approach the background level preceding the burst and only the delayed neutrons will remain. Since the prompt neutrons must all decay away before the delayed neutron contribution can be determined, the prompt neutron decay rate is a limiting factor in determining the pulse repetition rates and counting time intervals to be used. This rate of decay is dependent upon the system on which the measurements are being made. However, the faster the neutron spectrum is, the faster the decay rate will be. Also, the further subcritical a system is, the faster the decay rate will be. Therefore it is possible to obtain the same decay rate for two different degrees of subcriticality. It is this ambiguous feature of the prompt neutron decay which prevents it being used as a direct measurement of reactivity, although it is directly related to the reactivity of the given system. The rate of decay of the prompt neutrons can, however, be used to obtain an effective multiplication constant, k_{eff}, for the system by the following relationship:

$$\alpha_1 = \frac{1 - k_{eff}(1 - \beta_{eff})}{\ell}, \tag{3}$$

where α_1 is the decay rate, β_{eff} the effective delayed neutron fraction, and ℓ the neutron lifetime in the system. However, this requires a knowledge of ℓ and β_{eff} and ℓ is as difficult to calculate as k_{eff}. However, Equation 3 and the definition for reactivity,

$$\rho \equiv \frac{k - 1}{k}, \tag{4}$$

can be combined to obtain an expression for the reactivity of a system in units of β - i.e. dollars.

$$\frac{\rho}{\beta} = - \frac{\alpha_1 - k\beta/\ell}{k\beta/\ell}, \tag{5}$$

If the neutron generation time is assumed to be constant, Equation 5 can be reduced to:

$$\frac{\rho}{\beta} = - \frac{\alpha_1 - \alpha_c}{\alpha_c}, \tag{6}$$

where α_c is the prompt neutron decay rate at delayed critical (k = 1). However, the generation time does vary significantly with the degree of subcriticality. Also, α_c is a parameter not generally available for plant systems.

Three methods have been developed whereby the reactivity of a system can be determined directly from the raw data. The earlist technique was suggested by Sjostrand (Sjostrand 1956) who simply separated the data into a prompt neutron component and a delayed neutron component, as implied by Equations 1 and 2, and then approximated the reactivity by taking the ratio of the area under the prompt neutron curve to the area under the delayed neutron curve,

$$\left(\frac{\rho}{\beta}\right)_{SJ} = - \frac{\text{Prompt Neutron Area}}{\text{Delayed Neutron Area}} \tag{7}$$

Gozani (Gozani, et. al., 1965) improved on this by extrapolating the prompt neutron fundamental mode of decay back to time zero following the burst of neutrons, and taking the reactivity as:

$$\left(\frac{\rho}{\beta}\right)_{GO} = - \frac{\text{Prompt Neutron Fundamental Mode Area}}{\text{Delayed Neutron Area}} \qquad (8)$$

Garelis and Russell (Garelis and Russell 1963) developed a more rigorous theoretical model and showed that the prompt neutron count rates multiplied by a factor involving the reactivity of the system must equal the total area under the pulsed neutron source curve between time zero and 1/R following the burst of neutrons.

$$\int_0^{1/R} A_1 e^{-\alpha_1 t} \; e^{\frac{k\beta}{\ell} t} \, dt = \int_0^{1/R} A_1 e^{-\alpha_1 t} \, dt + \frac{N_D}{R} \qquad (9)$$

Where $A_1 e^{-\alpha_1 t}$ is the prompt neutron count rate at time t following the burst, N_D is the averaged delayed neutron count rate, and R is the pulse repetition rate. All the information needed to solve Equation 9 for $k\beta/\ell$ is available in the data obtained from the pulse neutron source measurement. Consequently, all the data needed to solve Equation 5 for the reactivity of the system is provided by the pulse neutron source data in the Garelis -Russell model. No other information is needed about the system.

Both the Gozani and Garelis - Russell methods were used in analyzing each of the pulse neutron source measurements covered by this report. The two analytical techniques respond differently to spatial harmonic effects (Gozani, et. al., 1965) such that the true value of subcriticality is bracketed by these two methods. The average of the value determined by these two methods should be closer to the true value of the measurement data than either one. However, neither method rigorously eliminates all spatial dependence. Calculational corrections (see Becker and Quisewberry 1966) should be made to the data to account for, or evaluate, modal shape differences not considered by the Gozani or Garelis - Russell analyses.

3.2.2 Description of Pulse Neutron System

The pulse neutron source measurements were made with a Kaman A808 pulsed neutron source capable of being repetitively pulsed up to 50 pulses per second and having a neutron yield of about 10^9 n/sec. The source is encased in a six-inch diameter oil filled cylinder, 36 inches long, and can be moved about. In all of the measurements the source was located outside the lattice plates, as indicated in Figure 2.3, at least 15 cm from the fuel rods and at an elevation such that its tritium target was located approximately at the horizontal mid plane of the assembly fuel region. The pulse neutron source measurement data were accumulated with a boron line proportional detector using a Canberra 8100 channel analyzer operating in the time mode with 1.3 microsecond dead time between the counting channels. The neutron detector (Data channel 3, Figure 2.3) was centered at mid plane, in the reflector region, directly across the fuel region from the pulse neutron source. A diagram of the pulsed neutron source control and data acquisition system is shown in Figure 3.6. A photograph of the system, including the neutron generator, is shown in Figure 3.7.

3.2.3 Pulse Neutron Experiments and Data

Pulse neutron source measurements were performed on each experimental assembly to determine subcritical k_{eff} values as incremental amounts of dissolved gadolinium nitrate were added to the originally critical assembly. The results of these measurements are presented in Table 3.3 for each experimental assembly; however, each set of measurements can be associated with the related criticality measurement data given in Tables 3.1 and 3.2 and elsewhere by means of the experiment reference number. As with the criticality measurement, a fuel loading diagram for each subcritical measurement is given in Appendix F. Computerized plots of the measurement data are presented in Appendix G. These plots are traceable to the results presented in Table 3.3 through the measurement identification number (for example BNFL 11-2, which is the second pulse measurement performed on the experimental assembly having a lattice identification of 11).

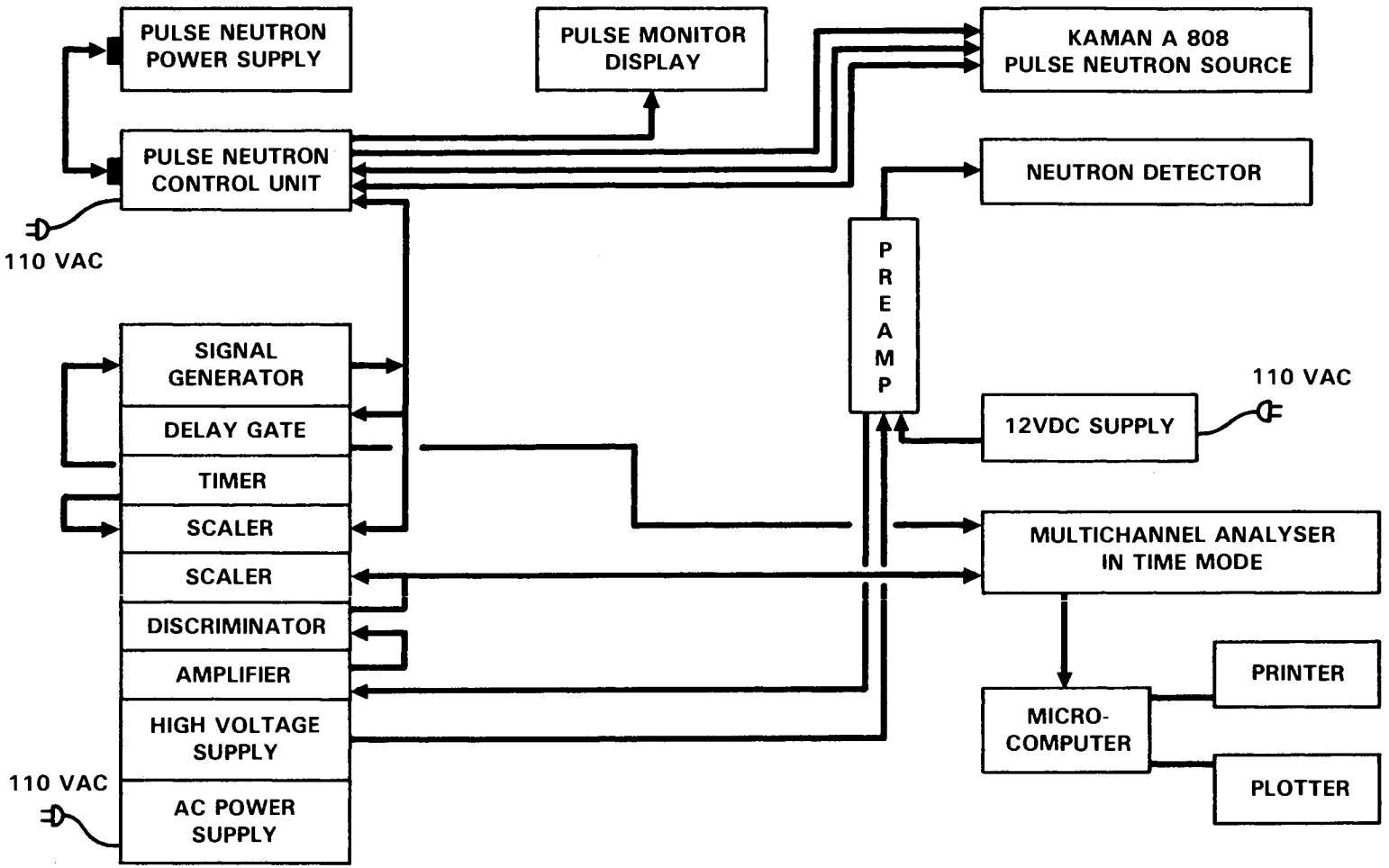

Figure 3.6 Pulse Neutron Source and Data Acquisition System

Figure 3.7 Pulse Neutron Source Control Units and Data Acquisition Equipment

TABLE 3.3 Experimental Results - Effect of Gadolinium Concentration on K_{eff}, Neutron Lifetime and Prompt Neutron Decay Rate

EXPERIMENT REFERENCE NUMBER	MEASUREMENT IDENTIFICATION NUMBER	LATTICE PITCH[a,b] (cm)	WATER-TO-FUEL VOLUME RATIO[b]	FUEL RODS			GADOLINIUM CONCENTRATION (g Gd/liter)[b]	k_{eff}			NEUTRON LIFETIME[f] (10^{-6} sec)	PROMPT NEUTRON DECAY RATE[b] (sec^{-1})
				TYPE	ENRICHMENT (wt%)	NUMBER		GR[c] (β = 0.0065)	GO[d] (β = 0.0065)	AVERAGE[e] (β = 0.0065)		
4.3-000-182	–	2.398 ± 0.005	2.711 ± 0.028	UO_2	4.31% ^{235}U	132	0	–	–	1.0	–	–
4.3-000-182	BNFL 11-2	2.398 ± 0.005	–	UO_2	4.31% ^{235}U	132	0.068 ± 0.007	0.980	0.976	0.978	17.4	1661 ± 25[j]
4.3-000-188	–	2.398 ± 0.005	–	UO_2	4.31% ^{235}U	593	0.482 ± 0.001	–	–	1.0	–	–
4.3-000-188	BNFL 11-3	2.398 ± 0.005	–	UO_2	4.31% ^{235}U	593	0.549 ± 0.008	0.977	0.973	0.975	19.5	1602 ± 6
4.3-000-188	BNFL 11-4	2.398 ± 0.005	–	UO_2	4.31% ^{235}U	593	0.549 ± 0.008	0.976	0.974	0.975	19.6	1606 ± 8
4.3-000-188	BNFL 11-5	2.398 ± 0.005	–	UO_2	4.31% ^{235}U	593	0.639 ± 0.017	0.953	0.934	0.944	21.5	2907 ± 32
4.3-000-188	BNFL 11-6	2.398 ± 0.005	–	UO_2	4.31% ^{235}U	593	0.639 ± 0.017	0.951	0.934	0.943	21.9	2907 ± 23
4.3-000-188	BNFL 11-7	2.398 ± 0.005	–	UO_2	4.31% ^{235}U	593	0.788 ± 0.011	0.899	0.838	0.869	24.1	5696 ± 95
4.3-000-188	BNFL 11-8	2.398 ± 0.005	–	UO_2	4.31% ^{235}U	593	0.788 ± 0.011	0.894	0.825	0.859	26.5	5565 ± 104
4.3-000-188	BNFL 11-9	2.398 ± 0.005	–	UO_2	4.31% ^{235}U	593	0.788 ± 0.011	0.891	0.818	0.855	27.2	5542 ± 87[j]
4.3-000-192	–	1.801 ± 0.005	0.984 ± 0.026	UO_2	4.31% ^{235}U	378	0	–	–	1.0	–	–
4.3-000-192	BNFL 12-1	1.801 ± 0.005	–	UO_2	4.31% ^{235}U	378	0.122 ± 0.001	0.944	0.932	0.938	26.4	2598 ± 21
4.3-000-204	–	1.801 ± 0.005	–	UO_2	4.31% ^{235}U	1260	1.247 ± 0.037	–	–	1.0	–	–
4.3-000-204	BNFL 12-3	1.801 ± 0.005	–	UO_2	4.31% ^{235}U	1260	1.371 ± 0.016	0.991	0.990	0.991	10.2	1552 ± 6
4.3-000-204	BNFL 12-4	1.801 ± 0.005	–	UO_2	4.31% ^{235}U	1260	1.456 ± 0.051	0.981	0.979	0.980	10.5	2485 ± 15
4.3-000-204	BNFL 12-5	1.801 ± 0.005	–	UO_2	4.31% ^{235}U	1260	1.456 ± 0.051	0.979	0.978	0.979	11.3	2495 ± 19
4.3-000-204	BNFL 12-6	1.801 ± 0.005	–	UO_2	4.31% ^{235}U	1260	1.664 ± 0.077	0.963	0.958	0.961	11.0	4170 ± 54
4.3-000-204	BNFL 12-7	1.801 ± 0.005	–	UO_2	4.31% ^{235}U	1260	2.195 ± 0.035	0.922	0.899	0.911	11.6	8183 ± 202
4.3-000-204	BNFL 12-8	1.801 ± 0.005	–	UO_2	4.31% ^{235}U	1260	2.195 ± 0.035	0.919	0.895	0.907	12.1	7682 ± 112
4.3-000-194	–	1.598 ± 0.005	0.509 ± 0.019	UO_2	4.31% ^{235}U	1185	0	–	–	1.0	–	–
4.3-000-194	BNFL 13-6	1.598 ± 0.005	–	UO_2	4.31% ^{235}U	1185	0.130 ± 0.001	0.960	0.949	0.955	17.9	2871 ± 24
4.3-000-194	BNFL 13-5	1.598 ± 0.005	–	UO_2	4.31% ^{235}U	1185	0.130 ± 0.001	0.958	0.945	0.952	17.3	3145 ± 23
4.3-000-194	BNFL 13-4	1.598 ± 0.005	–	UO_2	4.31% ^{235}U	1185	0.456 ± 0.001	0.941	0.905	0.923	15.1	5457 ± 59
4.3-000-194	BNFL 13-3	1.598 ± 0.005	–	UO_2	4.31% ^{235}U	1185	0.638 ± 0.008	0.920	0.884	0.902	14.3	7239 ± 103
4.3-000-194	BNFL 13-2	1.598 ± 0.005	–	UO_2	4.31% ^{235}U	1185	0.750 ± 0.006	0.918	0.879	0.899	13.4	8032 ± 93
4.3-000-194	BNFL 13-1	1.598 ± 0.005	–	UO_2	4.31% ^{235}U	1185	0.750 ± 0.006	0.920	0.886	0.903	13.0	7903 ± 93
2.35-000-160	–	1.895 ± 0.005	1.878 ± 0.038	UO_2	2.35% ^{235}U	431	0	–	–	1.0	–	–
2.35-000-160	BNFL 21-2	1.895 ± 0.005	–	UO_2	2.35% ^{235}U	431	0.120 ± 0.001	0.958	0.958	0.958	16.7	2891 ± 38
2.35-000-160	BNFL 21-4	1.895 ± 0.005	–	UO_2	2.35% ^{235}U	431	0.120 ± 0.001	0.964	0.960	0.962	15.0	2952 ± 53
2.35-000-165	–	1.895 ± 0.005	–	UO_2	2.35% ^{235}U	842	0.120 ± 0.001	–	–	1.0	–	–
2.35-000-165	BNFL 21-11	1.895 ± 0.005	–	UO_2	2.35% ^{235}U	842	0.218 ± 0.001	0.947	0.934	0.940	33.0	1996 ± 17
2.35-000-165	BNFL 21-12	1.895 ± 0.005	–	UO_2	2.35% ^{235}U	842	0.218 ± 0.001	0.945	0.930	0.938	33.1	2088 ± 28
2.35-000-165	BNFL 21-6	1.895 ± 0.005	–	UO_2	2.35% ^{235}U	842	0.262 ± 0.003	0.931	0.906	0.918	33.4	2612 ± 40
2.35-000-165	BNFL 21-7	1.895 ± 0.005	–	UO_2	2.35% ^{235}U	842	0.262 ± 0.003	0.932	0.907	0.920	33.5	2584 ± 37
2.35-000-165	BNFL 21-8	1.895 ± 0.005	–	UO_2	2.35% ^{235}U	842	0.262 ± 0.003	0.932	0.901	0.917	33.4	2672 ± 37
2.35-000-165	BNFL 21-9	1.895 ± 0.005	–	UO_2	2.35% ^{235}U	842	0.317 ± 0.003	0.899	0.850	0.875	37.2	3531 ± 111[j]
2.35-000-165	BNFL 21-10	1.895 ± 0.005	–	UO_2	2.35% ^{235}U	842	0.317 ± 0.003	0.902	0.852	0.877	36.1	3562 ± 79
2.35-000-170	–	1.598 ± 0.005	0.962 ± 0.025	UO_2	2.35% ^{235}U	1029	0	–	–	1.0	–	–
2.35-000-170	BNFL 22-2	1.598 ± 0.005	–	UO_2	2.35% ^{235}U	1029	0.055 ± 0.001	0.987	0.987	0.987	28.6	669 ± 5
2.35-000-170	BNFL 22-1	1.598 ± 0.005	–	UO_2	2.35% ^{235}U	1029	0.078 ± 0.001	0.964	0.962	0.963	31.7	1362 ± 10
2.35-000-170	BNFL 22-4	1.598 ± 0.005	–	UO_2	2.35% ^{235}U	1029	0.257 ± 0.001	0.904	0.876	0.890	35.4	3277 ± 53
4.3-002-196[g]	–	1.598 ± 0.005	0.509 ± 0.019 0.460 ± 0.001[h]	MO_2 & UO_2	2.0% PuO_2: 4.31% ^{235}U	1757	0	–	–	1.0	–	–
4.3-002-196[g]	BNFL 32-5	1.598 ± 0.005	–	MO_2 & UO_2	2.0% PuO_2: 4.31% ^{235}U	1757	0.194 ± 0.001	0.963	0.948	0.955	16.3	3071 ± 16
4.3-002-196[g]	BNFL 32-4	1.598 ± 0.005	–	MO_2 & UO_2	2.0% PuO_2: 4.31% ^{235}U	1757	0.408 ± 0.006	0.942	0.920	0.931	15.6	4808 ± 47
4.3-002-196[g]	BNFL 32-2	1.598 ± 0.005	–	MO_2 & UO_2	2.0% PuO_2: 4.31% ^{235}U	1757	0.626 ± 0.008	0.929	0.898	0.914	14.8	6413 ± 57
4.3-002-196[g]	BNFL 32-3	1.598 ± 0.005	–	MO_2 & UO_2	2.0% PuO_2: 4.31% ^{235}U	1757	0.918 ± 0.015	0.914	0.868	0.891	14.0	8218 ± 106
4.3-002-209[i]	–	1.598 ± 0.005	–	MO_2 & UO_2	2.0% PuO_2: 4.31% ^{235}U	2006	0.673 ± 0.001	–	–	1.0	–	–
4.3-002-209[i]	BNFL 32M-1	1.598 ± 0.005	–	MO_2 & UO_2	2.0% PuO_2: 4.31% ^{235}U	2006	0.760 ± 0.001	0.995	0.996	0.996	8.7	1280 ± 8
4.3-002-209[i]	BNFL 32M-3	1.598 ± 0.005	–	MO_2 & UO_2	2.0% PuO_2: 4.31% ^{235}U	2006	1.371 ± 0.001	0.972	0.969	0.970	8.6	4151 ± 40[j]
4.3-002-209[i]	BNFL 32M-4	1.598 ± 0.005	–	MO_2 & UO_2	2.0% PuO_2: 4.31% ^{235}U	2006	2.362 ± 0.002	0.949	0.925	0.937	8.3	8291 ± 167

[a] CENTER-TO-CENTER SPACING BETWEEN FUEL RODS IN A TRIANGULAR PATTERN
[b] ERROR LIMITS ARE ONE STANDARD DEVIATION ESTIMATES
[c] DETERMINED BY GARELIS-RUSSELL METHOD
[d] DETERMINED BY GOZANI METHOD
[e] SUBCRITICAL VALUES ARE AVERAGE OF GARELIS-RUSSELL AND GOZANI DETERMINED VALUES
[f] DETERMINED FROM AVERAGE VALUE FOR k_{eff}
[g] LATTICE OF PuO_2-UO_2 FUEL RODS AND UO_2 FUEL RODS IN A UNIFORM PATTERN OF ONE PuO_2-UO_2 ROD SURROUNDED BY SIX UO_2 RODS
[h] PuO_2-UO_2 LATTICE CELL WATER-TO-FUEL VOLUME RATIO
[i] LATTICE OF 1657 UO_2 FUEL RODS SURROUNDED BY 349 PuO_2-UO_2 FUEL RODS
[j] FUNDAMENTAL MODE OF DECAY NOT FIRMLY ESTABLISHED

Effective neutron multiplication constants, as determined by both the Garelis - Russell 1963 method and by the Gozani method are given in Table 3.3 for each subcritical assembly. As stated in the section describing the pulse neutron source technique, the true k_{eff} value for each assembly should lie somewhere between these two values due to spatial harmonics in the measurement data. If positive harmonics predominate in the data:

$$|\rho_{GO}| < |\rho| < |\rho_{GR}|$$

If negative harmonics predominate:

$$|\rho_{GO}| > |\rho| > |\rho_{GR}|$$

In general, an average of the k_{eff} values determined by the Garelis-Russell and Gozani methods is probably closer to the true value than either. Consequently an average of the Garelis-Russell and Gozani values is also given in Table 3.3 for each subcritical assembly. As indicated previously however, calculational corrections (see Becker and Quisenberry 1966) should be made to these values to evaluate and account for any "kinetic distortation" that may be present in the measured data.

Although the data shown in Table 3.3 indicate that negative harmonics predominate in each of the subcritical measurements, they become relatively negilible as the critical condition is approached. For k_{eff} values above about 0.95 the average value for k_{eff} is within 1% of the Garelis-Russell and Gozani values. As the assemblies become further subcritical the spread in k_{eff} values increase to about 2% at a k_{eff} level near 0.87.

In addition to subcritical k_{eff} values, values for the neutron lifetime and the rate of decay for prompt neutrons in each of the assemblies can be obtained from the pulse neutron source measurement data. These parameters may be of future use in developing calculational techniques, particularly

those involving neutron kinetics. These parameters, as will be discussed later, are also useful in indicating the consistancy and validity of the subcritical measurements. Consequently, neutron lifetimes and prompt neutron decay rates, obtained from the measurement data, are given in Table 3.3 for each subcritical assembly. These values, along with the k_{eff} values, are plotted in Figures 3.8, 3.9, 3.10, 3.11, 3.12, 3.13 and 3.14 as a function of the gadolinium concentration for each set of experimental assemblies (lattices) involving a series of measurements.

The neutron lifetime reported in Table 3.3 and Figures 3.8, 3.9, 3.10, 3.11, 3.12, 3.13 and 3.14 for each subcritical assembly is the average of that determined from the Garelis-Russell and the Gozani analyses of the measurement data. The prompt neutron decay rate reported in Table 3.3 and Figures 3.8, 3.9, 3.10, 3.11, 3.12, 3.13 and 3.14 for each subcritical assembly is the time rate of decay for the fundamental mode observed in the measurement data by least-squares fitting the data to a constant plus a single exponential term.

As indicated previously, and as can be seen in the computer plots of the measurement data presented in Appendix G, harmonics exist in the measurement data. To determine if a single mode of neutron decay eventually existed in each set of measurement data, a technique developed by Pfeiffer, Brown and Marshall (Pfeiffer, 1974) in a Fort St. Vrain startup test was used. The technique makes use of the standard deviation obtained on the fitted value for the prompt neutron decay rate, α, and the random fluctuation of the fitted value for α within the standard deviation as measurement data immediately following the neutron burst is successively ignored in the fitting process. If it can be demonstrated that a decay rate, and the associated standard deviation, fluctuates within the standard deviation as data are deleted, it can be concluded that a single time rate of decay predominates and is the fundamental mode of neutron decay for that experimental assembly. Examples of the variation observed in the prompt neutron decay rate as a function of time are shown in Figure 3.15 as typical. Except as noted in Table 3.3, a single mode of neutron decay eventually predominated in each of the subcritical measurements.

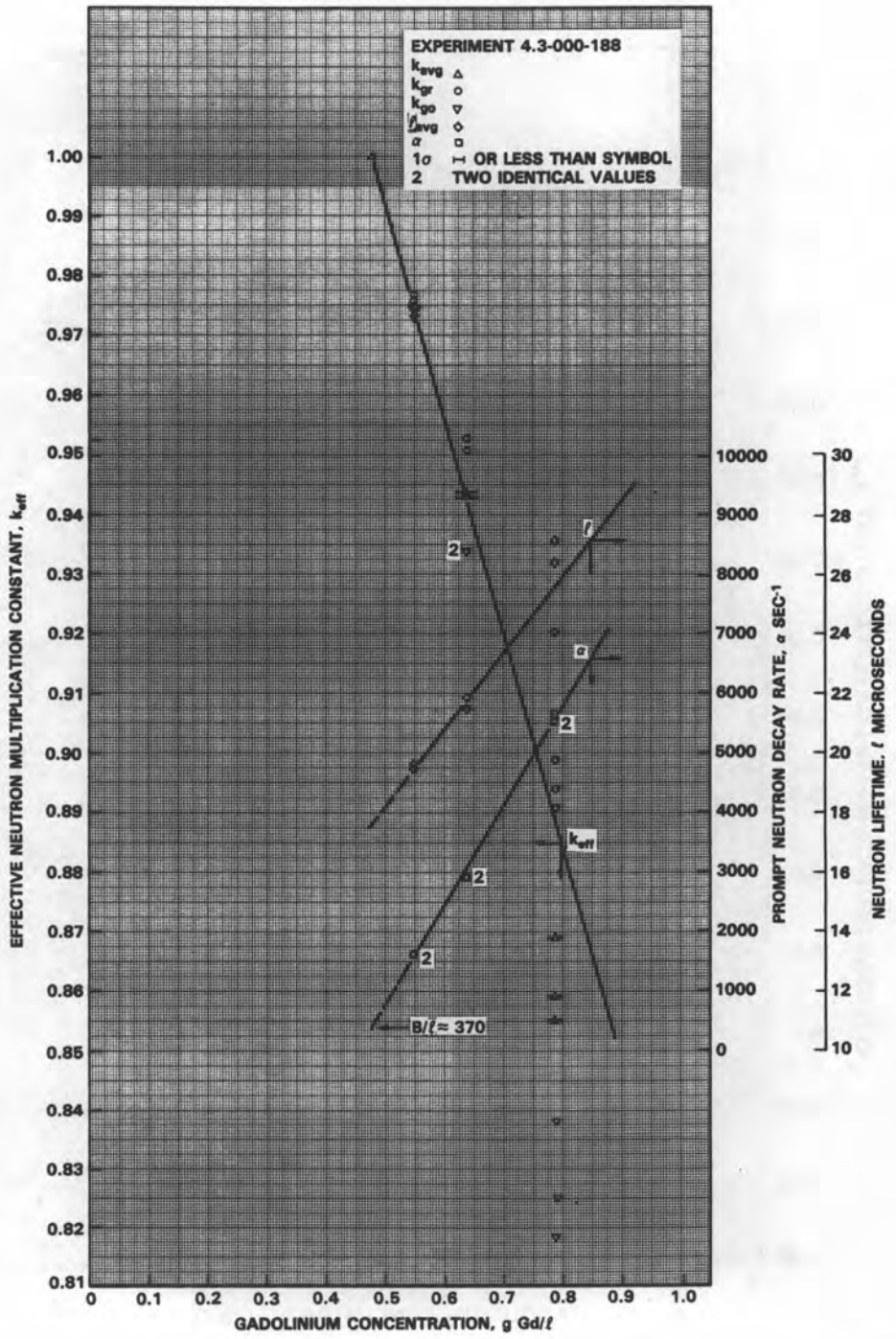

Figure 3.8 Measured Variations in k_{eff}, ℓ and α with Concentration of Dissolved Gadolinium in Fuel-Water Lattices of 4.31 wt% ^{235}U Enriched UO_2 Fuel Rods in a Triangular Pattern on 2.398 cm Center-to-Center Spacing

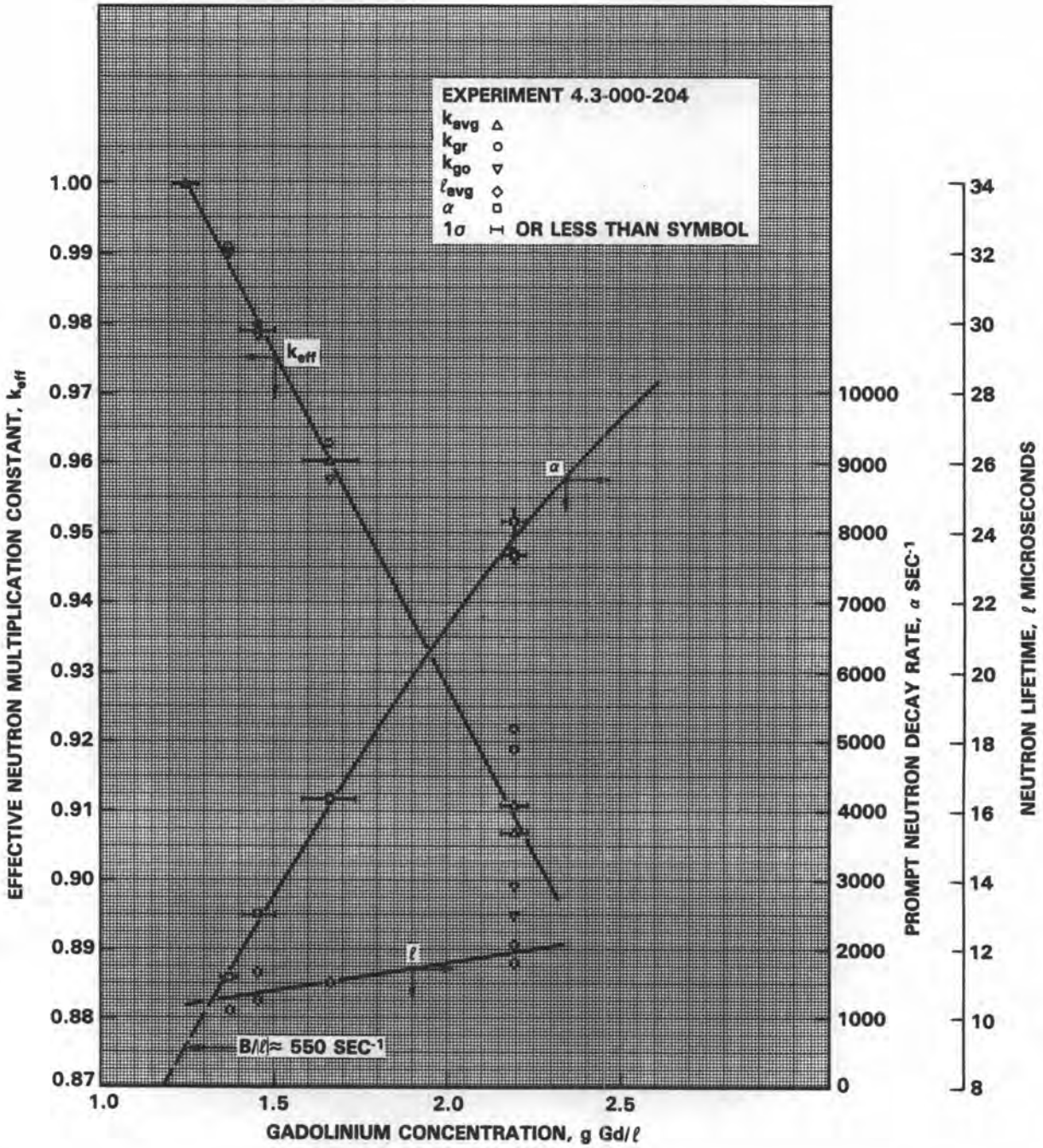

Figure 3.9 Measured Variations in k_{eff}, ℓ and α with Concentration of Dissolved Gadolinium in Fuel-Water Lattices of 4.31 wt% ^{235}U Enriched UO_2 Fuel Rods in a Triangular Pattern on 1.801 cm Center-to-Center Spacing

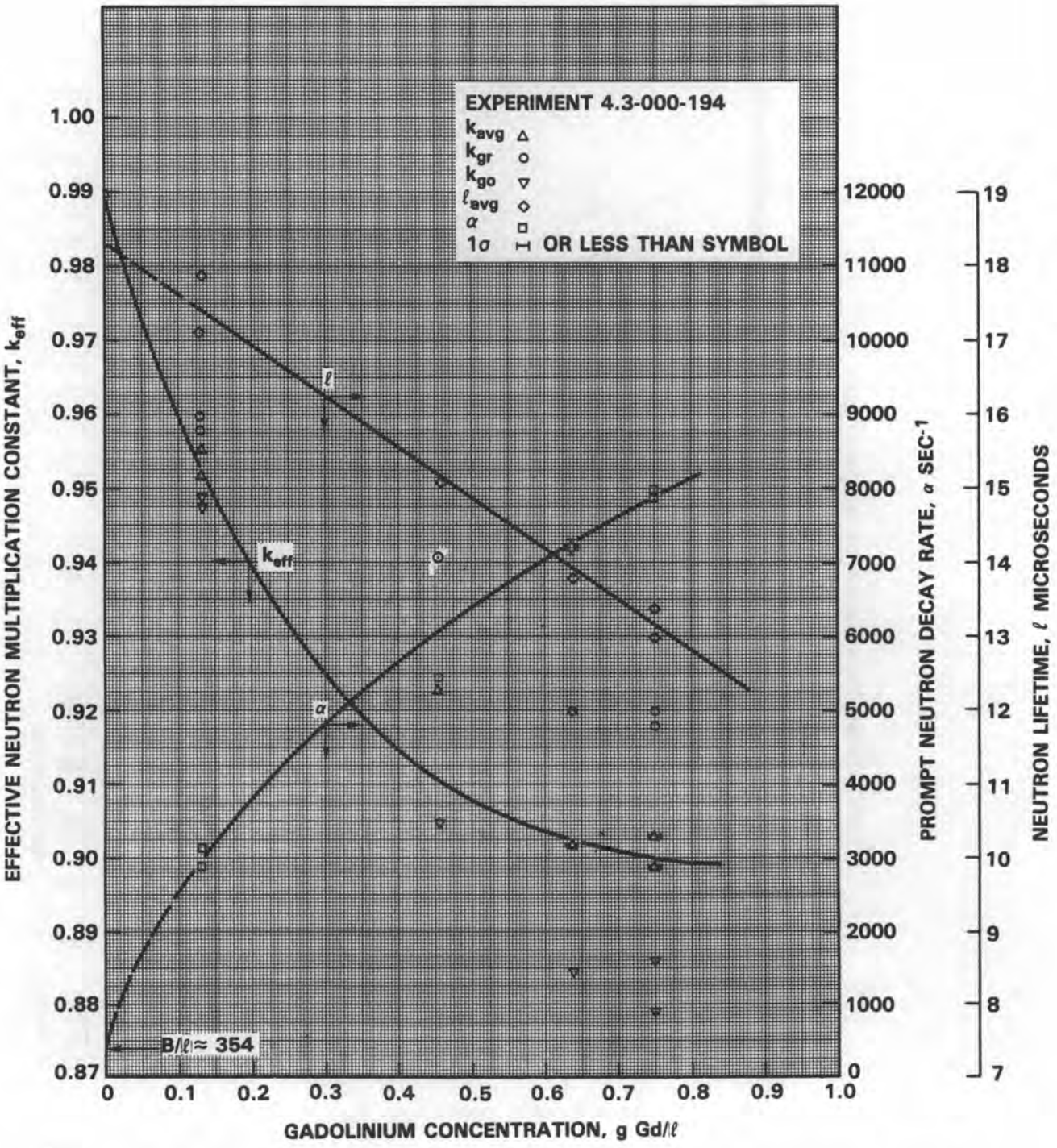

Figure 3.10 Measured Variations in k_{eff}, ℓ and α with Concentration of Dissolved Gadolinium in Fuel-Water Lattices of 4.31 wt% ^{235}U Enriched UO_2 Fuel Rods in a Triangular Pattern on 1.598 cm Center-to-Center Spacing

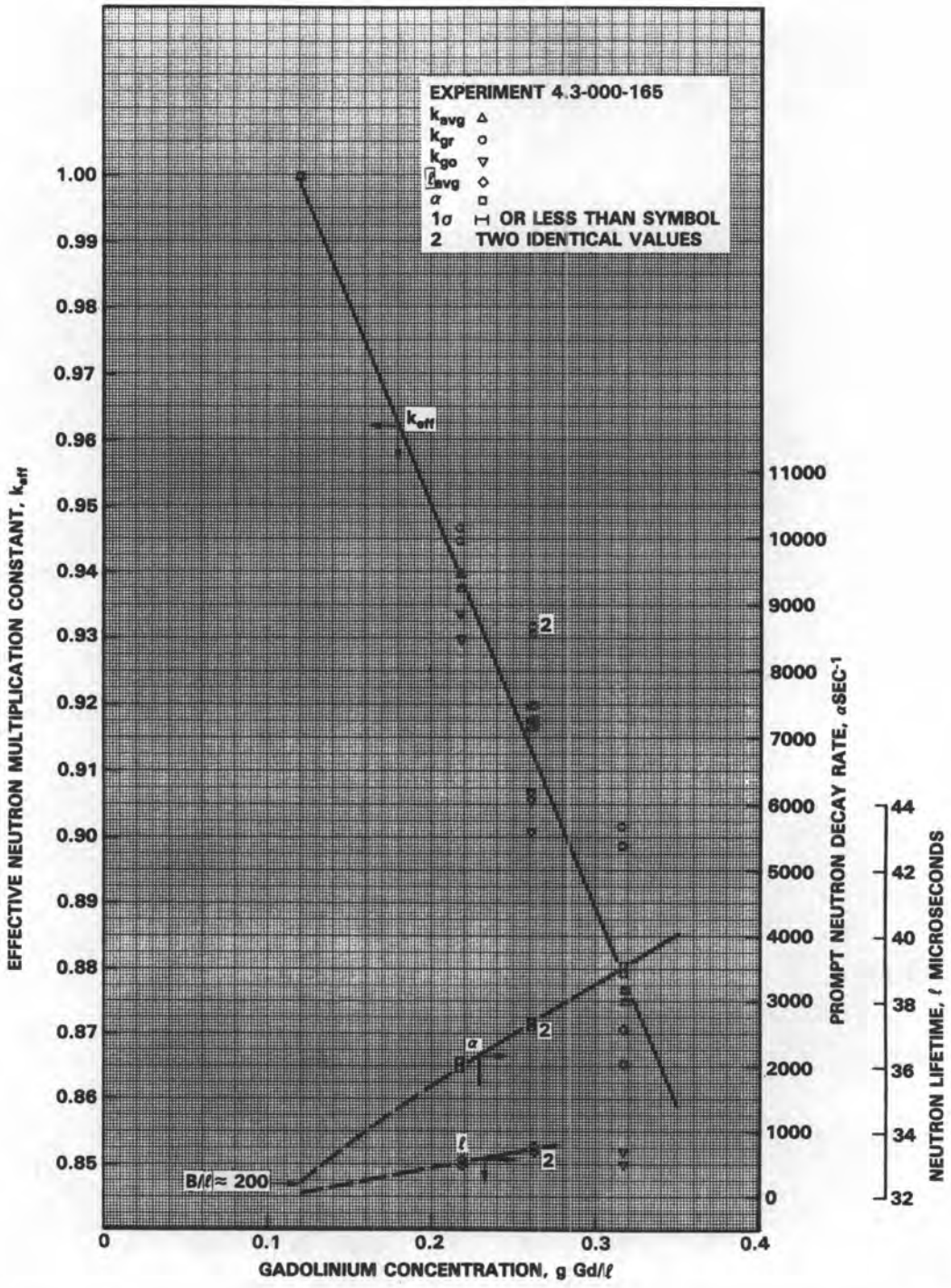

Figure 3.11 Measured Variations in k_{eff}, ℓ and α with Concentration of Dissolved Gadolinium in Fuel-Water Lattices of 2.35 wt% ^{235}U Enriched UO_2 Fuel Rods in a Triangular Pattern on a 1.895 cm Center-to-Center Spacing

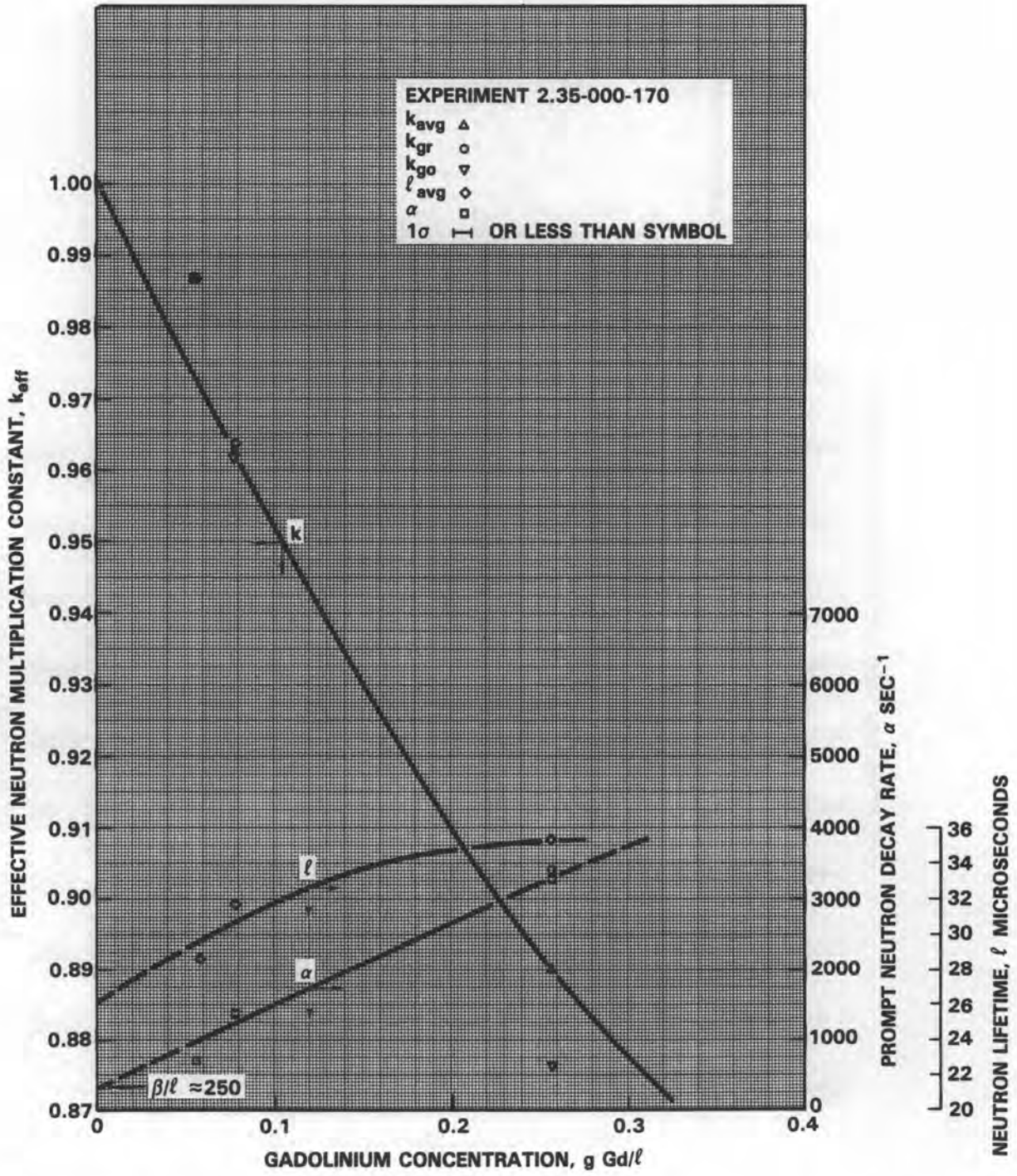

Figure 3.12 Measured Variations in k_{eff}, ℓ and α with Concentration of Dissolved Gadolinium in Fuel-Water Lattices of 2.35 wt% ^{235}U Enriched UO_2 Fuel Rods in a Triangular Pattern on a 1.598 cm Center-to-Center Spacing

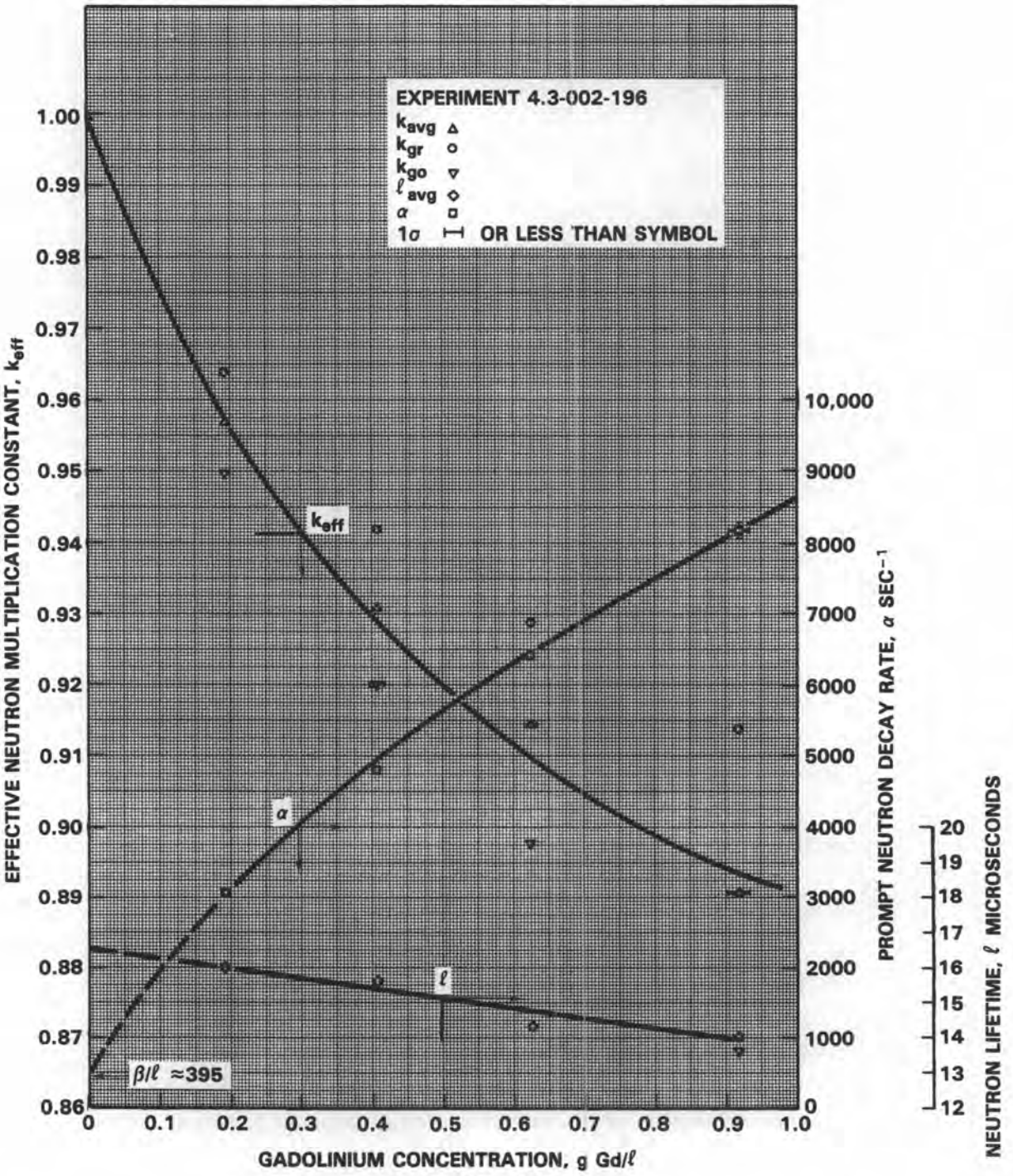

Figure 3.13 Measured Variations in k_{eff}, ℓ and α with Concentration of Dissolved Gadolinium in Fuel-Water Lattices of 4.31 wt% ^{235}U Enriched UO_2 Fuel Rods mixed with PuO_2-UO_2 Fuel Rods in a Triangular Pattern on a 1.598 cm Center-to-Center Spacing

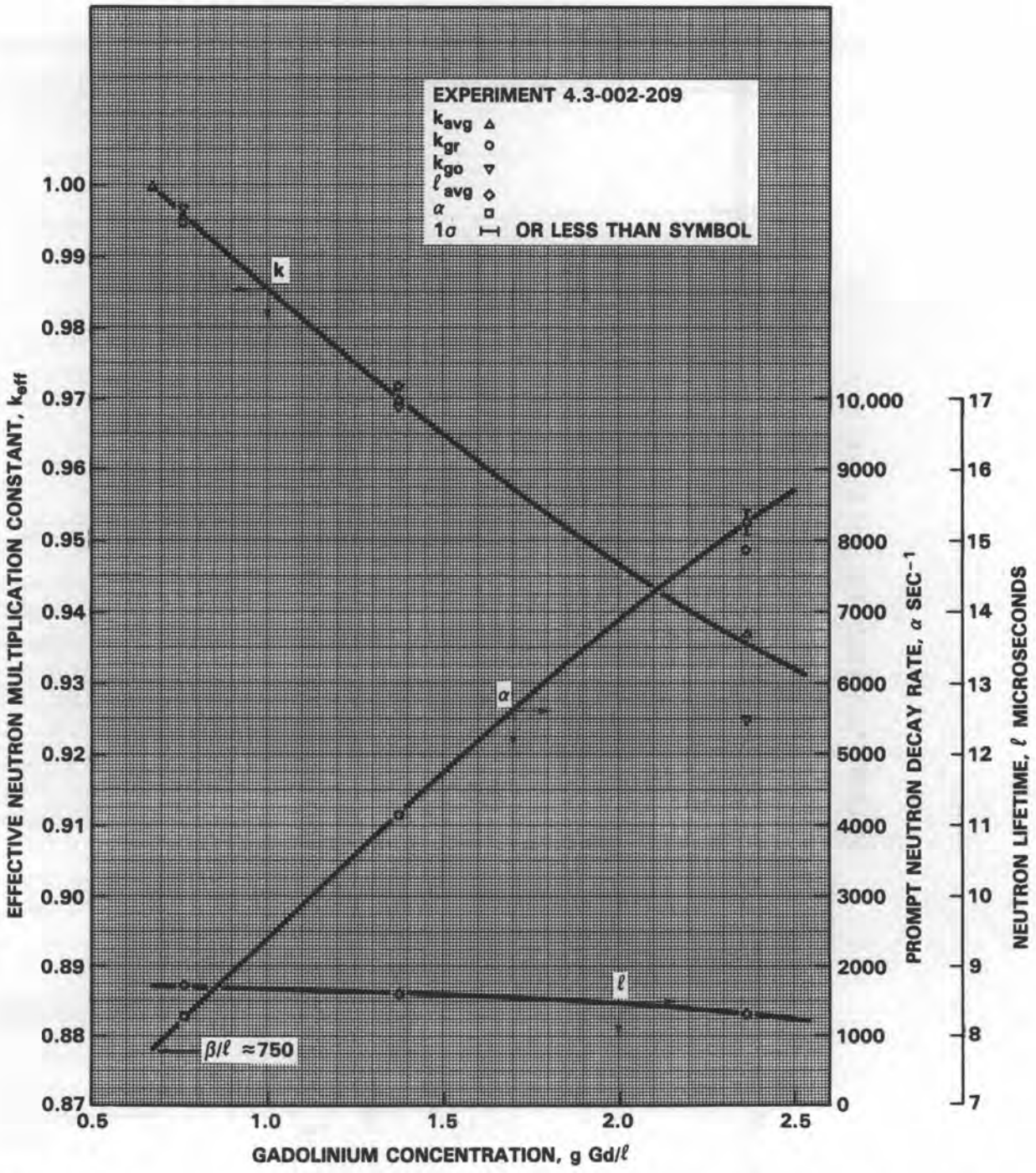

Figure 3.14 Measured Variations in k_{eff}, ℓ and α with Concentration of Dissolved Gadolinium in Fuel-Water Lattices of 4.31 wt% ^{235}U Enriched UO_2 Fuel Rods mixed with PuO_2-UO_2 Fuel Rods in a Triangular Pattern on a 1.598 cm Center-to-Center Spacing

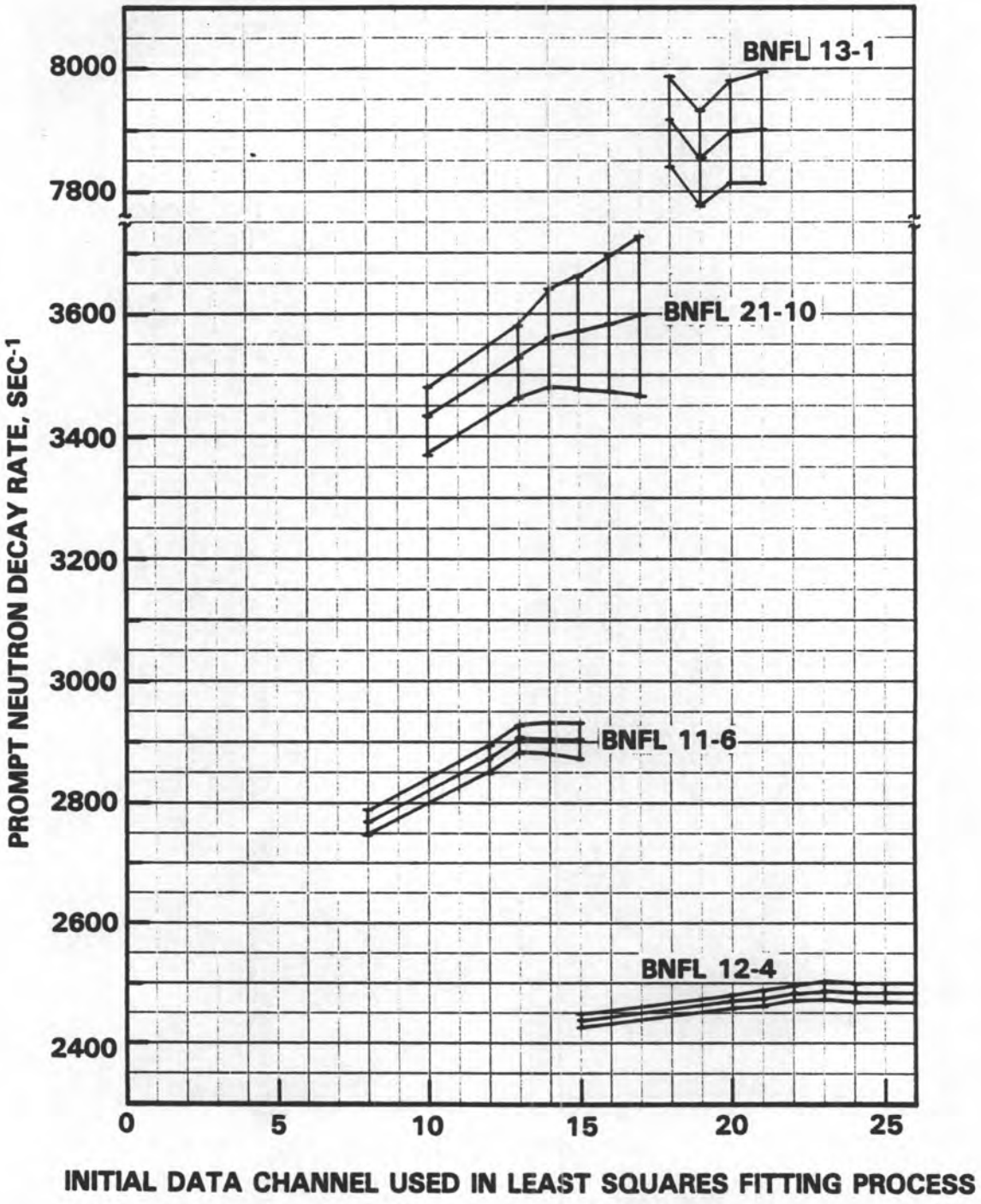

Figure 3.15 Illustration of Technique Used to Determine that a Fundamental Mode of Prompt Neutron Decay was Present in the Observed Measurement Data

Although the accuracy of the subcritical measurements cannot currently be verified by an independent method, the data reported in Table 3.3 indicate that multiple measurements reproduce k_{eff} to within about 0.005 or less. Also, except for measurement BNFL 11-2, the measurement data presented in Appendix G appear to be well behaved. Some perturbations appear in the measurement data for BNFL 11-2 (see computer plot in Appendix G). However, least-squares fitting and analyses of the data were performed to minimize the effect of those perturbations on the results given in Table 3.3.

An indication of the validity of the results can be obtained also by observing:

- The variation in k_{eff} as the critical condition is approached,
- the consistancy between the neutron lifetimes and the prompt neutron decay rates determined for a set of measurements.

As the delayed critical condition of an assembly is approached, the decay rate of the prompt neutrons in that assembly approaches β/ℓ, where β is the effective delayed neutron fraction and ℓ is the neutron lifetime (see section on Measurement Technique). Since β is essentially constant the neutron lifetimes in an assembly should approach a value at decayed critical that is consistant with the prompt neutron decay rate at delayed critical. Very near the delayed critical conditions, variations in both the neutron lifetimes and the decay rates can be approximated as a linear function of the gadolinium concentration. However, as neutron absorption or leakage begins to increase, the variation in both parameters, as well as k_{eff}, will begin to show some curvature and approach constant values.

By reviewing the data as presented in Figures 3.8 through 3.14 conclusions can be made on the validity of individual data points within a series of measurements. For example, although a linear extrapolation of the subcritical data presented in Figure 3.8 predicts the delayed critical conditions, the value for k_{eff} at the highest gadolinium concentrations of 0.788 g Gd/ℓ appears low and indicates some curvature should exist in the prompt neutron decay rate and/or the neutron lifetime data. For consistancy the k_{eff} value at the 0.788 g Gd/ℓ concentration should be at least 0.889

and the decay rate-neutron lifetime correspondingly smaller. However, considering the complex neutron spectral shifts that occur in a system as gadolinium is varied, calculations beyond the scope of work covered herein may demonstrate the validity of the measurement data at 0.788 g Gd/ℓ. Until this is demonstrated such data should be considered suspect. The data presented in Figure 3.9 for the 4.3-000-204 series of measurements are a more typical example of a complete set of consistant data having a high degree of reliability.

3.3 REACTION RATE MEASUREMENTS

Although reaction rate measurements were not a primary objective of the program, measurements were made in selected experimental assemblies, as indicated in Table 2.1, to obtain data for improving neutronic calculations. These measurements were performed in the critical assemblies of the 4.31 wt% ^{235}U enriched UO_2 fuel rods. Absolute ^{235}U fission rates, using solid state track recorders (SSTR), were measured in this fuel at all three degrees of neutron moderation (lattices 11, 12 and 13) with no gadolinium dissolved in the water, and at near optimum neutron moderation (lattice 11) with gadolinium in the water. Relative Conversion Ratio (RCR) and Fast Fission Ratio (FFR) measurements, using 4.31 wt% ^{235}U enriched UO_2 and depleted U foils, were made in the near optimum neutron moderated lattice 11 and in the undermoderated lattice 13 with and without gadolinium dissolved in the water. RCR and FFR measurements were also made in the slightly undermoderated lattice 12 with no gadolinium in the water.

3.3.1 Measurement Techniques

The use of solid state track recorder type devices to measure absolute fission rates is extensivley discussed in readily available publications (Gold 1968) and (Roberts 1968). Briefly, however, SSTR measurements are carried out using thin deposits of material in contact with a material such as mica. Fissions in the deposit create damage tracks in the mica that can be optically counted to obtain the number of fissions per atom of deposit.

Measurements to determine the Fast Fission Ratio ($^{238}U/^{235}U$) involve the simultaneous irradition of two uranium samples of different enrichments as discussed in detail in Appendix H. Measurements to determine the ^{238}U capture to ^{235}U fission ratio relative to that in a known thermal flux are also described in detail in Appendix H.

3.3.2 Reaction Rate Measurements and Data

The experimental assemblies in which reaction rate measurements were made are briefly described in Table 3.4. A fuel loading diagram (identified through the Experiment Reference Number) for each of these assemblies is presented in Appendix F. The measurement results obtained for each of the assemblies are summarized in Table 3.4 also. The results shown in Table 3.4 for the fission rates are based on the irradiation of a single SSTR in each assembly whereas each RCR and FFR result is the mean value obtained from three AEEW foil packs positioned in neutronically identical locations in the assemblies. The foil pack locations and the SSTR location in each assembly are identified in the loading diagrams of Appendix F.

For the ^{235}U fission rate measurements, a thin layer of ^{235}U, with an active diameter of 0.635 cm (0.25 in.), was electroplated onto a 1.11 cm (0.437 in.) diameter, 0.013 cm (0.005 in.) thick nickle plate. This was placed in close contact with a thin ($\sim$ 0.01 cm) disk of mica, and encapsulated in an aluminum holder by the Hanford Engineering Development Laboratory (HEDL) of Westinghouse Hanford Company (Ruddy 1983). A typical SSTR geometrical configuration is shown in Figure 3.16. The SSTR in each fission rate measurement was positioned between the first and second pellets of a three pellet column as indicated in Figure 3.17.

In each absolute fission rate measurement the SSTR was irradiated for a predetermined time at an integrated power level, P, given by

$$P = P_o \left[\tau \left(1 - e^{-\Delta t/\tau}\right) + t\right],$$

where t is the irradiation time at a constant power level, P_o, and τ is the period at which this power level was approached. Following each irradiation, the SSTR was given a 45 minute etch in 49% HF at 22° C and the fission fragment tracks counted by HEDL to obtain ^{235}U fission rates (Ruddy 1983).

TABLE 3.4 Experimental Results - Summary Table of Reaction Rates

EXPERIMENT REFERENCE NUMBER	LATTICE IDENTIFICATION NUMBER	LATTICE PITCH[b,c] (cm)	WATER-TO-FUEL VOLUME RATIO	FUEL RODS ENRICHMENT TYPE	FUEL RODS ENRICHMENT (wt%)[c]	FUEL RODS NUMBER	GADOLINIUM CONCENTRATION (g Gd/Liter)	ABSOLUTE FISSION RATE[c,d] (f/AT. ^{235}U SEC)	FAST FISSION RATE[c,e] (^{238}U/^{235}U)	RELATIVE CONVERSION RATIO[c,f] (^{238}Uc/^{235}Uf)
4.3-000-182D	11	2.398 ± 0.005	2.711 ± 0.028	UO_2	4.31% ^{235}U	132	0	1.59×10^{-13} ± 2.14%	-	-
4.3-000-182E	11	2.398 ± 0.005	2.711 ± 0.028	UO_2	4.31% ^{235}U	132	0	-	0.00196 ± 2.3%	2.70 ± 0.5%
4.3-000-188C	11	2.398 ± 0.005	-	UO_2	4.31% ^{235}U	615	0.482 ± 0.001	4.40×10^{-14} ± 2.21%	-	-
4.3-000-188D	11	2.398 ± 0.005	-	UO_2	4.31% ^{235}U	620	0.482 ± 0.001	-	0.00225 ± 2.4%	3.18 ± 0.3%
4.3-000-192D	12	1.801 ± 0.005	0.984 ± 0.026	UO_2	4.31% ^{235}U	374	0	4.83×10^{-14} ± 2.49%	-	-
4.3-000-192E	12	1.801 ± 0.005	0.984 ± 0.026	UO_2	4.31% ^{235}U	373	0	-	0.00396 ± 2.4%	5.08 ± 0.4%
4.3-000-194D	13	1.598 ± 0.005	0.509 ± 0.019	UO_2	4.31% ^{235}U	1151	0	4.71×10^{-15} ± 2.05%	-	-
4.3-000-194E	13	1.598 ± 0.005	0.509 ± 0.019	UO_2	4.31% ^{235}U	1154	0	-	0.00571 ± 2.3%	7.64%0.3%
4.3-000-198C	13	1.598 ± 0.005	-	UO_2	4.31% ^{235}U	1475	0.121 ± 0.002	-	0.00568 ± 3.3%	7.50 ± 0.3%

[a] DETAILS OF THE DATA REDUCTION AND ANALYSES OF THE REACTION RATE MEASUREMENTS ARE COVERED IN APPENDIX H AND RUDDY, 1983 REFERENCE

[b] CENTER-TO-CENTER SPACING BETWEEN FUEL RODS IN A TRIANGULAR PATTERN

[c] ERROR LIMITS ARE ONE STANDARD DEVIATIONS

[d] MEASUREMENTS WITH HEDL SOLID STATE TRACK RECORDERS

[e] FAST FISSION RATIO - ^{238}U FISSION RELATIVE TO ^{235}U FISSION MEASUREMENTS WITH AEEW FOIL PACKS

[f] RELATIVE CONVERSION RATIO - ^{238}U CAPTURE RELATIVE TO ^{235}U FISSION MEASUREMENTS WITH AEEW FOIL PACKS NORMALIZED TO SIMULTAINEOUS MEASUREMENTS IN THE NESTOR REACTOR

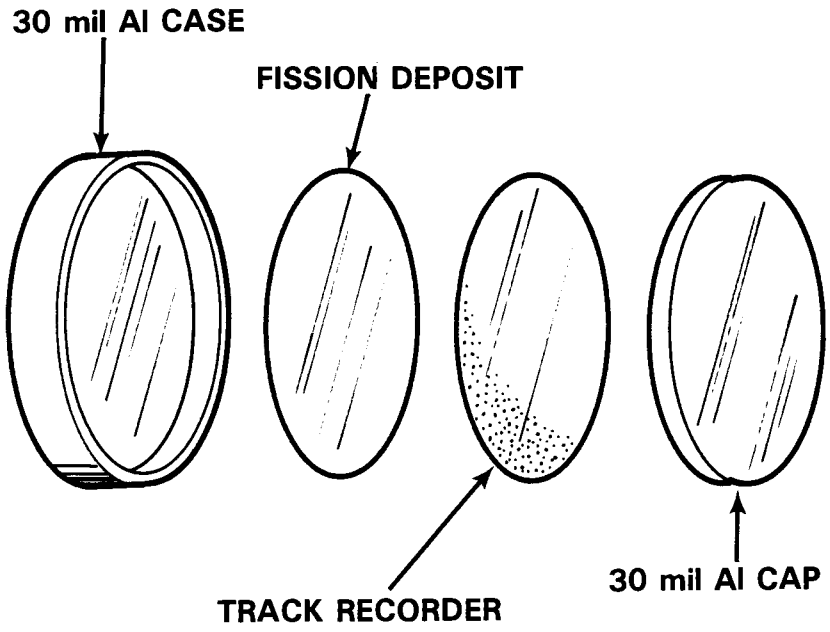

Figure 3.16 Typical SSTR Geometrical Configuration

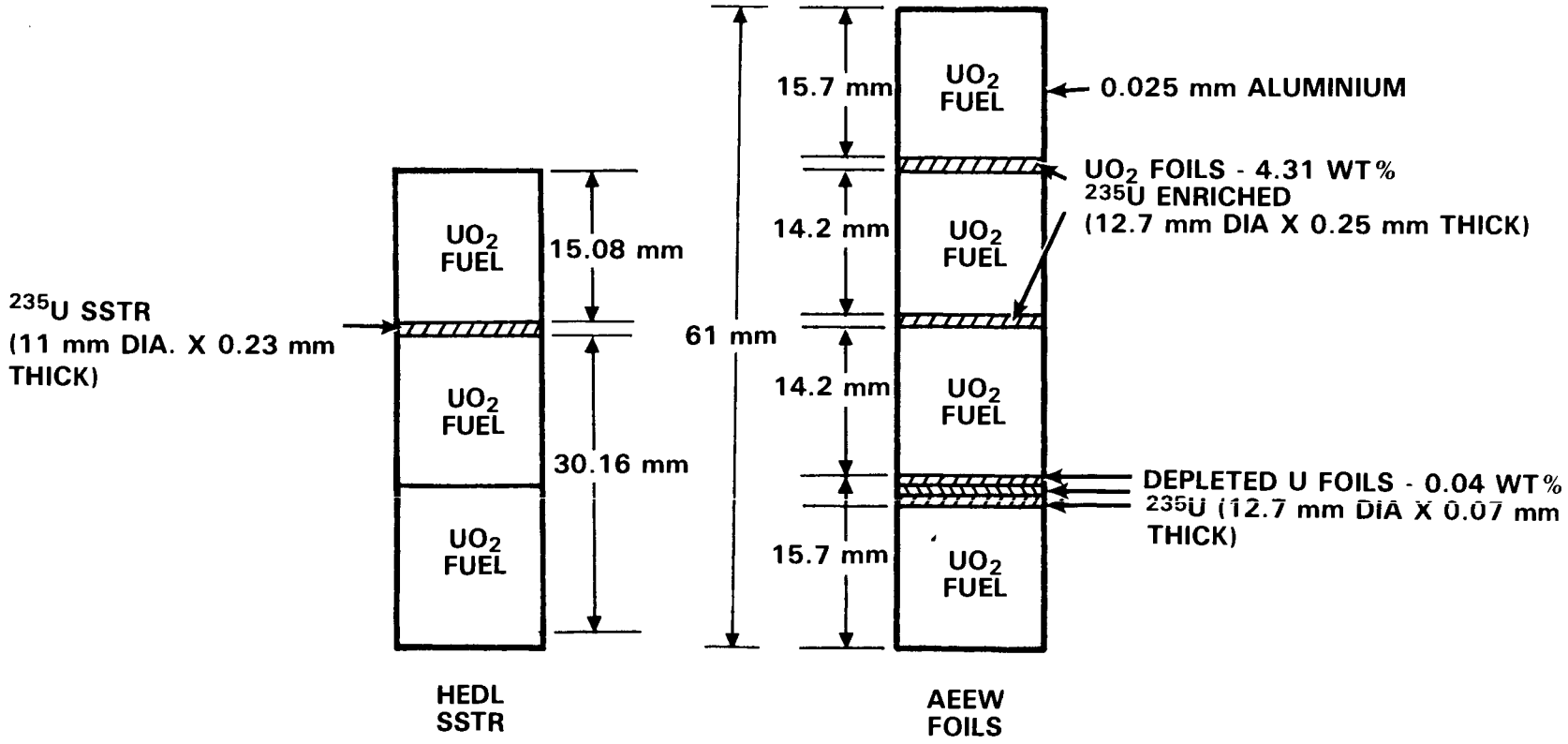

Figure 3.17 Description and Arrangement of Reaction Rate Packets

Preparation and assembly of the AEEW foil packs is covered in detail in Appendix H. A sketch of an assembled foil pack is shown in Figure 3.17. The Fast Fission Ratios reported in Table 3.4 were obtained by simultaneously irradiating 4.31 wt% ^{235}U enriched UO_2 foils and depleted U metal foils in the indicated experimental assemblies. To determine the Relative Conversion Ratios shown in Table 3.4, simultaneous irradiations were performed in the AEEW Nestor Reactor to obtain ^{238}U capture to ^{235}U fission ratios in a known thermal neutron flux. These irradiations were for exactly two hours at a constant thermal neutron flux of about 2×10^{8} n $cm^{-2}s^{-1}$ ($\sim 5 \times 10^{-14}$f at $.^{-1}s^{-1}$).

Due to the presence of the thermal neutron absorber, gadolinium, and the water-to-fuel ratios covered by the experiments, the neutron spectra varied considerably between experiments. To obtain thermal neutron fluxes of about 2×10^{8} n $cm^{-2}s^{-1}$ in each assembly, the power levels were ajusted based upon the absolute fission rates determined from the SSTR measurements. Photo reductions of the neutron flux recorder chart are presented in Appendix I.

Synchronization of the irradiations was achieved by maintaining a telephone connection between the control rooms of the Critical Mass Laboratory and the Nestor Reactor during the initial phase of each irradiation. To approximate the effects caused by the experimental assemblies approaching the power level on periods of about 60 seconds, the neutron shutter to the thermal column of the Nestor Reactor was opened each time when the experimental assembly reached 37% of full power. Therefore the total exposure time was slightly longer than two hours for each of the irradiations.

Following each irradiation the foil packs were removed from the experimental assembly, packaged and shipped to the AEEW for analyses as covered in Appendix H. Each set of foils were removed from the reaction rate fuel rods and packaged in a 6M shipping container approved by both the United States and the United Kingdom (USA/0002/X8) for this purpose. Shipment by road and air was coordinated to meet counting statistic requirements that each set of foils reach the AEEW within 30 hours following irradiation.

Three of the 4.31 wt% ^{235}U enriched UO_2 fuel rods were modified such that fuel pellets could be replaced with either an AEEW foil packet or a SSTR packet. Either a single SSTR was loaded into a reaction rate rod for irradiation or an AEEW foil pack was loaded into each of the three reaction rate rods for irradiation. A photograph of a modified fuel rod, disassembled and assembled, is shown in Figure 3.18. THe reaction rate packs were loaded in approximately the center of these fuel rods such that the bottom of each pack was at the same elevation when placed in an experimental assembly (see Figure 2.7, Experimental Assembly Elevations).

Since the reaction rate measurements are very sensitive to neutron moderation, special precautions were taken to assure that the neutron flux was uniformly characteristic of the region containing the reaction rate packet. As indicated previously, the reference elevation for the reaction rate packs was identical as defined in Figure 2.7 for all the experimental assemblies. The radial location of the reaction rate rods is given in the loading diagrams of Appendix F for each experimental assembly of interest. These locations are very accurately defined with respect to the center of each of the three lattice types in Figures 3.19, 3.20 and 3.21. In addition, the distance between each reaction rate fuel rod and the surrounding adjacent six fuel rods is given in Figures 3.19, 3.20 and 3.21 for the respective lattices. The distances reported in Figures 3.19, 3.20 and 3.21 are the result of multiple micrometer measurements over the length of the reaction rate packs. Machined Type 6061 aluminum spacers, shown in Figure 3.18, positioned above and below the reaction rate packs were used to maintain these uniform spacings over an elevation distance of about 24 cm as indicated in Figure 2.7.

To verify that the neutron flux was uniformly characteristic of the region containing the reaction rate packet, multiple FFR - RCR measurements were simultaneously performed in each of the five experimental assemblies. In each assembly AEEW foil packs were located in three neutronically identical positions as indicated in the loading diagrams of Appendix F and Figures 3.19, 3.20 and 3.21. As covered in Appendix H, the variations

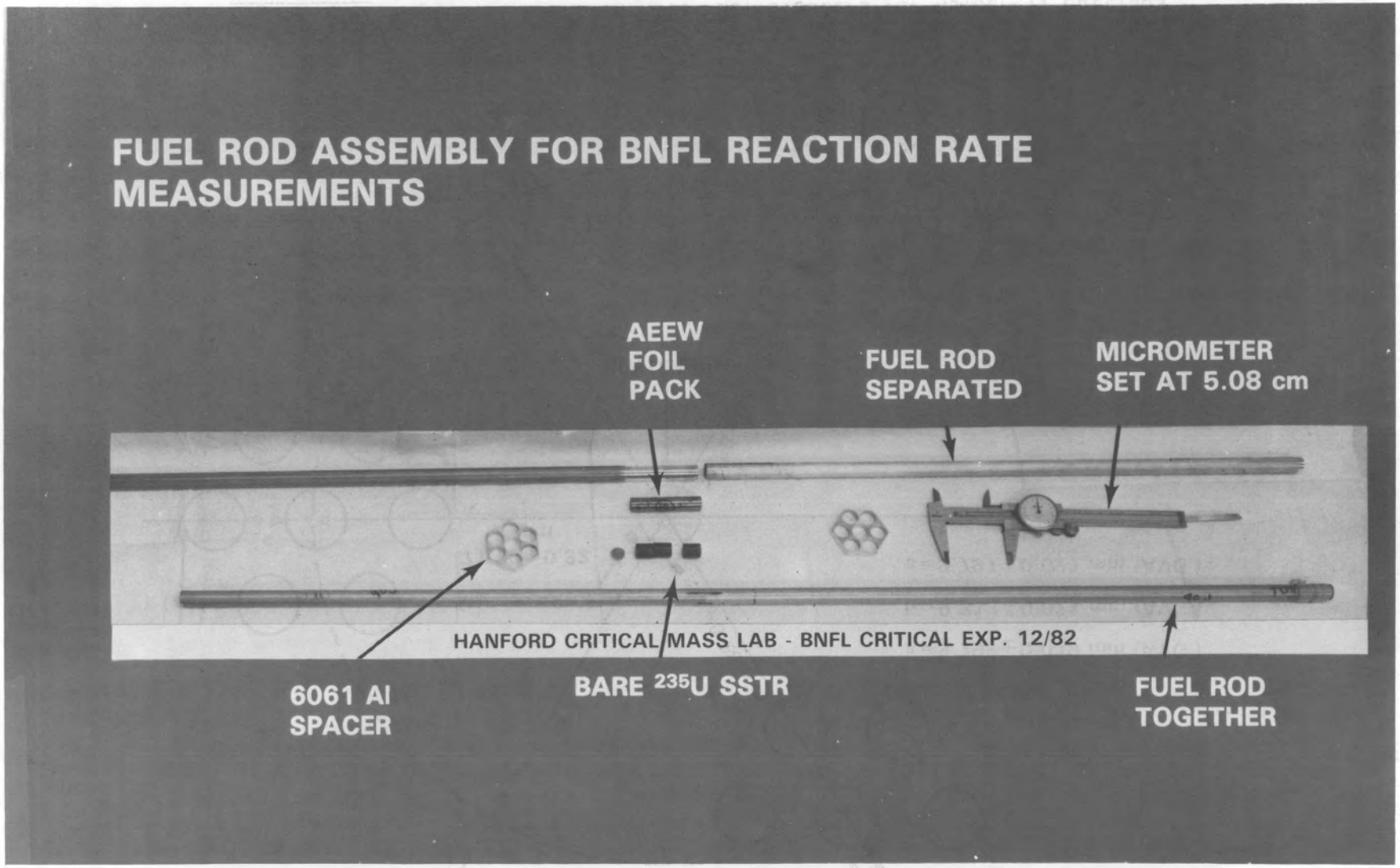

Figure 3.18 Photograph of Fuel Rod Assembly and Reaction Rate Devices Used in Experiments

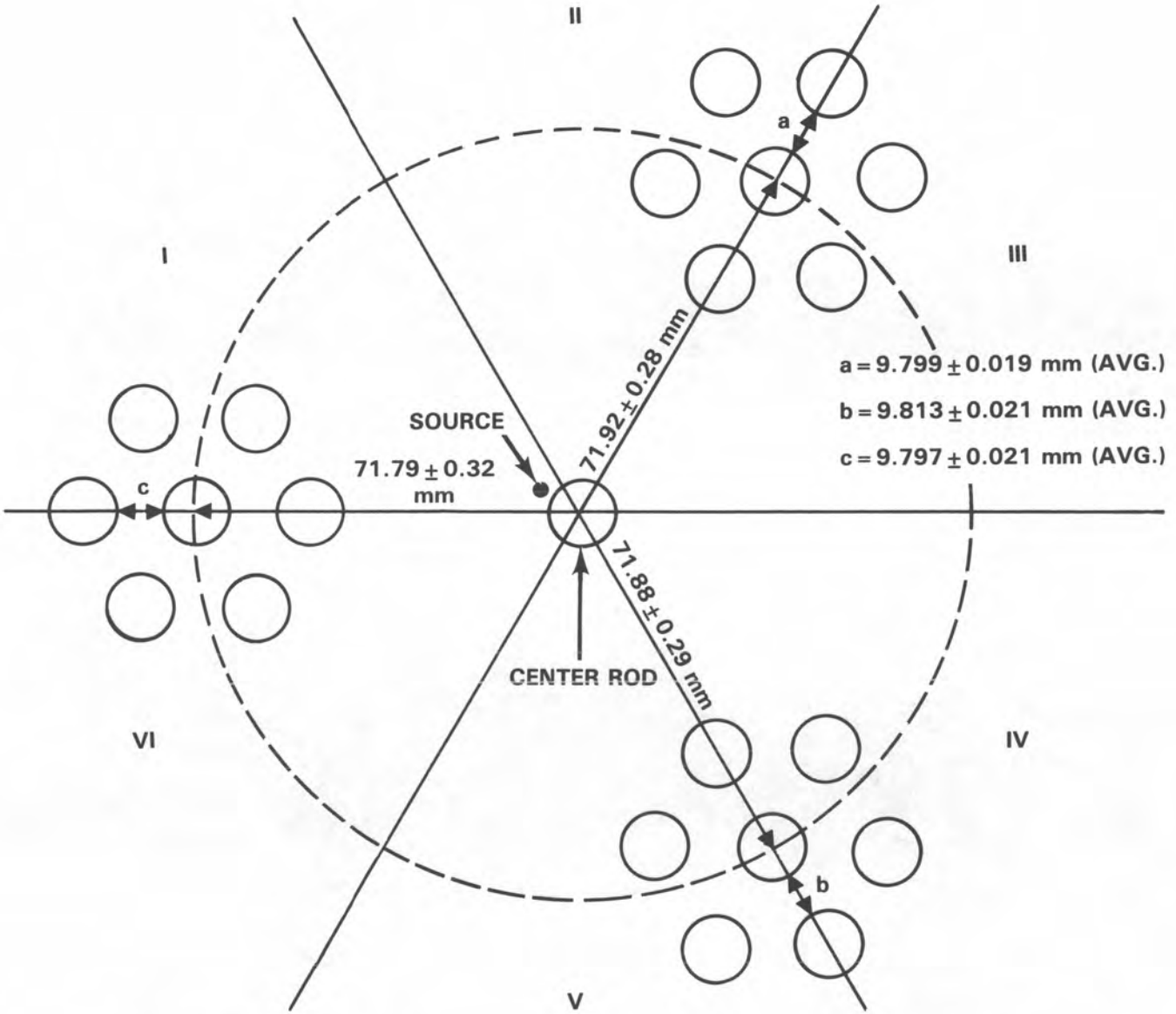

Figure 3.19 Layout of Reaction Rate Fuel Clusters for Number 11 Lattices

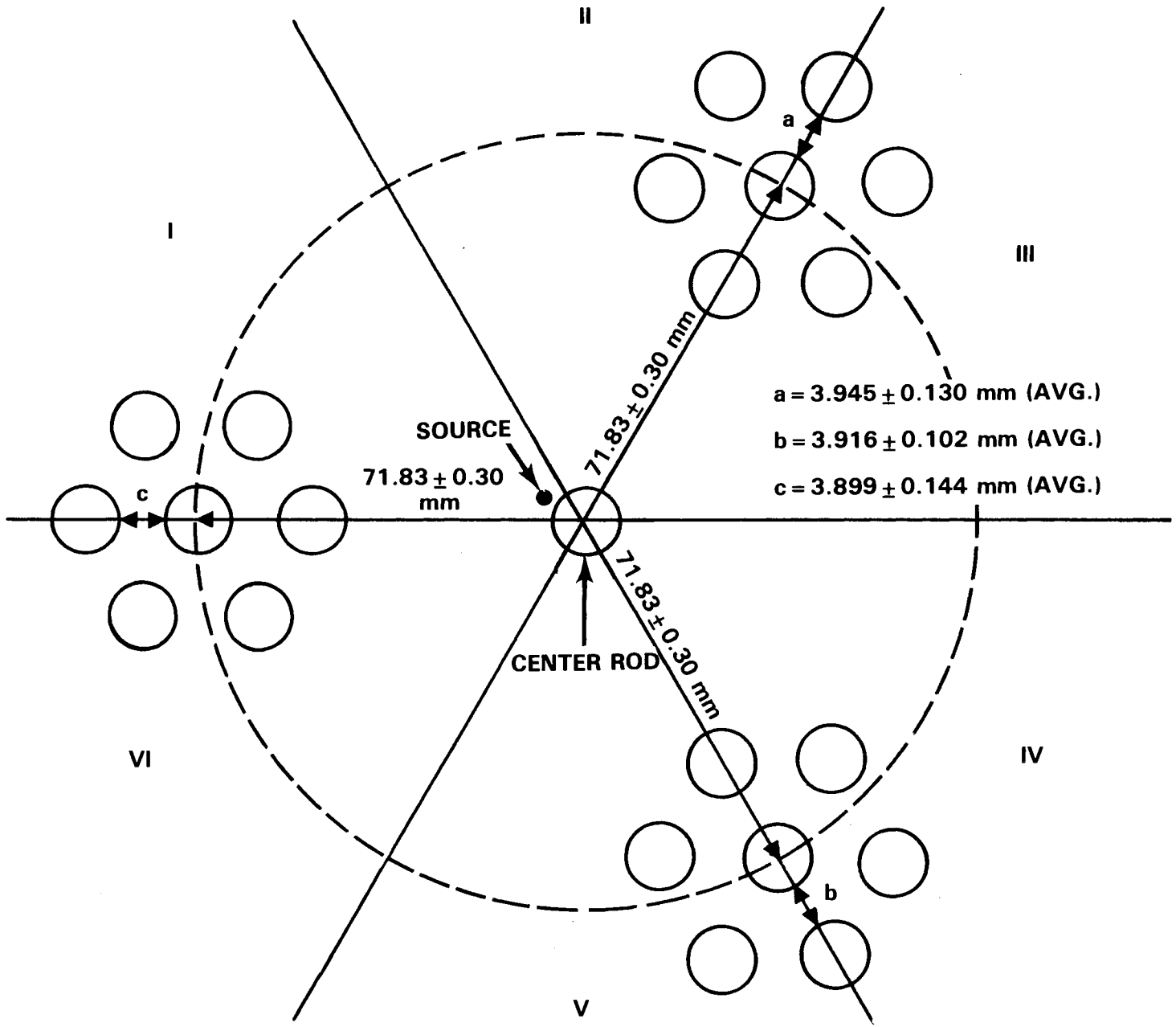

Figure 3.20 Layout of Reaction Rate Fuel Clusters for Number 12 Lattices

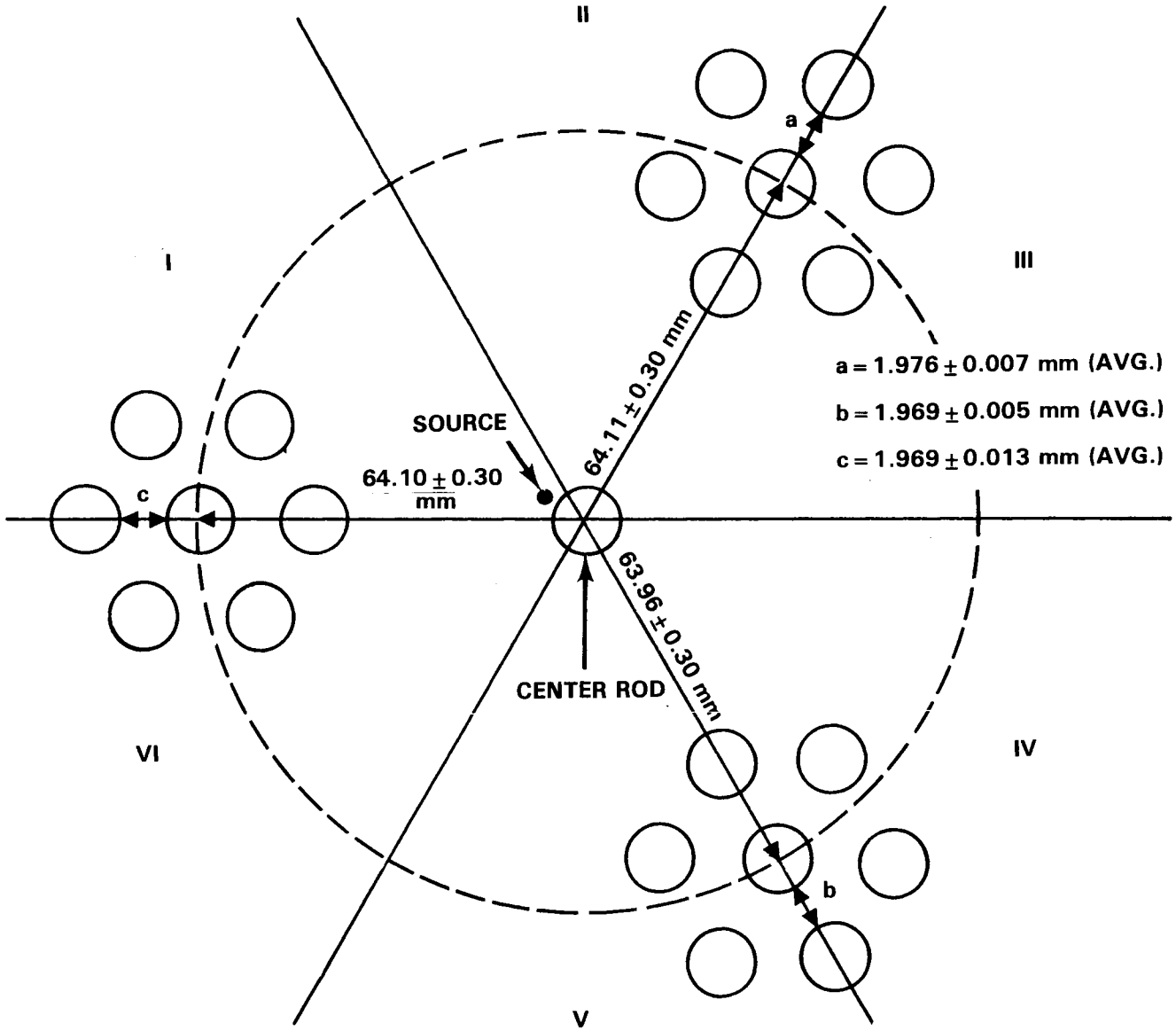

Figure 3.21 Layout of Reaction Rate Fuel Clusters for Number 13 Lattices

observed in these measurements indicate that the FFR and RCR measurements were relatively insensitive to the dimensional variations reported in Figures 3.19, 3.20 and 3.21.

4.0 CONCLUSIONS

The number of fuel rods required for delayed criticality have been experimentally determined for the following:

- Fuel-water lattices of 4.31 wt% ^{235}U enriched UO_2 fuel rods on center-to-center triangular spacings of 2,398 cm, 1.801 cm and 1.598 cm in water containing up to 1.481 g Gd/ℓ.
- Fuel-water lattices of 2.35 wt% ^{235}U enriched UO_2 fuel rods on center-to-center triangular spacings of 1.895 cm and 1.598 cm in water containing up to 0.12 g Gd/ℓ.
- Fuel-water lattices of 4.31 wt% ^{235}U enriched UO_2 fuel rods mixed with fuel rods of 2 wt% PuO_2 in natural UO_2 to obtain simulated irradiated fuel Pu/U compositions in lattices having a triangular center-to-center spacial of 1.598 cm between rods and up to 0.673 g/ℓ of gaddolinium dissolved in the water.

The critical size has also been experimentally determined for each of the above systems with fuel voided (i.e. water holes or columns) regions in the lattice assembly.

Using the pulse neutron source technique, subcritical k_{eff} valves, prompt neutron decay constants and neutron lifetimes have been experimentally measured for each of the above described systems as a function of gadolinium concentration in the water. The data obtained covers k_{eff} values down to about 0.85 and gadolinium concentrations up ot 2.362 g Gd/ℓ.

Absolute ^{235}U fission rates, fast fission ratios ($^{238}U/^{235}U$) and relative conversion ratios($^{238}U_c/^{235}U_f$) have been measured in the experimental assemblies of 4.31 wt% ^{235}U enriched UO_2 fuel. The absolute ^{235}U fission rates varied from 1.59×10^{-13} f at.$^{-1}$sec^{-1} for the near optimum (with no dissolved gadolinium in the water) neutron moderated 2.398cm lattice spacing to 4.71×10^{-15} for the undermoderated 1.598cm lattice spacing. Correspondingly, fast fission ratios of 0.00196 to 0.00571, and relative conversion ratios of 2.70 to 7.64 were observed in these same fuel-water lattices.

With respect to interpretation or use of the data presented herein, the following should be noted:

- Clean, easily defined critical assemblies to which experimentally determined corrections have been applied are provided (Table 3.1) for comparison with calculations. However, the experimental data from which these corrected data were derived are also provided (Table 3.2) for comparison purposes if desired.
- All of the subcritical k_{eff} values were obtained from data accumulated with the neutron detector located in the reflector region of each assembly. Consequently any calculational comparisons with the measured values of k_{eff} should include a coresponding calculationed spatial correction using the same nuclear data.
- The relative conversion ratios are relative to the thermal neutron flux in the AEEW Nestor reactor.
- The average gadolinium concentrations used herein to correlate the measurement data with the amount of dissolved gadolinium present may be about 2% high based on the analysis results obtained with the prepared control samples.

5.0 REFERENCES

Becker, M., and K. S. Quisenberry. 1966. "The Spatial Dependence of Pulsed Neutron Reactivity Measurements." In Proceedings of the Symposium on Neutron Dynamics and Control, Ser. 7, pp. 235-276, USAEC Symposium held at Tuscon, Arizona, May 1966. National Technical Information Service, Springfield, Virgina.

Bierman, S. R., and E. D. Clayton. 1981. "Criticality Experiments with Subcritical Clusters of 2.35 and 4.31 wt% ^{235}U-Enriched UO_2 Rods in Water with Steel Reflecting Walls." Nuclear Technology. 54: 131-144.

Bierman, S. R., B. M. Durst and E. D. Clayton. 1979. "Critical Separation Between Subcritical Clusters of Low Enriched UO_2 Rods in Water with Fixed Neutron Poisons." Nuclear Technology. 42: 237-249.

Broome, P. 1983. Minutes of a Meeting to Discuss the Chemical Analyses Performed in Connection with the Hanford Dissolver Experiment. TSCG/PEB/783/3. British Nuclear Fuels, Ltd., Risley, England.

Garelis, E., and J. L. Russell. 1963. "Theory of Pulsed Neutron Source Measurements." Nuclear Science and Engineering. 16: 263.

Gold, Raymond and Ronald J. Armani. 1968. "Absolute Fission Rate Measurements with Solid-State Track Recorders." Nuclear Science and Engineering. 34: 13-32.

Gozani, T., P. DeMarmels, T. Hurliman and H. Winkler. 1965. "On the Modified Pulse Source Techniques." In Proceedings of Symposium on Pulsed Neutron Research, Vol. II, pp. 49-62. Held by the International Atomic Energy Agency at Karlsruhe. International Atomic Energy Agency, Vienna, Austria.

Kaiz, G. H. 1969. N. S. Savannah Core II Nuclear Characteristics. NUS-597, prepared for Todd Shipyards, Corp. by NUS Corporation, Rockville, Maryland.

Pfeiffer, W., J. R. Brown and A. C. Marshall. 1974. "Fort St. Vrain Startup Test A-3: Pulsed Neutron Experiments." GA-A13079. Prepared for the United States Atomic Energy Commission, San Francisco Operations Office by General Atomic Company, San Diego, California, 92138.

Roberts, J. H., and Song-Teh Huang. 1968. "Fission Rate Measurements in Low-Power Fast Critical Assemblies with Solid-State Track Recorders." Nuclear Applications. 5: 247-252.

Ruddy, R. H. 1983. "SSTR Fission Rates Measured in British Nuclear Fuels, Limited Critical Cores." 8352257 (July 26, 1983). Pacific Northwest Laboratory, Richland, Washington.

Sjöstrand, N. G. 1956. "Measurements on a Subcritical Reactor Using a Pulsed Neutron Source." In Proceedings of United Nations International Conference on Peaceful Uses of Atomic Energy. 5: 52. Geneva, Switzerland.

Smith, R. I. and G. A. Konzek. 1978. Clean Critical Experiment Benchmarks for Plutonium Recycle in LWR's (Foil Activation Studies). NP-196. Vol. 2. Prepared for Electric Power Research Institute by Pacific Northwest Laboratory, Richland, Washington.

Smith, R. I. and G. J. Konzek. 1976. Clean Critical Experiment Benchmarks for Plutonium Recycle in LWR's. NP-196. Vol. 1. Prepared for Electric Power Research Institute by Pacific Northwest Laboratory, Richland, Washington.

Uotinen, V. O. and L. D. Williams. 1967. Experiments and Calculations for H_2O-Moderated Assemblies Containing UO_2-2 Wt% PuO_2 Fuel Rods. PNL-SA-1107. Pacific Northwest Laboratory, Richland, Washington.

APPENDIX A

Density and Chemical Composition of Type 6061, 1100 and 5052 Aluminum and for Zircalloy-2

APPENDIX A

Density and Chemical Composition of Type 6061, 1100 and 5052 Aluminum and Zircalloy-2

Density and American Society for Testing Materials (ASTM) chemical specifications for the aluminum and zircalloy-2 presented in the experimental assemblies are presented in this Appendix.

ASTM STANDARD B210-78 SPECIFICATIONS FOR TYPE 6061 ALUMINUM

Chemical Composition

Element	Wt%
Si	0.40-0.80
Fe	0.7 (Maximum)
Cu	0.15-0.40
Mn	0.15 (Maximum)
Mg	0.8-1.2
Cr	0.04-0.35
Zn	0.25 (Maximum)
Ti	0.15 (Maximum)
Al	Remainder

Maximum Impurities

Element	Wt%
Each	0.05
Total	0.15

Density: 2.69 g/cm^3 (Not part of standard - measured by volume displacement)

ASTM STANDARD B210-78 SPECIFICATIONS FOR TYPE 1100 ALUMINUM

Chemical Composition

Element	Wt%
Si	1.0 (Combined Maximum)
Fe	
Cr	0.05-0.20
Mn	0.05 (Maximum)
Zn	0.10 (Maximum)
Al	99.00 (Minimum)

Maximum Impurities

Element	Wt%
Each	0.05
Total	0.15

Density: 2.70 g/cm^3 (Not part of standard - measured by volume displacement)

ASTM STANDARD B210-78 SPECIFICATIONS FOR TYPE 5052 ALUMINUM

Chemical Composition

Element	Wt%
Si	0.45 (Combined Maximum)
Fe	
Cu	0.10 (Maximum)
Mn	0.10 (Maximum)
Mg	2.2-2.8
Cr	0.15-0.35
Zn	0.10 (Maximum)
Al	Remainder

Maximum Impurities

Element	WT%
Each	0.05
Total	0.15

Density: 2.69 g/cm^3 (Not Part of Standard)

ASTM STANDARD B 353-71 CHEMICAL SPECIFICATIONS FOR ZIRCALLOY-2

Chemical Composition

Element	Wt%
Sr	1.20-1.70
Fe	0.07-0.20
Cr	0.05-0.15
Ni	0.03-0.08
Fe + Cr + Ni	0.18-0.38
Zr	Remainder

Maximum Impurities

Element	Wt%
Al	0.0075
B	0.00005
Cd	0.00005
C	0.027
Cr	-
Co	0.0020
Cu	0.0050
Hf	0.020
Fe	-
H	0.0025
O	0.0025
Mg	0.0050
Ni	-
N	0.0080
Si	0.020
Ti	0.0050
W	0.010
U (Total)	0.00035

Density: 6.55 g/cm^3 (Not Part of Standard)

APPENDIX B

Description of Analytical Methods Used to Obtain Gadolinium Concentration and Comparison of Results on Prepared Solution Samples

APPENDIX B

Description of Analytical Methods Use to Obtain Gadolinium Concentration and Comparison of Results on Prepared Solution Samples

Water samples taken from the experimental assemblies were analyzed for gadolinium by four different laboratories. These laboratiries were:

- Hanford Environmental Health Foundation - Richland, Washington, U.S.A.
- Pacific Northwest Laboratories - Richland, Washington, U.S.A.
- Atomic Energy Establishment Winfrith, Dorechester, Dorset, U.K.
- British Nuclear Fuels, Ltd., Sellafield, Cumbria, U.K.

The analytical methods as used by these laboratories are described briefly in this Appendix. The results obtained by these analytical methods on prepared solution samples are also covered in this Appenix.

The Determination of Natural Gadolinium in Water Samples by Isotope Dilution Mass Spectrometry - Atomic Energy Establishment Winfrith

In Isotope Dilution Mass Spectrometry (IDMS), a known amount of an isotope, normally present as a minor constituent of the element being analysed, is added as a tracer to a sample aliquot. After adequate mixing of the spiked solution a portion is loaded onto a mass spectrometer (MS) filament and isotope ratios determined in the MS. Ion beam intensities of the added isotope and a reference isotope are measured and the ratio calculated. The difference between this ratio and the isotopic ratio in an unspiked sample is used to calculate the concentration of the element in the original solution.

Gadolinium has a natural isotopic composition as shown below. Although Gadolinium-154 would have been the preferred tracer because of its low natural abundance, Gadolinium-157 was chosen as the isotope dilution tracer, because of its ready availability from the stable isotope production unit at Harwell.

NATURAL ISOTOPIC COMPOSITION OF GADOLINIUM

Isotope	152	154	155	156	157	158	160
Atom %	0.20	2.15	14.73	20.47	15.68	24.87	21.90

Gadolinium-157 tracer in the form of Gd_2O_3 was dissolved in 50% nitric acid and diluted to an acid strength of 5% nitric acid at a nominal concentration of 100 µg Gd-157/ml. A second batch of tracer solution was prepared at 50 µg Gd-157/ml. Accurate concentration of each tracer solution was measured by IDMS using gadolinium standards prepared for ICP analyses. Results are listed below.

CALIBRATION RESULTS OF GADOLINIUM-157 TRACER SOLUTIONS

Tracer Solution No	^{157}Gd, µg/g	S.D.	RSD
1	96.72	0.57	0.59%
2	45.95	0.23	0.51%

Initially tracer solution 1 was used and, when exhausted, solution 2 was used.

The RSD values of 0.59% and 0.51% were calculated from actual determinations and include all errors associated with the method, i.e., balance weighings, mixing of tracer and aliquots, and mass spectrometry isotope ratio measurements. This can be compared with RSD values of 0.48% and 0.43% from Table 1 (ICP standards) which are calculated only on the instrument response for standards. For actual analysis of samples the errors for the responses of the samples will have to be combined giving RSD values of approximately 0.75% for analytical results on the ICP.

To analyze the experiment samples, aliquots of tracer solution containing 50-100 µg Gd-157 were weighed into clean tared 5 ml beakers and weight aliquts of sample containing 50-200 µg Gd added. Each spiked aliquot was mixed by swirling, slowly evaporated to dryness and the residue taken into solution with 3-4 drops of 4M nitric acid. Approximately 1-2 µg Gd from this solution was dried onto the side filaments of a triple rhenium filament mass spectrometer bead, loaded into the VG54E thermal ionisation mass spectrometer, and the Gd 157/Gd 156 isotope ratio measured. From this ratio the Gd content of the sample was calculated.

The Determination of Natural Gadolinium in Water Samples by Argon Plasma Emission Spectroscopy - Pacific Northwest Laboratory

Samples were analyzed for gadolinium using direct current argon plasma emission spectroscopy. The instrument used was a Spectrametrics Spectraspan IIIB Echelle spectrometer operated in sequential mode at the 4401.86 A line. Samples were aspirated directly into the DC source with a peristaltic pump. A SPEX Industries 995 ppm gadolinium solution was used as the primary reference standard. Samples were run undiluted and compared directly against the standard. A series of sequential dilutions of the standard were prepared to verify that the analytical line chosen was linear over the full range of interest. Distilled water was used as the low level reference blank. Accuracy and precision of the method is estimated to be 1-2%.

The Determination of Natural Gadolinium in Water Samples by Flame Emission Spectroscopy - Hanford Environmental Health Foundation

Flame emission is an analytical technique which is related to and complementary to atomic absorption. There are several basic differences between atomic absorption and flame emission spectroscopy. In atomic absorption, the only function of the flame is to convert the incoming aerosol into atomic vapor which can then absorb light from the primary light source, the hollow cathode lamp. The flame emission technique requires the flame to do two jobs: convert the aerosol into an atomic vapor and then thermally elevate the atoms to an excited electronic state. When these atoms return to the ground state, they emit light. The intensity of light emitted is related to the concentration of the element of interest in solution.

The Determination of Natural Gadolinium in Water Samples by Thermal Ionization Mass Spectrometry - British Nuclear Fuels, Ltd.

The method is based upon the principle of adding a known amount of gadolinium enriched with gadolinium 160 to a suitable portion of the sample. By measuring the isotopic ratio of the other isotopes of gadolinium to the 160 isotope it is possible to calculate the gadolinium content of the sample.

The tracer, an isotopically enriched standard of gadolinium consisting of 98% gadolinium 160, was first calibrated against three natural gadolinium standards. One made from "specification pure" gadolinium oxide and two from high purity gadolinium metal. In order to prevent any surface oxidation, the gadolinium metal was received in, and at all times handled in, an argon atmosphere. Each calibration was performed eight times.

Using pre-etched glassware to minimize the possibility of rare earth contamination of the samples from the glass surface, weighed portions of the tracer and sample were mixed together and taken to dryness to ensure isotopic equilibration.

To maintain the optimum sample to tracer ratio each analysis was performed using 20 micrograms of tracer and 100 micrograms of gadolinium from the sample.

A small portion of this mixture (1 microgram of gadolinium) was mounted upon a triple filament mass spectrometer bead and analyzed using a VG 54/38 double focussing thermal ionization mass spectrometer. Ratio measurements were made on 156, 157 and 158 to 160 for gadolinium and checks were made to assess whether any isobaric interference was caused by other rare earth elements. The total precision at the one standard deviation uncertainty level is estimated to be greater than 0.5%.

The Determination of Natural Gadolinium in Water Samples by Inductively Coupled Plasma Spectroscopy - Atomic Energy Establishment Winfrith

In inductively coupled plasma (ICP) spectroscopy an efficient radio frequency generator directs high frequency energy to an induction coil where an intense magnetic field is created. A stream of argon gas directed through the magnetic field by a quartz torch, is ionized to form a plasma, and a fine aerosol of the sample is injected into the core of the plasma. There the elements are thermally excited at temperatures near 11,000°C. These high temperatures insure the complete breakdown of chemical compounds and impedes the formation of other interfering compounds. The result is light energy emitted at identifiable wavelengths for each element (spectra). Precision entrance optics gather the light and directs it through a primary slit to a precision concave diffraction grating. The grating diffracts, resolves, and focuses the spectral light on exit slits at the spectrometer's focal curve. Exit slits are positioned to pass only specific wavelenghts for the elements of interest. Mirrors positioned behind the exit slits gather diverging light and focus it on the cathode of photomultiplier tubes, where light energy is converted to electrical signals proportional to individual elemental emission intensities.

Electrical signals from the photomultipliers are processed by the measuring electronics and are read direct from the operator's terminal in concentration units (e.g. ppm. ppb.%).

Analysis Results on Samples Containing Known Quantities of Gadolinium Dissolved in Water

Standard solutions containing 0.25 g Gd/ℓ 0.50 g Gd/ℓ and 1.0 g Gd/ℓ were prepared by the Springfields Works of BNFL for use in comparing results obtained by the analytical techniques described in this Appendix. Gadolinium nitrate (a solid) was used in the experiments. However the nitrate form is deliquescent and can possess up to six waters of hydration. Therefore, to assure good controlled standards, the standard solutions were prepared by two methods.

Pure gadolinium oxide (99.999 wt% Gd_2O_3) was heated at 800° for one hour. Weighed amounts (0.288 g, 0.5763 g, and 1.152 g) of this Gd_2O_3 were dissolved in a minimum quantity of nitric acid, an excess of nitric acid equivalent to 20 g/ℓ added, and then diluted with distilled water to 1 ℓ, producing 0.25 g, 0.5 g and 1.0 g Gd/ℓ. The solution was then bottled to obtain 100 ml samples. Samples were also prepared by dissolving weighed amounts (0.7176 g, 1.4352 g, and 2.8703 g) of the gadolinium nitrate powder used in the experiments in a minimum quanity of nitric acid, an excess of nitric acid equivalent to 20 g/ℓ added, and then diluted with distilled water to 1 ℓ, producing nominal 0.25, 0.5 and 1 g Gd/ℓ solutions. The solution was then bottled, 100 ml per bottle.

The results obtained with the various analytical methods are summarized in the following table.

Sample Description		Analytical Results				
Compound	g Gd/ℓ	HEHF[a] g Gd/ℓ	PNL[b] g Gd/ℓ	AEEW[c] g Gd/ℓ	AEEW[d] g Gd/ℓ	BNFL[e] g Gd/ℓ
Gd_2O_3	0.25	0.340	0.260	0.249	0.261 0.256	0.257
Gd_2O_3	0.50	0.575	0.498	0.506	0.503 0.507	0.516
Gd_2O_3	1.00	1.200	0.986	1.019	1.034 1.020	1.020
$Gd(NO_3)_3.6H_2O$	0.25	0.285	0.263 0.270	0.264	0.268 0.266	0.268
$Gd(NO_3)_3.6H_2O$	0.50	0.590	0.525 0.526	0.534	0.544 0.528	0.541
$Gd(NO_3)_3.6H_2O$	1.00	1.300	1.070 1.050	1.058	1.081 1.074	1.051

(a) Flame emission spectroscopy by Hanford Environmental Health Foundation.

(b) DC argon plasma emission spectroscopy analysis by Battelle-Northwest.

(c) Inductively coupled plasma emission spectroscopy analysis by Atomic Energy Establishment Winfrith.

(d) Isotope dilution mass spectrometry analysis by Atomic Energy Establishment Winfrith.

(e) Thermal ionization mass spectrometry analysis by British Nuclear Fuels, Ltd. Windscale.

To obtain exact agreement with the solution samples containing dissolved Gd_2O_3 the analytically determined concentrations, given above, require the factors indicated below:

Sample Description		Analytical Method				
Compound	g Gd/ℓ	HEHF (FES)	PNL (DAP)	AEEW (ICP)	AEEW (MS)	AEEW (MS)
Gd_2O_3	0.25	0.7353	0.9615	1.0040	0.9699	0.9728
Gd_2O_3	0.50	0.8696	1.0040	0.9881	0.9901	0.9690
Gd_2O_3	1.00	0.8333	1.0142	0.9814	0.9737	0.9804

Based on the above results and consultations with BNFL and AEEW staff, it was concluded that the average of the concentrations determined by mass spectrometry would provide consistent analytical values for the experimental solution samples as good as could be obtained. (Broome 1983).

In addition to the Springfield's solutions, samples were periodically prepared at the Critical Mass Laboratory by dissolving into distilled water containing 1 g nitric acid, weighed amounts of the gadolinium nitrate powder used in the experiments. The analysis results obtained for these samples are summarized below:

Sample Description g Compound/g Water[a]	Date	Analytical Results HEHF[b] g Gd/ℓ	PNL[c] g Gd/ℓ	BNFL[d] g Gd/ℓ
7.190×10^{-4}	08/11/82	0.306	-----	-----
7.190×10^{-4}	08/11/82	0.307	-----	-----
7.190×10^{-4}	11/16/82	0.310	0.259	-----
7.190×10^{-4}	11/16/82	-----	0.260	-----
7.185×10^{-4}	01/22/83	0.330	0.260	0.269

(a) Equivalent to 0.25 g Gd/ℓ if compound is the hexahydrate.
(b) Flame emission spectroscopy by Hanford Environmental Health Foundation.
(c) DC argon plasma emission spectroscopy analysis by Battelle-Northwest.
(d) Thermal ionization mass spectrometry analysis by British Nuclear Fuels, Ltd - Windscale.

Based on the concentrations determined for the gadolinium nitrate samples by mass spectrometry, an average of 4.91 ± 0.18 waters of hydration was calculated for the gadolinium powder used in the experiments.

APPENDIX C

Trace Impurities Present in Water and Gadolinium Nitrate Used in Experiments

APPENDIX C

Trace Impurities Present in Water and Gadolinium Nitrate Used in Experiments

Trace impurity levels are presented in this Appendix for the gadolinium nitrate powder and the gadolinium-water solutions. The gadolinium-water solutions are identified by sample numbers and experiment reference numbers which are tracable to the experimental assemblies described in the various sections of the report.

Impurities in the solutions were determined on a direct reading ICP which is capable of simultaneous analysis for 48 elements. A qualitative assessment of impurities was made by introducing a few millilitres of each sample solution into the argon plasma, and, while monitoring light emissions from the plasma on all the detectors, scanning across the detectors by moving the primary slit. The primary slit is the entrance slit to the spectrometer and small sideways movements have the same effect as moving the diffraction grating. Using this method, approximate concentrations of each element are obtained and interfering lines from other elements are highlighted. Those elements which gave a positive response were considered for quantitative analysis.

Standard solutions were prepared of those elements qualitatively identified. Following ICP calibration with these standards the samples were analysed.

Analysis of aluminum in the presence of gadolinium is a problem on the Winfrith ICP as the 308.20 nm Gd line overlaps the 308.2 nm Al line selected for aluminum analysis on the Winfrith ICP. (ICP direct readers have fixed slits so alternative lines cannot be used). To overcome this problem aluminum was determined by flame atomic absorption.

In the gadolinium-water impurity analyses the neodymium results tend to vary in direct relationship with the gadolinium concentration. Since

the gadolinium nitrate used in the experiments originated from the same batch, the neodymium impurities are probably due to gadolinium interference in the analyses. Also, it should be noted that the step-wise increase in aluminum inpurity in the gadolinium-water samples corresponds to the practice of adding a small amount of nitric acid to the experimental solution to assure precipitation of gadolinium compounds did not occur. Therefore, the increase in aluminum impurity is probably due to corrosion products resulting from this practice.

TRACE IMPURITIES PRESENT IN GADOLINIUM NITRATE POWDER USED IN EXPERIMENTS

Spectrographic Analysis by Supplier, Research Chemical, Phoenix, Arizona 85063

Element	Wt%
Eu	.03
Tb	.05
Dy	<.01
Y	.01
Sm	<.01
Si	<.01
Fe	<.01
Mg	<.01
Ca	<.01
Al	<.01

Impurity Analyses by Atomic Energy Establishment Winfrith, United Kingdom

Element	Wt%	Element	Wt%
Y	0.01	Ce	<0.005
Eu	0.005	Mg	<0.005
Cu	0.003	Rh	<0.005
Al	<0.1	W	<0.005
Be	<0.1	Zn	<0.003
Nd	<0.1	Ag	<0.002
Si	<0.1	Au	<0.002
Ti	<0.1	Ba	<0.002
B	<0.05	Cd	<0.002
Ca	<0.05	Co	<0.002
Na	<0.05	Cr	<0.002
Pb	<0.05	Fe	<0.002
Ru	<0.05	Hf	<0.002
Sn	<0.05	Li	<0.002
Ln	<0.01	Mn	<0.002
K	<0.01	Mo	<0.002
Ni	<0.01	Sr	<0.002
Pt	<0.01	V	<0.002
Sm	<0.01	Zr	<0.002
U	<0.01		

TRACE IMPURITIES PRESENT IN GADOLINIUM-WATER SOLUTIONS

ICP Analysis by Atomic Energy Establishment Winfrith

Microgram of Element per Gram of Sample

Experiment Reference Number	Sample Identification Number	Al	B	Ca	Cu	Eu	Pb	Mg	Nd	Ni	Si	Ni	Y	Zn
4.3-000-182	1-1-1	< 0.25	< 0.05	0.9	< 0.03	< 0.03	< 0.25	0.04	< 0.5	< 0.1	2.6	6.6	< 0.01	< 0.03
4.3-000-185	1-1-2	< 0.25	< 0.05	1.5	5.6	< 0.03	1.0	1.3	1.1	< 0.1	< 0.2	0.6	< 0.01	3.7
4.3-000-186	1-1-3	< 0.25	< 0.05	1.6	0.15	0.04	0.37	1.3	4.0	< 0.1	< 0.2	0.6	< 0.01	0.19
4.3-000-188	1-1-4	< 0.25	< 0.05	2.9	0.15	0.04	0.42	2.4	4.4	0.1	< 0.2	6.8	< 0.01	0.22
4.3-000-188	1-1-5	< 0.25	< 0.05	2.7	0.15	0.05	0.44	2.9	4.9	0.1	< 0.2	7.3	0.01	0.22
4.3-000-188	1-1-6	< 0.25	< 0.05	2.9	0.15	0.06	0.52	3.1	5.7	0.2	< 0.2	8.9	0.02	0.22
4.3-000-188	1-1-7	0.3	< 0.05	1.8	0.16	0.06	0.57	3.3	7.2	0.2	< 0.2	0.5	0.04	0.23
4.3-000-194	1-3-3	< 0.25	< 0.05	4.0	0.15	0.07	0.52	3.6	7.1	0.2	< 0.2	4.0	0.04	0.23
4.3-000-194	1-3-4	< 0.25	< 0.05	7.0	0.13	0.07	0.44	3.9	5.9	0.1	< 0.2	4.4	0.02	0.23
4.3-000-194	1-3-5	< 0.25	< 0.05	15.4	0.03	0.06	< 0.25	4.7	1.1	< 0.1	1.2	3.0	< 0.01	0.12
4.3-000-194	1-3-6	< 0.25	< 0.05	5.0	0.12	0.05	0.30	2.7	4.0	0.1	< 0.2	3.4	< 0.01	0.18
4.3-000-198	1-3-7	< 0.25	< 0.05	15.7	< 0.03	0.07	< 0.25	4.9	1.1	< 0.1	1.2	3.1	0.02	0.15
2.35-000-160	2-1-1	< 0.25	< 0.05	< 0.5	< 0.03	< 0.03	< 0.25	0.03	< 0.5	< 0.1	< 0.2	0.4	< 0.01	< 0.03
2.35-000-160 a)	2-1-2	< 0.25	< 0.05	1.5	18.2	< 0.03	1.9	1.4	2.4	0.3	< 0.2	0.6	< 0.01	10.6
2.35-000-165	2-1-3	< 0.25	< 0.05	2.7	0.04	< 0.03	< 0.25	0.86	0.6	< 0.1	1.5	6.1	< 0.01	0.14
2.35-000-165	2-1-4	< 0.25	< 0.05	1.5	11.2	< 0.03	1.6	1.4	2.9	0.1	< 0.2	0.5	< 0.01	7.2
2.35-000-165	2-1-5	< 0.25	< 0.05	6.0	14.2	0.03	1.4	2.4	1.9	0.3	< 0.2	0.9	< 0.01	6.1
None b)	3-2-1	< 0.25	< 0.05	10.3	< 0.03	0.05	< 0.25	2.5	< 0.5	< 0.1	2.1	4.0	< 0.01	< 0.03
4.3-002-196	3-2-2	< 0.25	< 0.05	3.9	0.20	0.06	0.57	3.5	5.6	0.1	< 0.2	4.6	0.08	0.26
4.3-002-196	3-2-3	< 0.25	0.07	3.7	0.18	0.08	0.75	3.3	7.9	0.2	< 0.2	5.3	0.11	0.26
4.3-002-196	3-2-5	< 0.25	< 0.05	11.4	0.63	0.06	0.40	3.7	1.7	< 0.1	0.6	2.7	0.02	0.18
4.3-000-192	1-2-2	< 0.25	< 0.05	< 0.05	< 0.03	< 0.03	< 0.25	0.04	< 0.5	< 0.1	< 0.2	0.5	< 0.01	< 0.03
4.3-000-192	1-2-3	< 0.25	< 0.05	18.2	< 0.03	0.08	< 0.25	4.9	< 0.5	< 0.1	3.1	6.9	< 0.01	0.05
4.3-000-201	1-2-5	3.8	< 0.05	19.2	0.05	0.08	1.0	5.5	1.1	< 0.1	2.2	4.4	0.02	0.34
4.3-000-202	1-2-6	5.0	< 0.05	19.1	0.10	0.06	1.3	5.6	3.5	< 0.1	< 0.2	4.3	0.05	0.43
4.3-000-203	1-2-7	5.7	< 0.05	18.8	0.22	0.05	1.7	5.5	8.1	0.2	< 0.2	4.1	0.11	0.56
4.3-000-204	1-2-8	7.3	0.06	18.6	0.30	0.06	2.1	5.7	10.7	0.3	< 0.2	3.5	0.15	0.65
4.3-000-204	1-2-9	8.6	0.08	18.8	0.34	0.07	2.4	5.9	12.0	0.3	< 0.2	3.5	0.16	0.75
4.3-000-204	1-2-10	8.3	0.09	18.4	0.36	0.07	2.5	5.9	12.0	0.3	< 0.2	3.4	0.17	0.75
4.3-000-204	1-2-11	8.5	0.09	18.2	0.40	0.07	2.6	5.8	13.3	0.4	< 0.2	3.3	0.19	0.77
4.3-000-204	1-2-12	10.0	0.13	18.4	0.51	0.08	2.9	5.8	17.8	0.4	< 0.2	3.3	0.25	0.81
4.3-000-205	1-2-13	6.1	0.09	18.5	0.35	0.07	2.1	5.5	12.0	0.3	< 0.2	3.3	0.17	0.60
4.3-000-206	1-2-14	6.4	0.08	18.6	0.35	0.07	2.1	5.5	12.2	0.3	< 0.2	3.4	0.17	0.61
2.35-000-170	2-2-1	1.2	< 0.05	2.7	0.03	< 0.03	0.4	0.8	< 0.5	< 0.1	2.1	1.6	0.01	0.74
2.35-000-170	2-2-2	3.8	< 0.05	7.0	0.03	0.03	0.3	2.2	< 0.5	< 0.1	2.2	1.7	0.01	1.2
2.35-000-170	2-2-3	8.0	0.05	9.0	0.09	0.04	0.6	3.3	1.2	< 0.1	1.3	1.4	0.03	2.0
4.3-002-207	3-2M-1	2.5	< 0.05	18.0	0.13	0.07	0.8	5.0	2.0	0.1	< 0.2	3.3	0.06	0.49
4.3-002-208	3-2M-2	3.1	< 0.05	13.0	0.08	< 0.03	0.7	3.7	1.7	< 0.1	< 0.2	2.1	0.05	0.26
4.3-002-209	3-2M-3	5.4	< 0.05	13.0	0.10	0.03	0.8	4.0	2.0	< 0.1	< 0.2	1.6	0.06	0.38
4.3-002-209	3-2M-4	6.5	< 0.05	13.0	0.11	0.03	0.8	4.0	2.2	0.1	< 0.2	2.2	0.06	0.48
4.3-002-209	3-2M-5	6.5	0.09	18.0	0.31	0.06	1.5	5.5	6.0	0.3	< 0.2	3.3	0.16	0.89
4.3-002-209	3-2M-6	7.6	0.12	18.0	0.50	0.03	1.9	5.4	8.3	0.5	< 0.2	3.0	0.26	0.93

a) Includes experiment 165.

b) Control sample.

APPENDIX D

Trace Impurities Measured In Lattice Plate Material

APPENDIX D

Trace Impurities Measured In Lattice Plate Material

Trace impurity levels are presented in this Appendix for the polypropylene material used in fabricating the lattice plates for these experiments. The analytical results are from a spark source mass spectrographic analysis of a sample taken from, and considered representative of, the polypropylene during fabrication of the lattice plates. The spectrographic analysis were performed by the Hanford Engineering Development Laboratory, Richland, Washington, on June 14, 1982.

Trace Impurities Present in Lattice Plates

Element	Parts Per Million by Weight
B	<1
F	2
Na	3
Mg	100
Al	90
Si	80
P	2
Cl	3
K	2
Ca	20
Ti	200
V	20
Cr	40
Mn	0.3
Fe	<20
Cu	40
Zn	40
Ge	10
As	20
Rb	8
Y	10
Zr	200
Mo	15
Sn	4
Br	10

APPENDIX E

Center-to-Center Spacing Between Fuel Rods

APPENDIX E

Center-to-Center Spacing Between Fuel Rods

Measurements to determine the center-to-center spacing between the fuel rods in each experimental assembly are covered in this Appendix. Each experimental assembly was provided with three plates of polypropylene into which equally spaced holes, having diameters 0.013 cm larger than the fuel rods, had been milled on specified center-to-center spacings within ± 0.013 cm. These plates were positioned approximately equal distance apart in the experimental assembly to maintain a constant distance between the fuel rods over their entire length. Corresponding center-to-center spacings between holes were measured along two diameters, 60° apart, of each lattice plate to obtain an average lattice spacing for each experimental assembly and to determine if the holes were uniformly spaced as specified.

Lattice 11 Center-to-Center Spacings

Top Plate (inch)	Middle Plate (inch)	Bottom Plate (inch)
0.945	0.946	0.945
0.944	0.944	0.945
0.946	0.944	0.946
0.943	0.944	0.944
0.944	0.945	0.944
0.945	0.945	0.946
0.946	0.946	0.946
0.944	0.943	0.944
0.943	0.943	0.944
0.943	0.942	0.943
0.944	0.943	0.944
0.944	0.943	0.944
Average: 0.944 ± 0.001	0.944 ± 0.001	0.945 ± 0.001

Overall Average Center-to-Center Spacing: 0.944 ± 0.002 inch (2.398 cm)

Lattice 12 Center-To-Center Spacings

Top Plate (inch)	Middle Plate (inch)	Bottom Plate (inch)
0.710	0.714	0.713
0.712	0.712	0.712
0.712	0.712	0.710
0.712	0.713	0.713
0.712	0.712	0.712
0.714	0.713	0.712
0.711	0.714	0.713
0.713	0.712	0.712
0.712	0.712	0.712
0.711	0.712	0.712
0.712	0.713	0.711
0.711	0.712	0.713
0.713	0.712	0.712
0.709	0.711	0.708
0.711	0.712	0.712
0.712	0.713	0.712
0.712	0.711	0.712
0.712	0.712	0.712
Average: 0.709 ± 0.002	0.709 ± 0.001	0.709 ± 0.001

Overall Average Center-To-Center Spacing: 0.709 ± 0.002 inch (1.801 cm)

Lattice 13[(a)] Center-To-Center Spacings

Top Plate (inch)	Middle Plate (inch)	Bottom Plate (inch)
0.629	0.630	0.635
0.629	0.632	0.624
0.629	0.630	0.633
0.629	0.629	0.627
0.629	0.630	0.634
0.630	0.629	0.628
0.628	0.631	0.626
0.629	0.630	0.624
0.628	0.627	0.631
0.631	0.631	0.631
0.628	0.629	0.627
0.630	0.628	0.635
0.630	0.630	0.628
0.629	0.631	0.632
0.628	0.627	0.627
0.631	0.630	0.631
0.630	0.625	0.629
0.630	0.633	0.631
0.629	0.625	0.630
0.630	0.629	0.628
0.632	0.631	0.631
0.626	0.624	0.633
0.629	0.626	0.621
0.628	0.628	0.629
0.630	0.626	0.629
0.629	0.626	0.630
0.631	0.632	0.629
0.629	0.627	0.631
0.630	0.633	0.630
0.630	0.624	0.629
Average: 0.629 ± 0.001	0.629 ± 0.004	0.629 ± 0.005

Overall Average Center-To-Center Spacing: 0.629 ± 0.002 inch (1.598 cm)

(a) Lattice plates also used in experiments identified by Lattice Identification Number: 32 and 32M.

Lattice 21 Center-To-Center Spacings

Top Plate (inch)	Middle Plate (inch)	Bottom Plate (inch)
0.746	0.745	0.746
0.746	0.746	0.746
0.746	0.746	0.746
0.746	0.746	0.746
0.746	0.746	0.746
0.746	0.745	0.746
0.745	0.746	0.746
0.745	0.746	0.746
0.747	0.747	0.746
0.746	0.747	0.747
0.746	0.747	0.746
0.745	0.748	0.745
0.747	0.746	0.747
0.746	0.748	0.746
0.745	0.746	0.746
0.747	0.747	0.747
Average: 0.746 ± 0.001	0.746 ± 0.001	0.746 ± 0.001

Overall Average Center-To-Center Spacing: 0.746 ± 0.002 inch (1.895 cm)

Lattice 22 Center-To-Center Spacings

Top Plate (inch)	Middle Plate (inch)	Bottom Plate (inch)
0.628	0.629	0.632
0.630	0.630	0.628
0.629	0.629	0.632
0.631	0.629	0.629
0.628	0.629	0.630
0.629	0.629	0.631
0.630	0.630	0.629
0.628	0.629	0.629
0.630	0.629	0.630
0.630	0.629	0.630
0.629	0.630	0.629
0.629	0.629	0.629
0.630	0.630	0.629
0.630	0.630	0.630
0.630	0.630	0.630
0.630	0.630	0.630
Average: 0.629 ± 0.001	0.629 ± 0.001	0.630 ± 0.001

Overall Average Center-To-Center Spacing: 0.629 ± 0.002 inch (1.598 cm)

APPENDIX F

Loading Diagrams for Critical and Subcritical Assemblies

APPENDIX F

Loading Diagrams for Critical and Subcritical Assemblies

A loading diagram for each critical and subcritical assembly is presented in this Appendix. Each diagram identifies the type or types of fuel involved, the amount of fuel required for criticality and the location of the fuel in the assembly. Each diagram also identifies any irregular features present in the experimental assemblies. The location of control and safety rod guide sleeves and the location of reaction rate devices are shown when present. Lattice and experiment identification numbers are provided in each diagram for cross reference with tables presented in the text.

In an attempt to minimize computational input errors, lattice spacings, gadolinium concentrations and, when applicable, subcritical k_{eff} values are also given on each diagram.

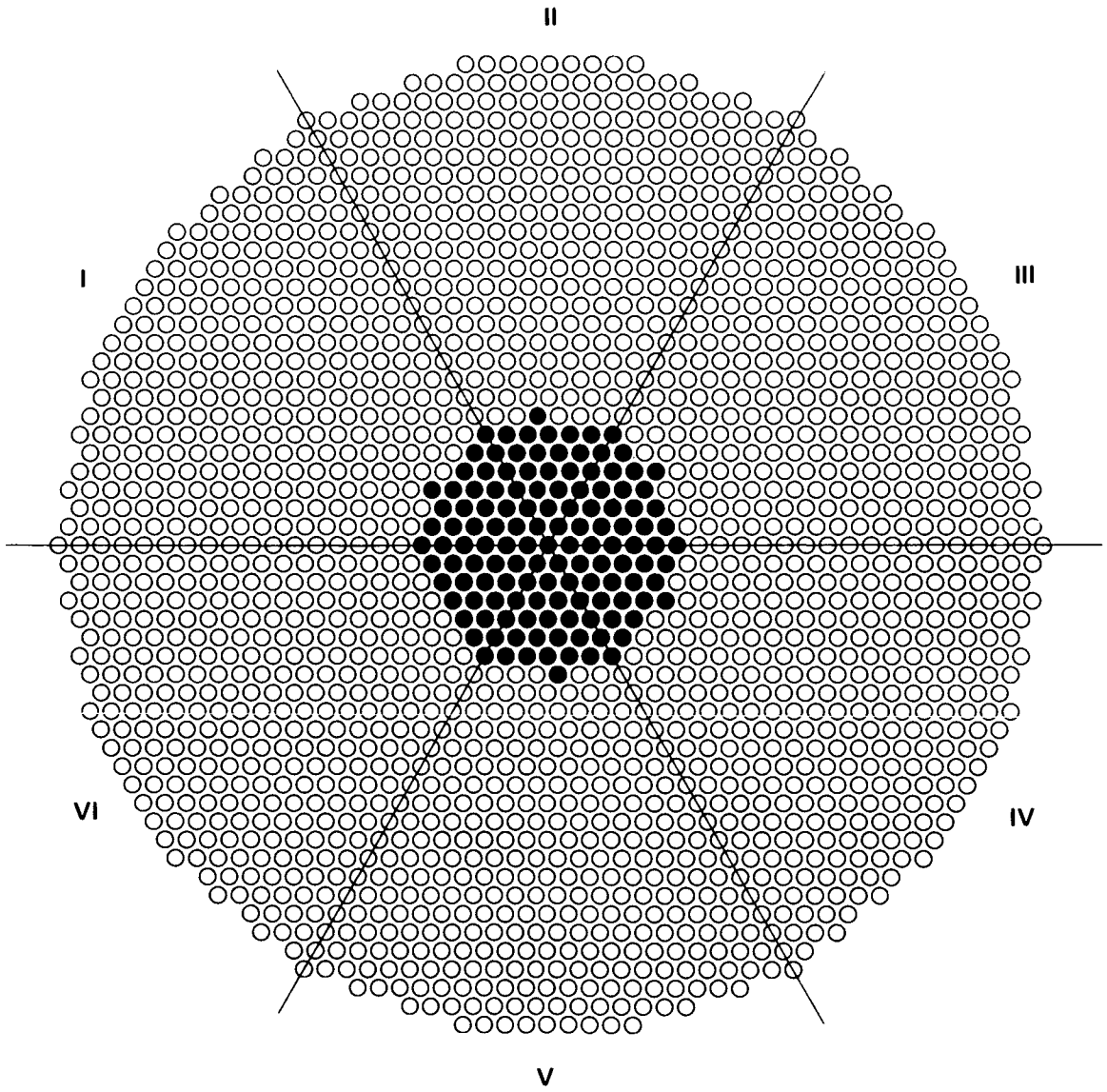

FUEL: 4.31 wt% ^{235}U ENRICHED UO_2

EXPERIMENT: 4.3-000-182

LATTICE: 11

PITCH: 2.398 ± 0.005

GADOLINIUM: SEE COMMENTS

CONTROL ROD: NONE

SAFETY ROD: NONE

REACTION RATES: NONE

RODS: 132 UO_2 RODS AT ●

k_{eff}: SEE COMMENTS

COMMENTS:

$k_{eff} = 1.0$ AT ZERO g Gd/liter

$k_{eff} = 0.985$ AT 0.068 ± 0.001 g Gd/liter

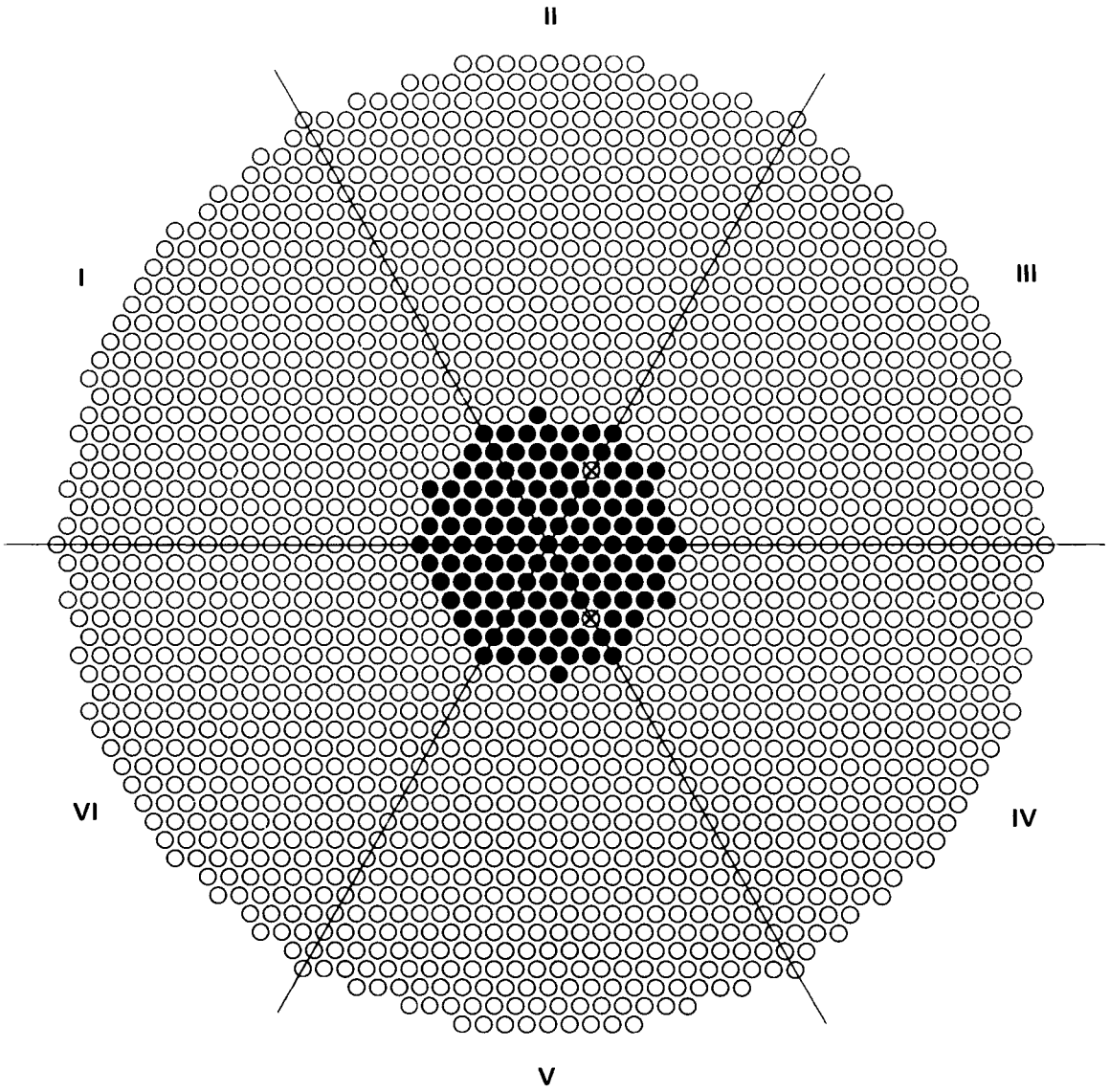

FUEL: 4.31 wt% ^{235}U ENRICHED UO_2

EXPERIMENT: 4.3-000-182A

LATTICE: 11

PITCH: 2.398 ± 0.005 cm

GADOLINIUM: 0

CONTROL ROD: OUT

SAFETY ROD: OUT

REACTION RATES: NONE

RODS: 130 UO_2 RODS AT ●

k_{eff}: 1.0

COMMENTS: WATER FILLED ALUMINUM SLEEVES AT ⊗

F.3

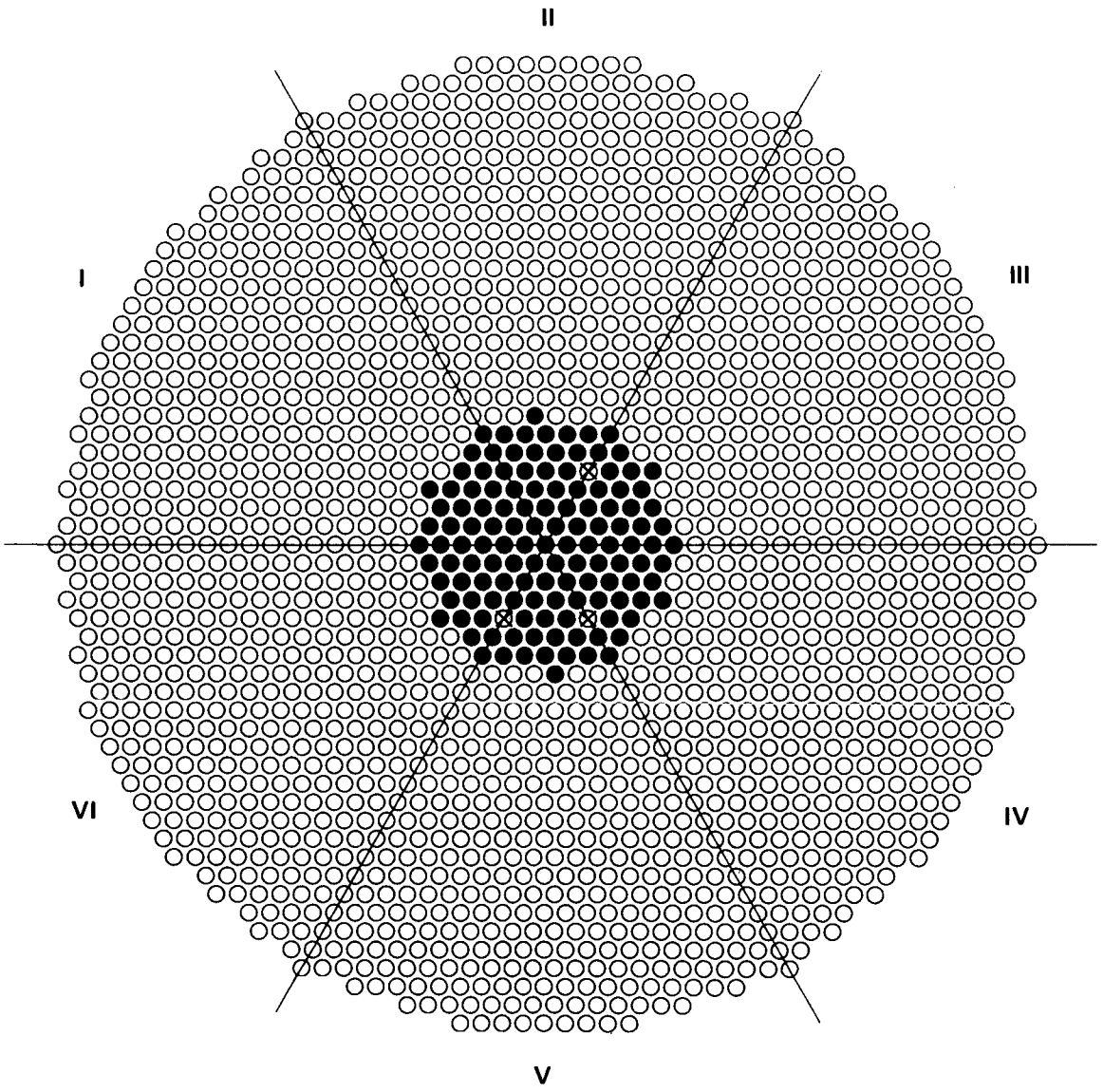

FUEL: 4.31 wt% ^{235}U ENRICHED UO_2

EXPERIMENT: 4.3-000-182B

LATTICE: 11

PITCH: 2.398 ± 0.005

GADOLINIUM: 0

CONTROL ROD: OUT

SAFETY ROD: OUT

REACTION RATES: NONE

RODS: 130 UO_2 RODS AT ●

k_{eff}: 1.0

COMMENTS: WATER FILLED ALUMINUM SLEEVES AT ⊗

F.4

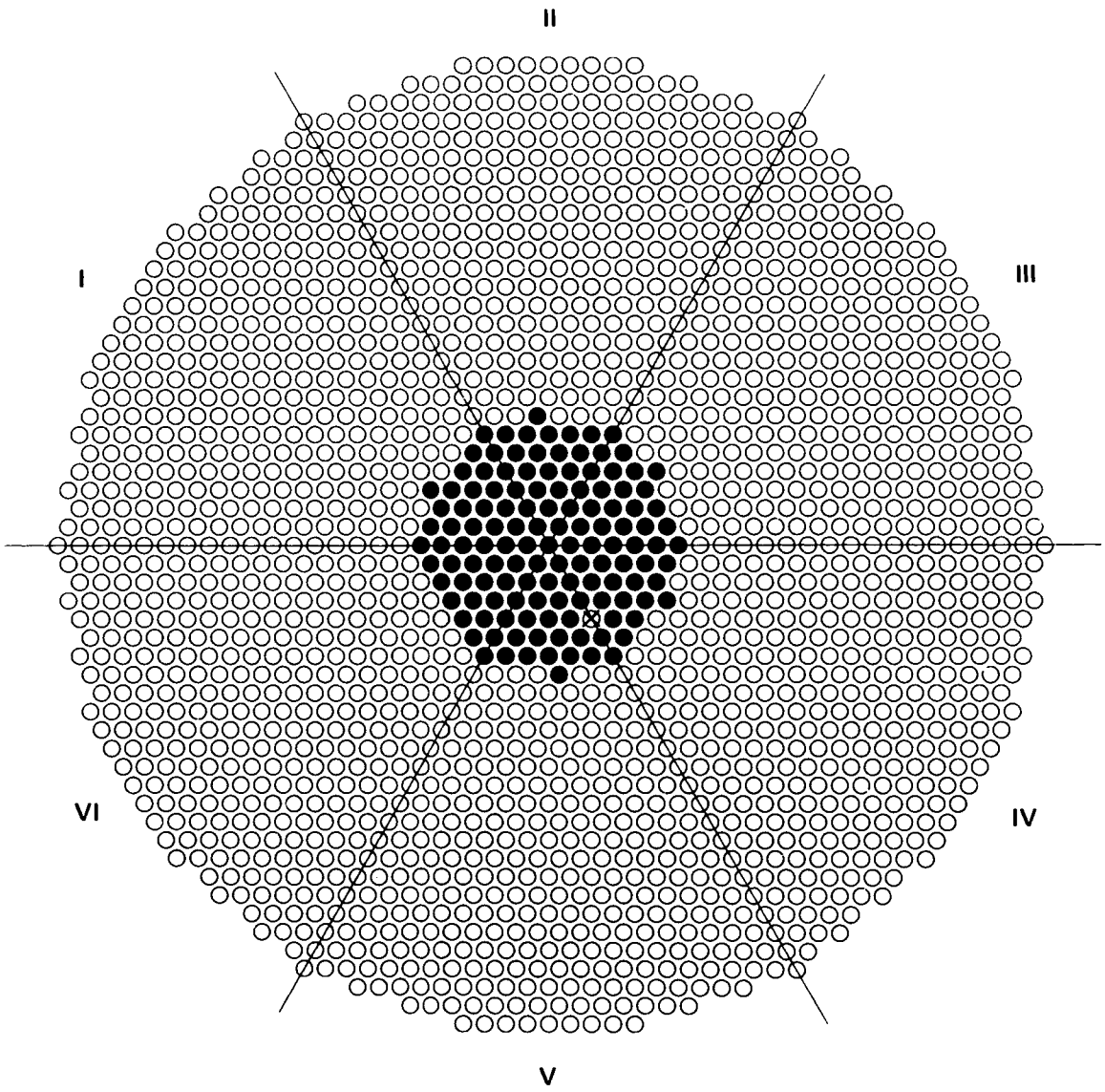

FUEL: 4.31 wt% ^{235}U ENRICHED UO_2

EXPERIMENT: 4.3-000-182C

LATTICE: 11

PITCH: 2.398 ± 0.005 cm

GADOLINIUM: 0

CONTROL ROD: OUT

SAFETY ROD: NONE

REACTION RATES: NONE

RODS: 131 UO_2 RODS AT ●

k_{eff}: 1.0

COMMENTS: WATER FILLED ALUMINUM SLEEVES AT ⊠

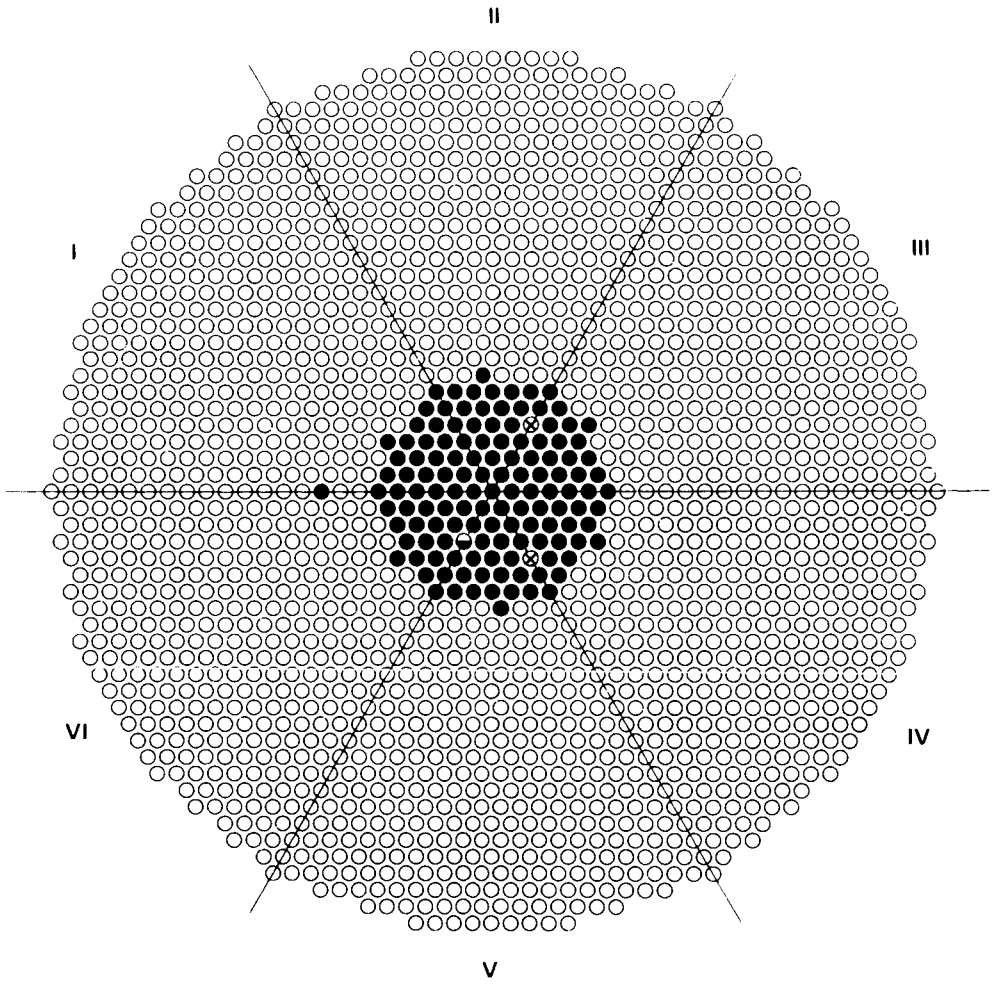

FUEL: 4.31 wt% ^{235}U ENRICHED UO_2

EXPERIMENT: 4.3-000-182D

LATTICE: 11

PITCH: 2.398 ± 0.005 cm

GADOLINIUM: NONE

CONTROL ROD: OUT 52.4 ± 0.3 cm FROM BOTTOM OF FUEL (LOCATION V ⊗)

SAFETY ROD: OUT

REACTION RATES: SOLID STATE ^{235}U TRACK RECORDER IN ◒

RODS: 132 UO_2 RODS AT ●

k_{eff}: 1.0

COMMENTS: CONTROL AND SAFETY ROD ALUMINUM GUIDE SLEEVES AT ⊗

F. 6.9

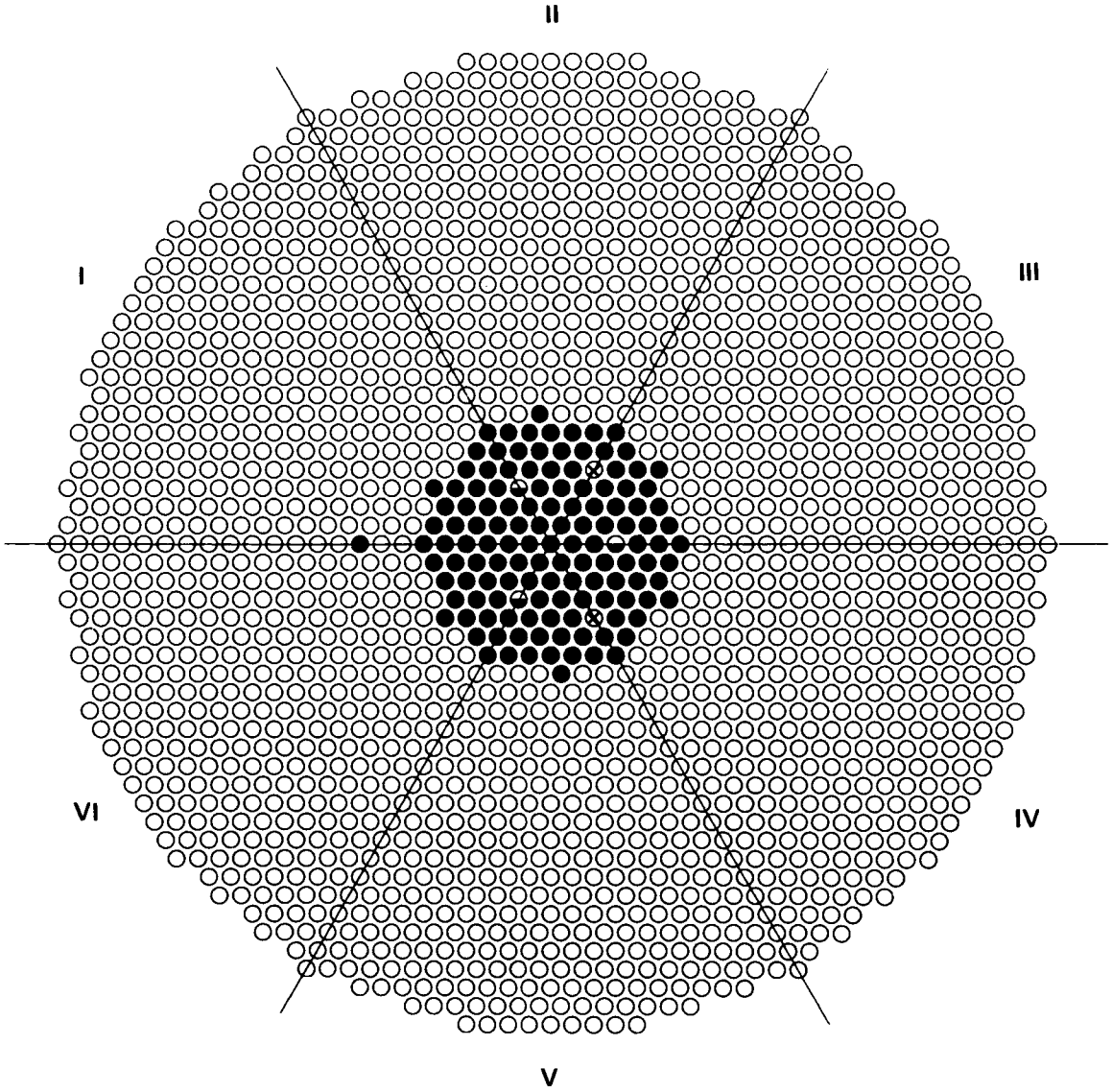

FUEL: 4.31 wt% ^{235}U ENRICHED UO_2

EXPERIMENT: 4.3-000-182E

LATTICE: 11

PITCH: 2.398 ± 0.005

GADOLINIUM: NONE

CONTROL ROD: OUT 58.4 ± 0.3 cm FROM BOTTOM OF FUEL (LOCATION V ⊗)

SAFETY ROD: OUT

REACTION RATES: ^{238}U AND ^{235}U FOILS IN ◒ (SEE COMMENTS)

RODS: 132 UO_2 RODS AT ●

k_{eff}: 1.0

COMMENTS: CONTROL AND SAFETY ROD ALUMINUM GUIDE SLEEVES AT ⊗
AEEW 3 FOIL PACKET IN II ◒
AEEW 4 FOIL PACKET IN IV ◒
AEEW 11 FOIL PACKET IN VI ◒

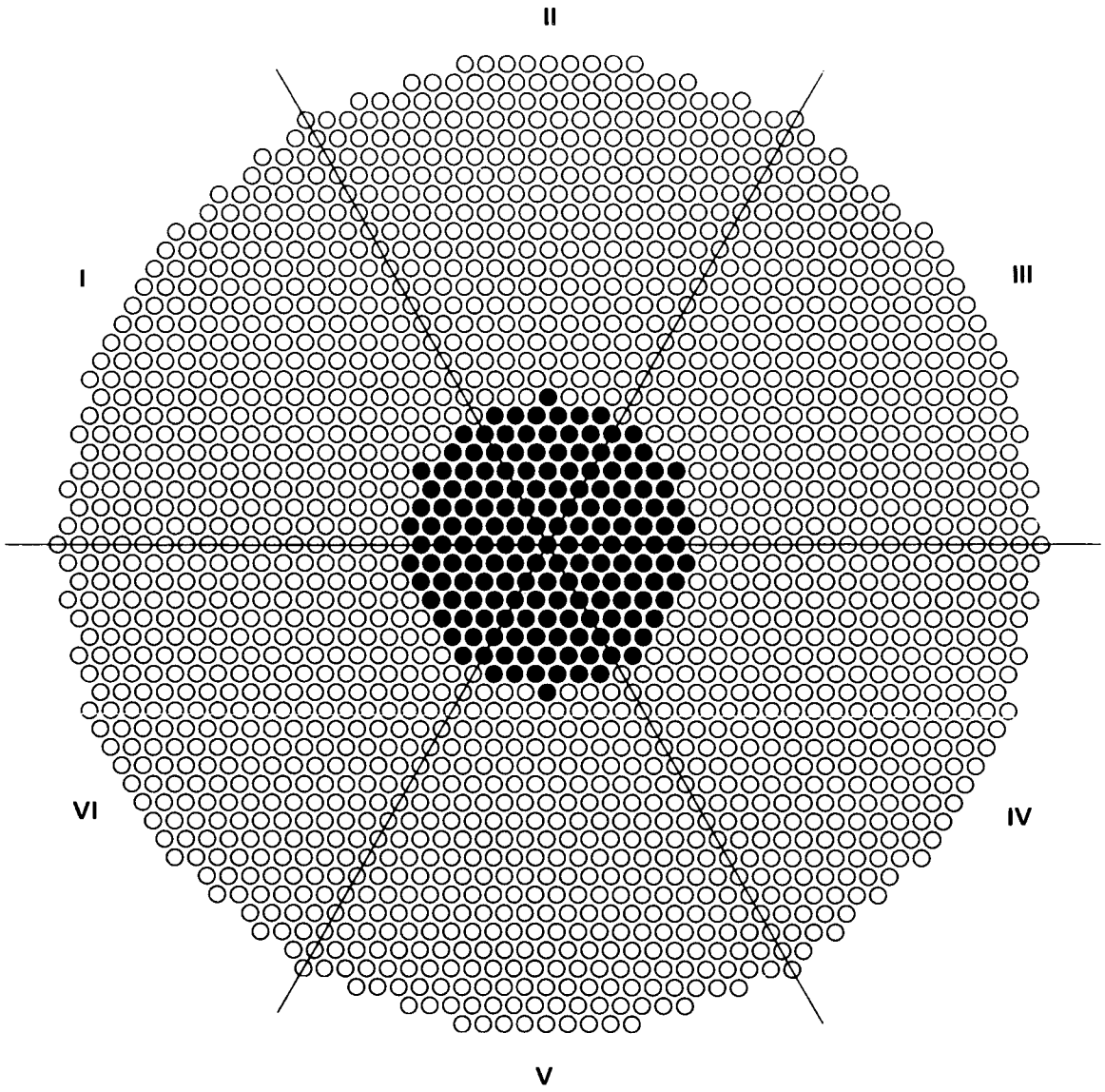

FUEL: 4.31 wt% ^{235}U ENRICHED UO_2

EXPERIMENT: 4.3-000-185

LATTICE: 11

PITCH: 2.398 ± 0.005

GADOLINIUM: 0.068 ± 0.001 g Gd/liter

CONTROL ROD: NONE

SAFETY ROD: NONE

REACTION RATES: NONE

RODS: 167 UO_2 RODS AT ●

k_{eff}: 1.0

COMMENTS:

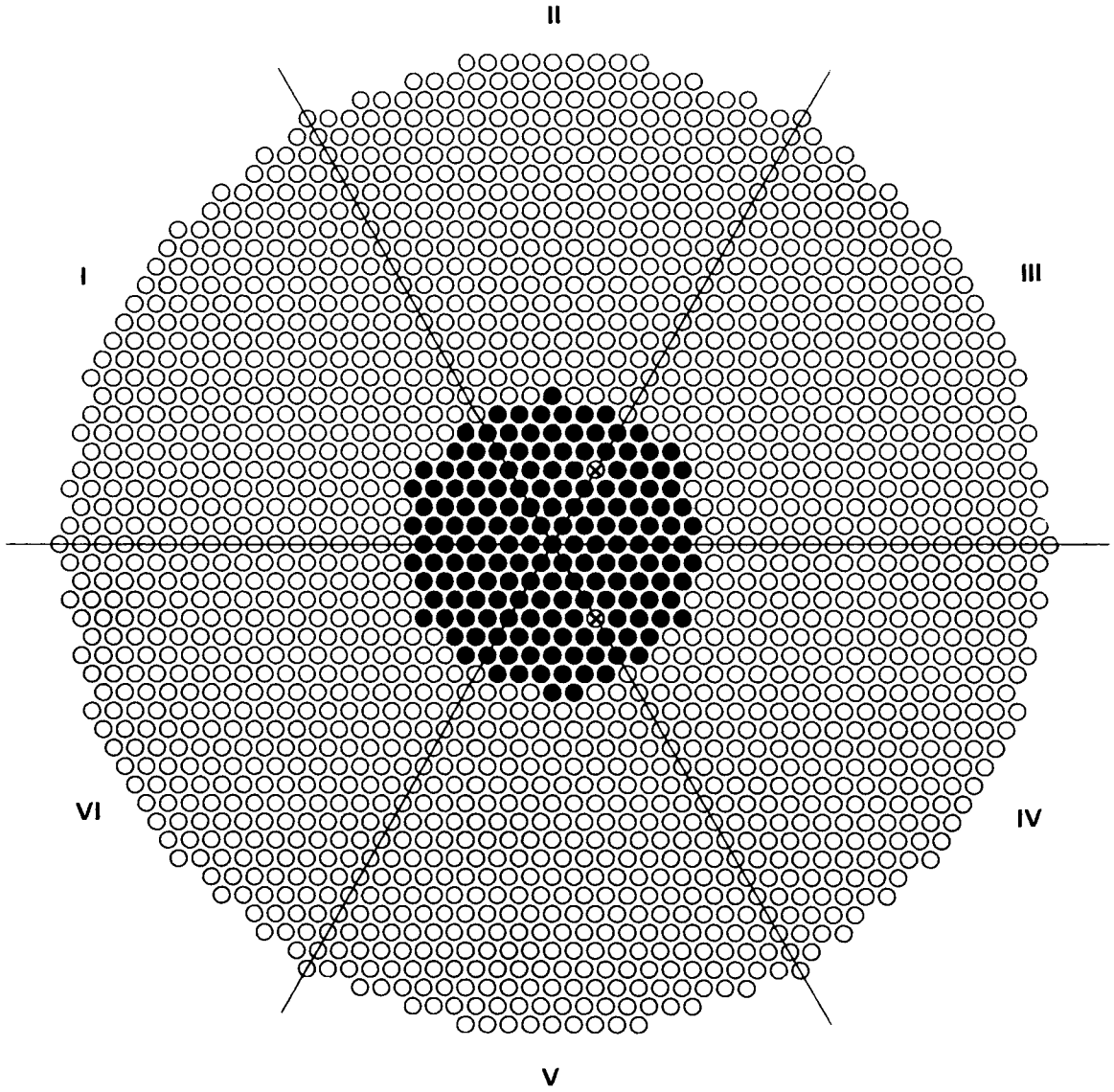

FUEL: 4.31 wt% ^{235}U ENRICHED UO_2

EXPERIMENT: 4.3-000-185A

LATTICE: 11

PITCH: 2.398 ± 0.005

GADOLINIUM: 0.068 ± 0.001 g Gd/liter

CONTROL ROD: OUT

SAFETY ROD: OUT

REACTION RATES: NONE

RODS: 170 UO_2 RODS AT ●

k_{eff}: 1.0

COMMENTS: WATER FILLED ALUMINUM SLEEVES AT ⊗

F.9

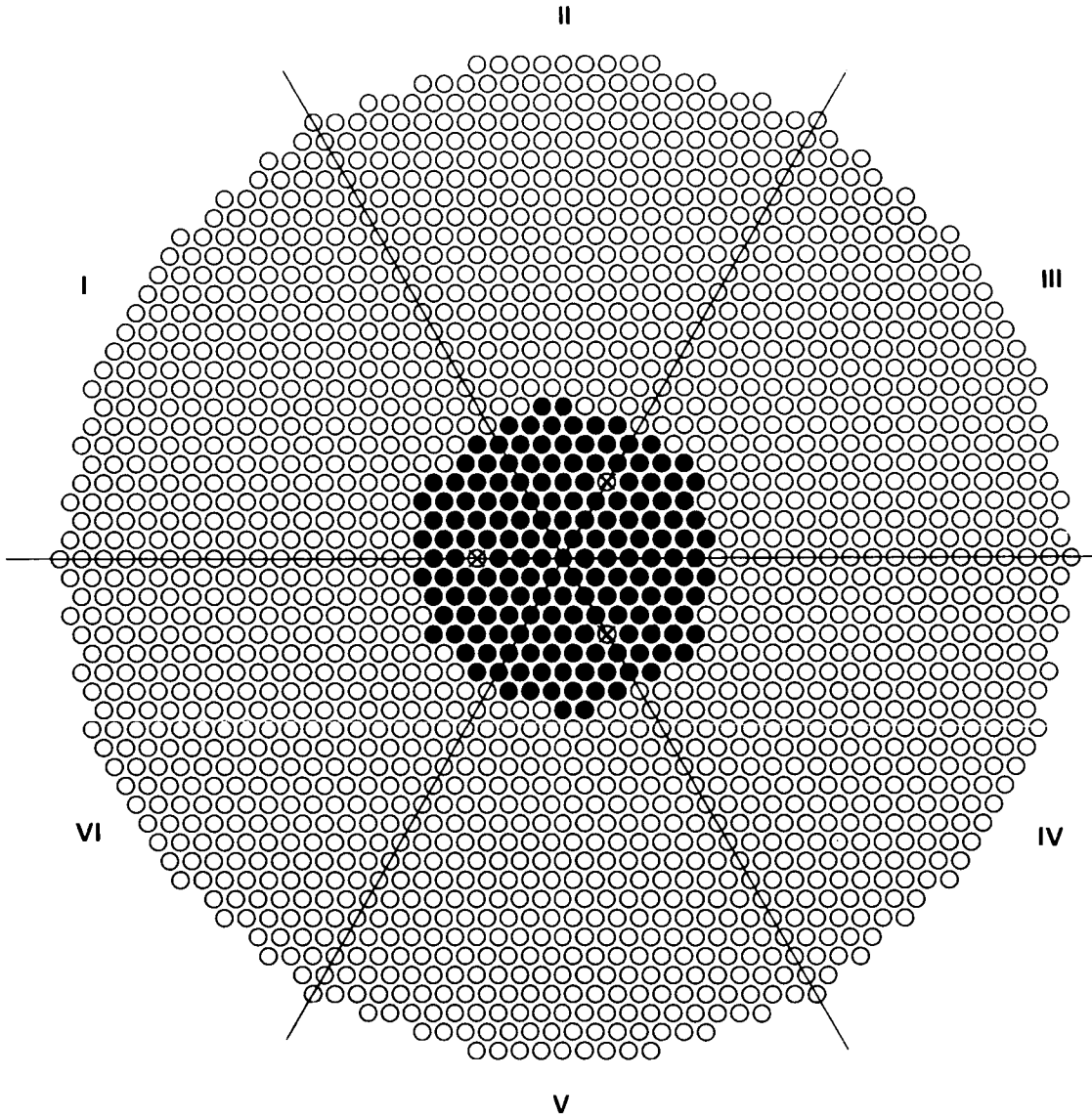

FUEL: 4.31 wt% ^{235}U ENRICHED UO_2

EXPERIMENT: 4.3-000-185B

LATTICE: 11

PITCH: 2.398 ± 0.005

GADOLINIUM: 0.068 ± 0.001 g Gd/liter

CONTROL ROD: OUT

SAFETY ROD: OUT

REACTION RATES: NONE

RODS: 171 UO_2 RODS AT ●

k_{eff}: 1.0

COMMENTS: WATER FILLED ALUMINUM SLEEVES AT ⊠

F.10

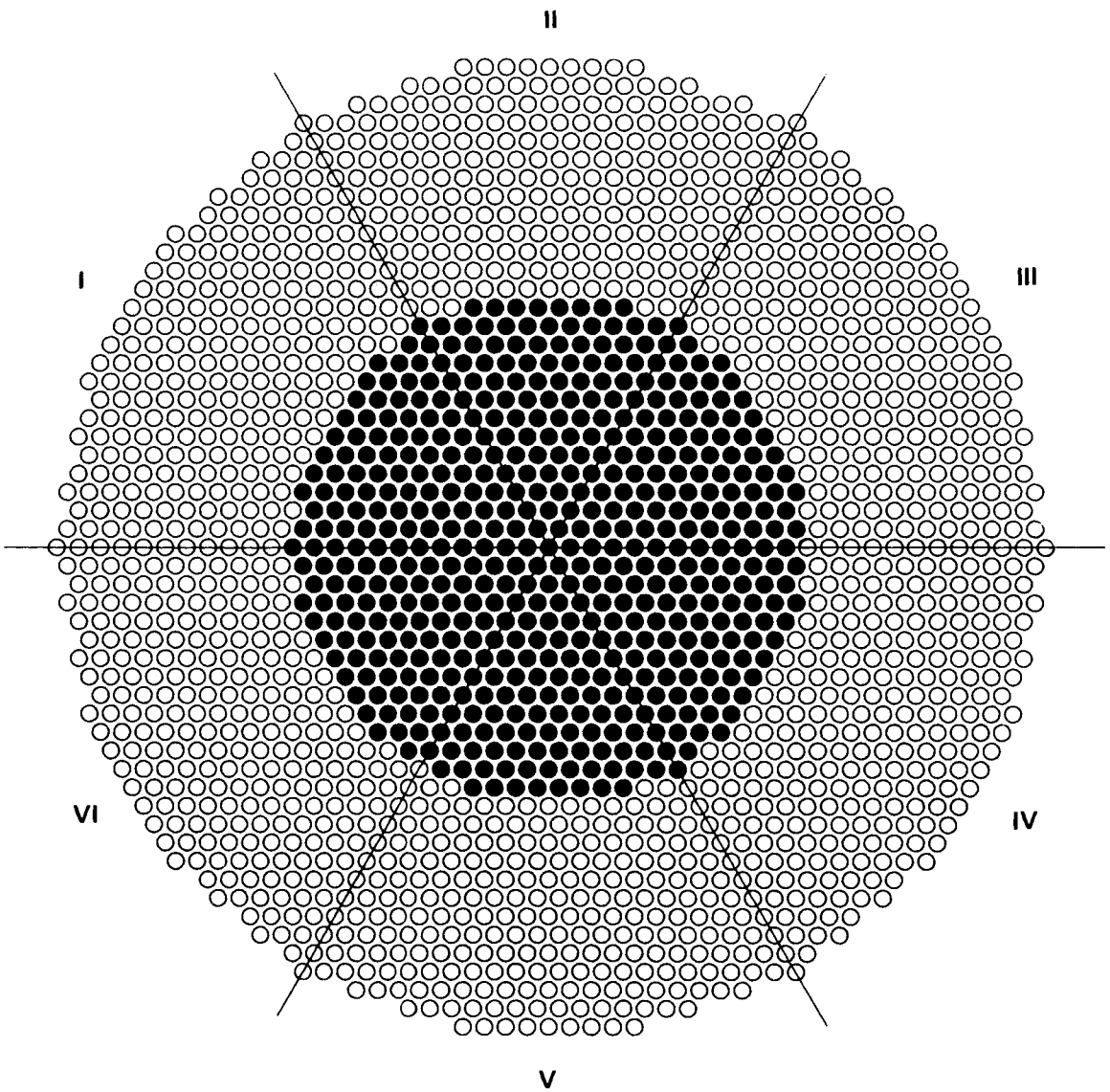

FUEL: 4.31 wt% ^{235}U ENRICHED UO_2

EXPERIMENT: 4.3-000-186

LATTICE: 11

PITCH: 2.398 ± 0.005

GADOLINIUM: 0.438 ± 0.004 g Gd/liter

CONTROL ROD: NONE

SAFETY ROD: NONE

REACTION RATES: NONE

RODS: 515 UO_2 RODS AT ●

k_{eff}: 1.0

COMMENTS:

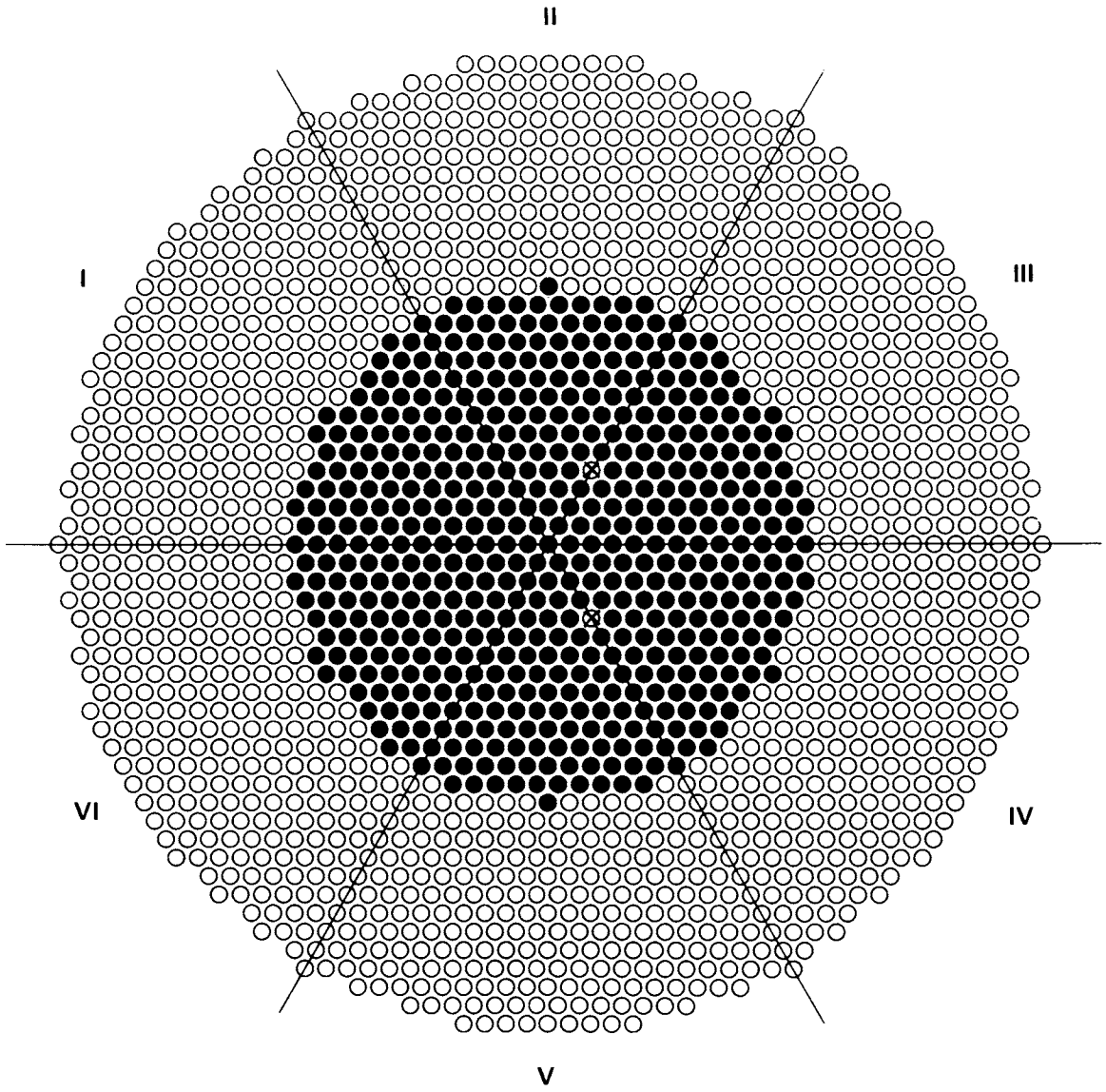

FUEL: 4.31 wt% ^{235}U ENRICHED UO_2

EXPERIMENT: 4.3-000-186A

LATTICE: 11

PITCH: 2.398 ± 0.005

GADOLINIUM: 0.438 ± 0.004 g Gd/liter

CONTROL ROD: OUT

SAFETY ROD: OUT

REACTION RATES: NONE

RODS: 536 UO_2 RODS AT ●

k_{eff}: 1.0

COMMENTS: WATER FILLED ALUMINUM SLEEVES AT ⊗

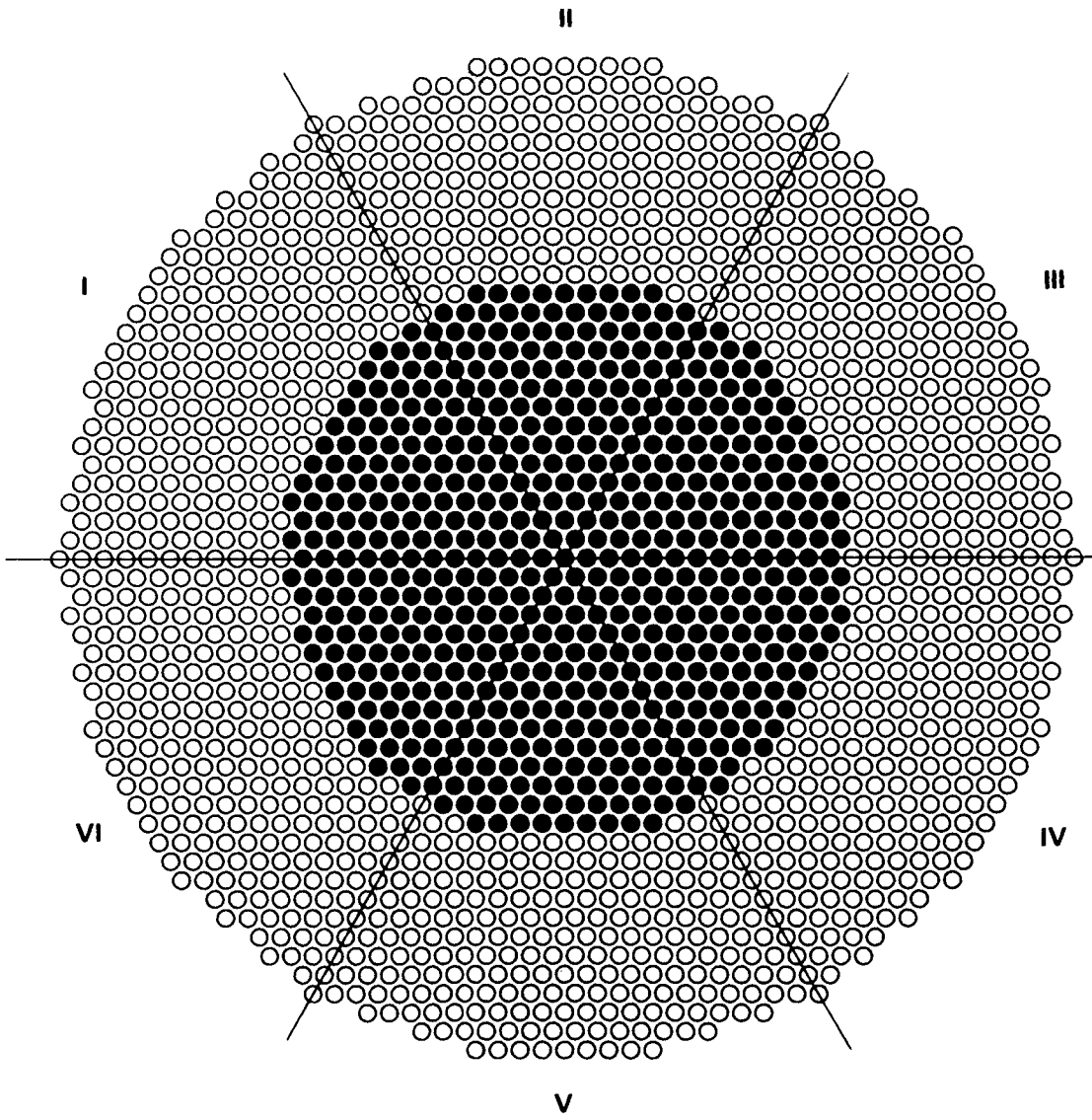

FUEL: 4.31 wt% ^{235}U ENRICHED UO_2

EXPERIMENT: 4.3-000-188

LATTICE: 11

PITCH: 2.398 ± 0.005

GADOLINIUM: SEE COMMENTS

CONTROL ROD: NONE

SAFETY ROD: NONE

REACTION RATES: NONE

RODS: 593 UO_2 RODS AT ●

k_{eff}: SEE COMMENTS

COMMENTS:

k_{eff} = 1.00 AT 0.482 ± 0.001 g Gd/liter
k_{eff} = 0.975 AT 0.549 ± 0.008 g Gd/liter
k_{eff} = 0.944 AT 0.639 ± 0.017 g Gd/liter
k_{eff} = 0.861 AT 0.788 ± 0.011 g Gd/liter

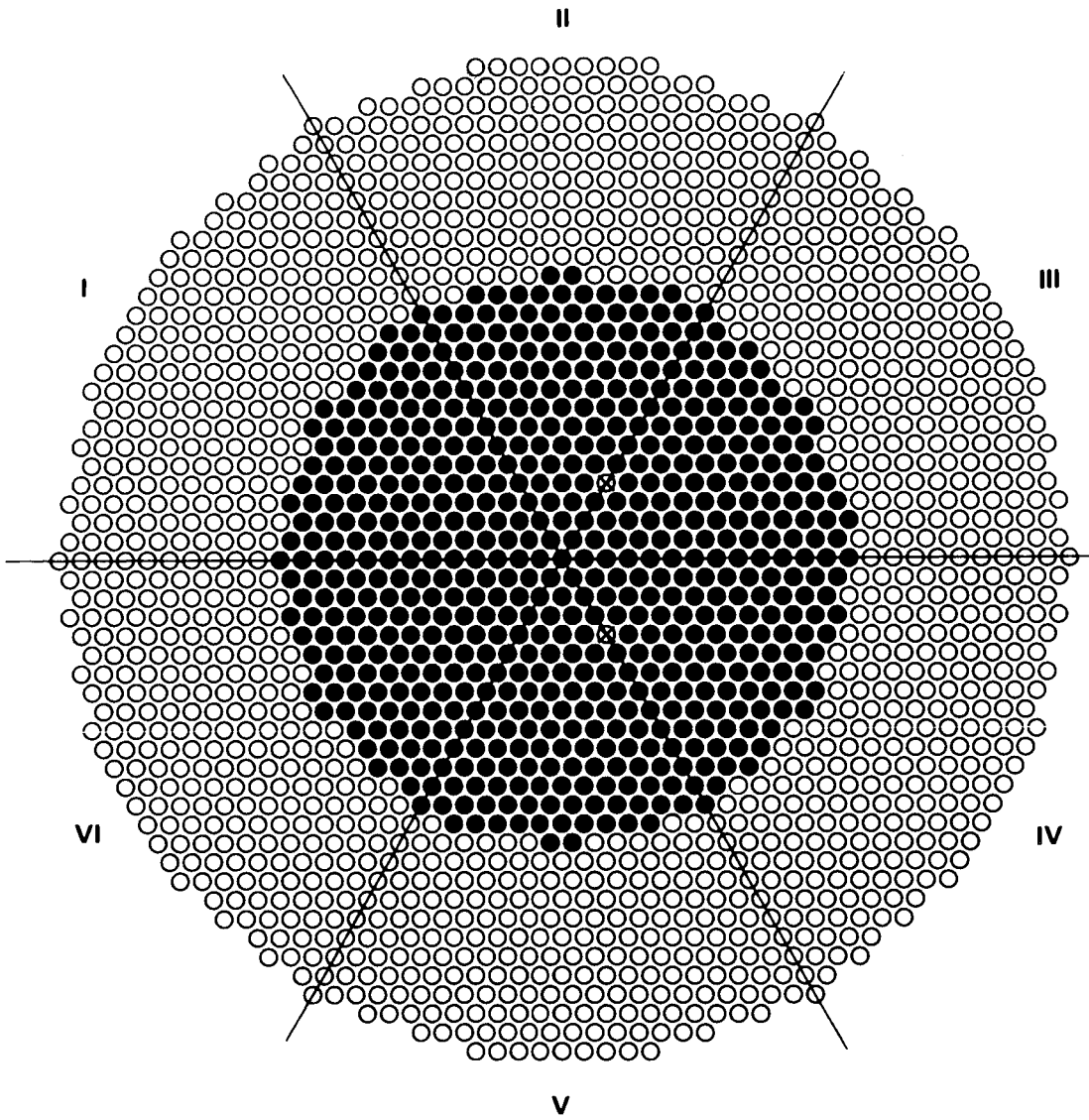

FUEL: 4.31 wt% ^{235}U ENRICHED UO_2

EXPERIMENT: 4.3-000-188A

LATTICE: 11

PITCH: 2.398 ± 0.005

GADOLINIUM: 0.482 ± 0.001 g Gd/liter

CONTROL ROD: OUT

SAFETY ROD: OUT

REACTION RATES: NONE

RODS: 615 UO_2 RODS AT ●

k_{eff}: 1.0

COMMENTS: WATER FILLED ALUMINUM SLEEVES AT ⊗

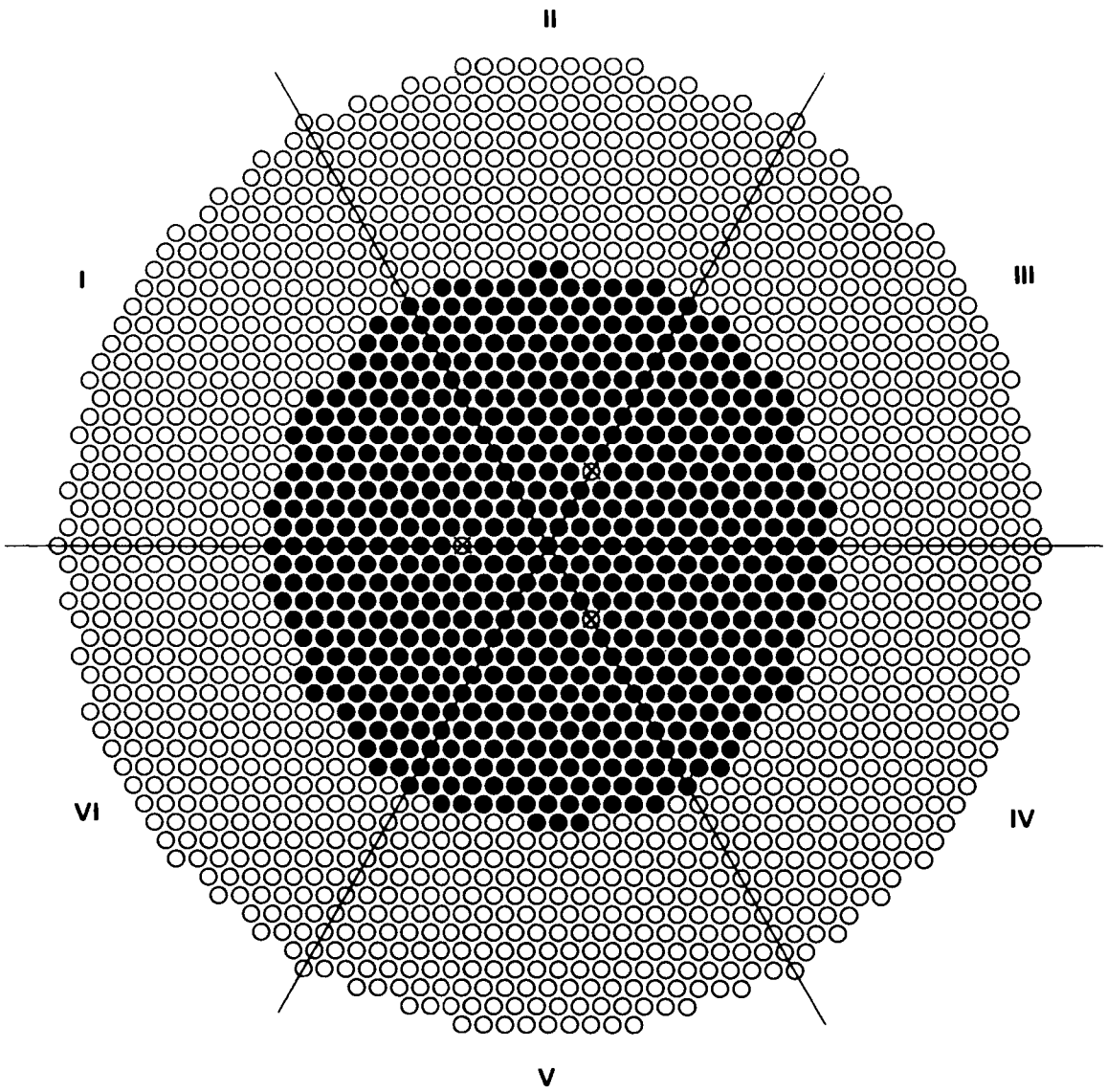

FUEL: 4.31 wt% ^{235}U ENRICHED UO_2

EXPERIMENT: 4.3-000-188B

LATTICE: 11

PITCH: 2.398 ± 0.005

GADOLINIUM: 0.482 ± 0.001 g Gd/liter

CONTROL ROD: OUT

SAFETY ROD: OUT

REACTION RATES: NONE

RODS: 625 UO_2 RODS AT ●

k_{eff}: 1.0

COMMENTS: WATER FILLED ALUMINUM SLEEVES AT ⊗

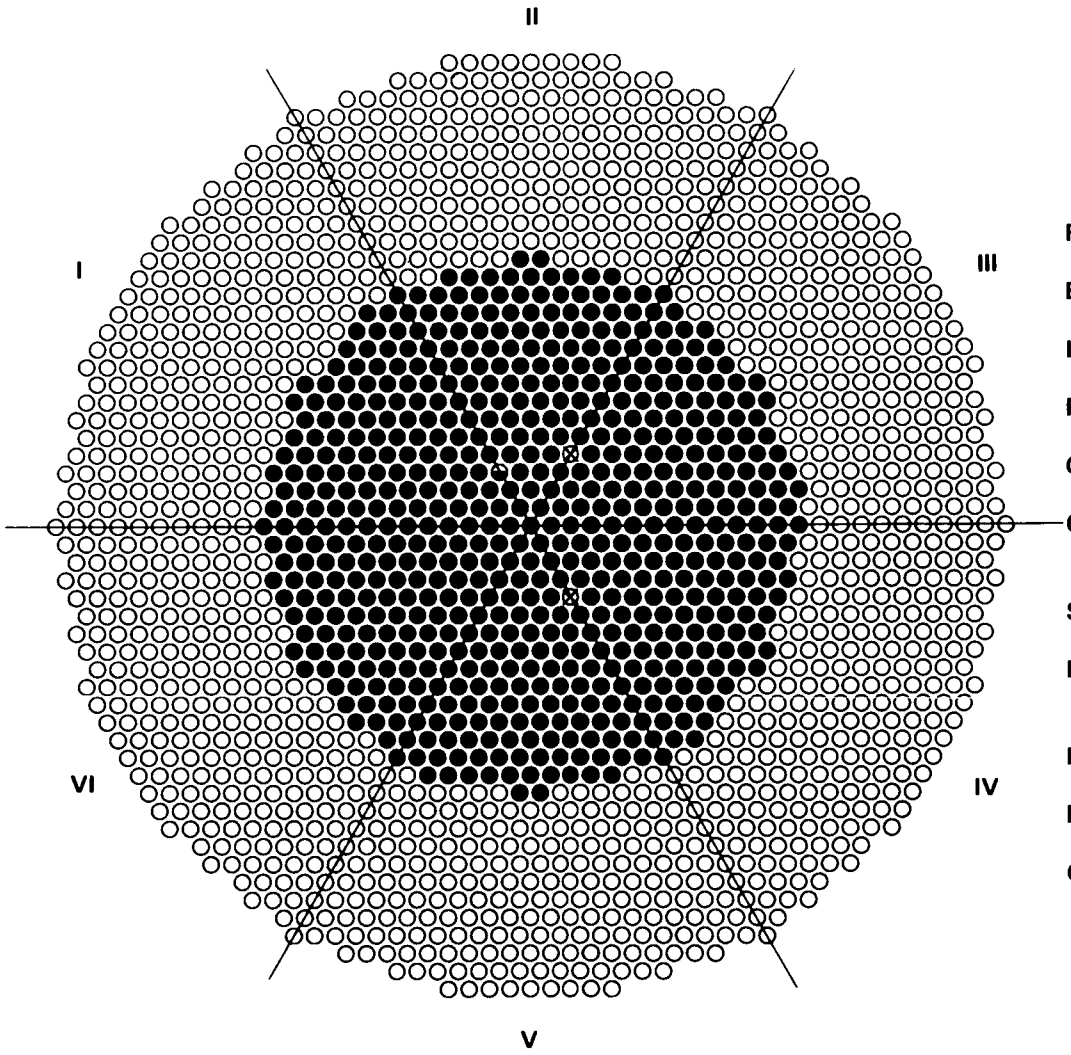

FUEL: 4.31 wt% ^{235}U ENRICHED UO_2

EXPERIMENT: 4.3-000-188C

LATTICE: 11

PITCH: 2.398 ± 0.005

GADOLINIUM: 0.482 ± 0.001 g Gd/liter

CONTROL ROD: OUT 29.2 ± 0.3 cm FROM BOTTOM OF FUEL (LOCATION V ⊠)

SAFETY ROD: OUT

REACTION RATES: SOLID STATE ^{235}U TRACK RECORDER IN ⊖

RODS: 615 UO_2 RODS AT ●

k_{eff}: 1.0

COMMENTS: CONTROL AND SAFETY ROD ALUMINUM GUIDE SLEEVES AT ⊠

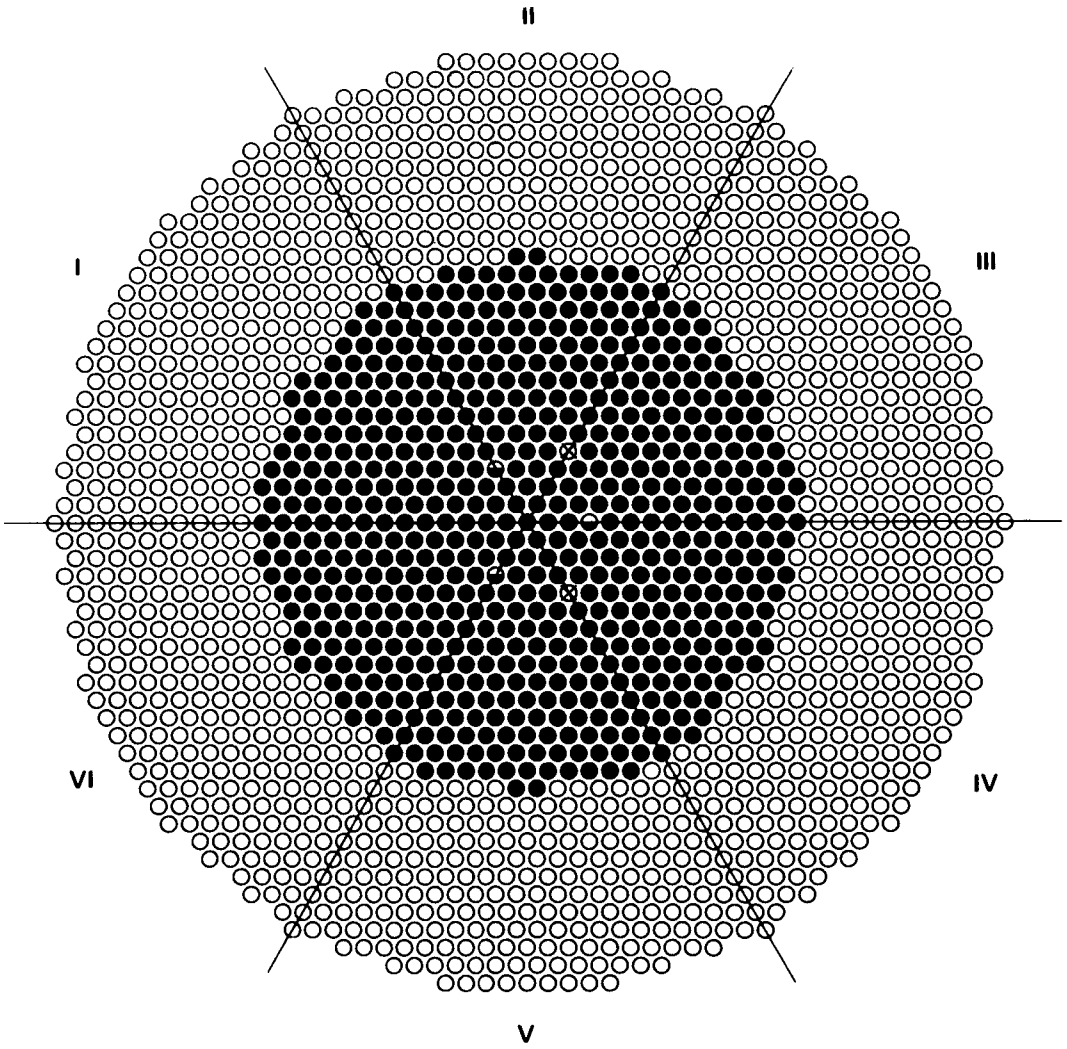

FUEL: 4.31 wt% ^{235}U ENRICHED UO_2

EXPERIMENT: 4.3-000-188D

LATTICE: 11

PITCH: 2.398 ± 0.005

GADOLINIUM: 0.482 ± 0.001 g Gd/liter

CONTROL ROD: OUT 26.0 ± 0.3 cm FROM BOTTOM OF FUEL (LOCATION V ⊗)

SAFETY ROD: OUT

REACTION RATES: ^{238}U AND ^{235}U FOILS IN ◒ (SEE COMMENTS)

RODS: 620 UO_2 RODS AT ●

k_{eff}: 1.0

COMMENTS: CONTROL AND SAFETY ROD ALUMINUM GUIDE SLEEVES AT ⊗
AEEW 2 FOIL PACKET IN II ◒
AEEW 5 FOIL PACKET IN IV ◒
AEEW 1 FOIL PACKET IN VI ◒

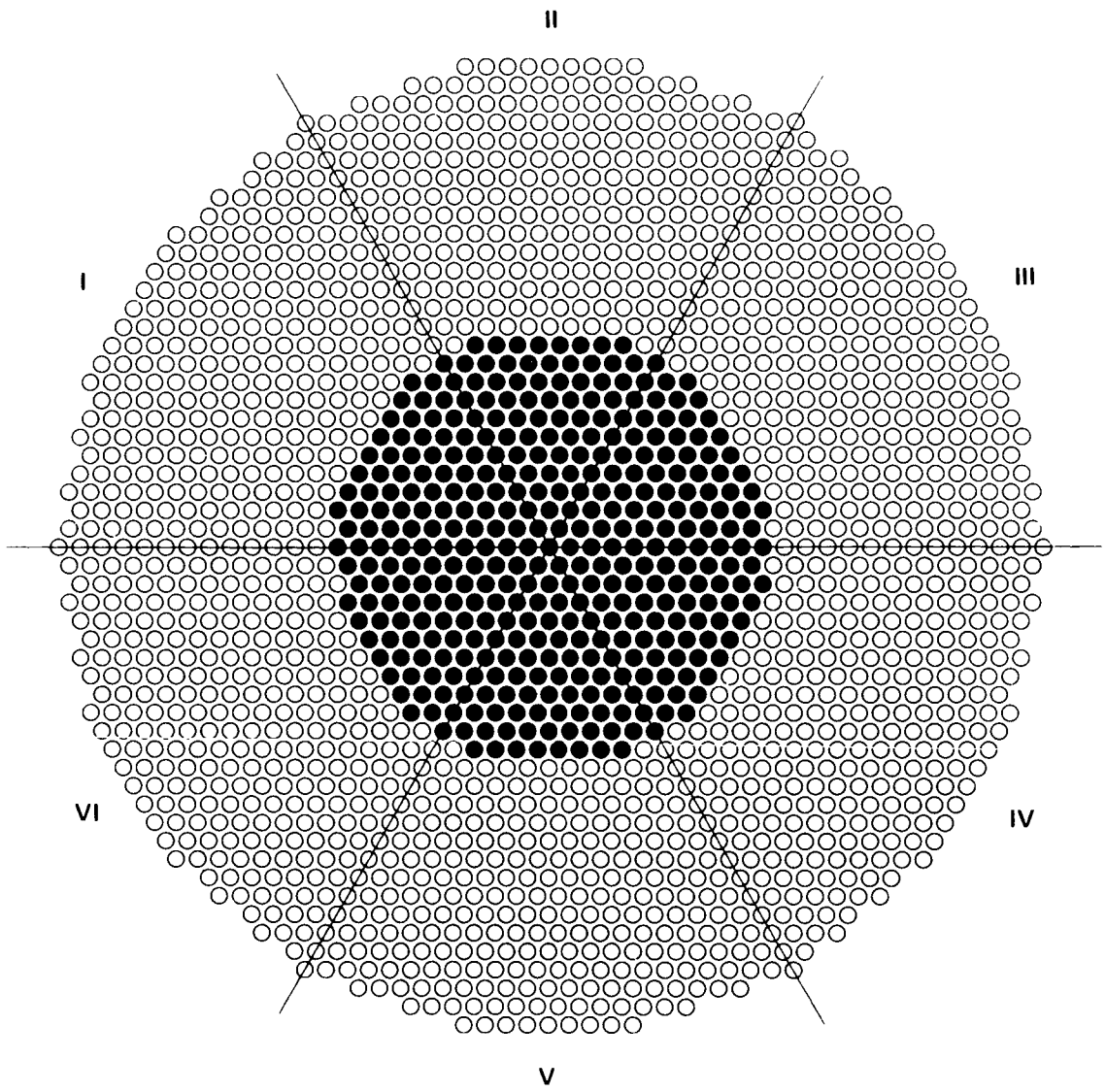

FUEL: 4.31 wt% ^{235}U ENRICHED UO_2

EXPERIMENT: 4.3-000-192

LATTICE: 12

PITCH: 1.801 ± 0.005 cm

GADOLINIUM: SEE COMMENTS

CONTROL ROD: NONE

SAFETY ROD: NONE

REACTION RATES: NONE

RODS: 378 UO_2 RODS AT ●

k_{eff}: SEE COMMENTS

COMMENTS: k_{eff} = 1.0 @ ZERO g Gd/liter
k_{eff} = 0.938 @ 0.122 ± 0.001 g Gd/liter

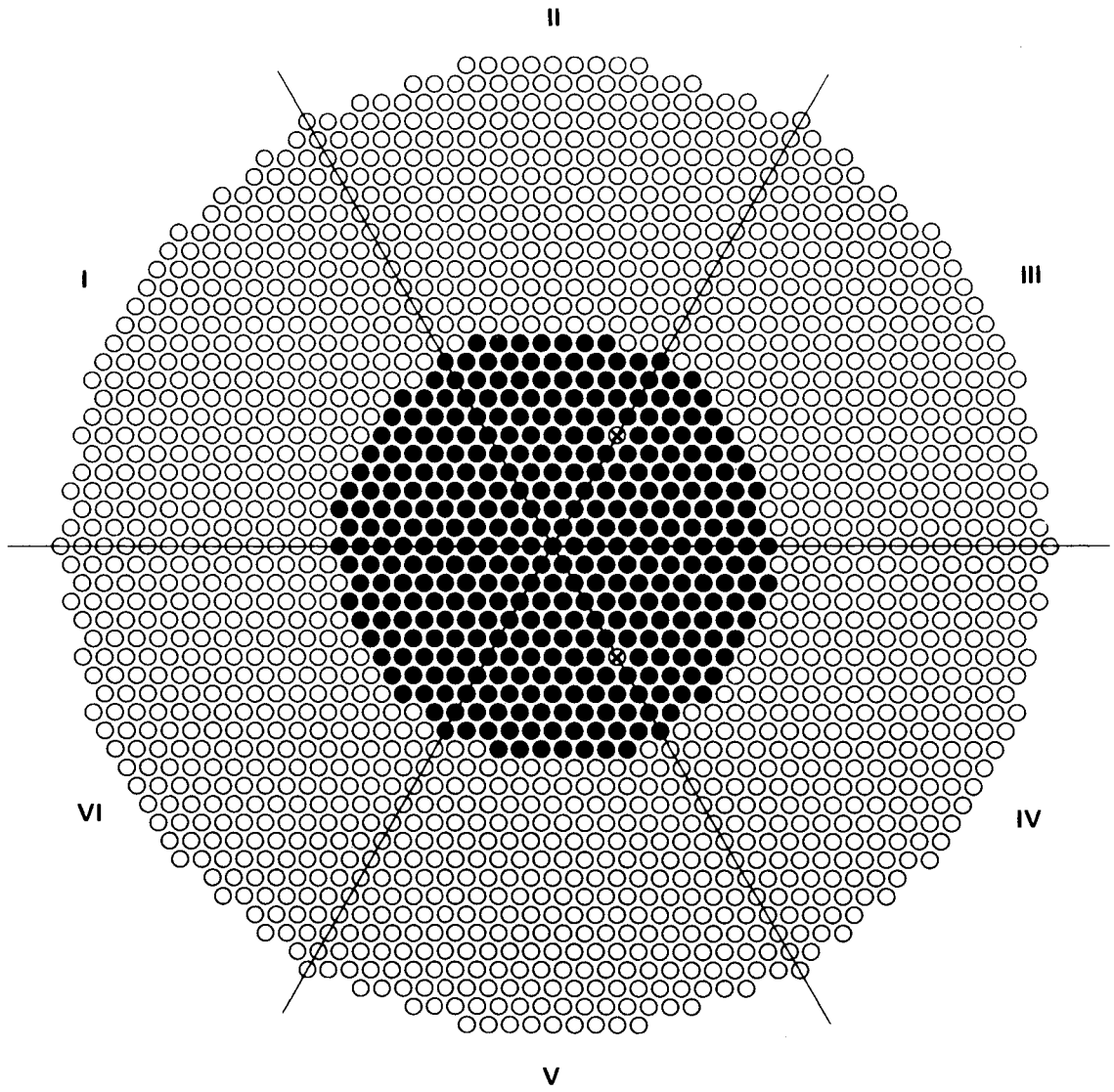

FUEL: 4.31 wt% ^{235}U ENRICHED UO_2

EXPERIMENT: 4.3-000-192A

LATTICE: 12

PITCH: 1.801 ± 0.005 cm

GADOLINIUM: NONE

CONTROL ROD: OUT

SAFETY ROD: OUT

REACTION RATES: NONE

RODS: 370 UO_2 RODS AT ●

k_{eff}: 1.0

COMMENTS: WATER FILLED ALUMINUM SLEEVES AT ⊗

F°19

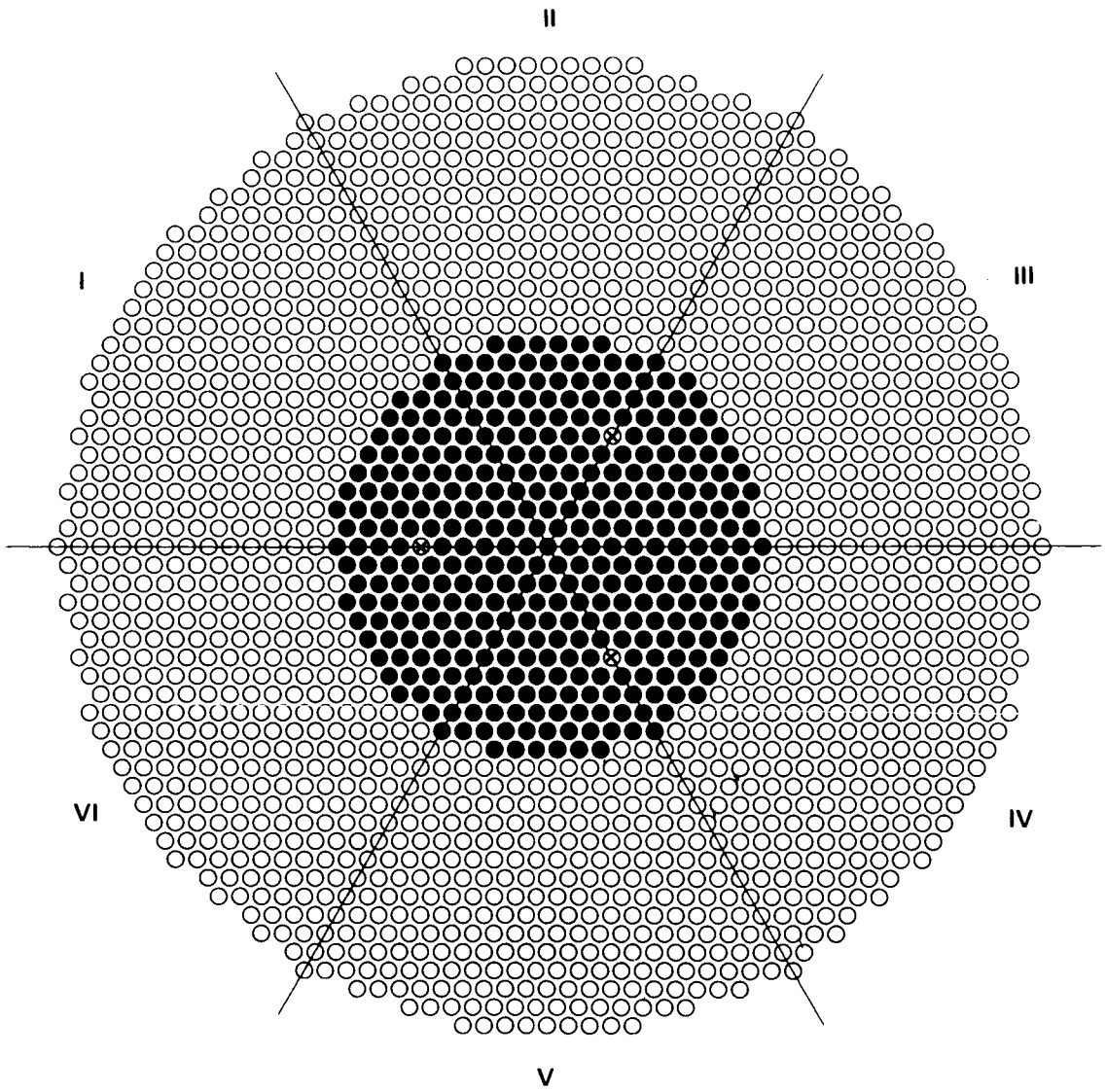

FUEL: 4.31 wt% ^{235}U ENRICHED UO_2

EXPERIMENT: 4.3-000-192B

LATTICE: 12

PITCH: 1.802 ± 0.005 cm

GADOLINIUM: NONE

CONTROL ROD: OUT

SAFETY ROD: OUT

REACTION RATES: NONE

RODS: 366 UO_2 RODS AT ●

k_{eff}: 1.0

COMMENTS: WATER FILLED ALUMINUM SLEEVES AT ⊗

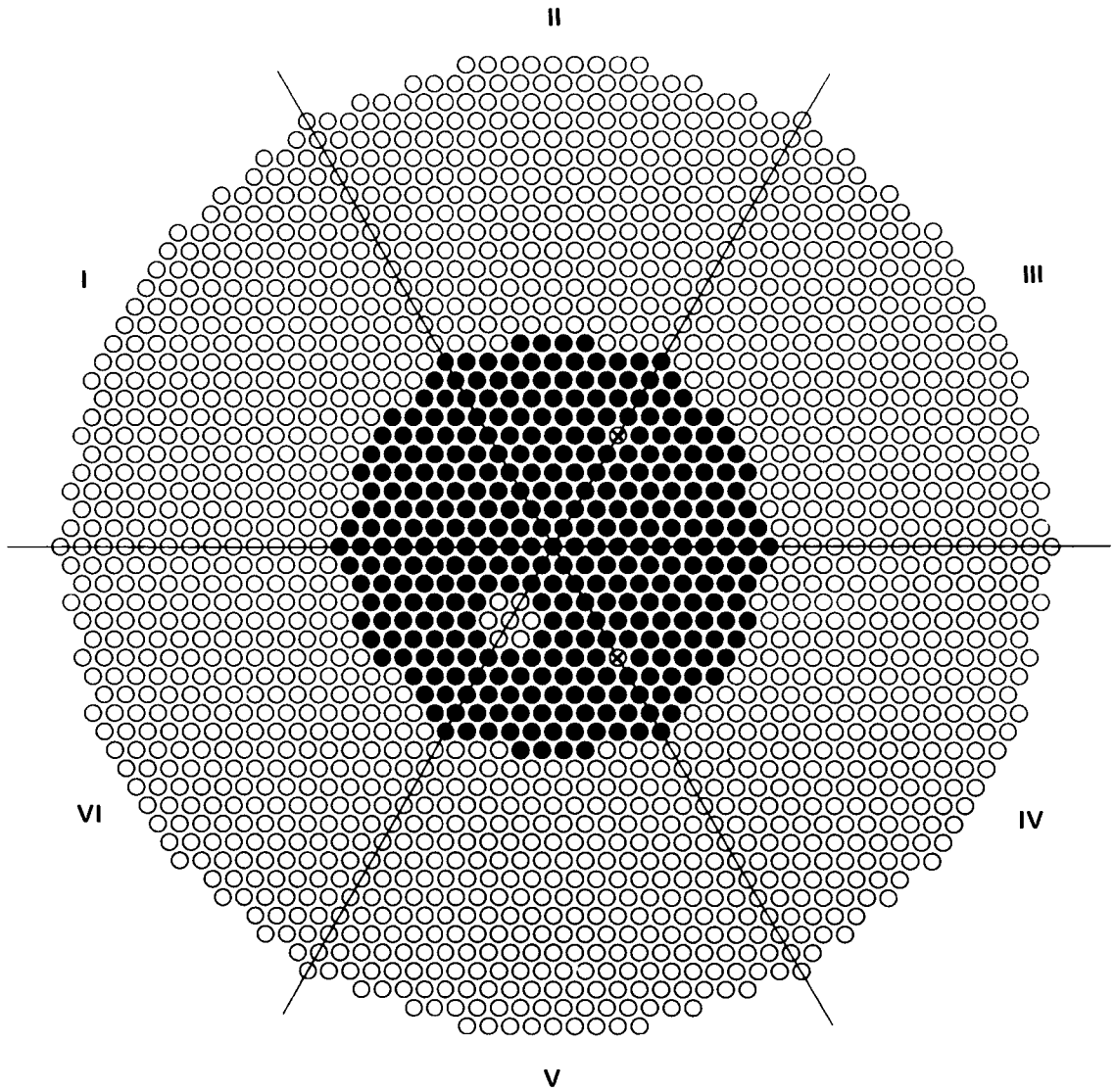

FUEL: 4.31 wt% ^{235}U ENRICHED UO_2

EXPERIMENT: 4.3-000-192C

LATTICE: 12

PITCH: 1.801 ± 0.005 cm

GADOLINIUM: NONE

CONTROL ROD: OUT

SAFETY ROD: OUT

REACTION RATES: NONE

RODS: 345 UO_2 RODS AT ●

k_{eff}: 1.0

COMMENTS: WATER FILLED ALUMINUM SLEEVES AT ⊗

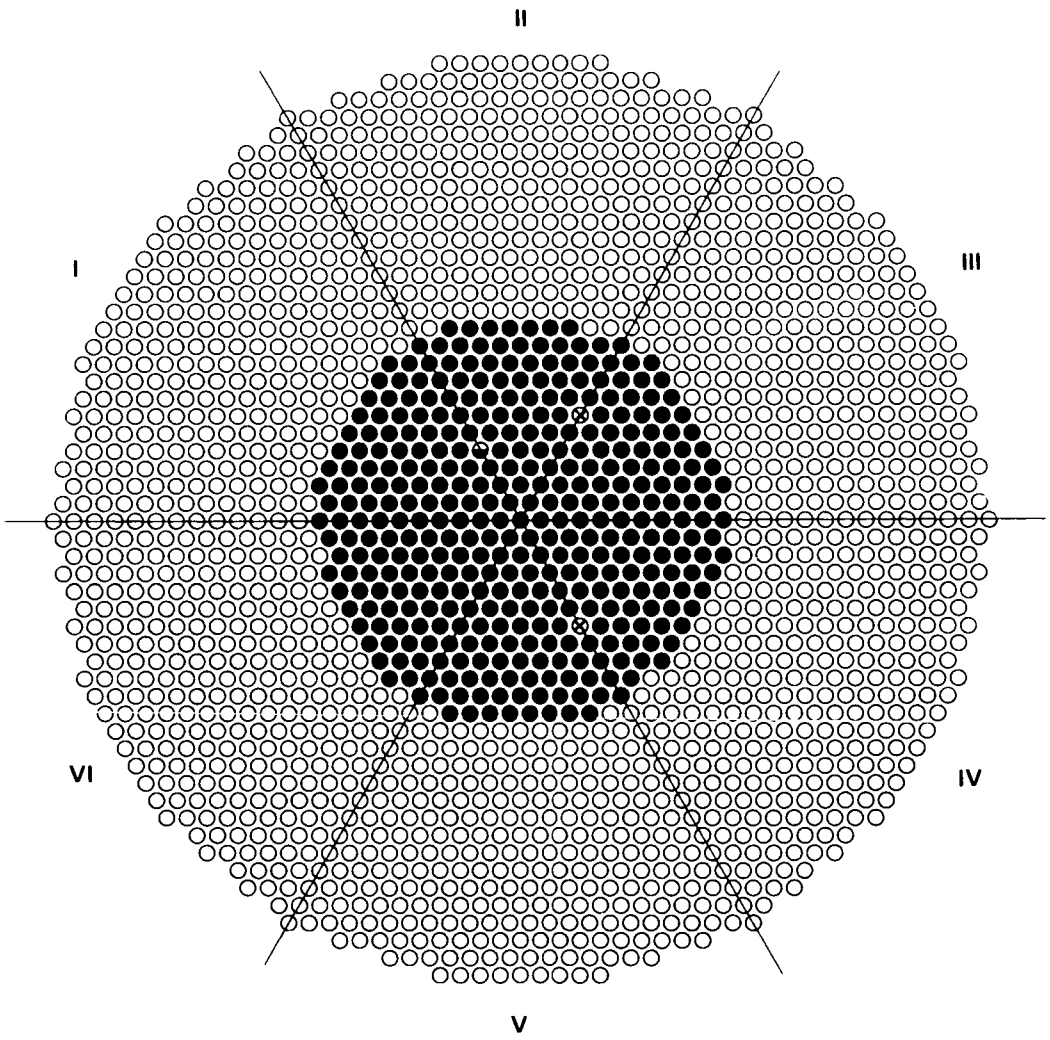

FUEL: 4.31 wt% ^{235}U ENRICHED UO_2

EXPERIMENT: 4.3-000-192D

LATTICE: 12

PITCH: 1.801 ± 0.005 cm

GADOLINIUM: NONE

CONTROL ROD: OUT 52.2 ± 0.3 cm FROM BOTTOM OF FUEL (LOCATION V ⊠)

SAFETY ROD: OUT

REACTION RATES: SOLID STATE ^{235}U TRACK RECORDER AT ◒

RODS: 374 UO_2 RODS AT ●

k_{eff}: 1.0

COMMENTS: CONTROL AND SAFETY ROD ALUMINUM GUIDE SLEEVES AT ⊗

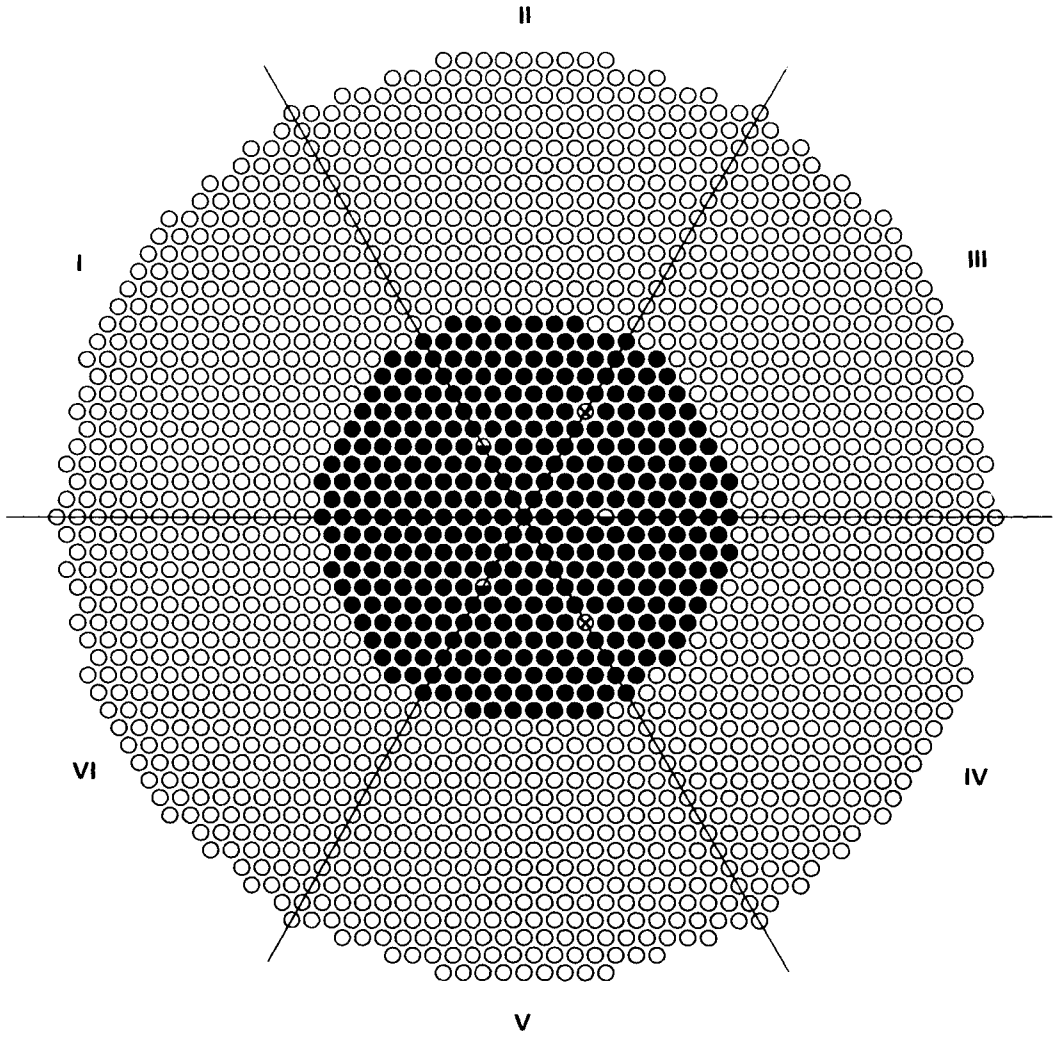

FUEL: 4.31 wt% ^{235}U ENRICHED UO_2

EXPERIMENT: 4.3-000-192E

LATTICE: 12

PITCH: 1.801 ± 0.005 cm

GADOLINIUM: NONE

CONTROL ROD: OUT 50.0 ± 0.3 cm FROM BOTTOM OF FUEL (LOCATION V ⊗)

SAFETY ROD: OUT

REACTION RATES: ^{238}U AND ^{235}U FOILS IN ◒ (SEE COMMENTS)

RODS: 373 UO_2 RODS AT ●

k_{eff}: 1.0

COMMENTS: CONTROL AND SAFETY ROD ALUMINUM GUIDE SLEEVES AT ⊗
AEEW 8 FOIL PACKET IN II ◒
AEEW 6 FOIL PACKET IN IV ◒
AEEW 7 FOIL PACKET IN VI ◒

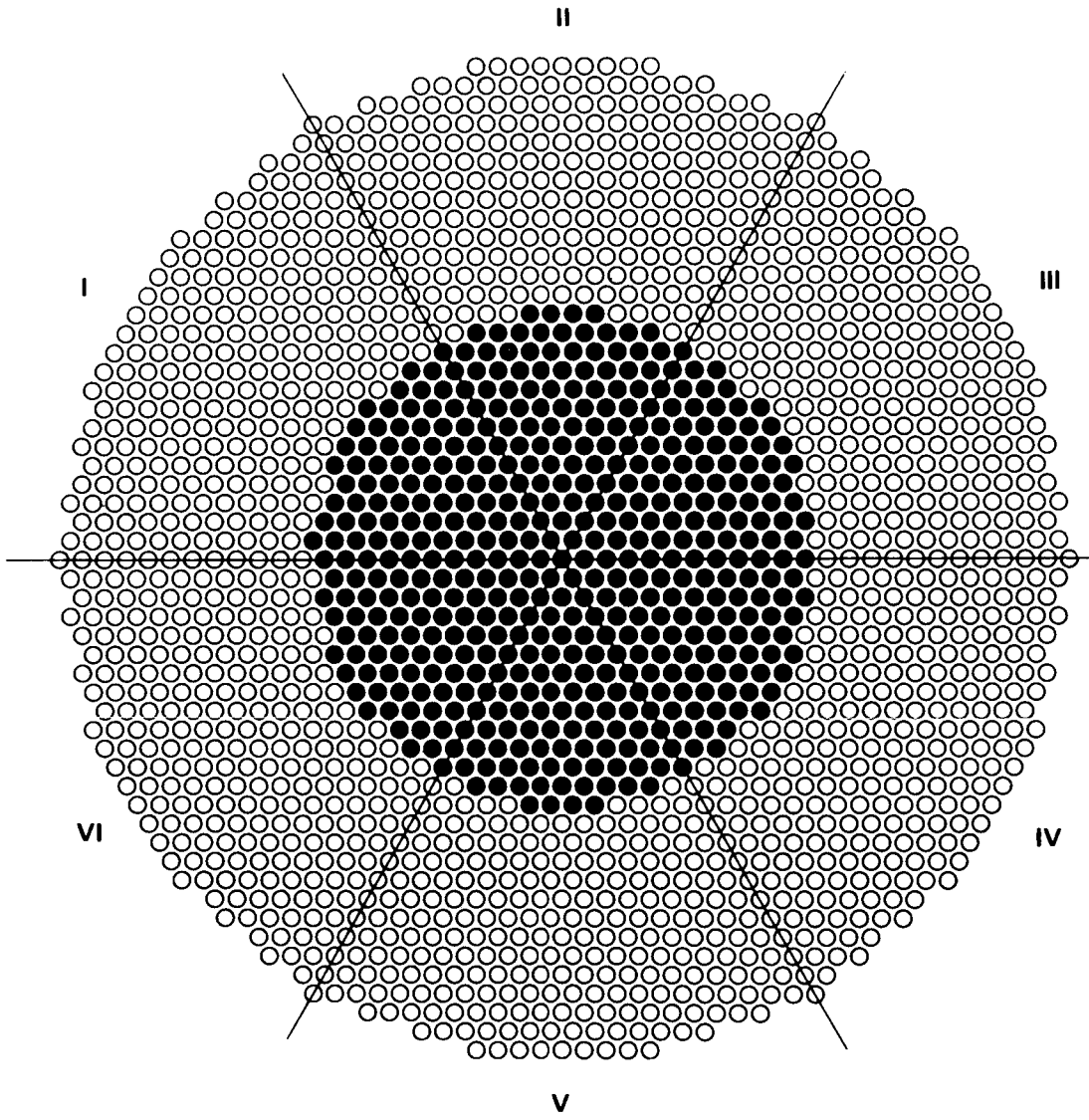

FUEL: 4.31 wt% ^{235}U ENRICHED UO_2

EXPERIMENT: 4.3-000-201

LATTICE: 12

PITCH: 1.801 ± 0.005 cm

GADOLINIUM: 0.122 ± 0.001 g Gd/liter

CONTROL ROD: NONE

SAFETY ROD: NONE

REACTION RATES: NONE

RODS: 476 UO_2 RODS AT ●

k_{eff}: 1.0

COMMENTS:

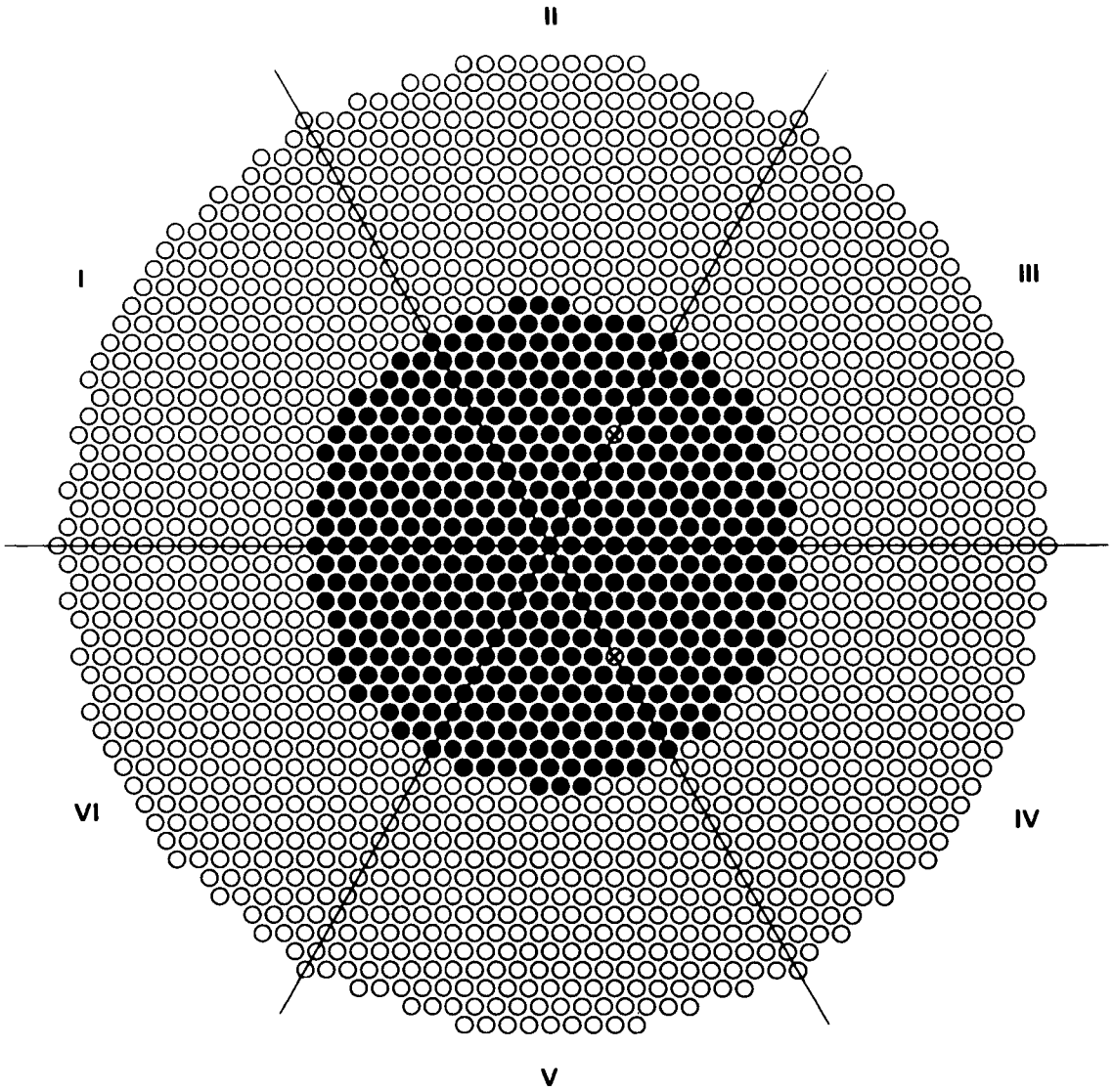

FUEL: 4.31 wt% ^{235}U ENRICHED UO_2

EXPERIMENT: 4.3-000-201A

LATTICE: 12

PITCH: 1.801 ± 0.005 cm

GADOLINIUM: 0.122 ± 0.001 g Gd/liter

CONTROL ROD: OUT

SAFETY ROD: OUT

REACTION RATES: NONE

RODS: 468 UO_2 RODS AT ●

k_{eff}: 1.0

COMMENTS: WATER FILLED ALUMINUM SLEEVES AT ⊗

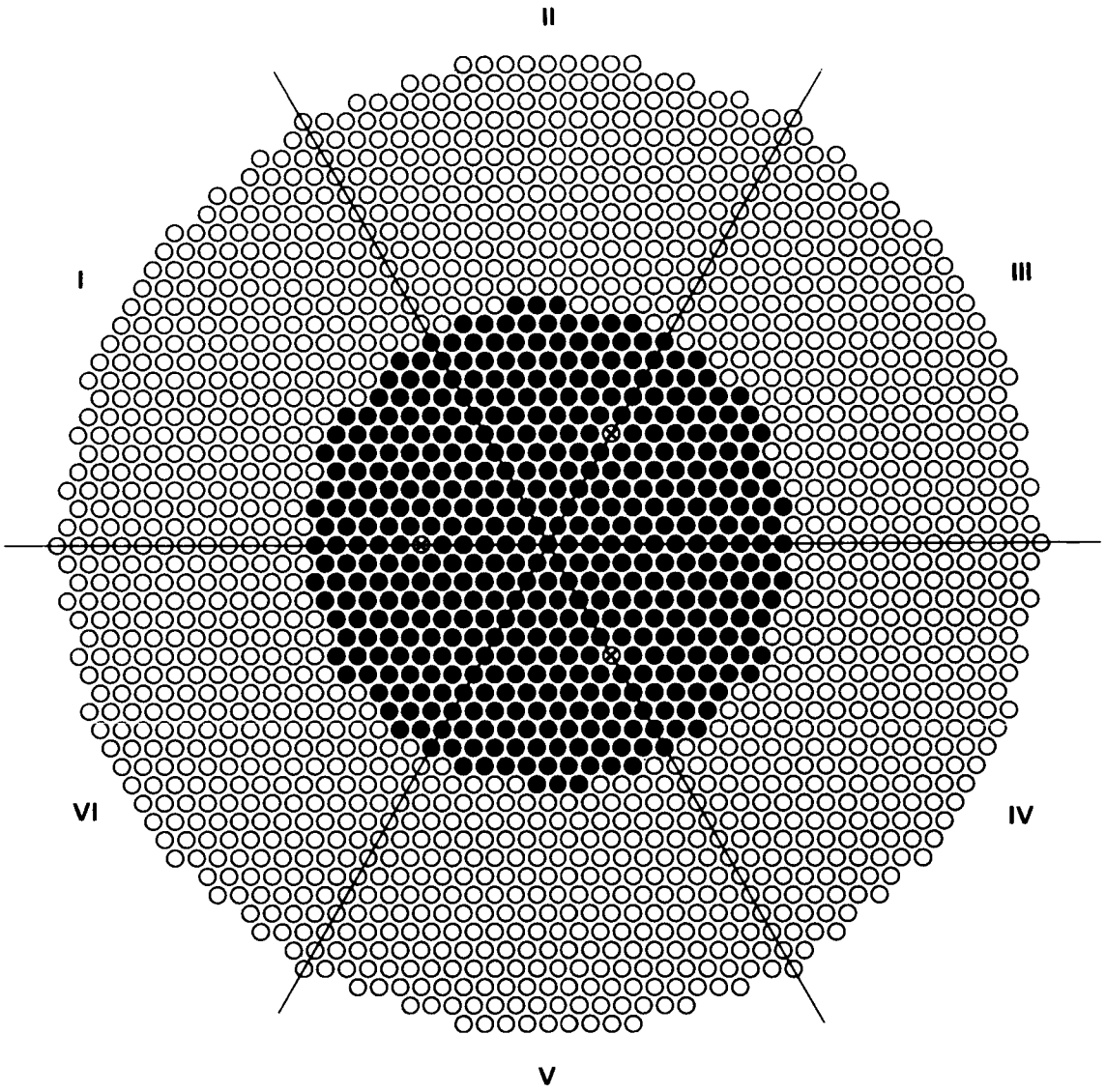

FUEL: 4.31 wt% ^{235}U ENRICHED UO_2

EXPERIMENT: 4.3-000-201B

LATTICE: 12

PITCH: 1.801 ± 0.005 cm

GADOLINIUM: 0.122 ± 0.001 g Gd/liter

CONTROL ROD: OUT

SAFETY ROD: OUT

REACTION RATES: NONE

RODS: 464 UO_2 RODS AT ●

k_{eff}: 1.0

COMMENTS: WATER FILLED ALUMINUM SLEEVES AT ⊗

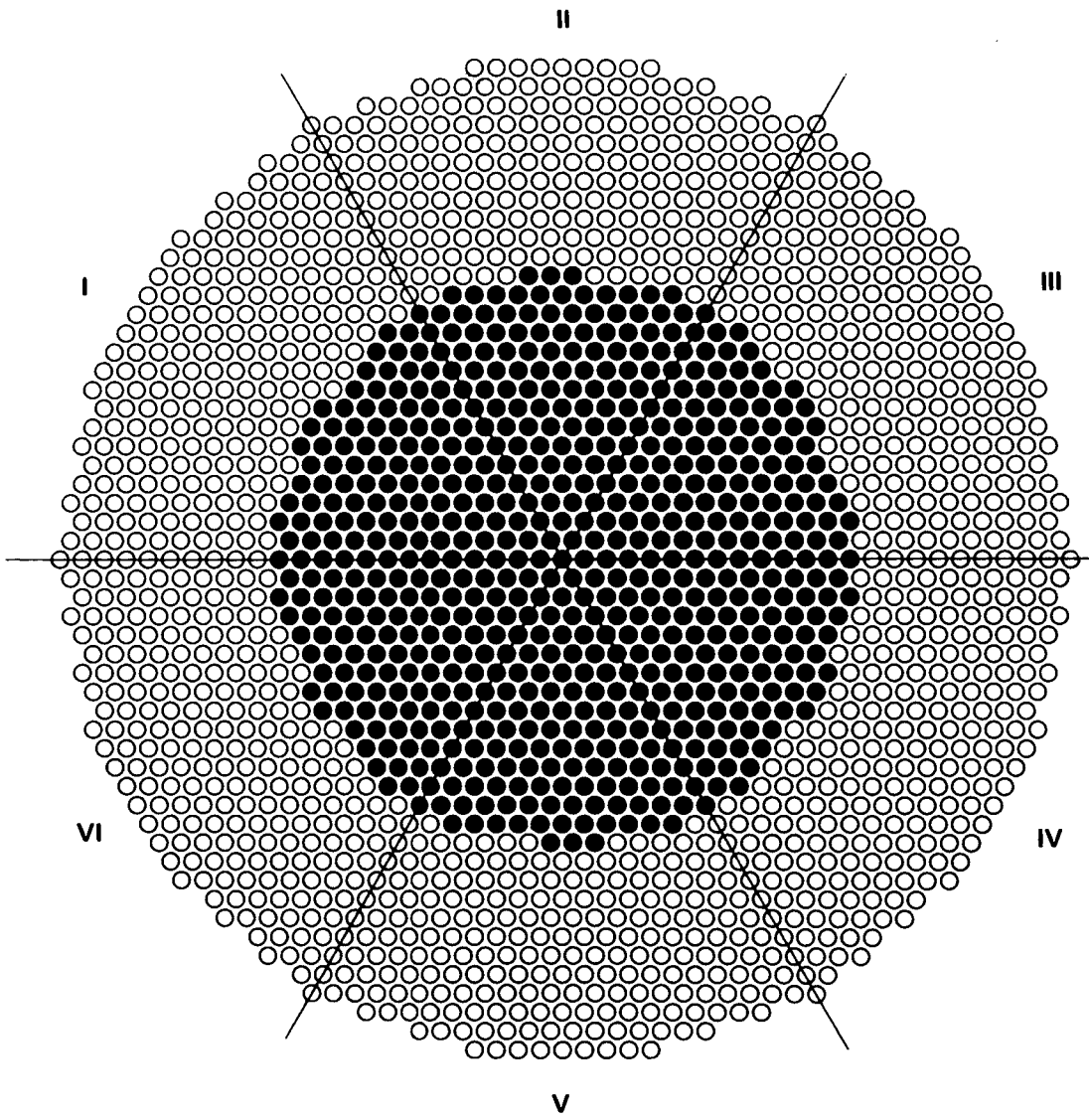

FUEL: 4.31 wt% ^{235}U ENRICHED UO_2

EXPERIMENT: 4.3-000-202

LATTICE: 12

PITCH: 1.801 ± 0.005 cm

GADOLINIUM: 0.400 ± 0.021 g Gd/liter

CONTROL ROD: NONE

SAFETY ROD: NONE

REACTION RATES: NONE

RODS: 630 UO_2 RODS AT ●

k_{eff}: 1.0

COMMENTS:

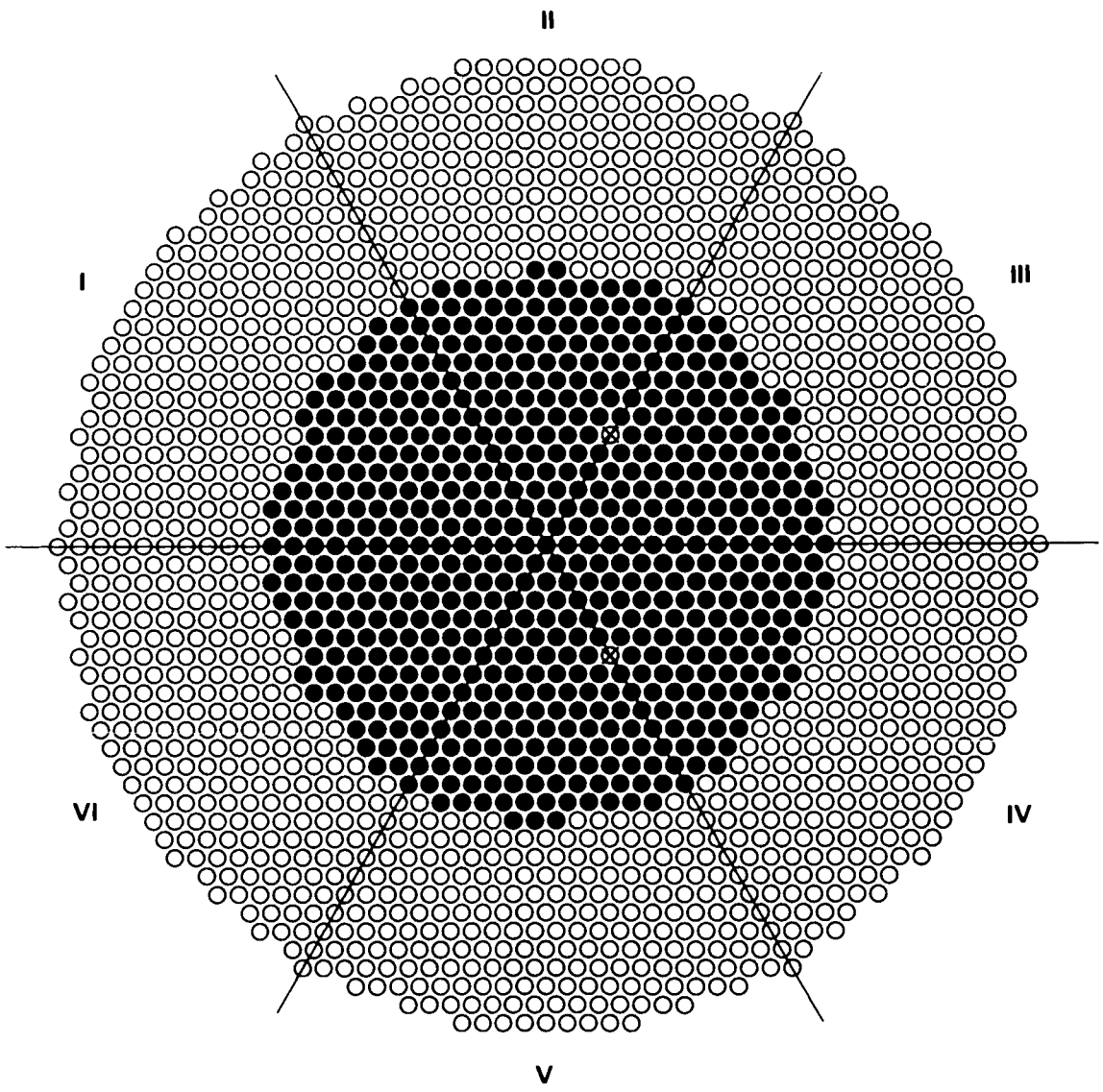

FUEL: 4.31 wt% ^{235}U ENRICHED UO_2

EXPERIMENT: 4.3-000-202A

LATTICE: 12

PITCH: 1.801 ± 0.005 cm

GADOLINIUM: 0.400 ± 0.021 g Gd/liter

CONTROL ROD: OUT

SAFETY ROD: OUT

REACTION RATES: NONE

RODS: 625 UO_2 RODS AT ●

k_{eff}: 1.0

COMMENTS: WATER FILLED ALUMINUM SLEEVES AT ⊠

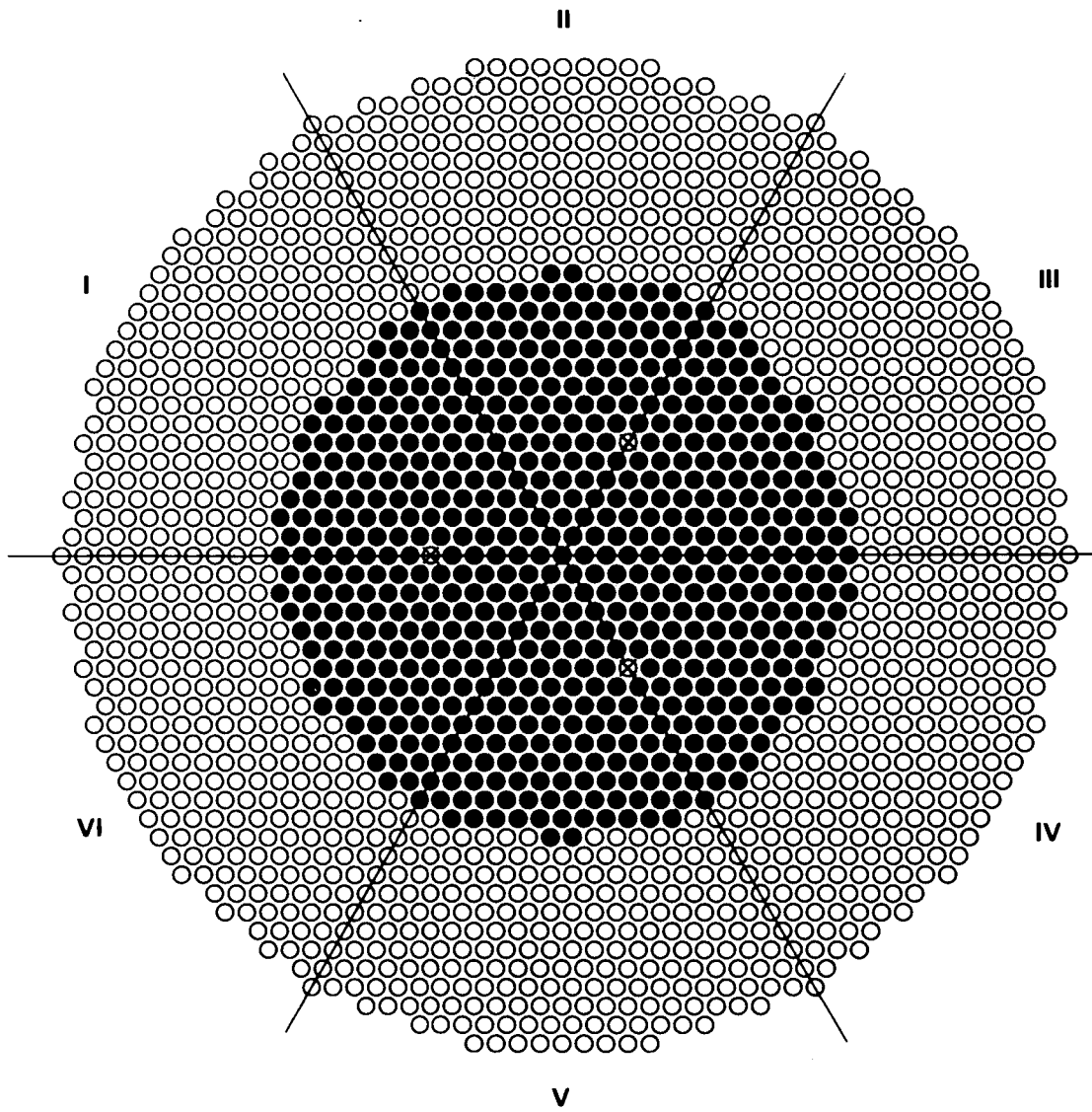

FUEL: 4.31 wt% ^{235}U ENRICHED UO_2

EXPERIMENT: 4.3-000-202B

LATTICE: 12

PITCH: 1.801 ± 0.005 cm

GADOLINIUM: 0.400 ± 0.021 g Gd/liter

CONTROL ROD: OUT

SAFETY ROD: OUT

REACTION RATES: NONE

RODS: 623 UO_2 RODS AT ●

k_{eff}: 1.0

COMMENTS: WATER FILLED ALUMINUM SLEEVES AT ⊗

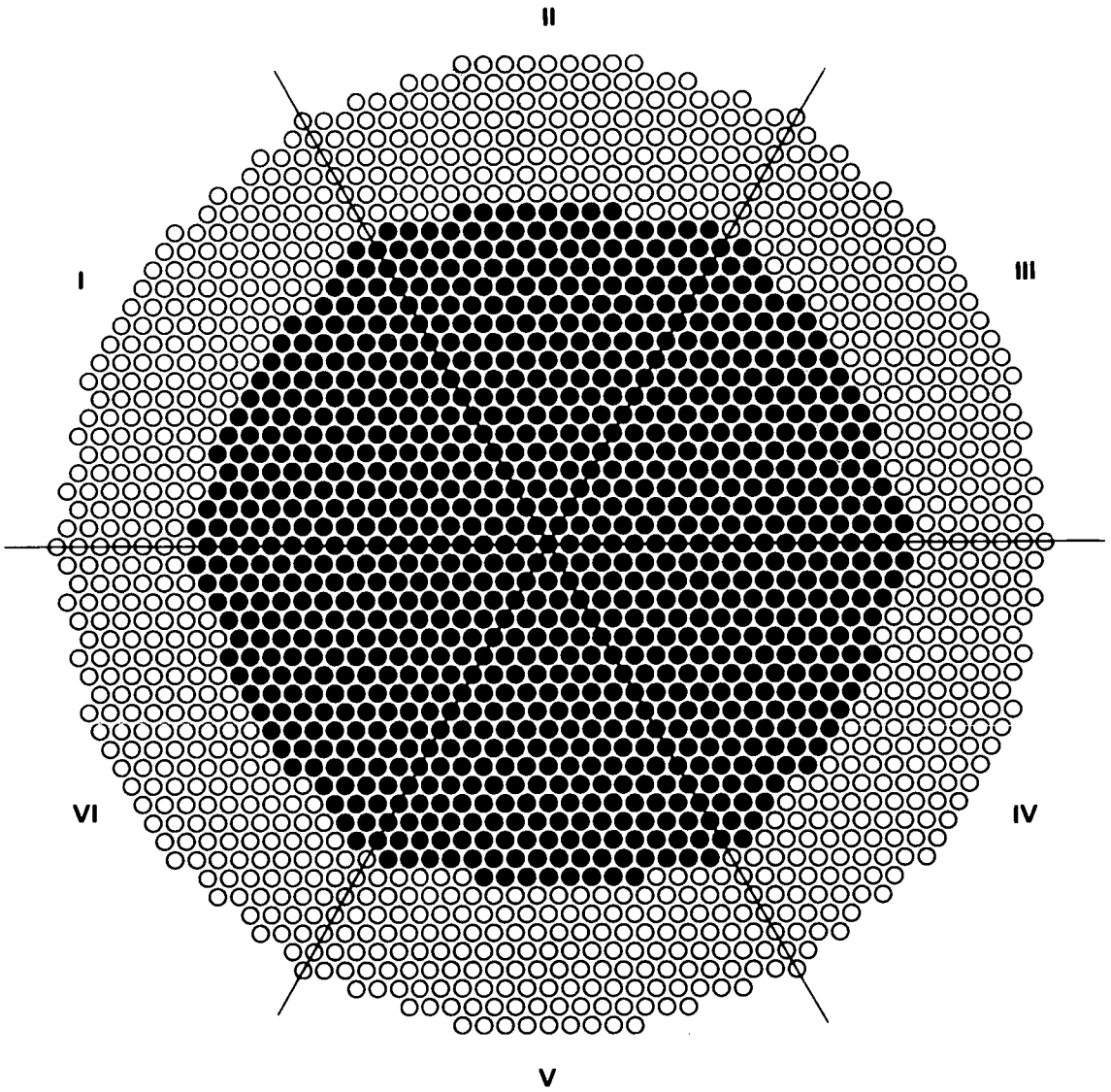

FUEL: 4.31 wt% ^{235}U ENRICHED UO_2

EXPERIMENT: 4.3-000-203

LATTICE: 12

PITCH: 1.801 ± 0.005 cm

GADOLINIUM: 0.908 ± 0.06 g Gd/liter

CONTROL ROD: NONE

SAFETY ROD: NONE

REACTION RATES: NONE

RODS: 959 UO_2 RODS AT ●

k_{eff}: 1.0

COMMENTS:

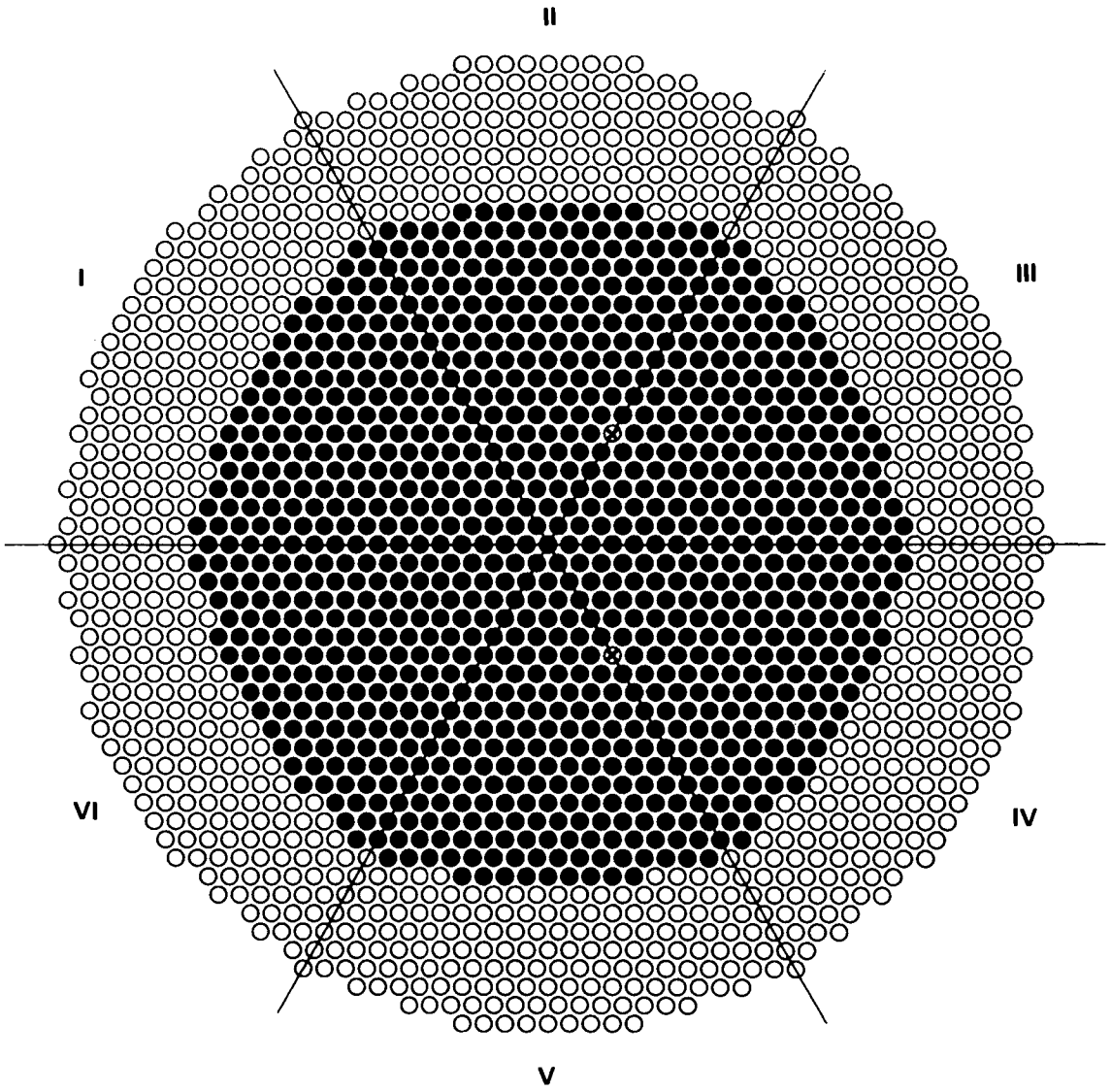

FUEL: 4.31 wt% ^{235}U ENRICHED UO_2

EXPERIMENT: 4.3-000-203A

LATTICE: 12

PITCH: 1.801 ± 0.005 cm

GADOLINIUM: 0.908 ± 0.006 g Gd/liter

CONTROL ROD: OUT

SAFETY ROD: OUT

REACTION RATES: NONE

RODS: 965 UO_2 RODS AT ●

k_{eff}: 1.0

COMMENTS: WATER FILLED ALUMINUM SLEEVES AT ⊗

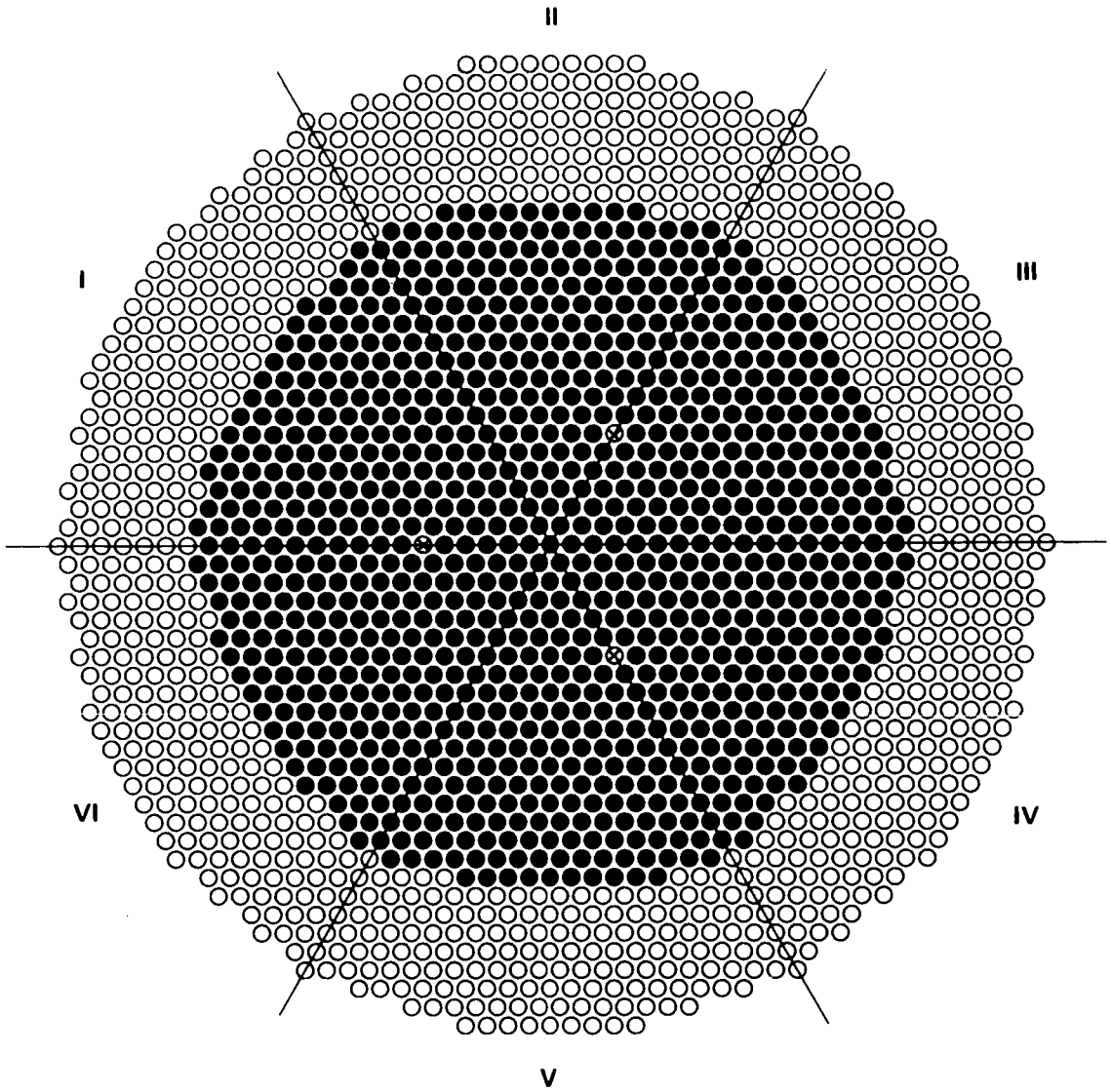

FUEL: 4.31 wt% ^{235}U ENRICHED UO_2

EXPERIMENT: 4.3-000-203B

LATTICE: 12

PITCH: 1.801 ± 0.005 cm

GADOLINIUM: 0.908 ± 0.006 g Gd/liter

CONTROL ROD: OUT

SAFETY ROD: OUT

REACTION RATES: NONE

RODS: 968 UO_2 RODS AT ●

k_{eff}: 1.0

COMMENTS: WATER FILLED ALUMINUM SLEEVES AT ⊗

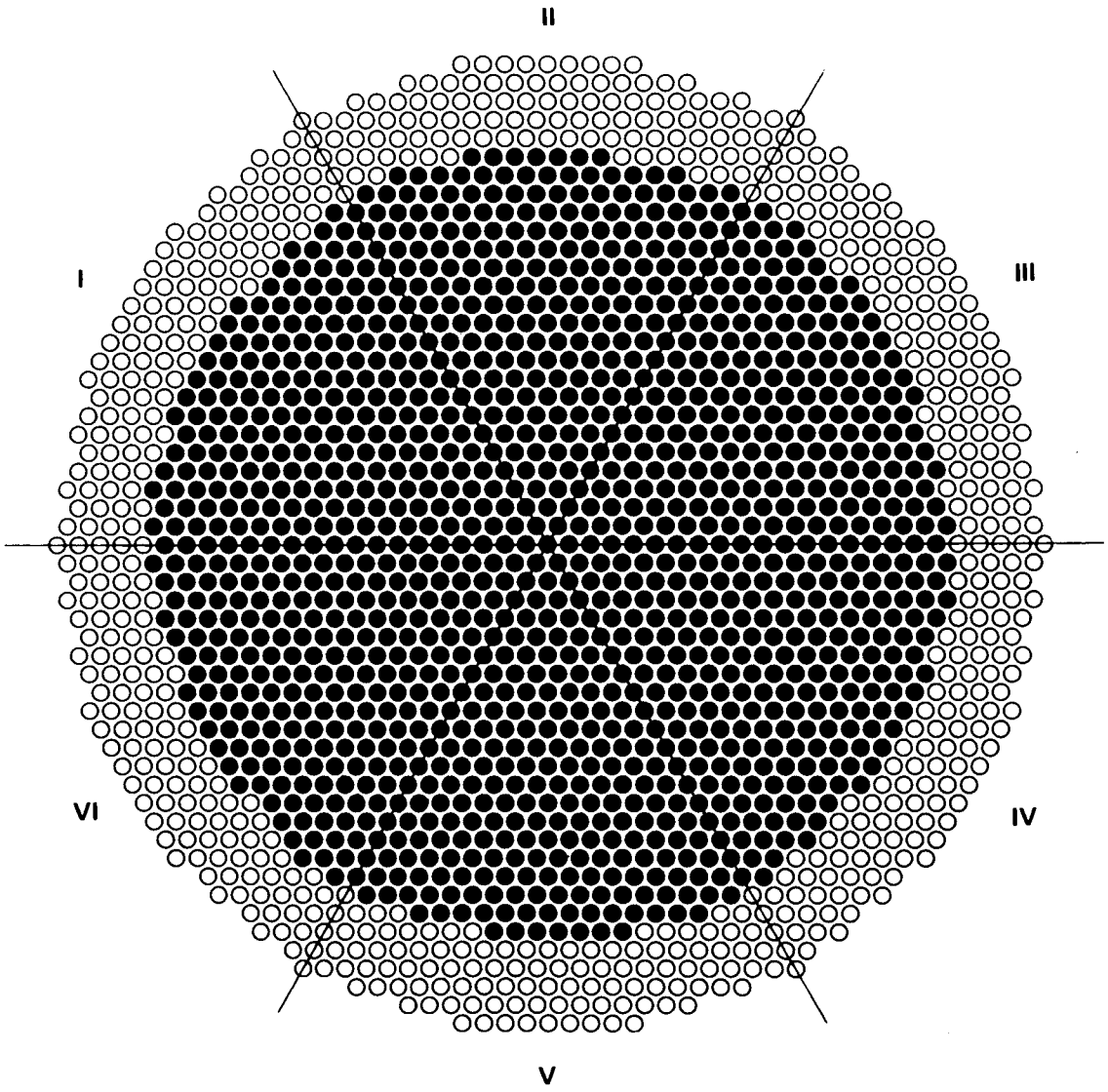

FUEL: 4.31 wt% ^{235}U ENRICHED UO_2

EXPERIMENT: 4.3-000-204

LATTICE: 12

PITCH: 1.801 ± 0.005 cm

GADOLINIUM: SEE COMMENTS

CONTROL ROD: OUT

SAFETY ROD: OUT

REACTION RATES: NONE

RODS: 1260 UO_2 RODS AT ●

k_{eff}: SEE COMMENTS

COMMENTS:

$k_{eff} = 1.0$ AT 1.247 ± 0.038 g GD/liter
$k_{eff} = 0.991$ AT 1.371 ± 0.051 g GD/liter
$k_{eff} = 0.980$ AT 1.456 ± 0.051 g GD/liter
$k_{eff} = 0.961$ AT 1.664 ± 0.077 g GD/liter
$k_{eff} = 0.909$ AT 2.195 ± 0.035 g GD/liter

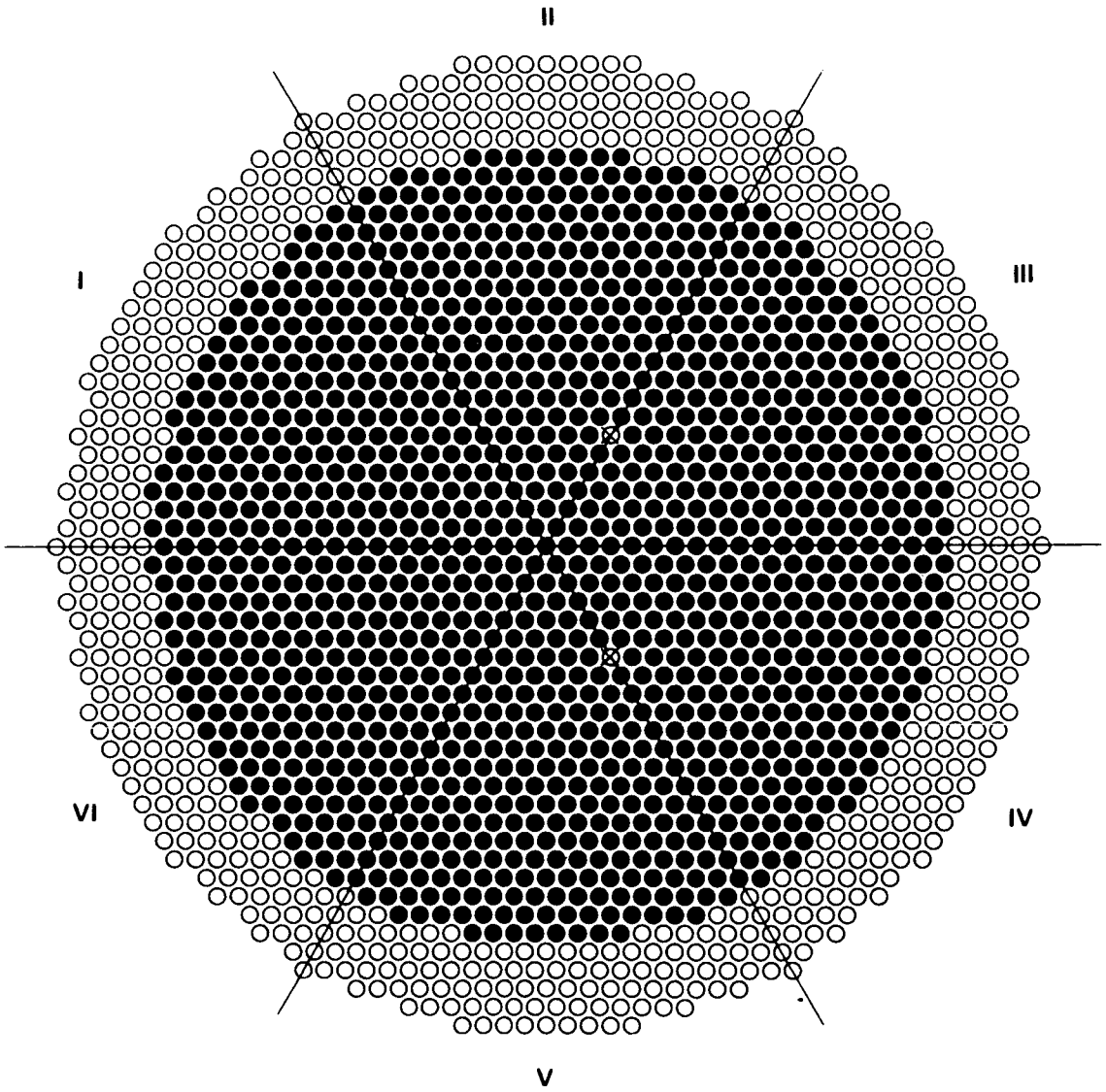

FUEL: 4.31 wt% ^{235}U ENRICHED UO_2

EXPERIMENT: 4.3-000-204A

LATTICE: 12

PITCH: 1.801 ± 0.005 cm

GADOLINIUM: 1.246 ± 0.038 g Gd/liter

CONTROL ROD: OUT

SAFETY ROD: OUT

REACTION RATES: NONE

RODS: 1270 UO_2 RODS AT ●

k_{eff}: 1.0

COMMENTS: WATER FILLED ALUMINUM SLEEVES AT ⊠

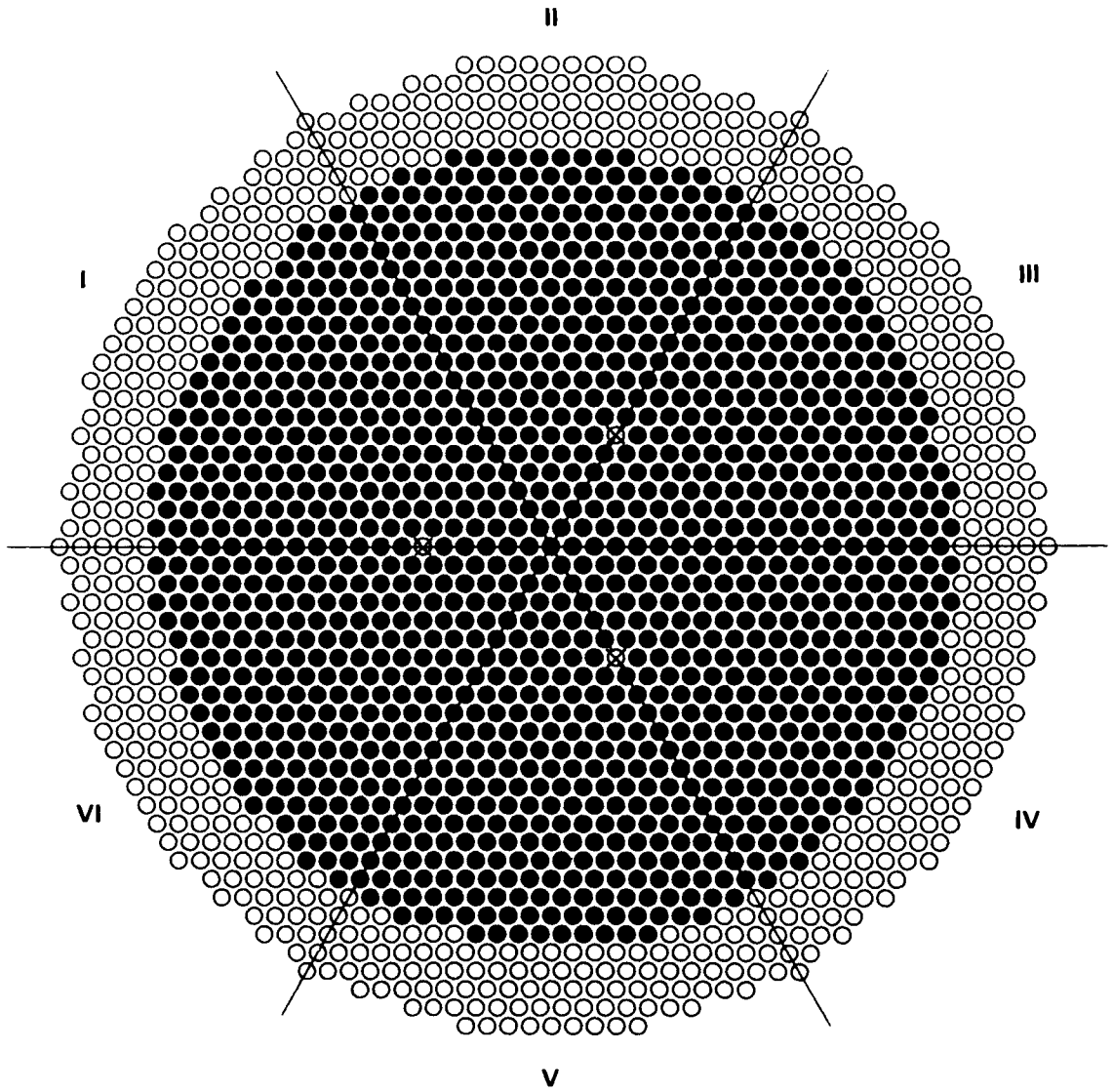

FUEL: 4.31 wt% ^{235}U ENRICHED UO_2

EXPERIMENT: 4.3-000-204B

LATTICE: 12

PITCH: 1.801 ± 0.005 cm

GADOLINIUM: 1.246 ± 0.038 g Gd/liter

CONTROL ROD: OUT

SAFETY ROD: OUT

REACTION RATES: NONE

RODS: 1275 UO_2 RODS AT ●

k_{eff}: 1.0

COMMENTS: WATER FILLED ALUMINUM SLEEVES AT ⊠

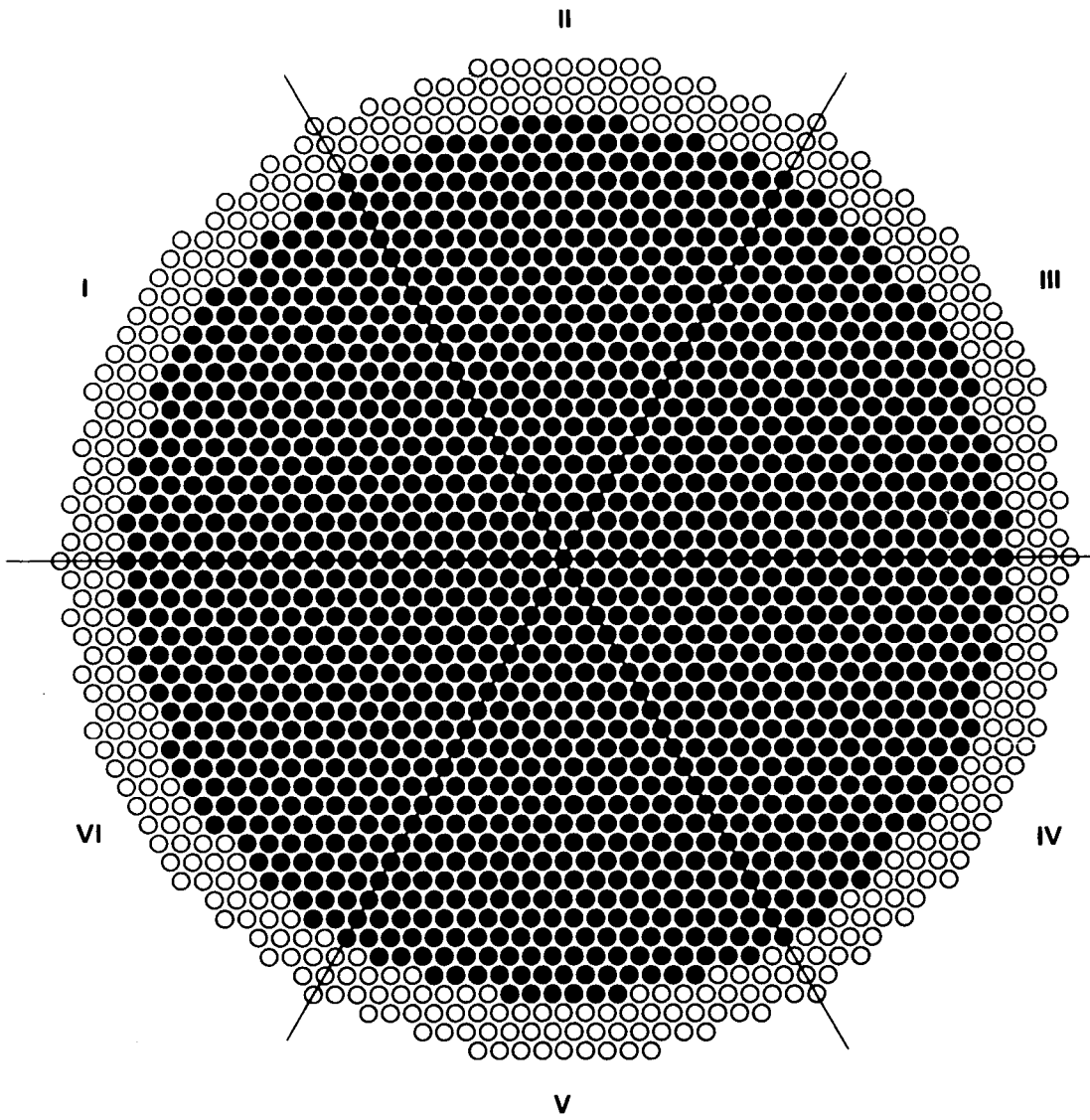

FUEL: 4.31 wt% ^{235}U ENRICHED UO_2

EXPERIMENT: 4.3-000-205

LATTICE: 12

PITCH: 1.801 ± 0.005 cm

GADOLINIUM: 1.448 ± 0.025 g Gd/liter

CONTROL ROD: NONE

SAFETY ROD: NONE

REACTION RATES: NONE

RODS: 1482 UO_2 RODS AT ●

k_{eff}: 1.0

COMMENTS:

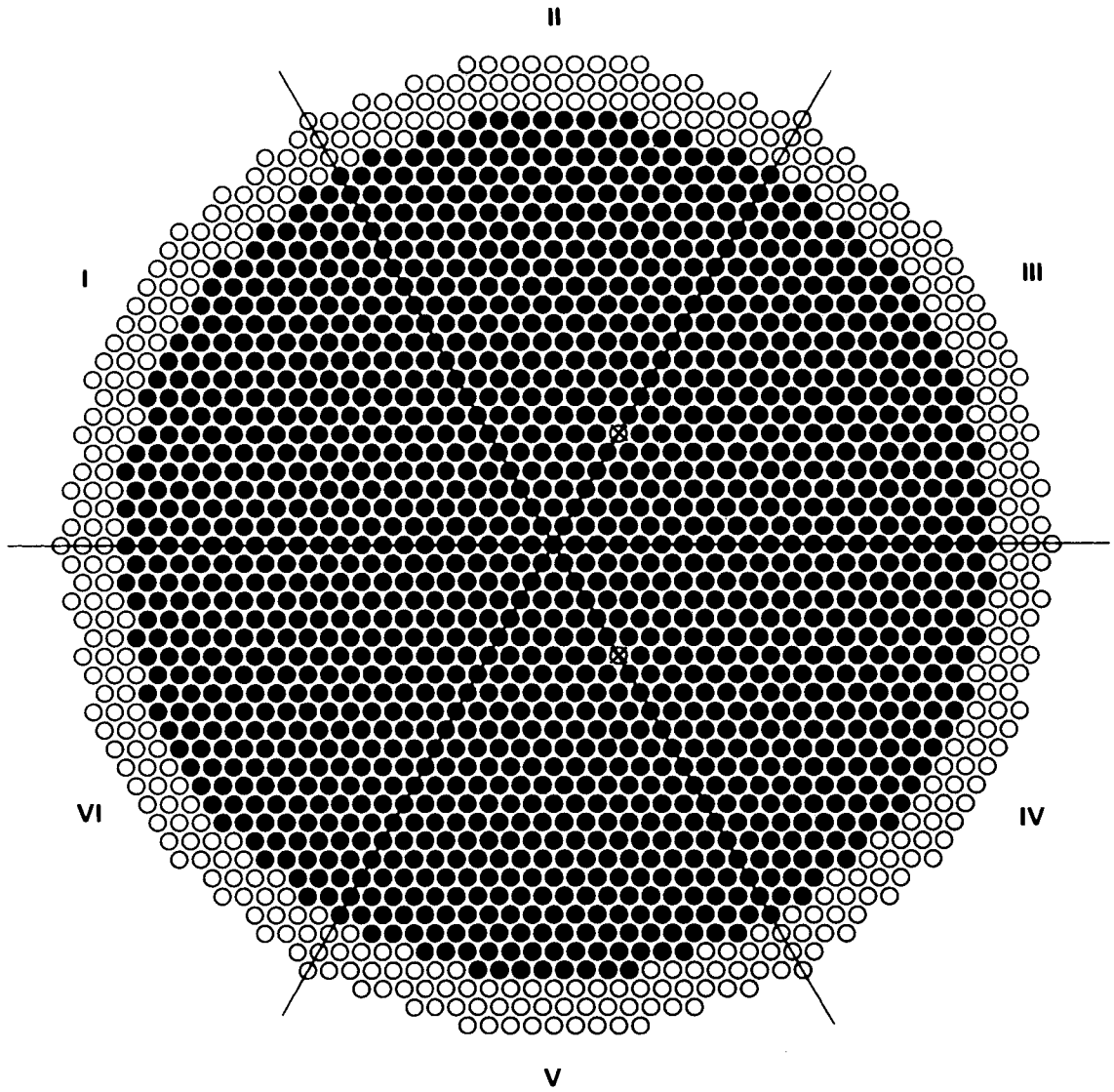

FUEL: 4.31 wt% ^{235}U ENRICHED UO_2

EXPERIMENT: 4.3-000-205A

LATTICE: 12

PITCH: 1.801 ± 0.005 cm

GADOLINIUM: 1.448 ± 0.025 g Gd/liter

CONTROL ROD: OUT

SAFETY ROD: OUT

REACTION RATES: NONE

RODS: 1494 UO_2 RODS AT ●

k_{eff}: 1.0

COMMENTS: WATER FILLED ALUMINUM SLEEVES AT ⊠

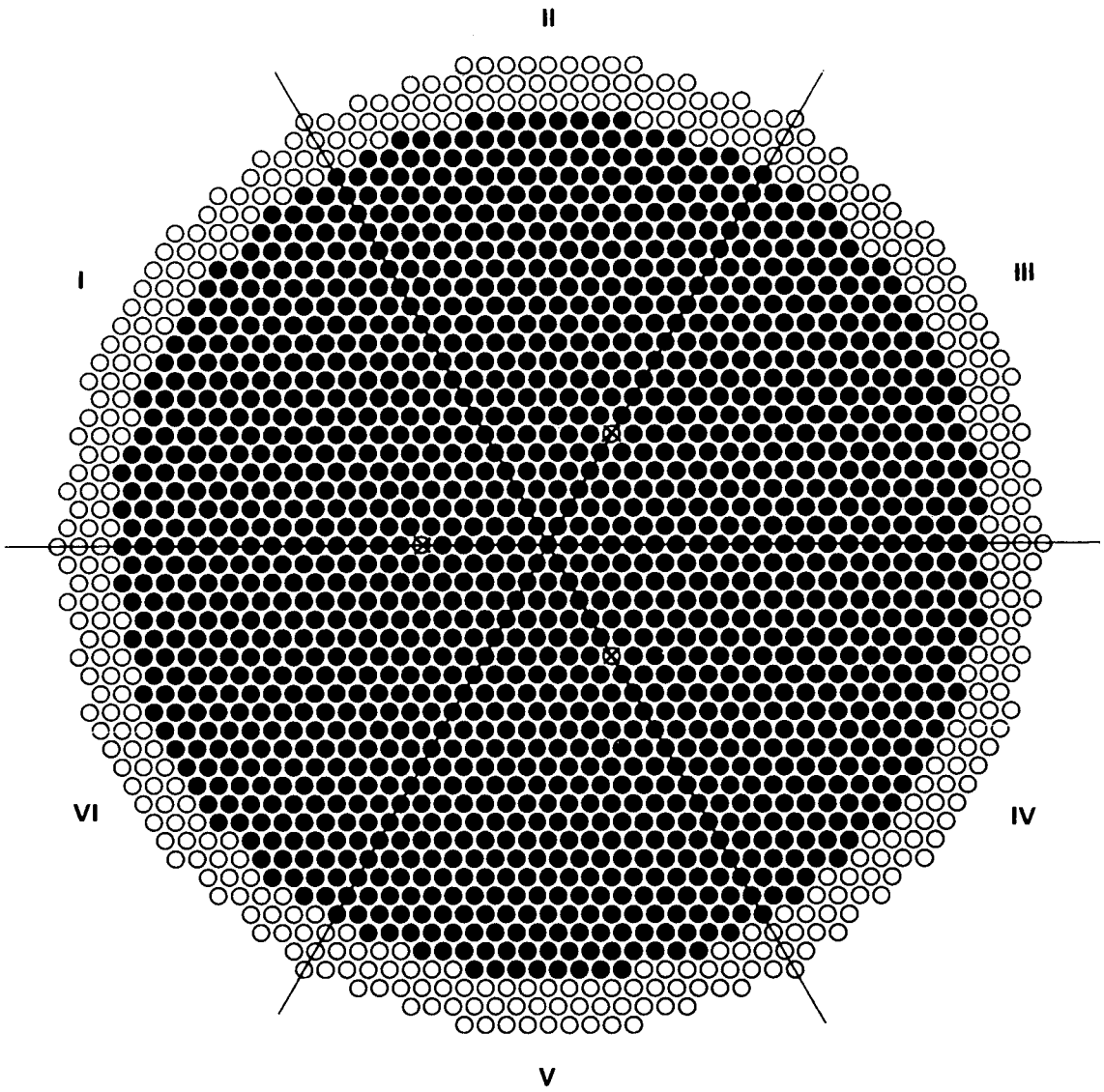

FUEL: 4.31 wt% ^{235}U ENRICHED UO_2

EXPERIMENT: 4.3-000-205B

LATTICE: 12

PITCH: 1.801 ± 0.005 cm

GADOLINIUM: 1.448 ± 0.025 g Gd/liter

CONTROL ROD: OUT

SAFETY ROD: OUT

REACTION RATES: NONE

RODS: 1500 UO_2 RODS AT ●

k_{eff}: 1.0

COMMENTS: WATER FILLED ALUMINUM SLEEVES AT ⊠

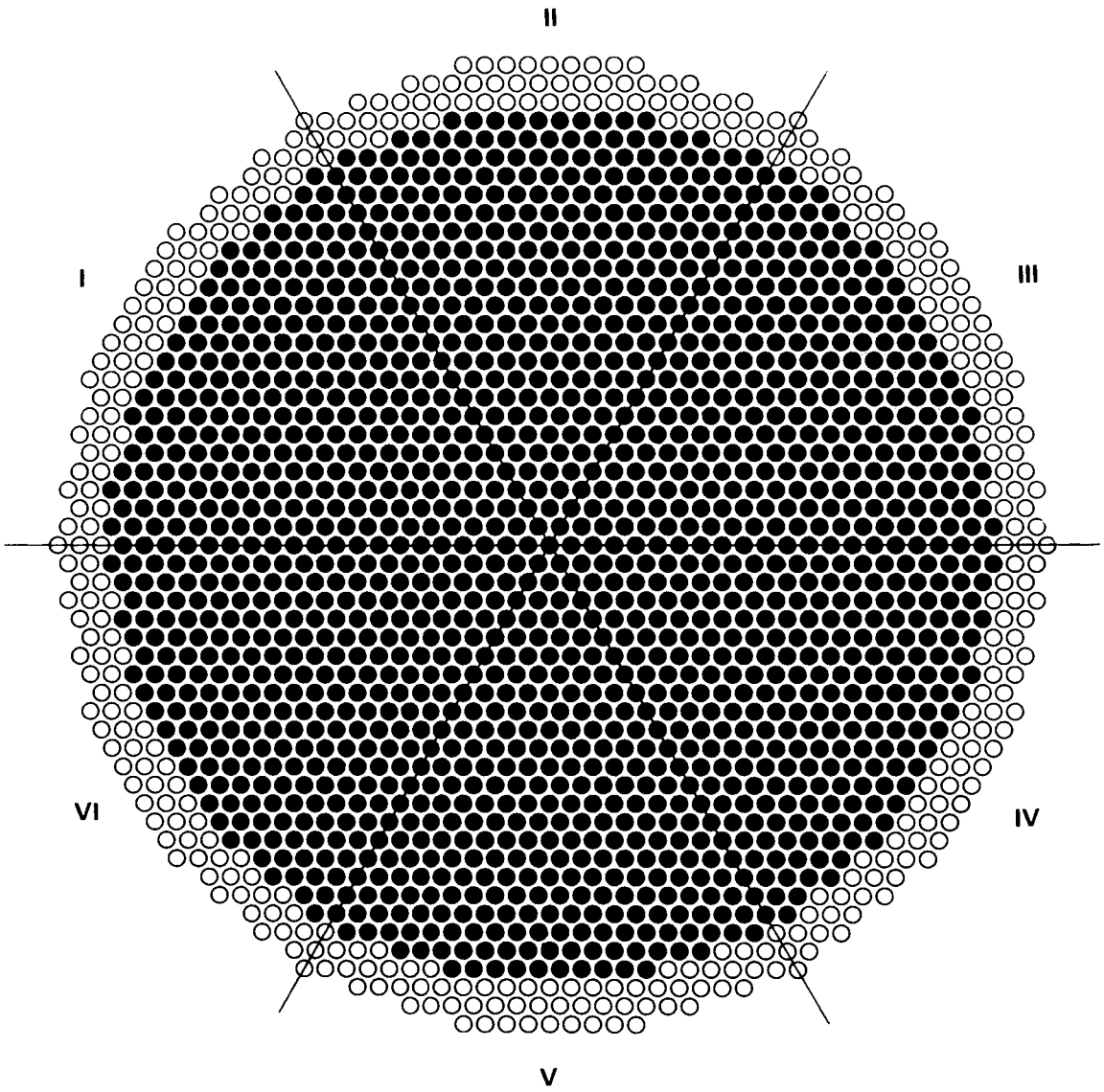

FUEL: 4.31 wt% ^{235}U ENRICHED UO_2

EXPERIMENT: 4.3-000-206

LATTICE: 12

PITCH: 1.801 ± 0.005 cm

GADOLINIUM: 1.481 ± 0.044 g Gd/liter

CONTROL ROD: NONE

SAFETY ROD: NONE

REACTION RATES: NONE

RODS: 1533 UO_2 RODS AT ●

k_{eff}: 1.0

COMMENTS:

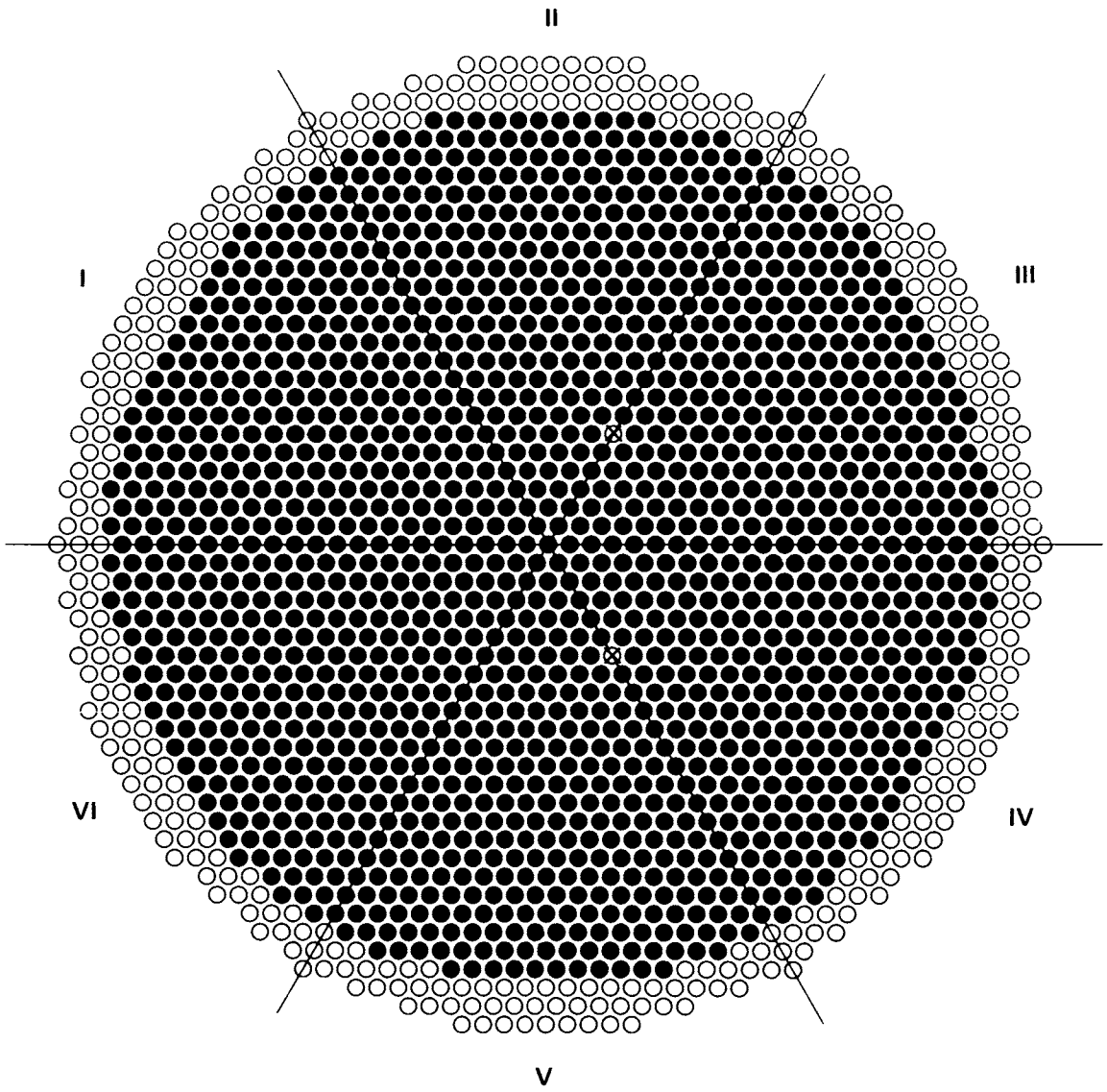

FUEL: 4.31 wt% ^{235}U ENRICHED UO_2

EXPERIMENT: 4.3-000-206A

LATTICE: 12

PITCH: 1.801 ± 0.005 cm

GADOLINIUM: 1.481 ± 0.044 g Gd/liter

CONTROL ROD: OUT

SAFETY ROD: OUT

REACTION RATES: NONE

RODS: 1548 UO_2 RODS AT ●

k_{eff}: 1.0

COMMENTS: WATER FILLED ALUMINUM SLEEVES AT ⊠

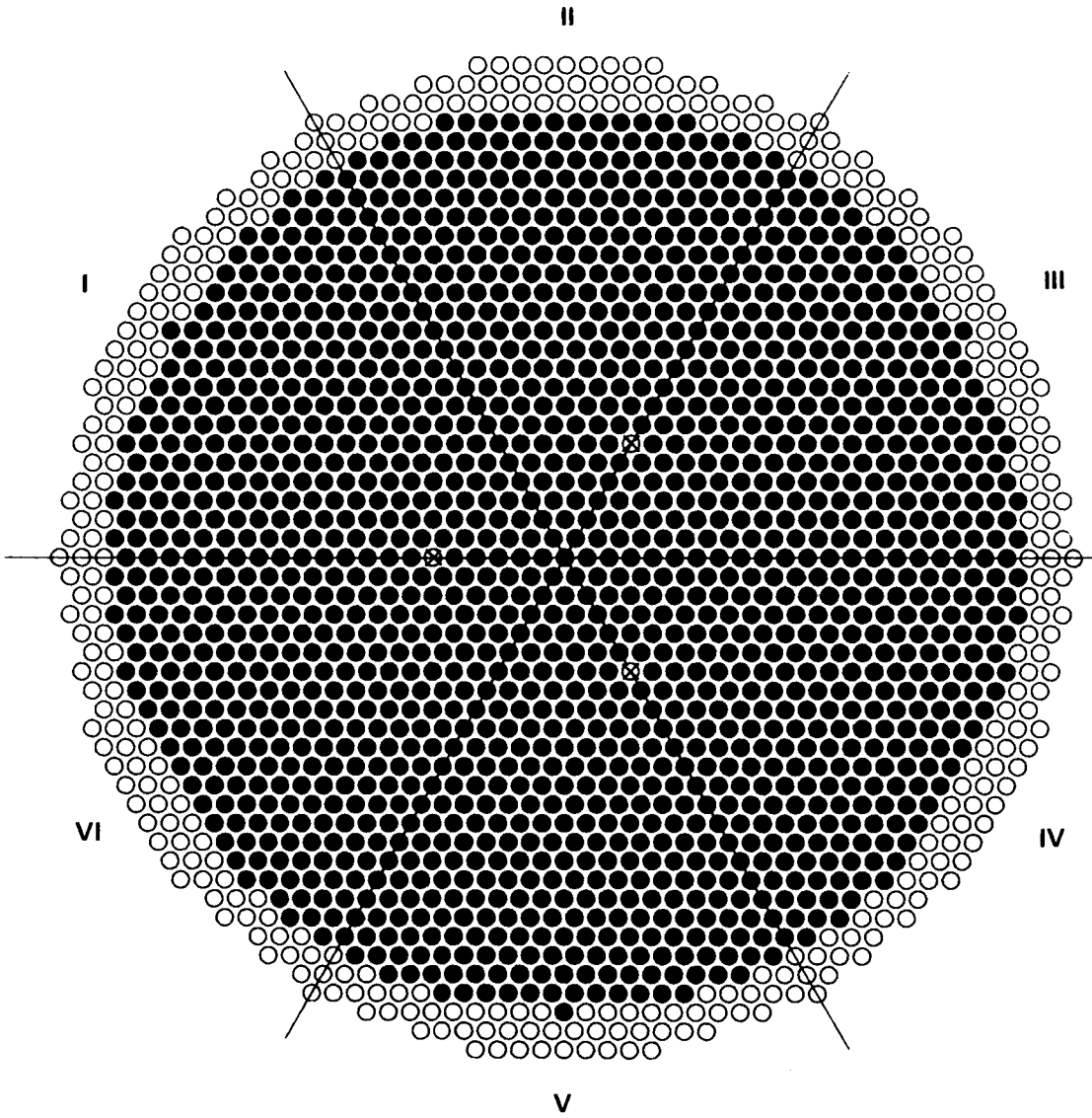

FUEL: 4.31 wt% ^{235}U ENRICHED UO_2

EXPERIMENT: 4.3-000-206B

LATTICE: 12

PITCH: 1.801 ± 0.005 cm

GADOLINIUM: 1.481 ± 0.044 g Gd/liter

CONTROL ROD: OUT

SAFETY ROD: OUT

REACTION RATES: NONE

RODS: 1555 UO_2 RODS AT ●

k_{eff}: 1.0

COMMENTS: WATER FILLED ALUMINUM SLEEVES AT ⊠

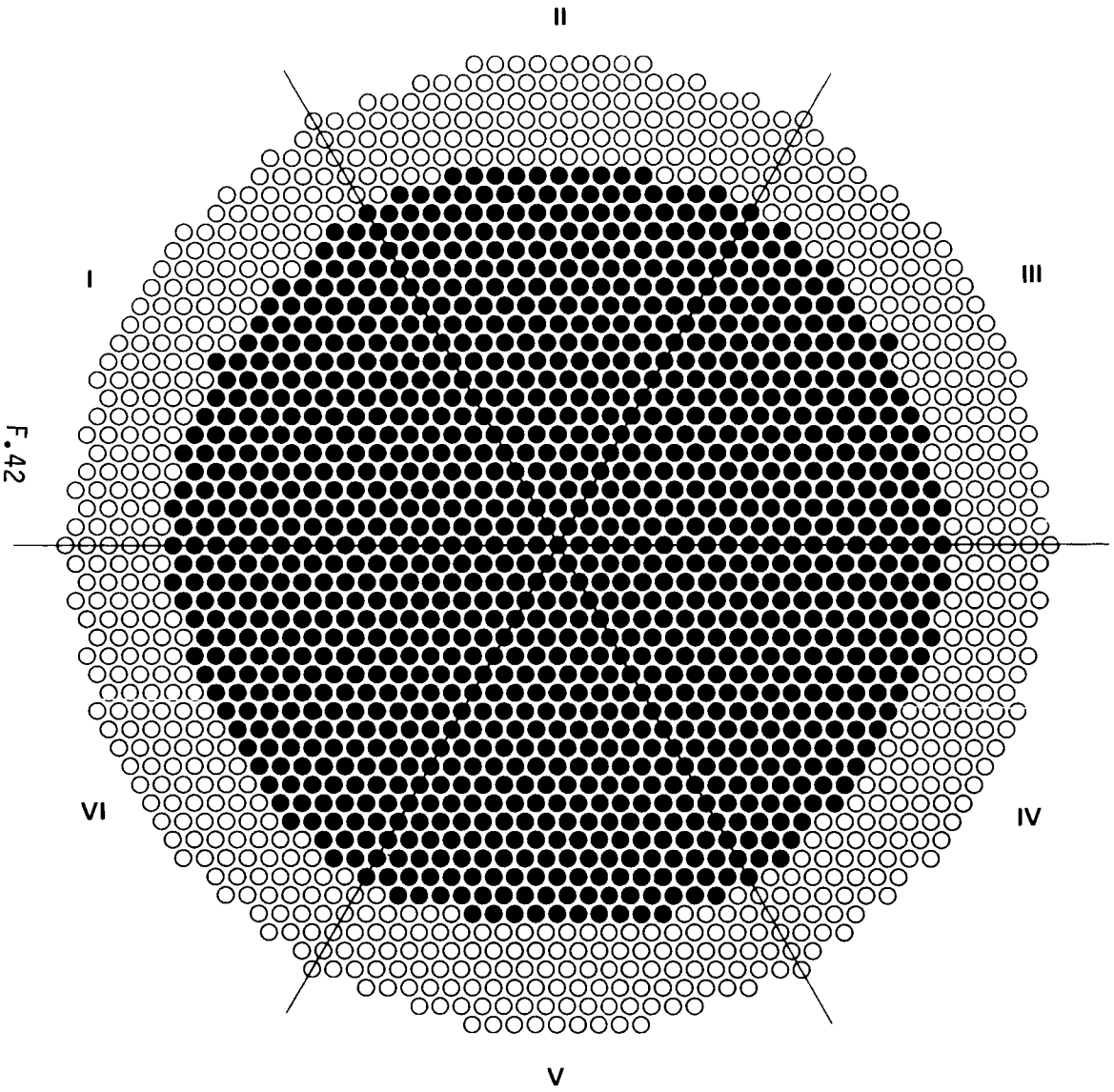

FUEL: 4.31 wt% ^{235}U ENRICHED UO_2

EXPERIMENT: 4.3-000-194

LATTICE: 13

PITCH: 1.598 ± 0.005 cm

GADOLINIUM: SEE COMMENTS

CONTROL ROD: NONE

SAFETY ROD: NONE

REACTION RATES: NONE

RODS: 1185 UO_2 RODS AT ●

k_{eff}: SEE COMMENTS

COMMENTS:

$k_{eff} = 1.0$ AT ZERO g Gd/liter
$k_{eff} = 0.953$ AT 0.130 ± 0.001 g Gd/liter
$k_{eff} = 0.923$ AT 0.456 ± 0.001 g Gd/liter
$k_{eff} = 0.902$ AT 0.638 ± 0.008 g Gd/liter
$k_{eff} = 0.901$ AT 0.750 ± 0.008 g Gd/liter

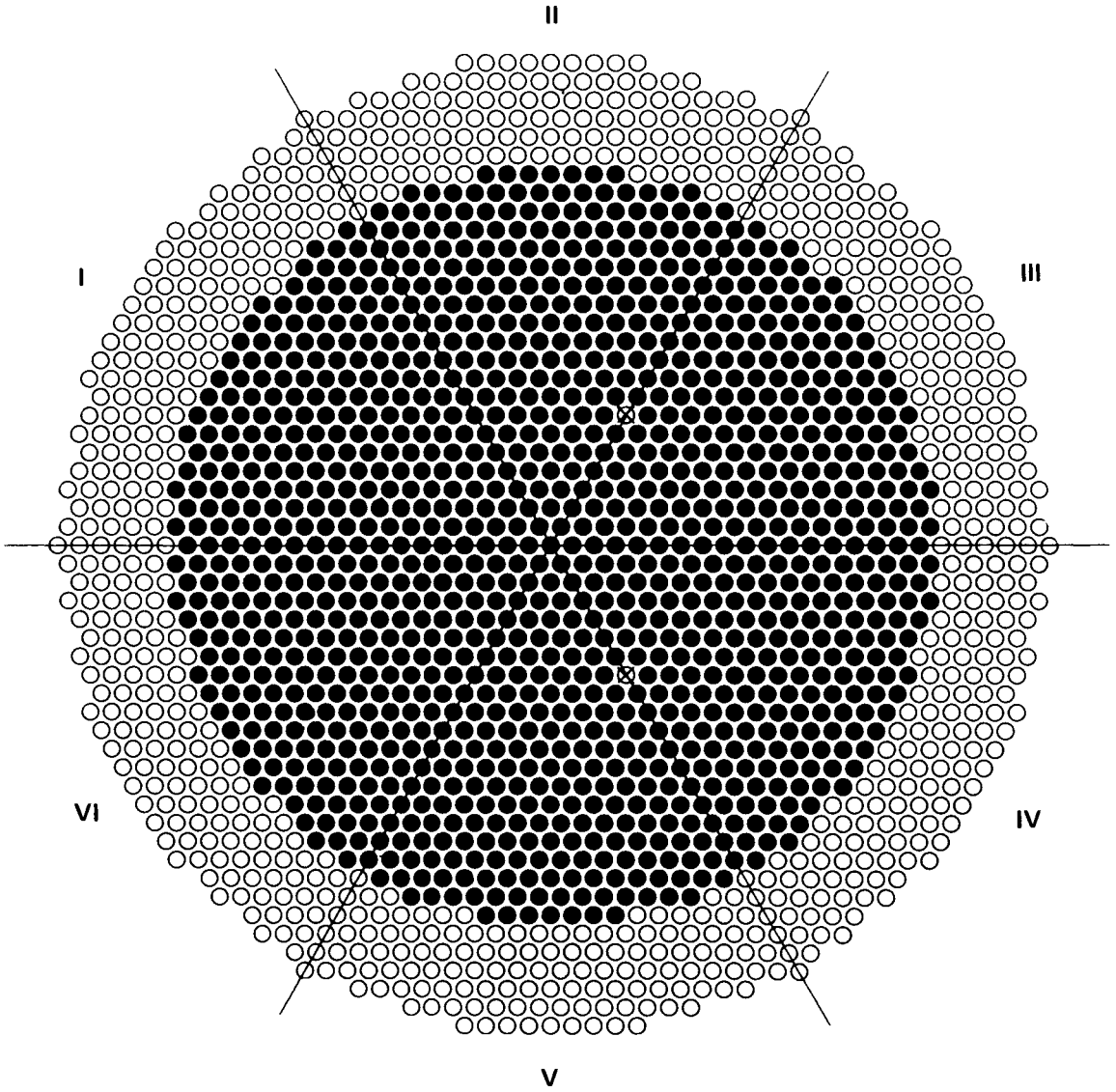

FUEL: 4.31 wt% ^{235}U ENRICHED UO_2

EXPERIMENT: 4.3-000-194A

LATTICE: 13

PITCH: 1.598 ± 0.005 cm

GADOLINIUM: NONE

CONTROL ROD: OUT

SAFETY ROD: OUT

REACTION RATES: NONE

RODS: 1147 UO_2 RODS AT ●

k_{eff}: 1.0

COMMENTS: WATER FILLED ALUMINUM SLEEVES AT ⊠

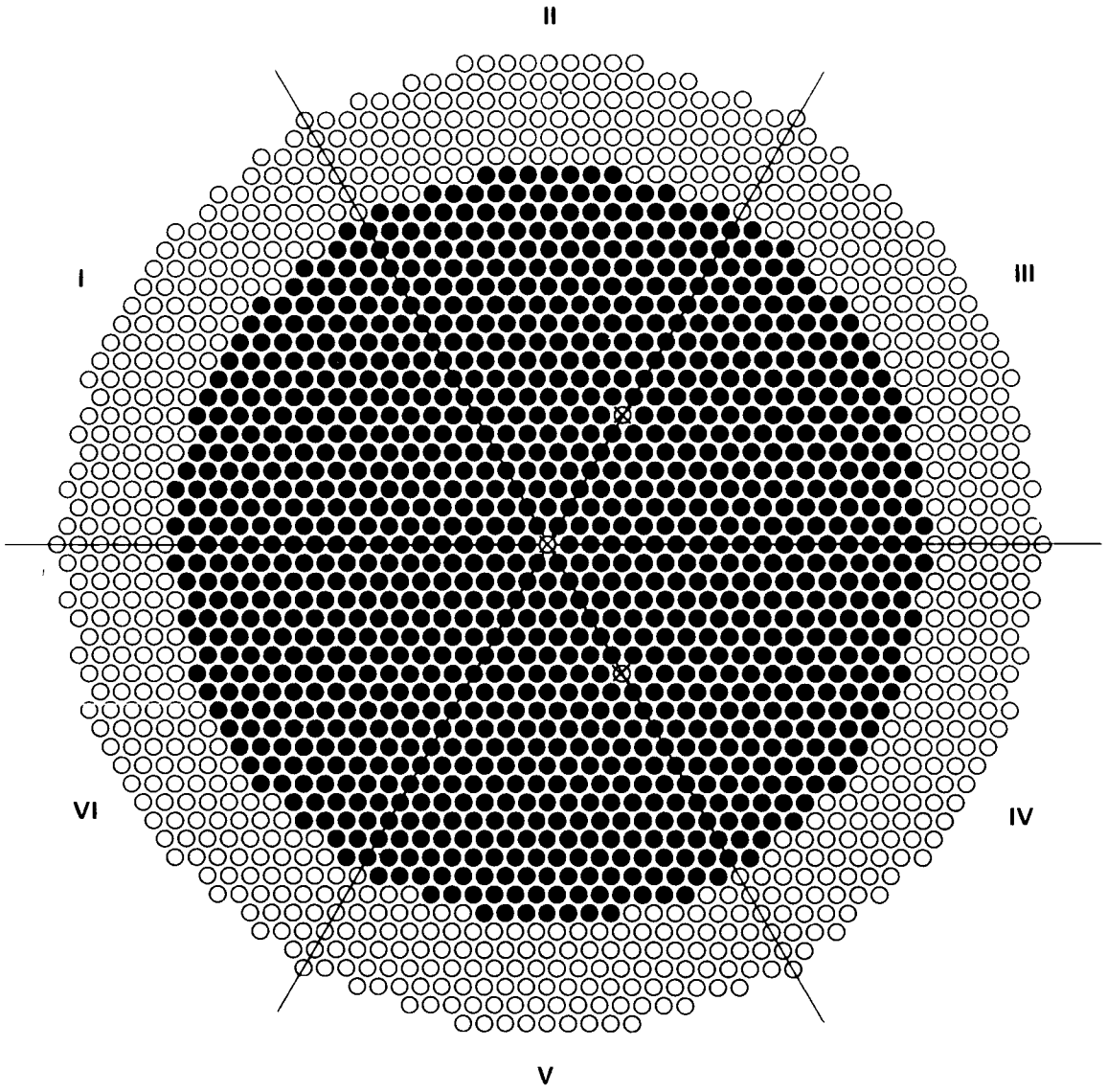

FUEL: 4.31 wt% ^{235}U ENRICHED UO_2

EXPERIMENT: 4.3-000-194B

LATTICE: 13

PITCH: 1.598 ± 0.005 cm

GADOLINIUM: NONE

CONTROL ROD: OUT

SAFETY ROD: OUT

REACTION RATES: NONE

RODS: 1135 UO_2 RODS AT ●

k_{eff}: 1.0

COMMENTS: WATER FILLED ALUMINUM SLEEVES AT ⊠

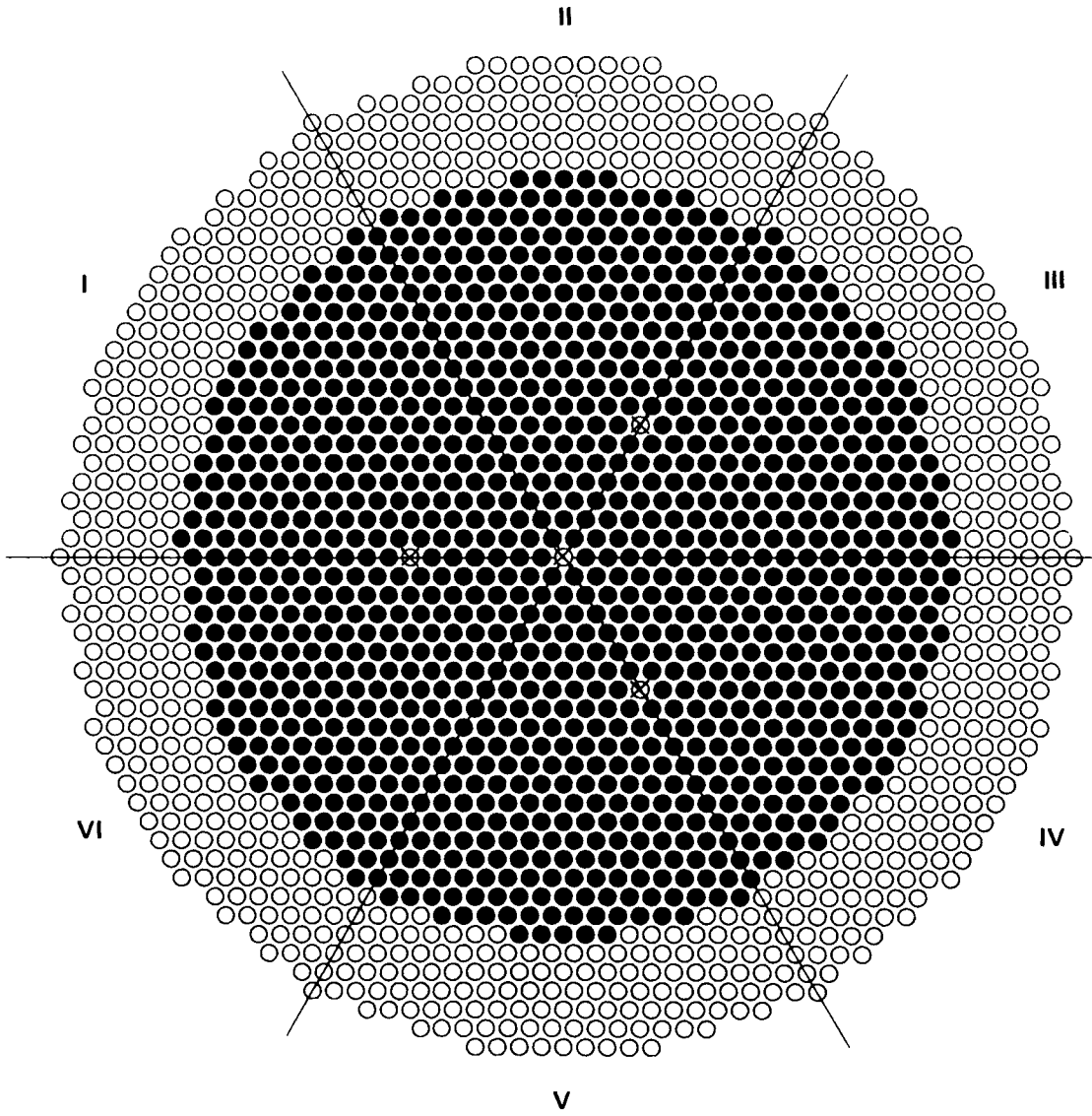

FUEL: 4.31 wt% ^{235}U ENRICHED UO_2

EXPERIMENT: 4.3-000-194C

LATTICE: 13

PITCH: 1.598 ± 0.005 cm

GADOLINIUM: NONE

CONTROL ROD: OUT

SAFETY ROD: OUT

REACTION RATES: NONE

RODS: 1116 UO_2 RODS AT ●

k_{eff}: 1.0

COMMENTS: WATER FILLED ALUMINUM SLEEVES AT ⊠

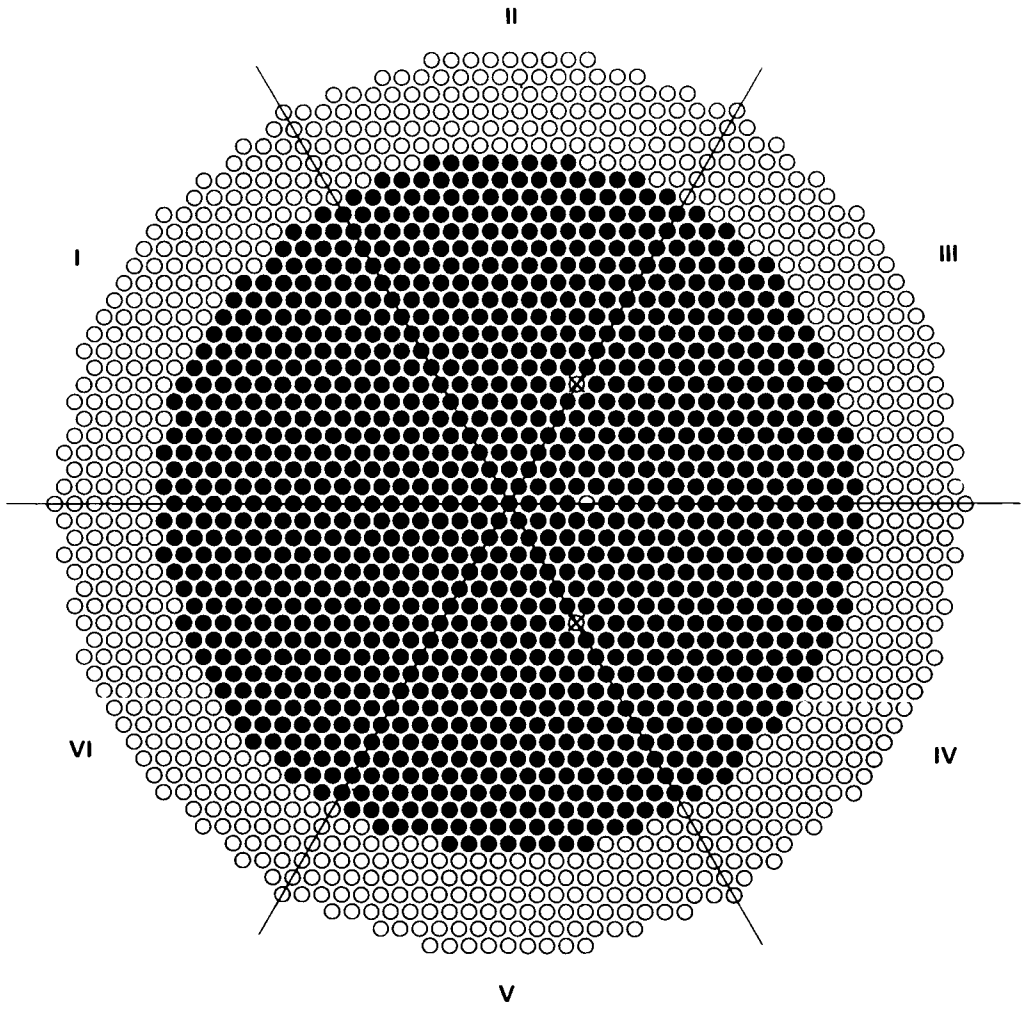

FUEL: 4.31 wt% ^{235}U ENRICHED UO_2

EXPERIMENT: 4.3-000-194D

LATTICE: 13

PITCH: 1.598 ± 0.005 cm

GADOLINIUM: NONE

CONTROL ROD: OUT 52.4 ± 0.3 cm FROM BOTTOM OF FUEL (LOCATION V ⊠)

SAFETY ROD: OUT

REACTION RATES: SOLID STATE ^{235}U TRACK RECORDER AT ◒

RODS: 1151 UO_2 RODS AT ●

k_{eff}: 1.0

COMMENTS: CONTROL AND SAFETY ROD ALUMINUM GUIDE SLEEVES AT ⊠

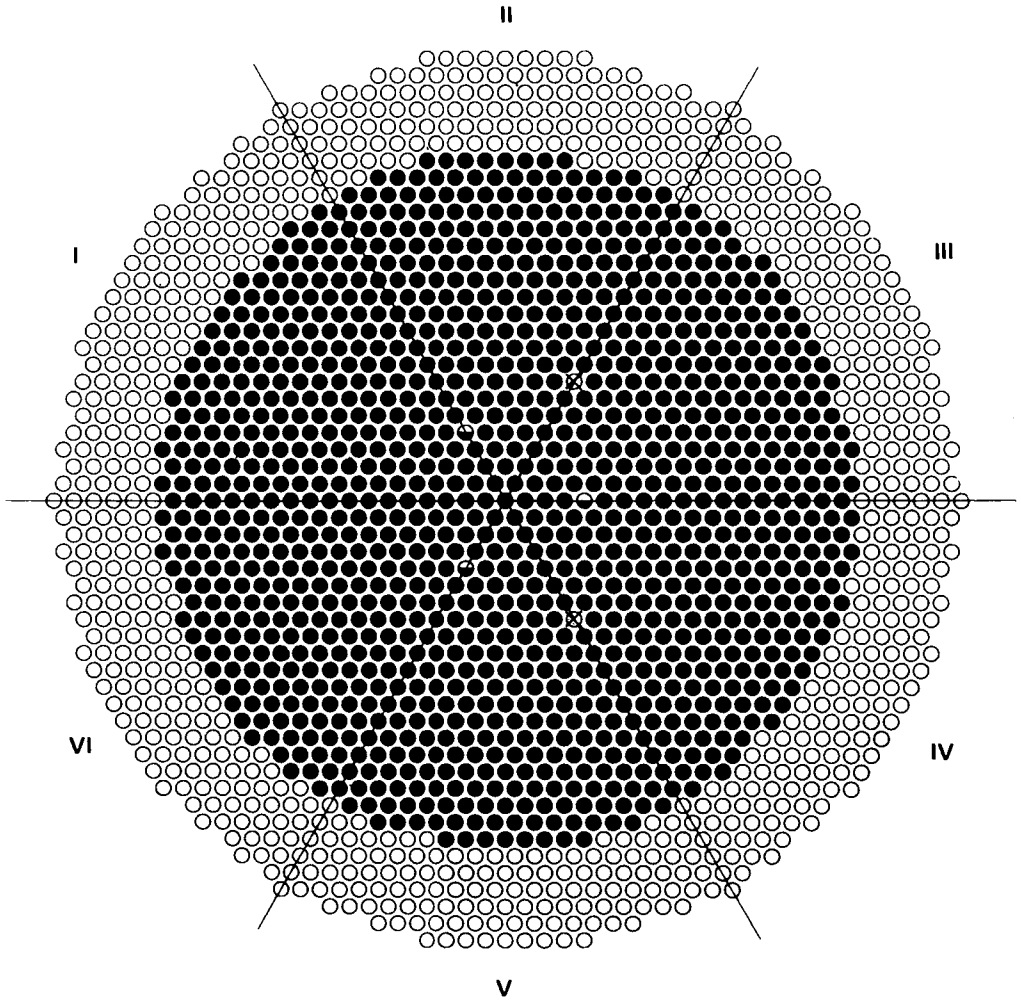

FUEL: 4.31 wt% ^{235}U ENRICHED UO_2

EXPERIMENT: 4.3-000-194E

LATTICE: 13

PITCH: 1.598 ± 0.005 cm

GADOLINIUM: NONE

CONTROL ROD: OUT 56.5 ± 0.3 cm FROM BOTTOM OF FUEL (LOCATION V ⊠)

SAFETY ROD: OUT

REACTION RATES: ^{238}U AND ^{235}U FOILS IN ◒ (SEE COMMENTS)

RODS: 1151 UO_2 RODS AT ●

k_{eff}: 1.0

COMMENTS: CONTROL AND SAFETY ROD ALUMINUM GUIDE SLEEVES AT ⊠
AEEW 9 FOIL PACKET IN II ◒
AEEW 10 FOIL PACKET IN IV ◒
AEEW 12 FOIL PACKET IN VI ◒

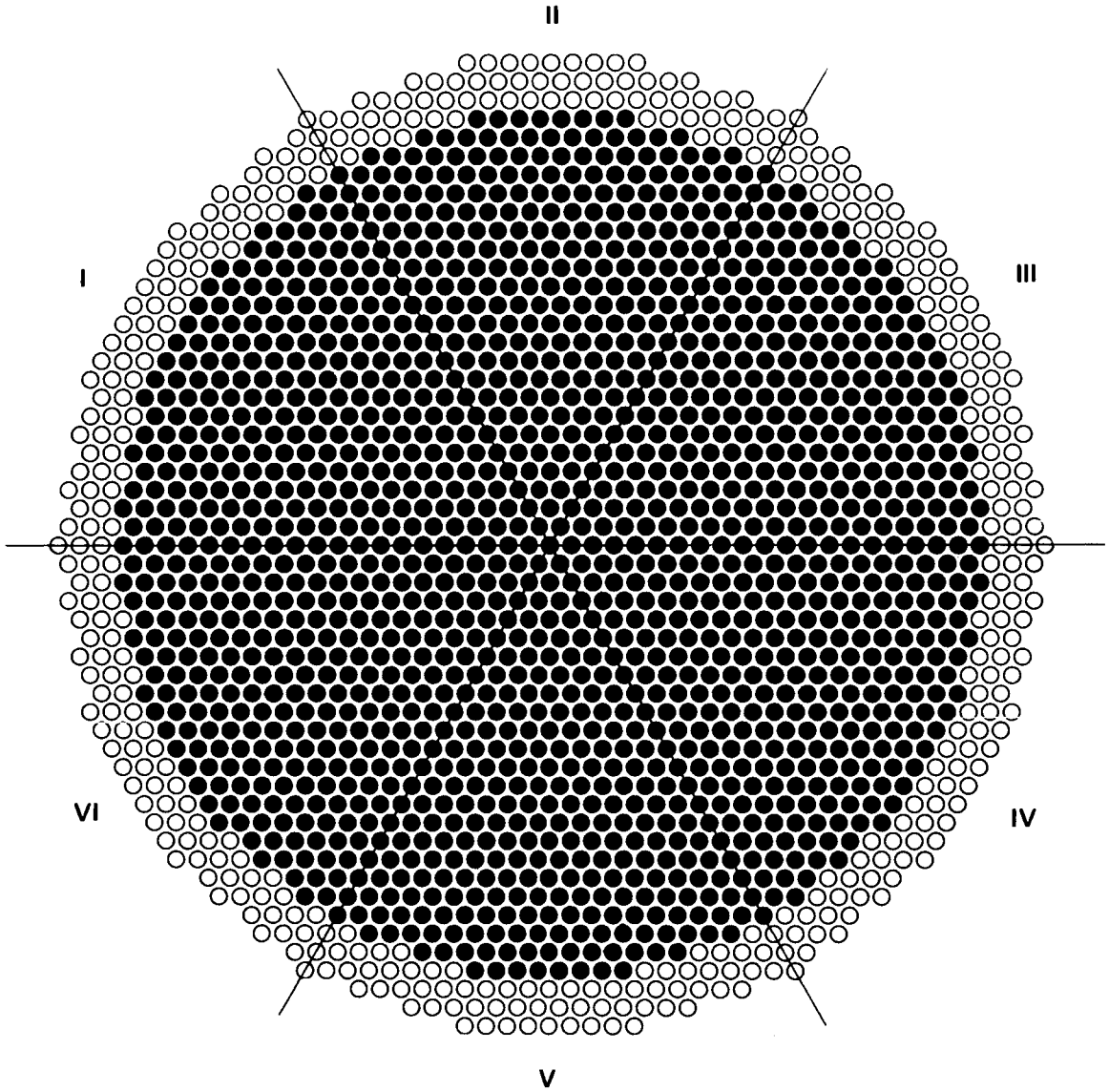

FUEL: 4.31 wt% ^{235}U ENRICHED UO_2

EXPERIMENT: 4.3-000-198

LATTICE: 13

PITCH: 1.598 ± 0.005 cm

GADOLINIUM: 0.121 ± 0.002 g Gd/liter

CONTROL ROD: NONE

SAFETY ROD: NONE

REACTION RATES: NONE

RODS: 1495 UO_2 RODS AT ●

k_{eff}: 1.0

COMMENTS:

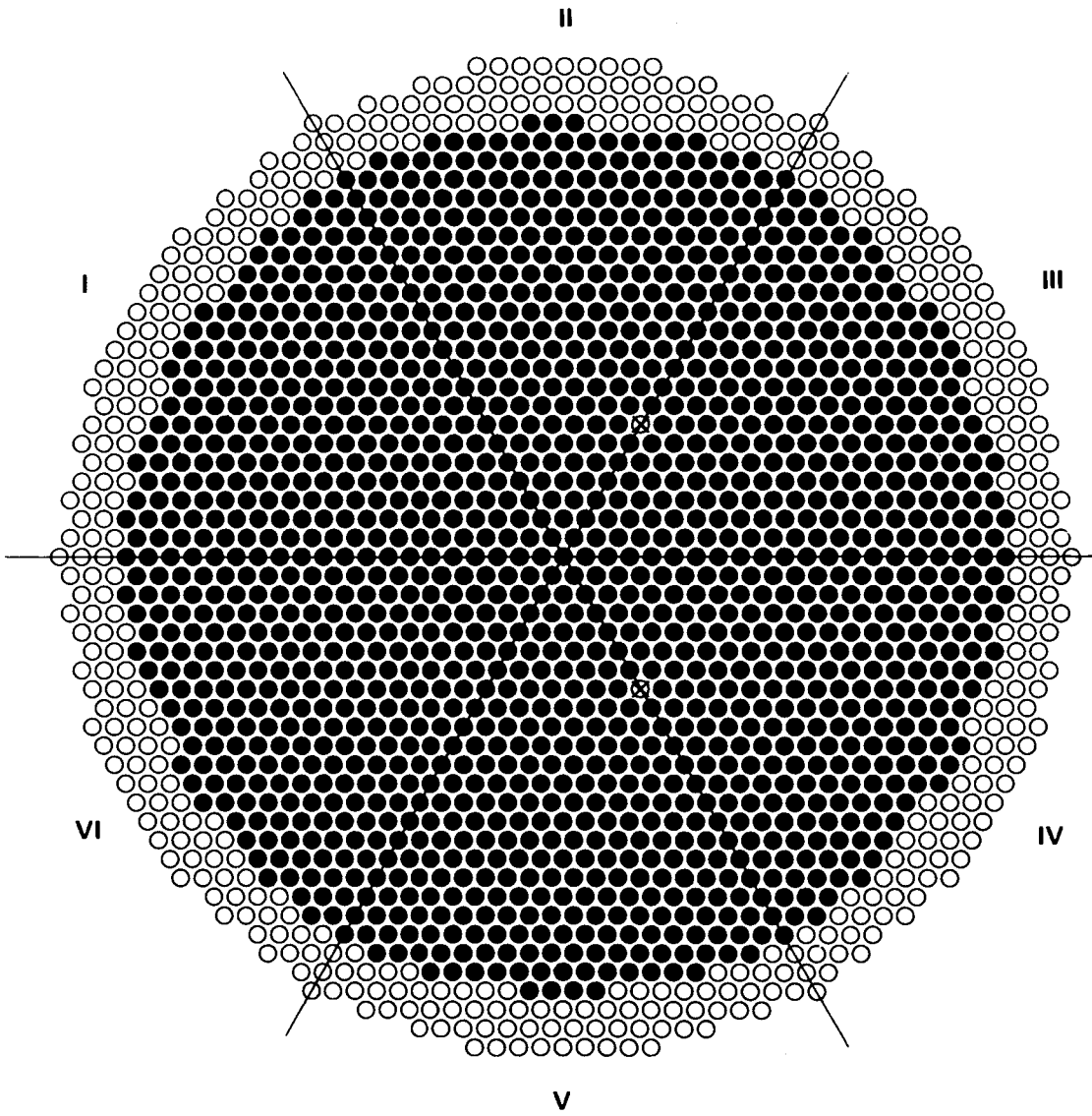

FUEL: 4.31 wt% ^{235}U ENRICHED UO_2

EXPERIMENT: 4.3-000-198A

LATTICE: 13

PITCH: 1.598 ± 0.005 cm

GADOLINIUM: 0.121 ± 0.002 g Gd/liter

CONTROL ROD: OUT

SAFETY ROD: OUT

REACTION RATES: NONE

RODS: 1466 UO_2 RODS AT ●

k_{eff}: 1.0

COMMENTS: WATER FILLED ALUMINUM SLEEVES AT ⊠

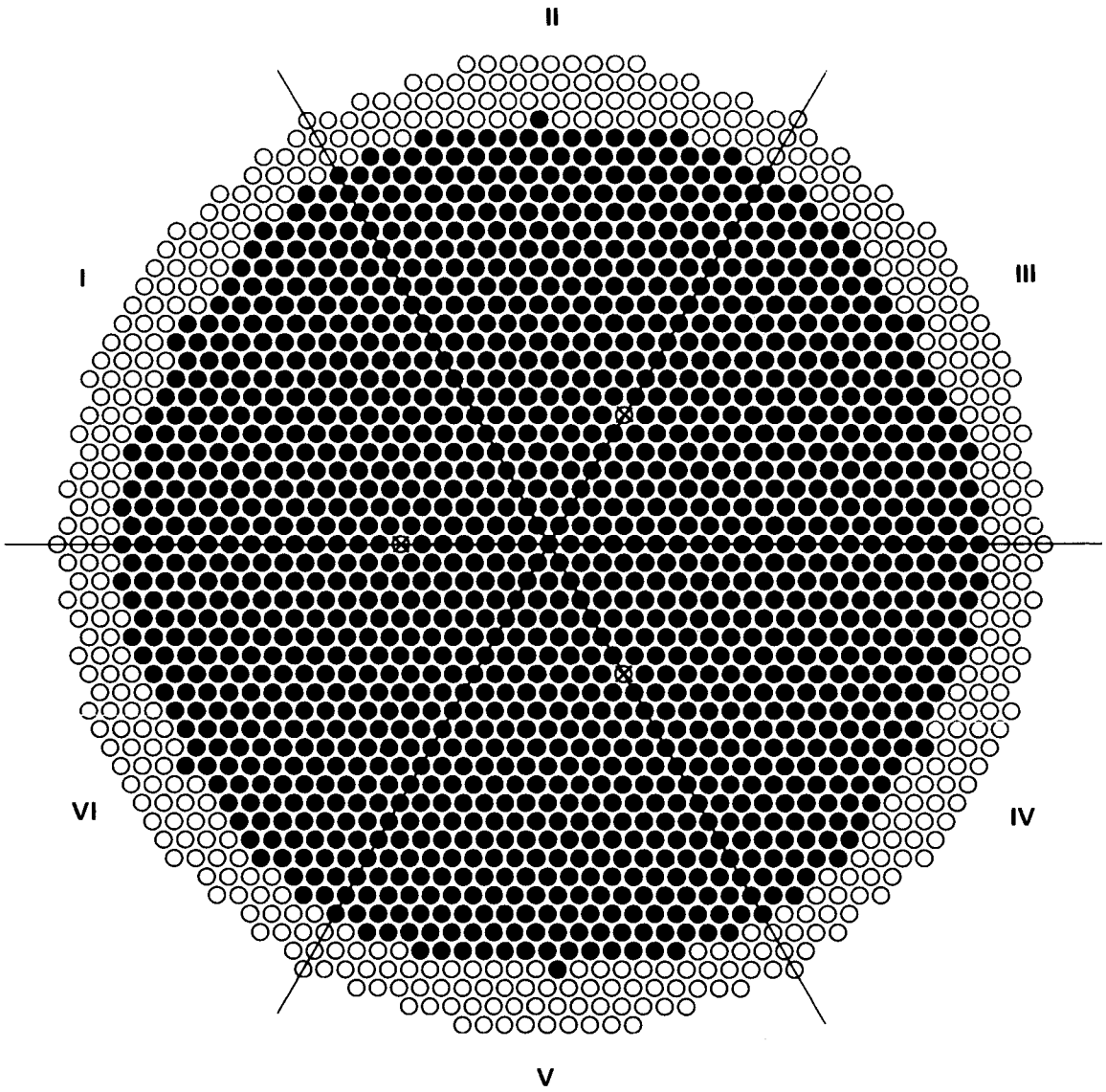

FUEL: 4.31 wt% ^{235}U ENRICHED UO_2

EXPERIMENT: 4.3-000-198B

LATTICE: 13

PITCH: 1.598 ± 0.005 cm

GADOLINIUM: 0.121 ± 0.002 g Gd/liter

CONTROL ROD: OUT

SAFETY ROD: OUT

REACTION RATES: NONE

RODS: 1451 UO_2 RODS AT ●

k_{eff}: 1.0

COMMENTS: WATER FILLED ALUMINUM SLEEVES AT ⊠

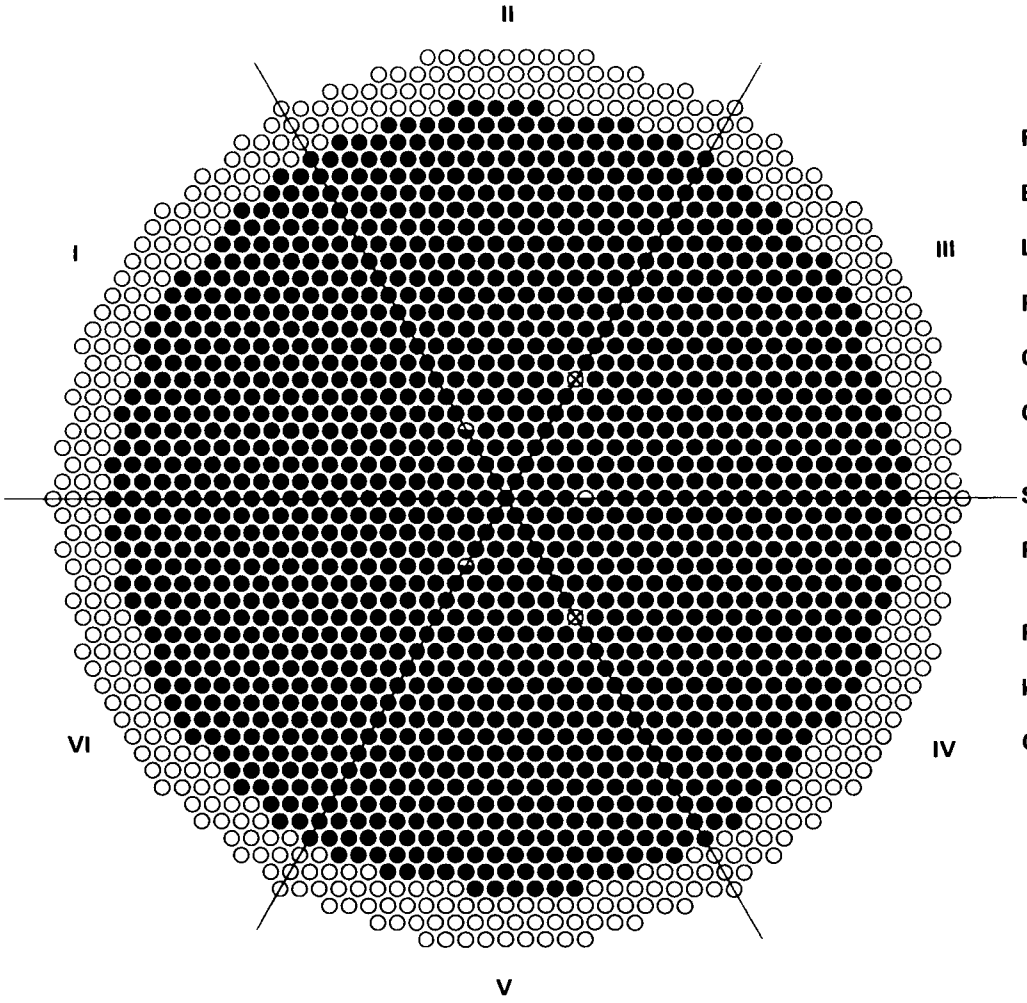

FUEL: 4.31 wt% ^{235}U ENRICHED UO_2

EXPERIMENT: 4.3-000-198C

LATTICE: 13

PITCH: 1.598 ± 0.005 cm

GADOLINIUM: 0.121 ± 0.002 g Gd/liter

CONTROL ROD: OUT 50.6 ± 0.3 cm FROM BOTTOM OF FUEL (LOCATION V ⊠)

SAFETY ROD: OUT

REACTION RATES: ^{238}U AND ^{235}U FOILS IN ◒ (SEE COMMENTS)

RODS: 1475 UO_2 RODS AT ●

k_{eff}: 1.0

COMMENTS: CONTROL AND SAFETY ROD ALUMINUM GUIDE SLEEVES AT ⊠
AEEW 15 FOIL PACKET IN II ◒
AEEW 14 FOIL PACKET IN IV ◒
AEEW 13 FOIL PACKET IN VI ◒

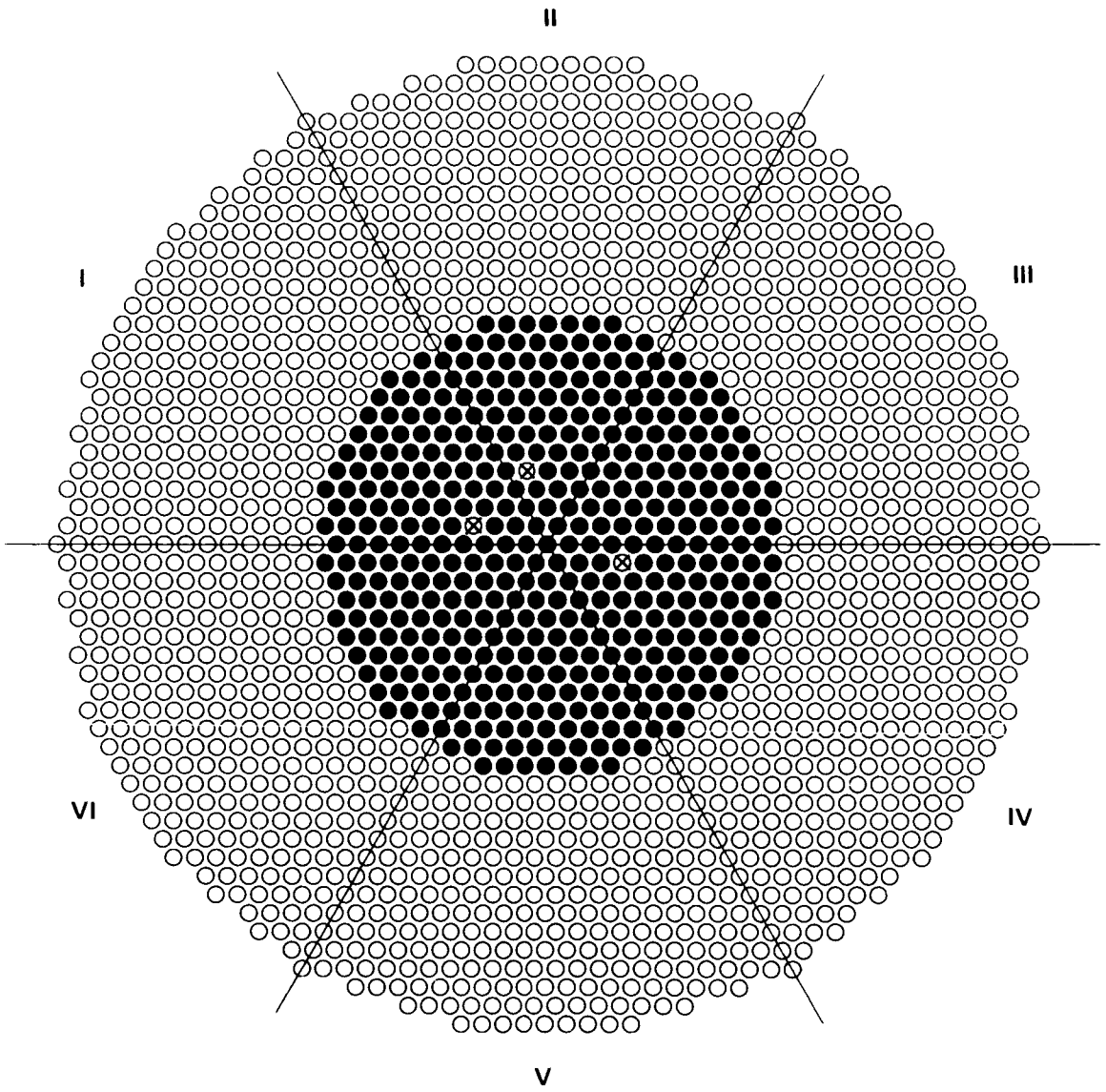

FUEL: 2.35 wt% ^{235}U ENRICHED UO_2

EXPERIMENT: 2.35-000-159A

LATTICE: 21

PITCH: 1.895 ± 0.005 cm

GADOLINIUM: NONE

CONTROL ROD: OUT

SAFETY ROD: OUT

REACTION RATES: NONE

RODS: 428 UO_2 RODS AT ●

k_{eff}: 1.0

COMMENTS: WATER FILLED ALUMINUM SLEEVES AT ⊠

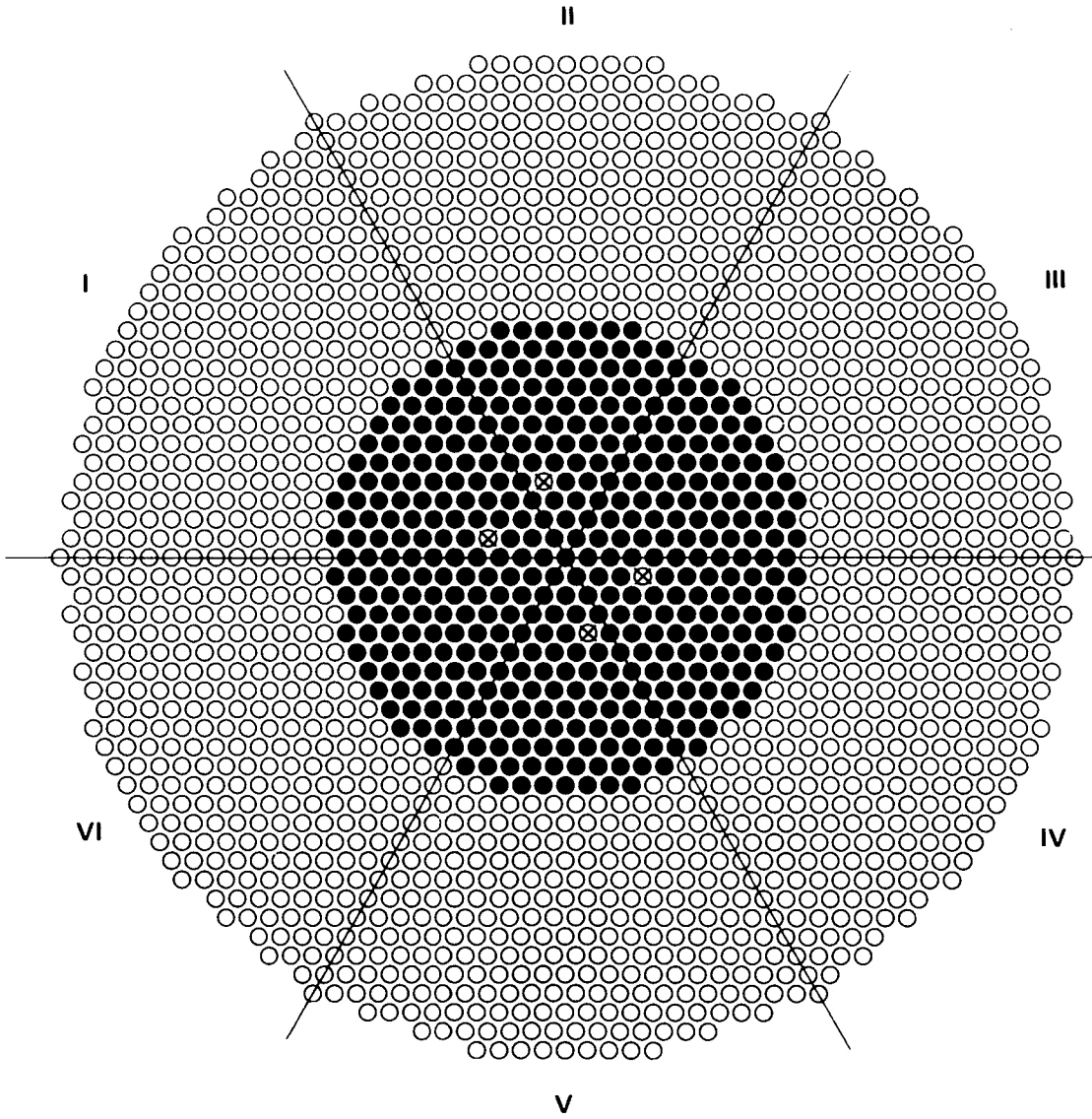

FUEL: 2.35 wt% ^{235}U ENRICHED UO_2

EXPERIMENT: 2.35-000-159B

LATTICE: 21

PITCH: 1.895 ± 0.005 cm

GADOLINIUM: NONE

CONTROL ROD: OUT

SAFETY ROD: OUT

REACTION RATES: NONE

RODS: 427 UO_2 RODS AT ●

k_{eff}: 1.0

COMMENTS: WATER FILLED ALUMINUM SLEEVES AT ⊠

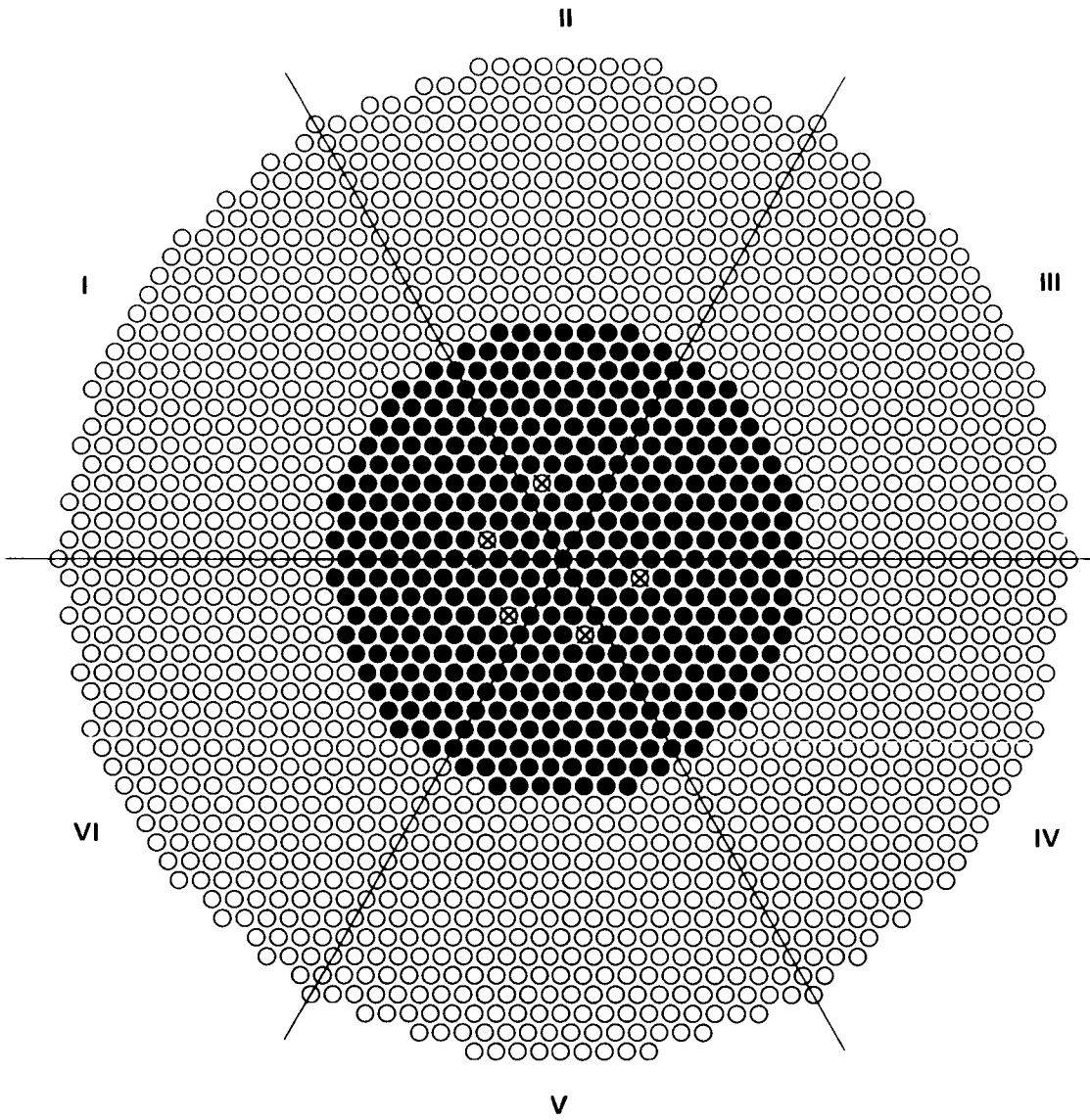

FUEL: 2.35 wt% ^{235}U ENRICHED UO_2

EXPERIMENT: 2.35-000-159C

LATTICE: 21

PITCH: 1.895 ± 0.005 cm

GADOLINIUM: NONE

CONTROL ROD: OUT

SAFETY ROD: OUT

REACTION RATES: NONE

RODS: 426 UO_2 RODS AT ●

k_{eff}: 1.0

COMMENTS: WATER FILLED ALUMINUM SLEEVES AT ⊠

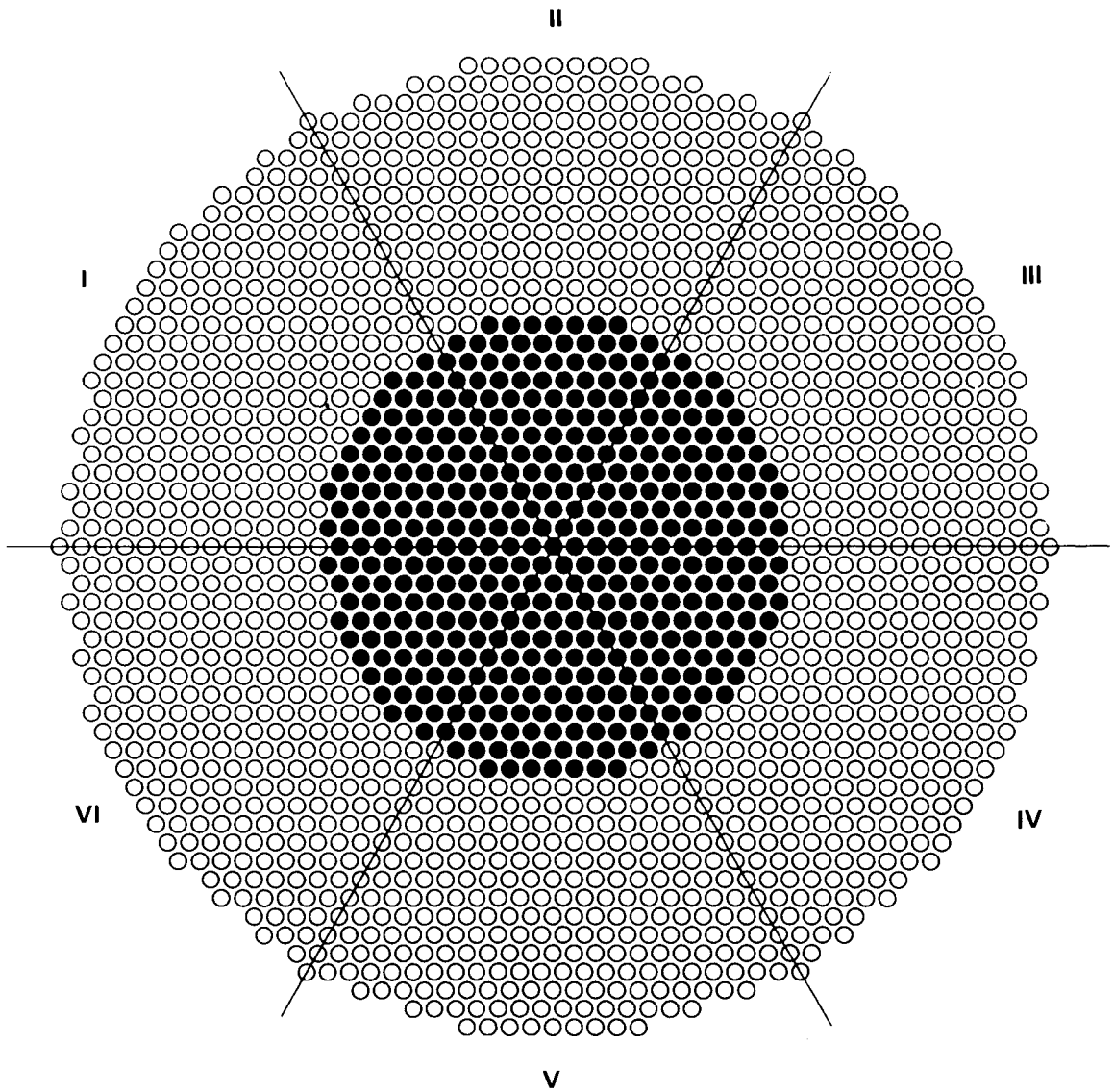

FUEL: 2.35 wt% ^{235}U ENRICHED UO_2

EXPERIMENT: 2.35-000-160

LATTICE: 12

PITCH: 1.895 ± 0.005

GADOLINIUM: SEE COMMENTS

CONTROL ROD: NONE

SAFETY ROD: NONE

REACTION RATES: NONE

RODS: 431 UO_2 RODS AT ●

k_{eff}: SEE COMMENTS

COMMENTS:

k_{eff} = 1.0 AT ZERO g Gd/liter

k_{eff} = 0.960 AT 0.120 ± 0.001 g Gd/Liter

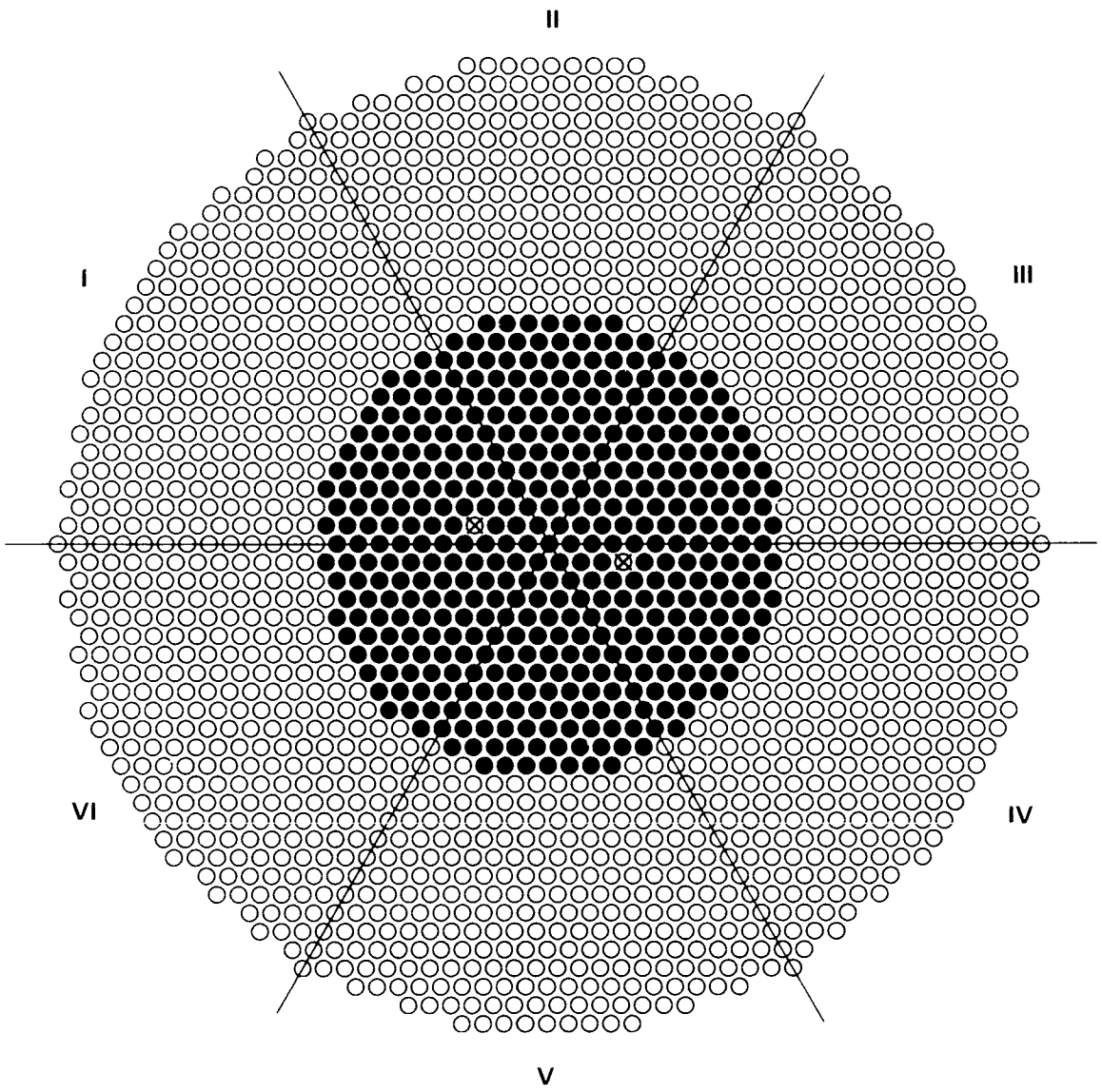

FUEL: 2.35 wt% ^{235}U ENRICHED UO_2

EXPERIMENT: 2.35-000-160A

LATTICE: 21

PITCH: 1.895 ± 0.005 cm

GADOLINIUM: NONE

CONTROL ROD: OUT

SAFETY ROD: OUT

REACTION RATES: NONE

RODS: 429 UO_2 RODS AT ●

k_{eff}: 1.0

COMMENTS: WATER FILLED ALUMINUM SLEEVES AT ⊠

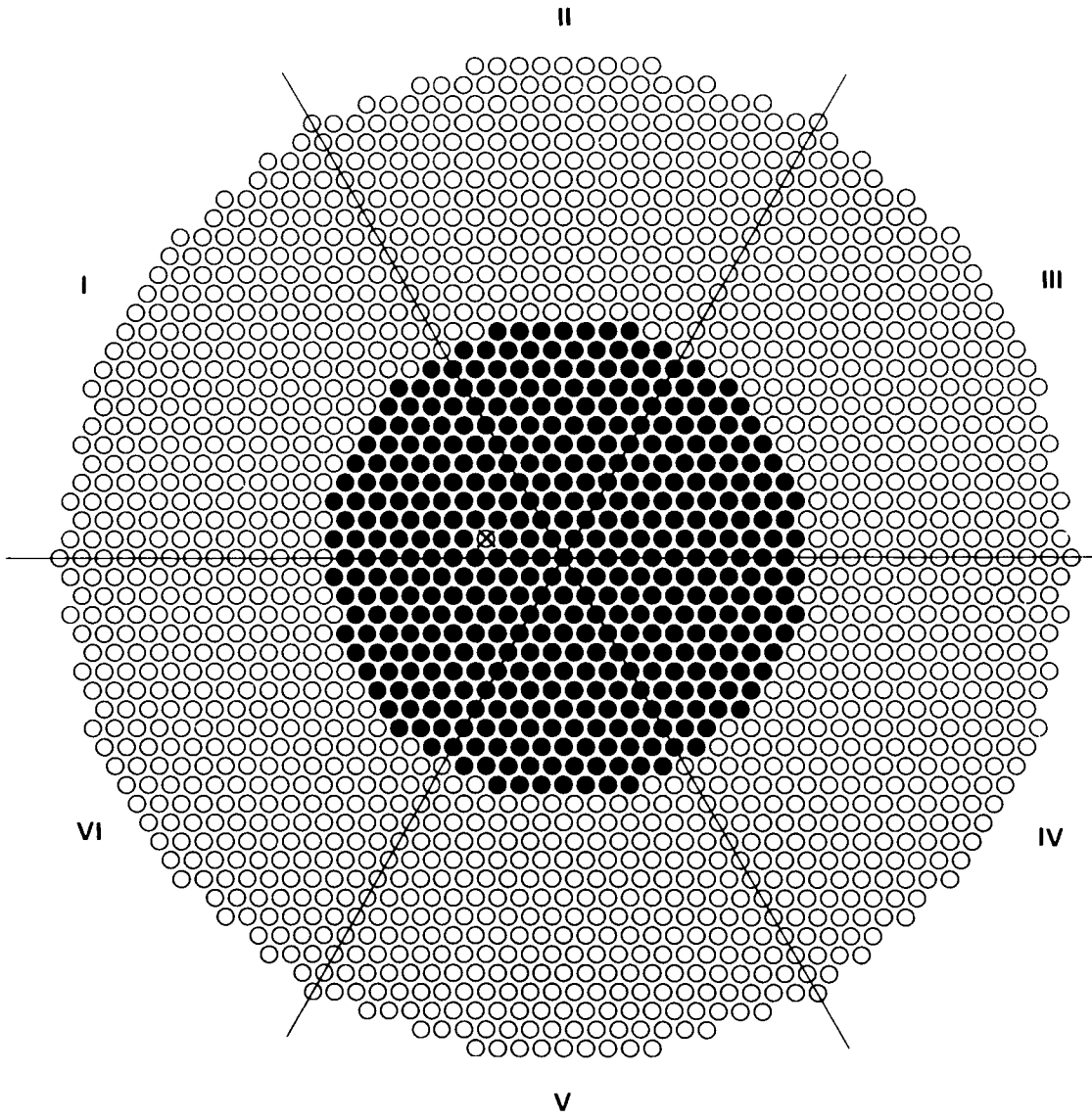

FUEL: 2.35 wt% ^{235}U ENRICHED UO_2

EXPERIMENT: 2.35-000-160B

LATTICE: 21

PITCH: 1.895 ± 0.005 cm

GADOLINIUM: NONE

CONTROL ROD: OUT

SAFETY ROD: OUT

REACTION RATES: NONE

RODS: 430 UO_2 RODS AT ●

k_{eff}: 1.0

COMMENTS: WATER FILLED ALUMINUM SLEEVES AT ⊠

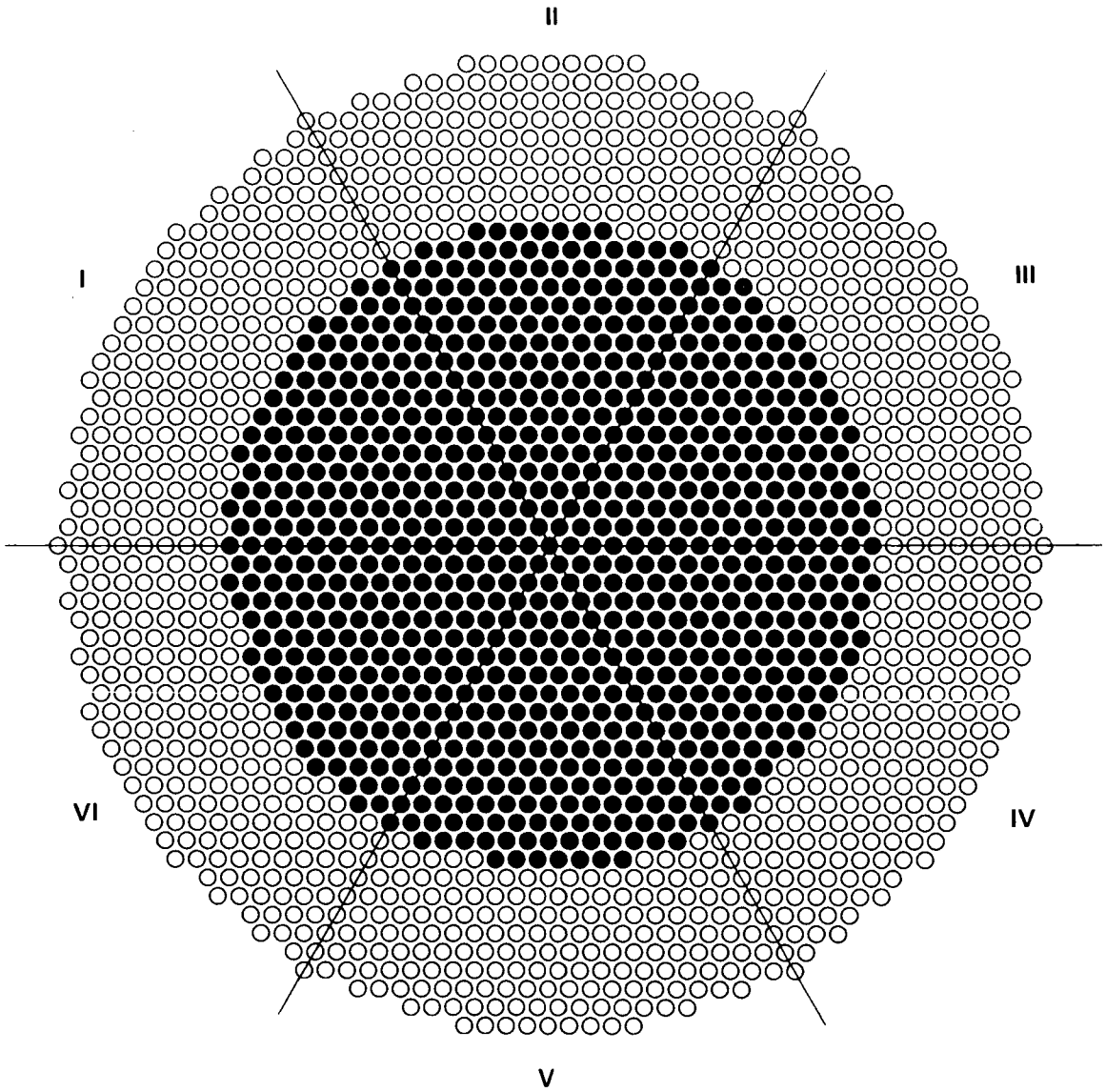

FUEL: 2.35 wt% ^{235}U ENRICHED UO_2

EXPERIMENT: 2.35-000-165

LATTICE: 21

PITCH: 1.895 ± 0.005

GADOLINIUM: SEE COMMENTS

CONTROL ROD: NONE

SAFETY ROD: NONE

REACTION RATES: NONE

RODS: 842 UO_2 RODS AT ●

k_{eff}: SEE COMMENTS

COMMENTS:

$k_{eff} = 1.0$ AT 0.120 ± 0.001 g Gd/liter
$k_{eff} = 0.939$ AT 0.218 ± 0.001 g Gd/liter
$k_{eff} = 0.918$ AT 0.262 ± 0.003 g Gd/liter
$k_{eff} = 0.876$ AT 0.317 ± 0.001 g Gd/liter

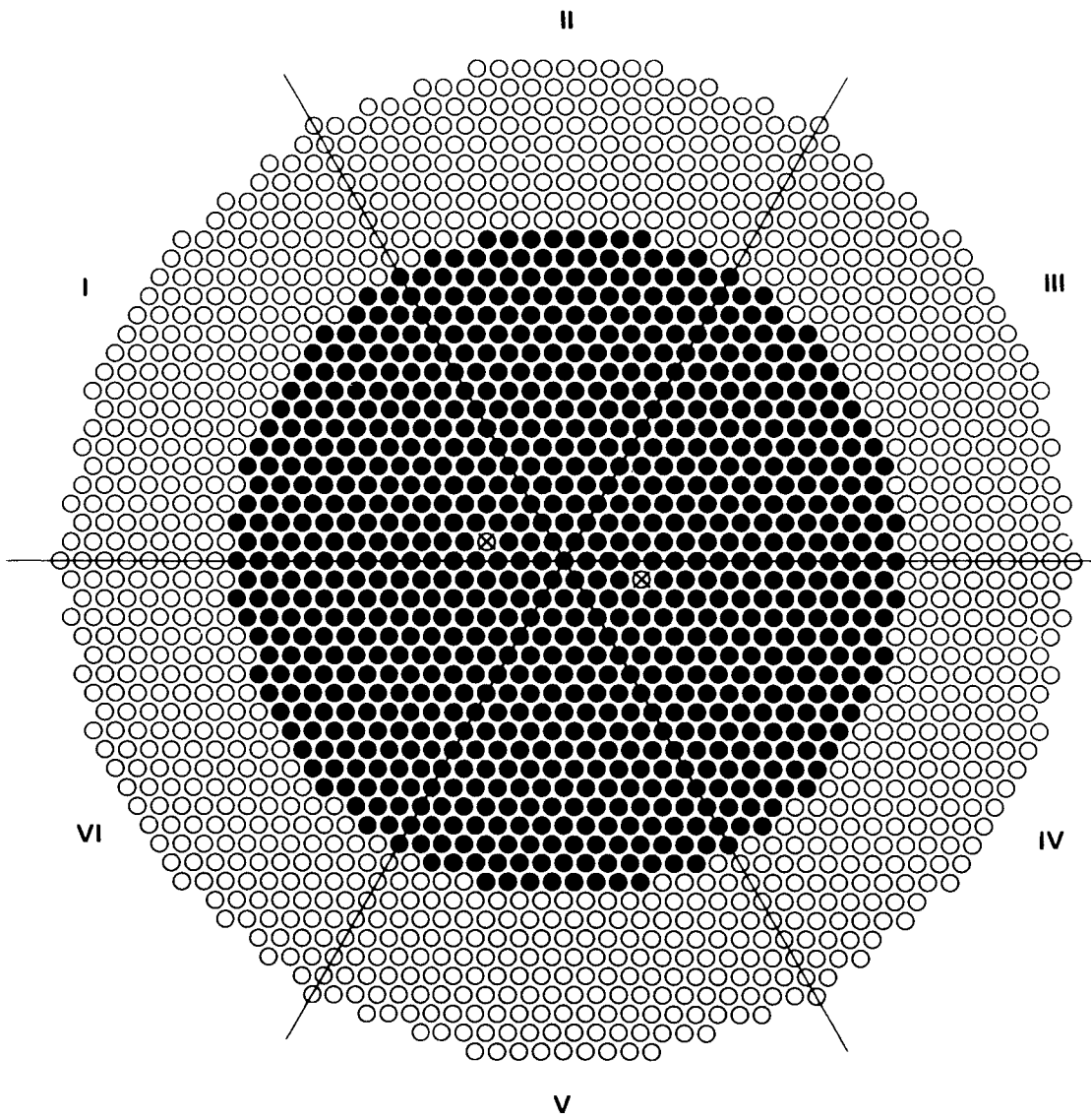

FUEL: 2.35 wt% ^{235}U ENRICHED UO_2

EXPERIMENT: 2.35-000-165A

LATTICE: 21

PITCH: 1.895 + 0.005

GADOLINIUM: 0.120 ± 0.001 g Gd/liter

CONTROL ROD: OUT

SAFETY ROD: OUT

REACTION RATES: NONE

RODS: 842 UO_2 RODS AT ●

k_{eff}: 1.0

COMMENTS: WATER FILLED ALUMINUM SLEEVES AT ⊠

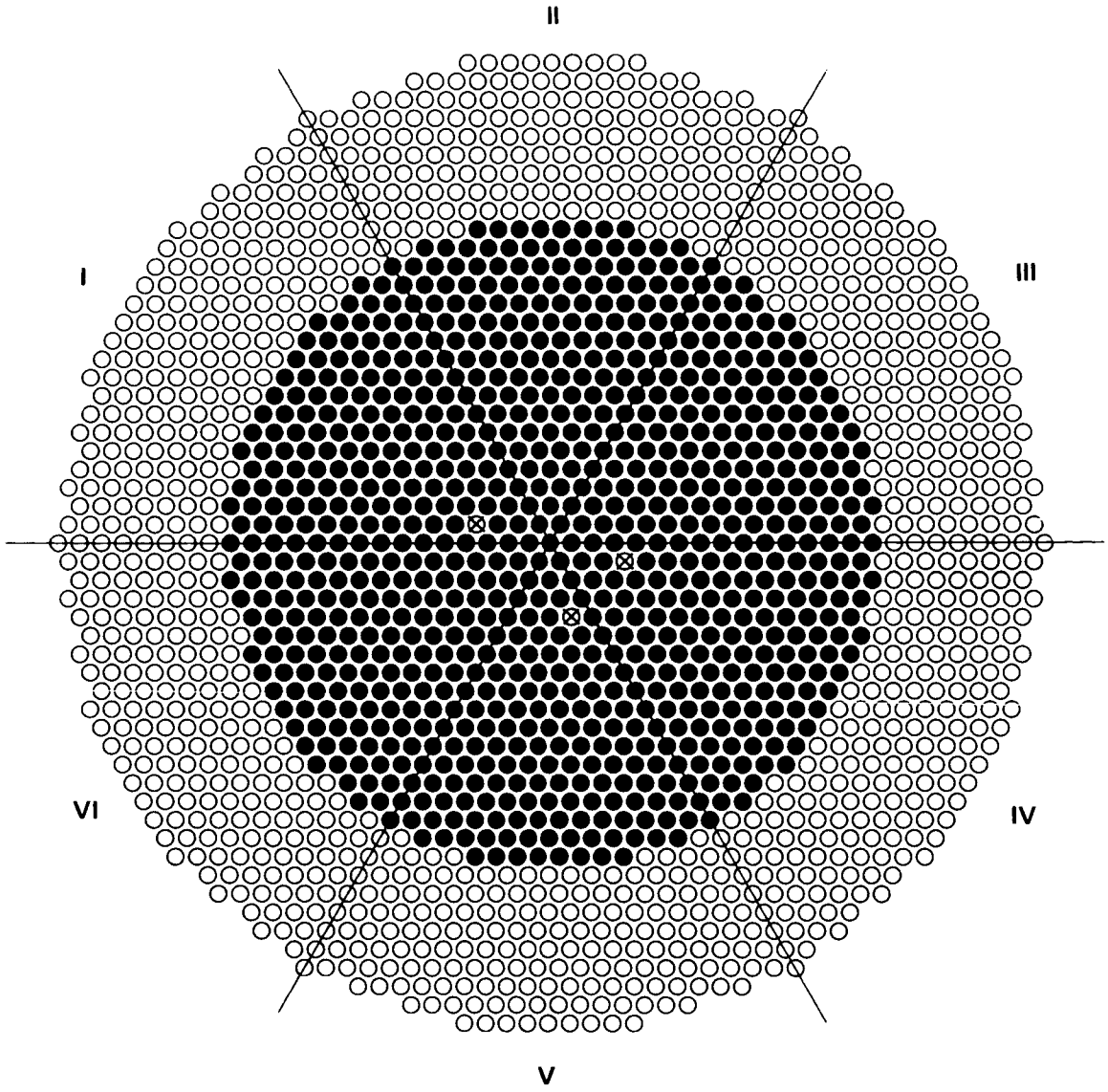

FUEL: 2.35 wt% ^{235}U ENRICHED UO_2

EXPERIMENT: 2.35-000-165 B

LATTICE: 21

PITCH: 1.895 ± 0.005

GADOLINIUM: 0.120 ± 0.001 g Gd/liter

CONTROL ROD: OUT

SAFETY ROD: OUT

REACTION RATES: NONE

RODS: 842 UO_2 RODS AT ●

k_{eff}: 1.0

COMMENTS: WATER FILLED ALUMINUM SLEEVES AT ⊠

F-60

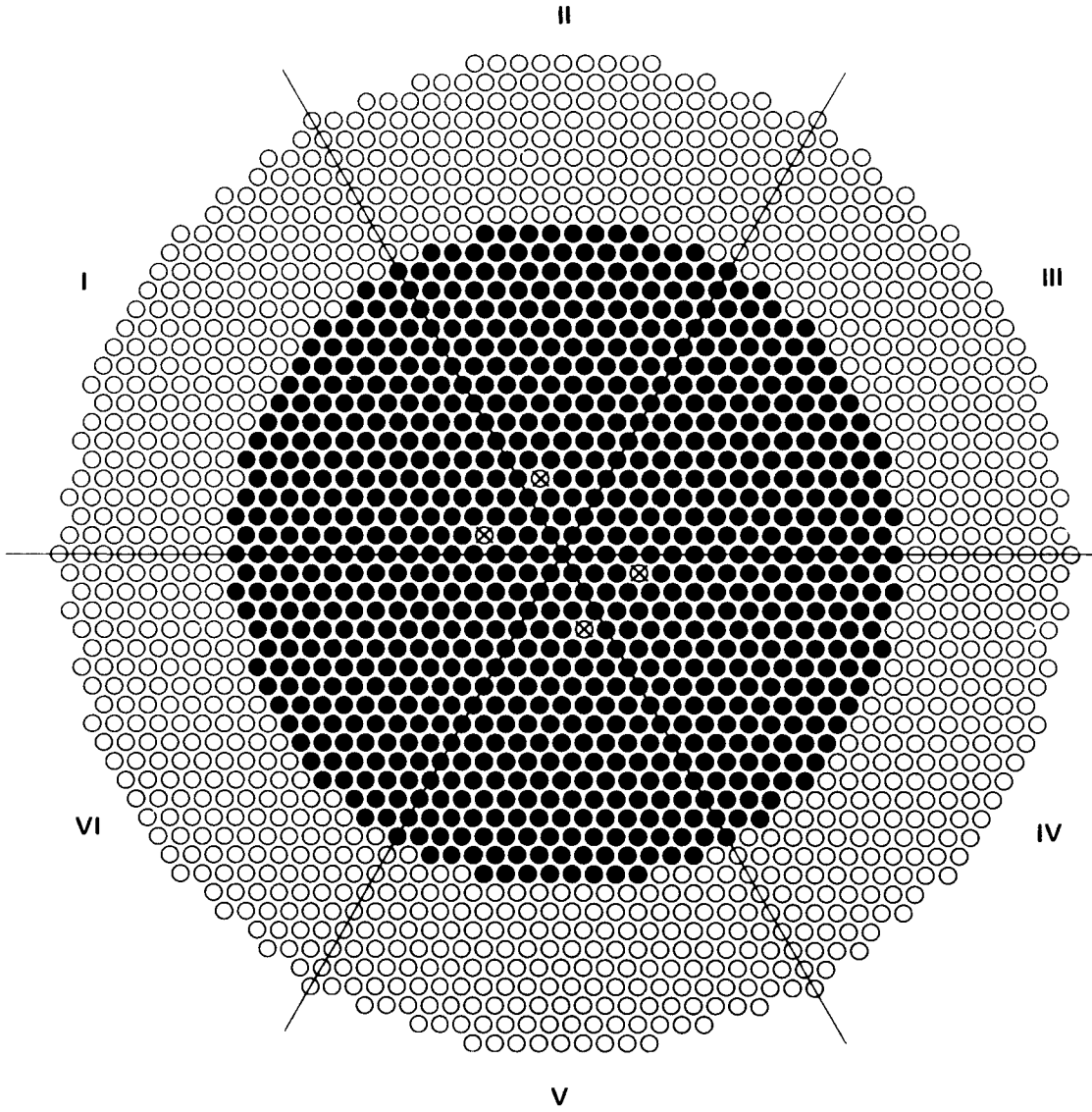

FUEL: 2.35 wt% ^{235}U ENRICHED UO_2

EXPERIMENT: 2.35-000-165C

LATTICE: 21

PITCH: 1.895 ± 0.005

GADOLINIUM: 0.120 ± 0.001 g Gd/liter

CONTROL ROD: OUT

SAFETY ROD: OUT

REACTION RATES: NONE

RODS: 842 UO_2 RODS AT ●

k_{eff}: 1.0

COMMENTS: WATER FILLED ALUMINUM SLEEVES AT ⊠

F.61

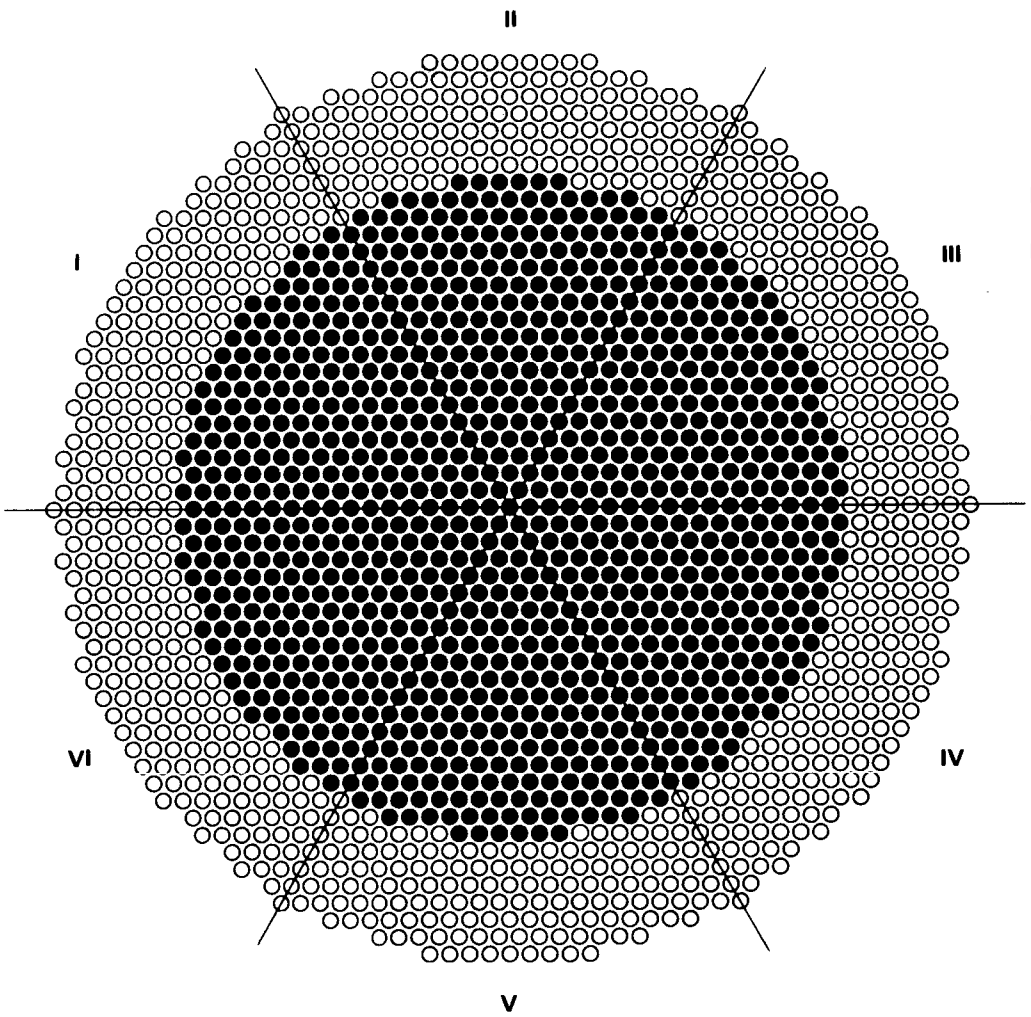

FUEL: 2.35 wt% ^{235}U ENRICHED UO_2

EXPERIMENT: 2.35-000-170

LATTICE: 22

PITCH: 1.598 ± 0.005 cm

GADOLINIUM: SEE COMMENTS

CONTROL ROD: NONE

SAFETY ROD: NONE

REACTION RATES: NONE

RODS: 1029 UO_2 RODS AT ●

k_{eff}: SEE COMMENTS

COMMENTS:

$k_{eff} = 1.0$ AT ZERO g Gd/liter
$k_{eff} = 0.987$ AT 0.055 ± 0.001 g Gd/liter
$k_{eff} = 0.963$ AT 0.078 ± 0.001 g Gd/liter
$k_{eff} = 0.890$ AT 0.257 ± 0.001 g Gd/liter

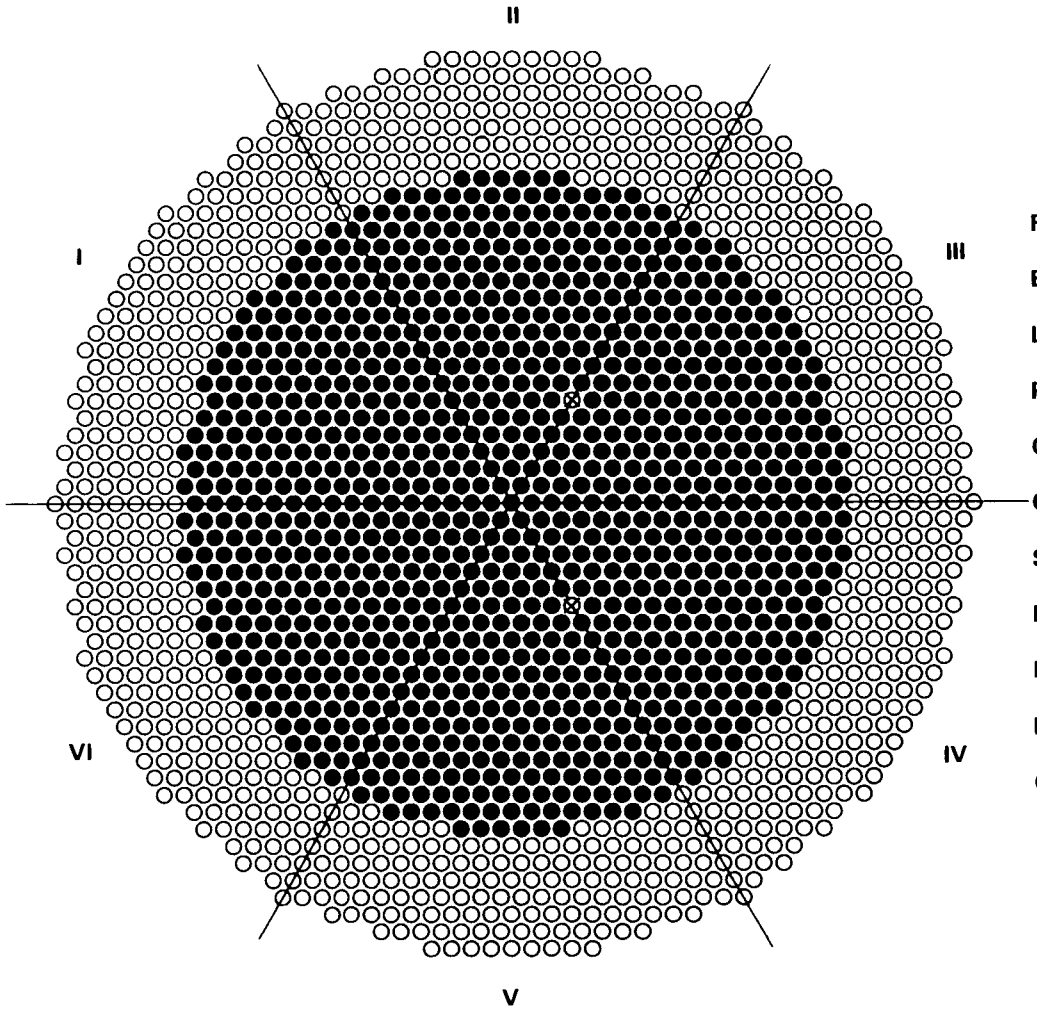

FUEL: 2.35 wt% ^{235}U ENRICHED UO_2

EXPERIMENT: 2.35-000-170A

LATTICE: 22

PITCH: 1.598 ± 0.005 cm

GADOLINIUM: NONE

CONTROL ROD: OUT

SAFETY ROD: OUT

REACTION RATES: NONE

RODS: 1025 UO_2 RODS AT ●

k_{eff}: 1.0

COMMENTS: WATER FILLED ALUMINUM SLEEVES AT ⊠

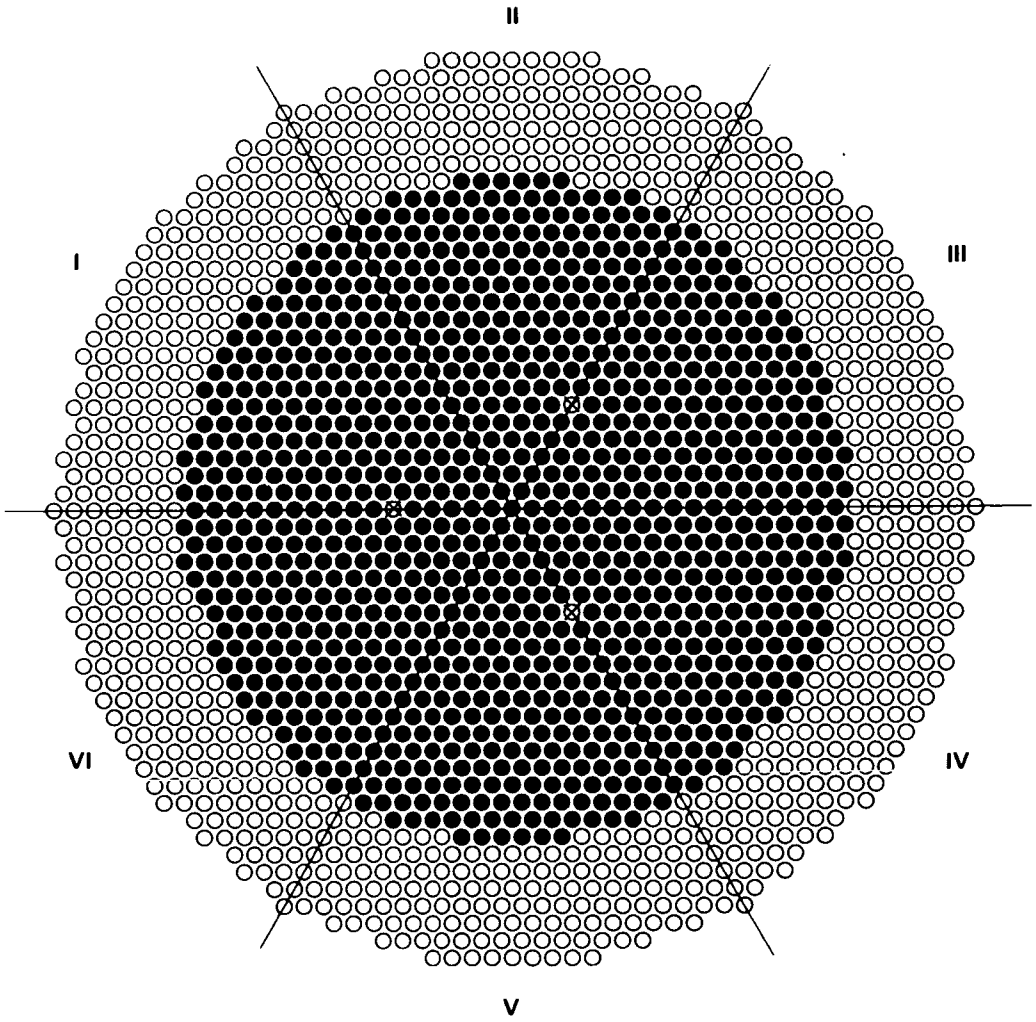

FUEL: 2.35 wt% ^{235}U ENRICHED UO_2

EXPERIMENT: 2.35-000-170B

LATTICE: 22

PITCH: 1.598 ± 0.005 cm

GADOLINIUM: NONE

CONTROL ROD: OUT

SAFETY ROD: OUT

REACTION RATES: NONE

RODS: 1023 UO_2 RODS AT ●

k_{eff}: 1.0

COMMENTS: WATER FILLED ALUMINUM SLEEVES AT ⊠

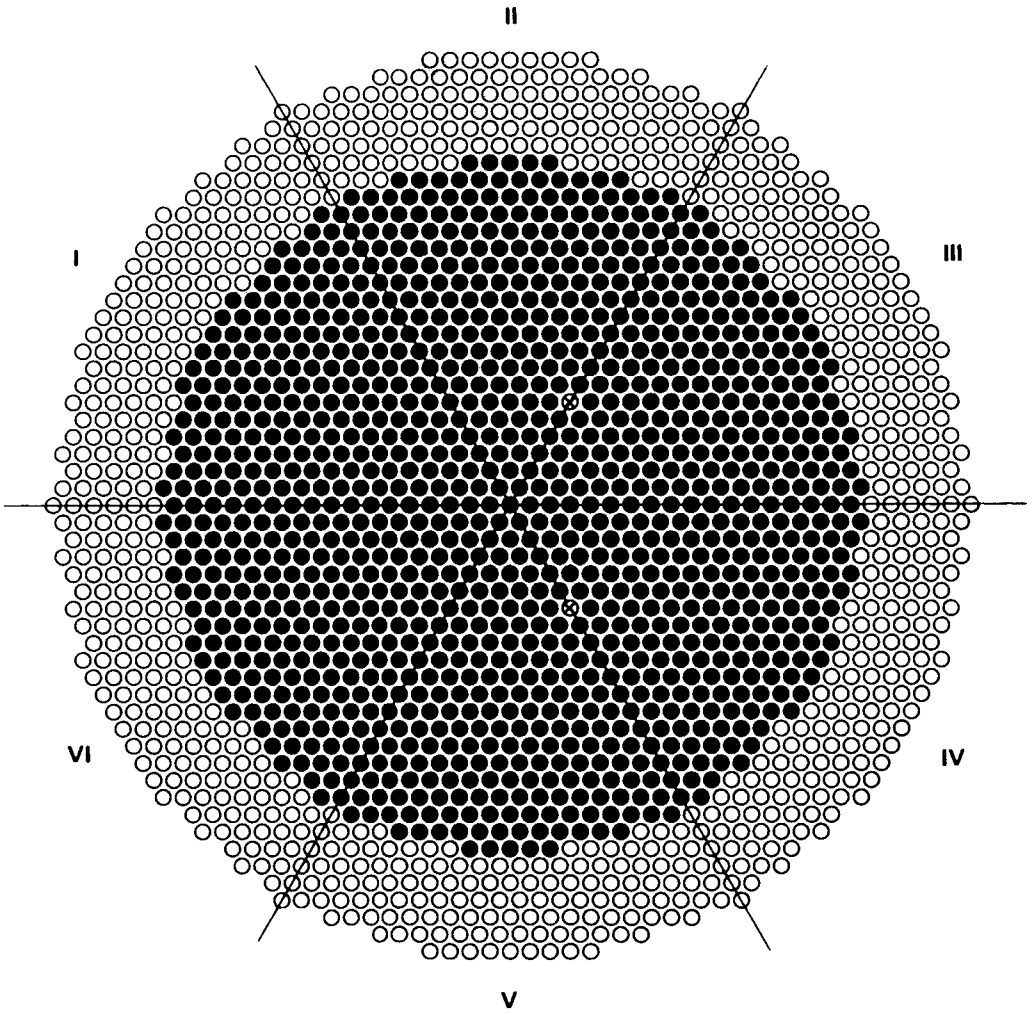

FUEL: 2.35 wt% ^{235}U ENRICHED UO_2

EXPERIMENT: 2.35-000-172

LATTICE: 22

PITCH: 1.598 ± 0.005 cm

GADOLINIUM: 0.055 ± 0.001 g Gd/liter

CONTROL ROD: OUT

SAFETY ROD: OUT

REACTION RATES: NONE

RODS: 1122 UO_2 RODS AT ●

k_{eff}: 1.0

COMMENTS: WATER FILLED ALUMINUM SLEEVES AT ⊗

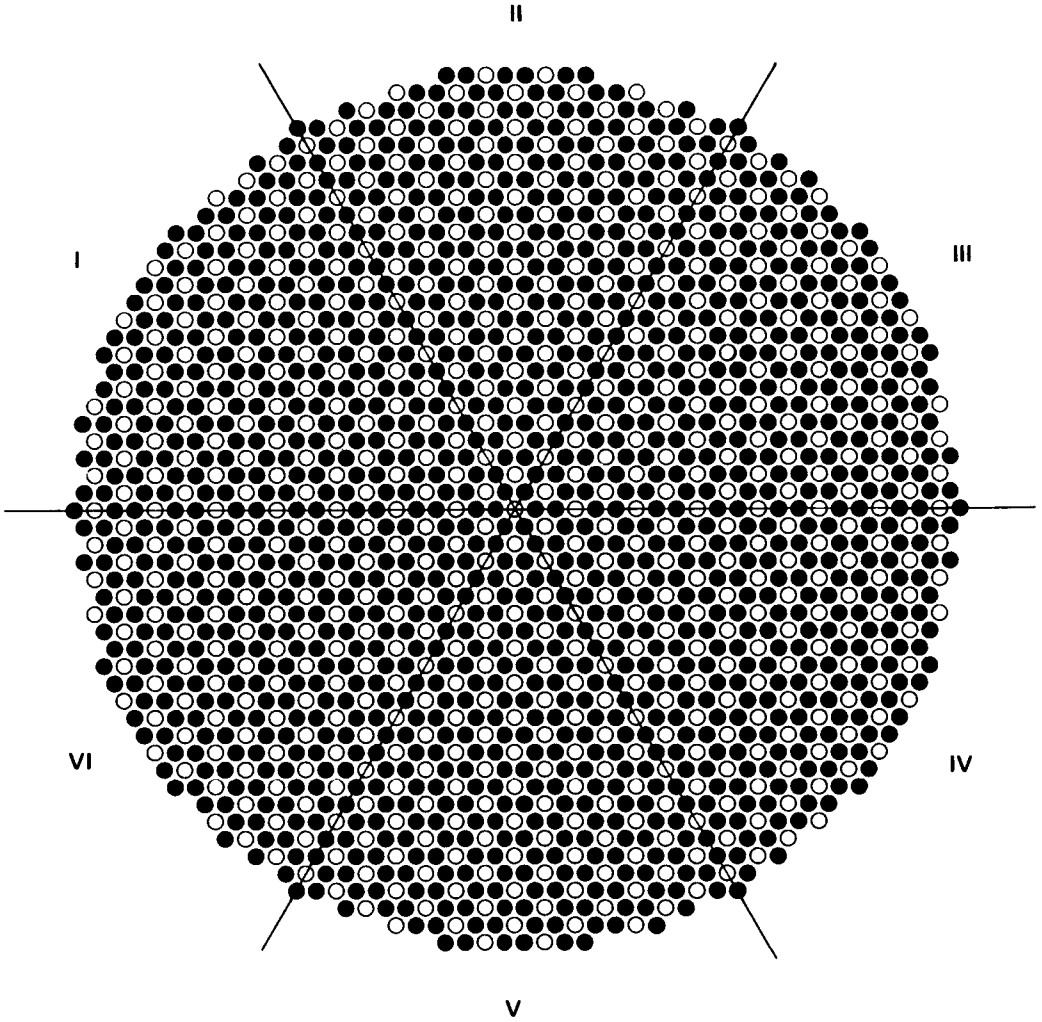

FUEL: 4.31 wt% ^{235}U ENRICHED UO_2 AND PuO_2-NATURAL UO_2 CONTAINING 2.0 wt% PuO_2

EXPERIMENT: 4.3-002-196

LATTICE: 32

PITCH: 1.598 ± 0.005 cm

GADOLINIUM: SEE COMMENTS

CONTROL ROD: NONE

SAFETY ROD: NONE

REACTION RATES: NONE

RODS: 583 MO_2 RODS AT ○ PLUS 1174 UO_2 RODS AT ●

k_{eff}: SEE COMMENTS

COMMENTS: PERIPHERIAL UNUSED LATTICE LOCATIONS NOT SHOWN

$k_{eff} = 1.0$ AT ZERO g Gd/liter
$k_{eff} = 0.957$ AT 0.194 ± 0.001 g Gd/liter
$k_{eff} = 0.931$ AT 0.408 ± 0.006 g Gd/liter
$k_{eff} = 0.914$ AT 0.626 ± 0.008 g Gd/liter
$k_{eff} = 0.891$ AT 0.918 ± 0.015 g Gd/liter

F.66

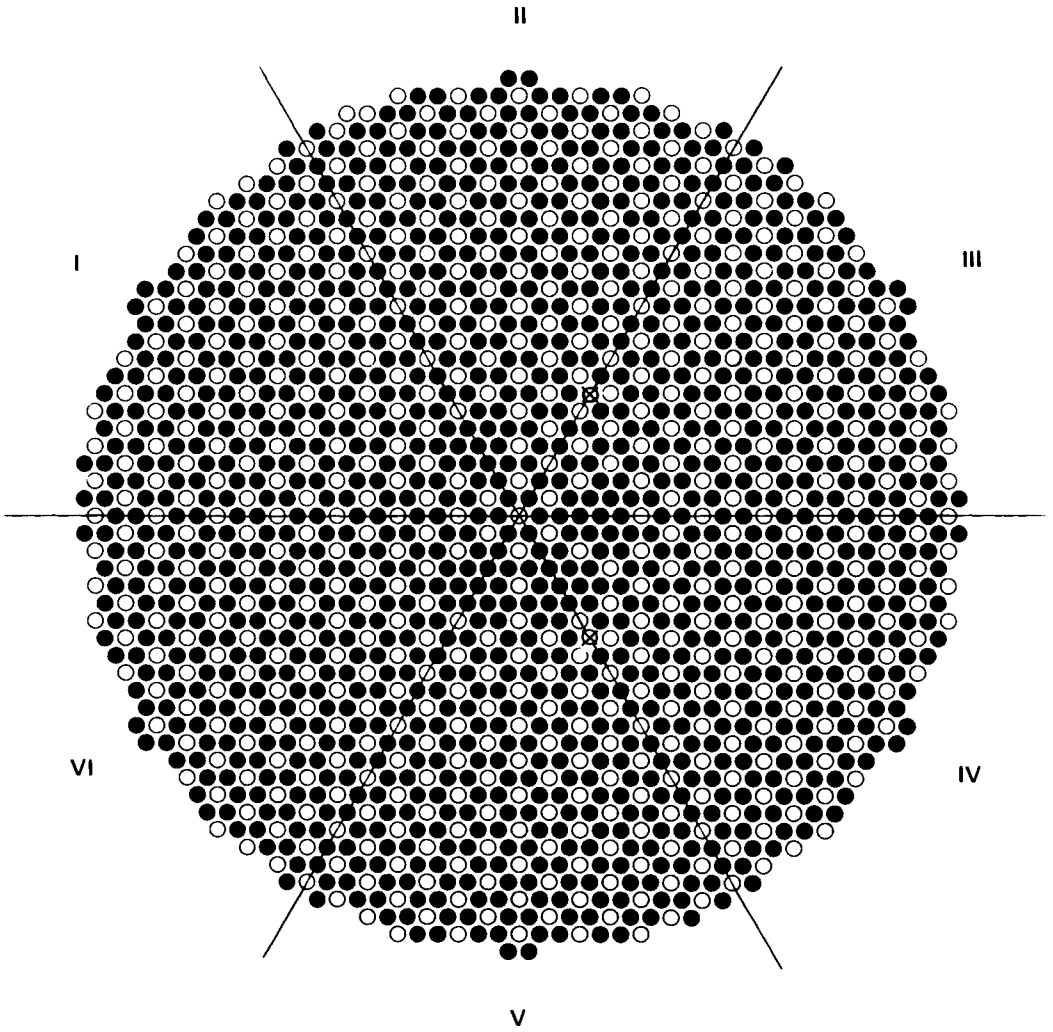

FUEL: 4.31 wt% ^{235}U ENRICHED UO_2 AND PuO_2-NATURAL UO_2 CONTAINING 2.0 wt% PuO_2

EXPERIMENT: 4.3-002-196A

LATTICE: 32

PITCH: 1.598 ± 0.005 cm

GADOLINIUM: NONE

CONTROL ROD: OUT

SAFETY ROD: OUT

REACTION RATES: NONE

RODS: 559 MO_2 RODS AT ○ PLUS
1142 UO_2 RODS AT ●

k_{eff}: 1.0

COMMENTS: WATER FILLED ALUMINIUM SLEEVES AT ⊠
PERIPHERIAL UNUSED
LATTICE LOCATIONS NOT SHOWN

F.67

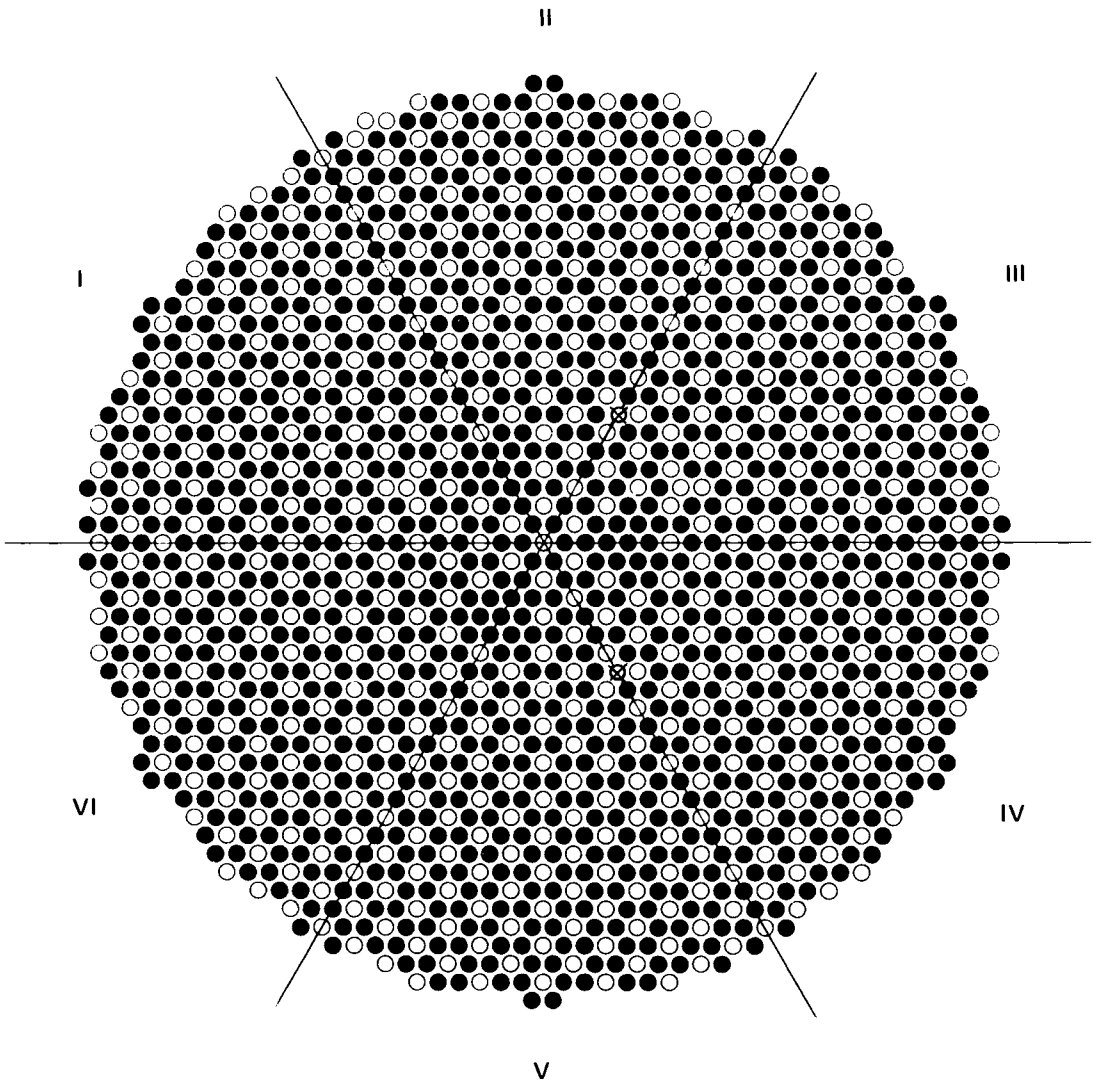

FUEL: 4.31 wt% ^{235}U ENRICHED UO_2 AND PuO_2-
NATURAL UO_2 CONTAINING 2.0 wt% PuO_2

EXPERIMENT: 4.3-002-196B

LATTICE: 32

PITCH: 1.598 ± 0.005 cm

GADOLINIUM: NONE

CONTROL ROD: OUT

SAFETY ROD: OUT

REACTION RATES: NONE

RODS: 562 MO_2 RODS AT ○ PLUS
1146 UO_2 RODS AT ●

k_{eff}: 1.0

COMMENTS: WATER FILLED ALUMINUM
SLEEVES AT ⊠
PERIPHERIAL UNUSED LATTICE
LOCATIONS NOT SHOWN

F-68

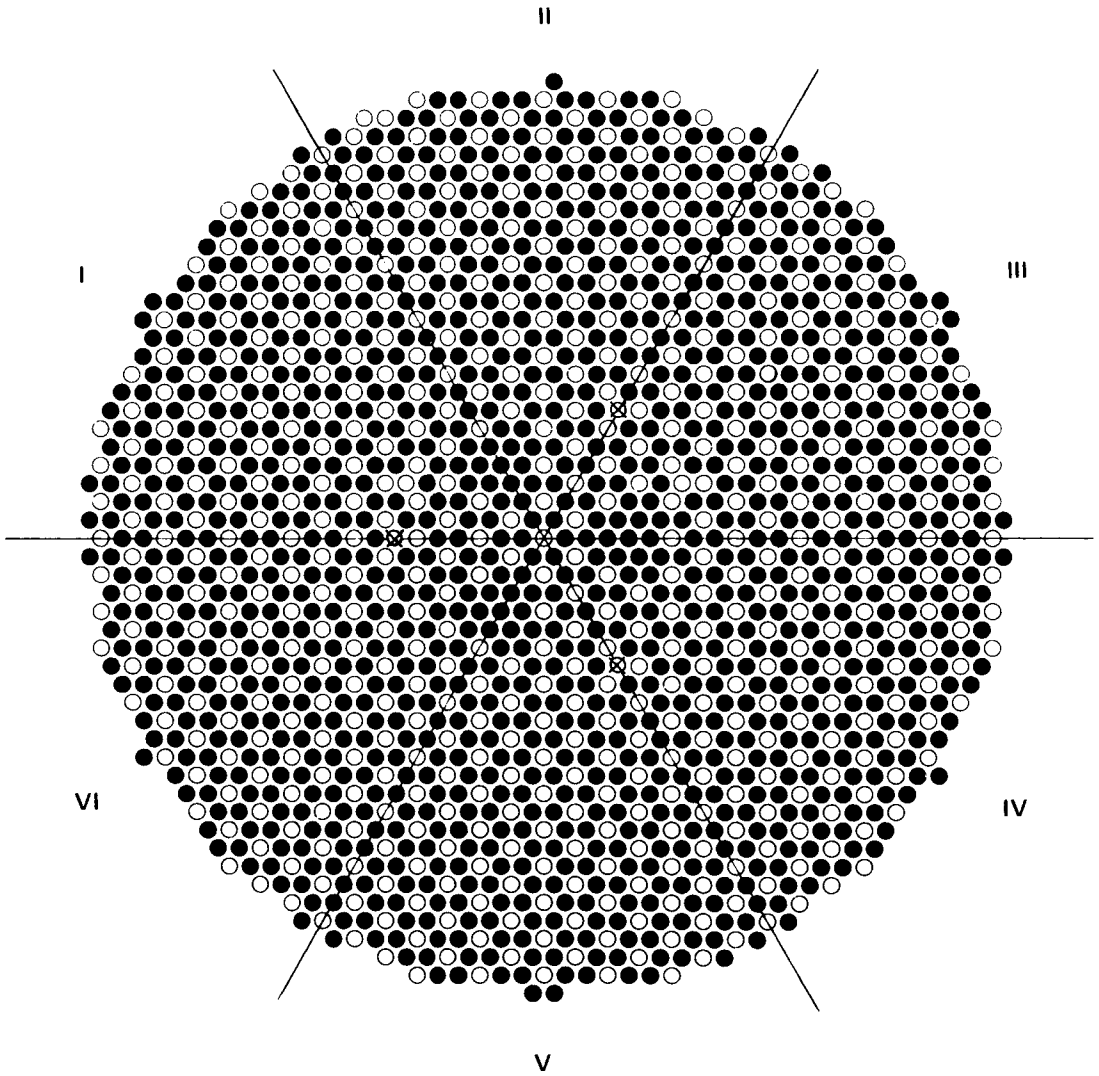

FUEL: 4.31 wt% ^{235}U ENRICHED UO_2 AND PuO_2-NATURAL UO_2 CONTAINING 2.0 wt% PuO_2

EXPERIMENT: 4.3-002-196C

LATTICE: 32

PITCH: 1.598 ± 0.005 cm

GADOLINIUM: NONE

CONTROL ROD: OUT

SAFETY ROD: OUT

REACTION RATES: NONE

RODS: 562 PuO_2-UO_2 RODS AT ○ PLUS
1131 UO_2 RODS AT ●

k_{eff}: 1.0

COMMENTS: WATER FILLED ALUMINUM SLEEVES AT ⊠
PERIPHERIAL UNUSED LATTICE LOCATIONS NOT SHOWN

F.69

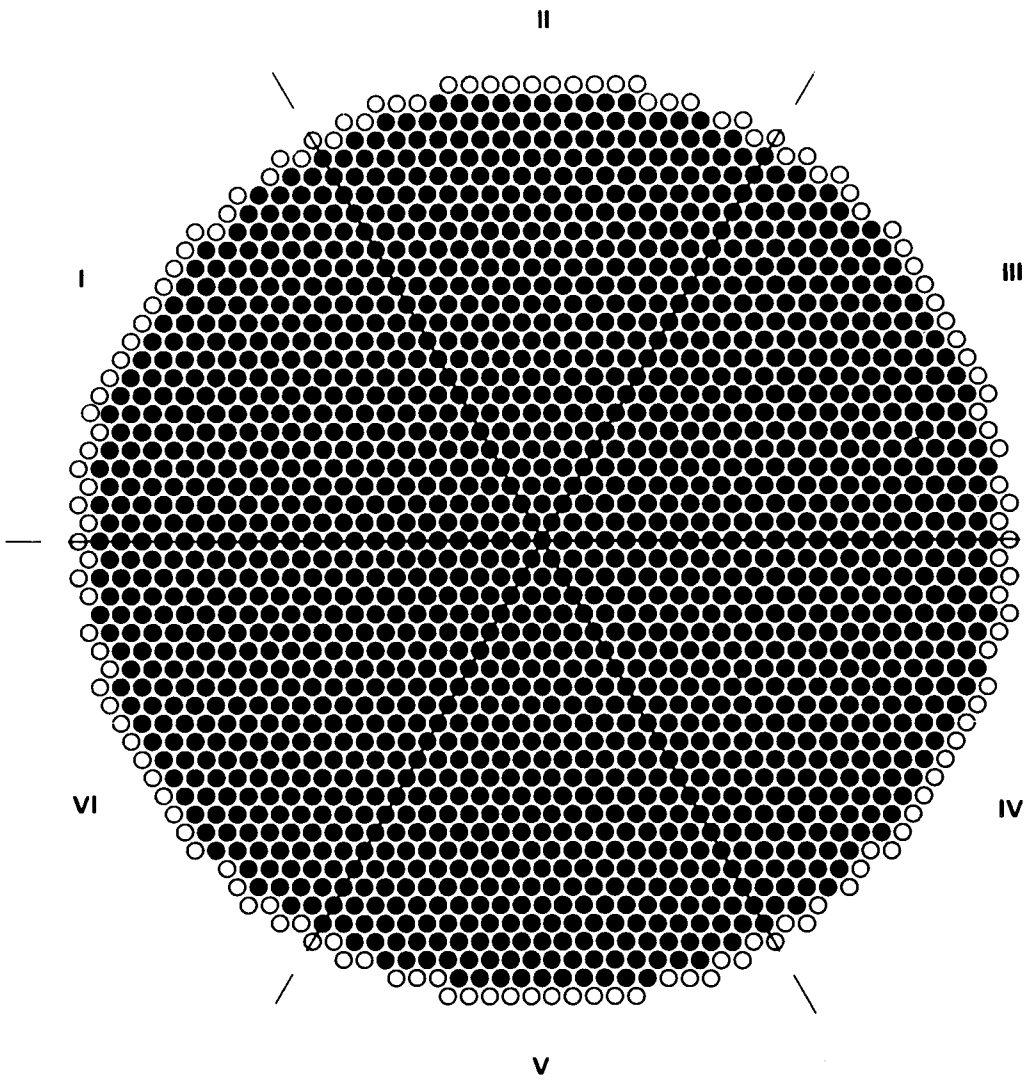

FUEL: 4.31 wt% ^{235}U ENRICHED UO_2 AND PuO_2-NATURAL UO_2 CONTAINING 2.0 wt% PuO_2

EXPERIMENT: 4.3-000-207

LATTICE: 32M

PITCH: 1.598 ± 0.005 cm

GADOLINIUM: 0.466 ± 0.001 g Gd/liter

CONTROL ROD: OUT

SAFETY ROD: OUT

REACTION RATES: NONE

RODS: 139 MO_2 RODS AT ○ PLUS 1657 UO_2 RODS AT ●

k_{eff}: 1.0

COMMENTS: . PERIPHERIAL UNUSED LATTICE LOCATIONS NOT SHOWN.

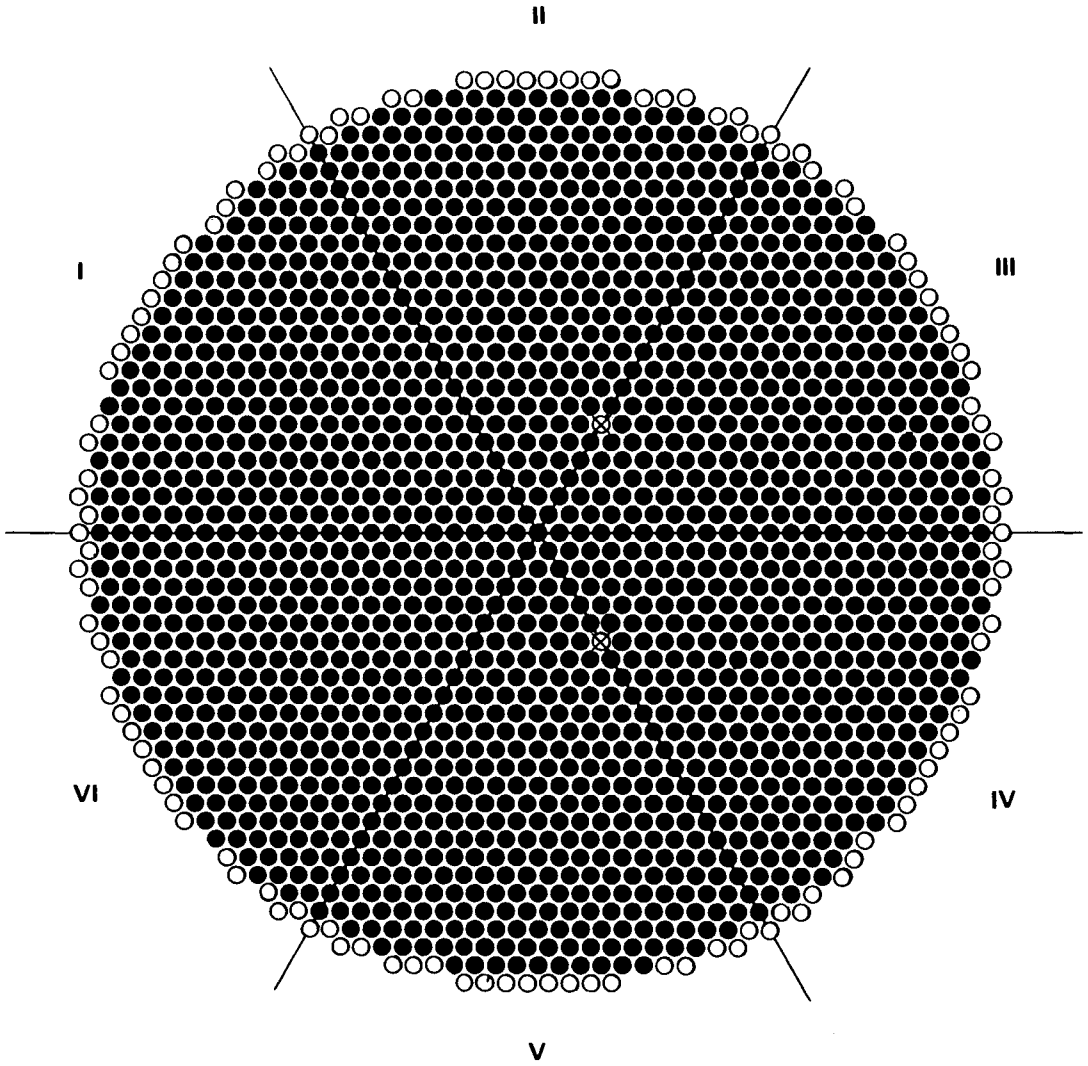

FUEL: 4.31 wt% ^{235}U ENRICHED UO_2 AND PuO_2-NATURAL UO_2 CONTAINING 2.0 wt% PuO_2

EXPERIMENT: 4.3-000-207A

LATTICE: 32M

PITCH: 1.598 ± 0.005 cm

GADOLINIUM: 0.466 ± 0.001 g Gd/liter

CONTROL ROD: OUT

SAFETY ROD: OUT

REACTION RATES: NONE

RODS: 120 MO_2 RODS AT ○ PLUS 1655 UO_2 RODS AT ●

k_{eff}: 1.0

COMMENTS: WATER FILLED ALUMINUM SLEEVE AT ⊠. PERIPHERIAL UNUSED LATTICE LOCATIONS NOT SHOWN.

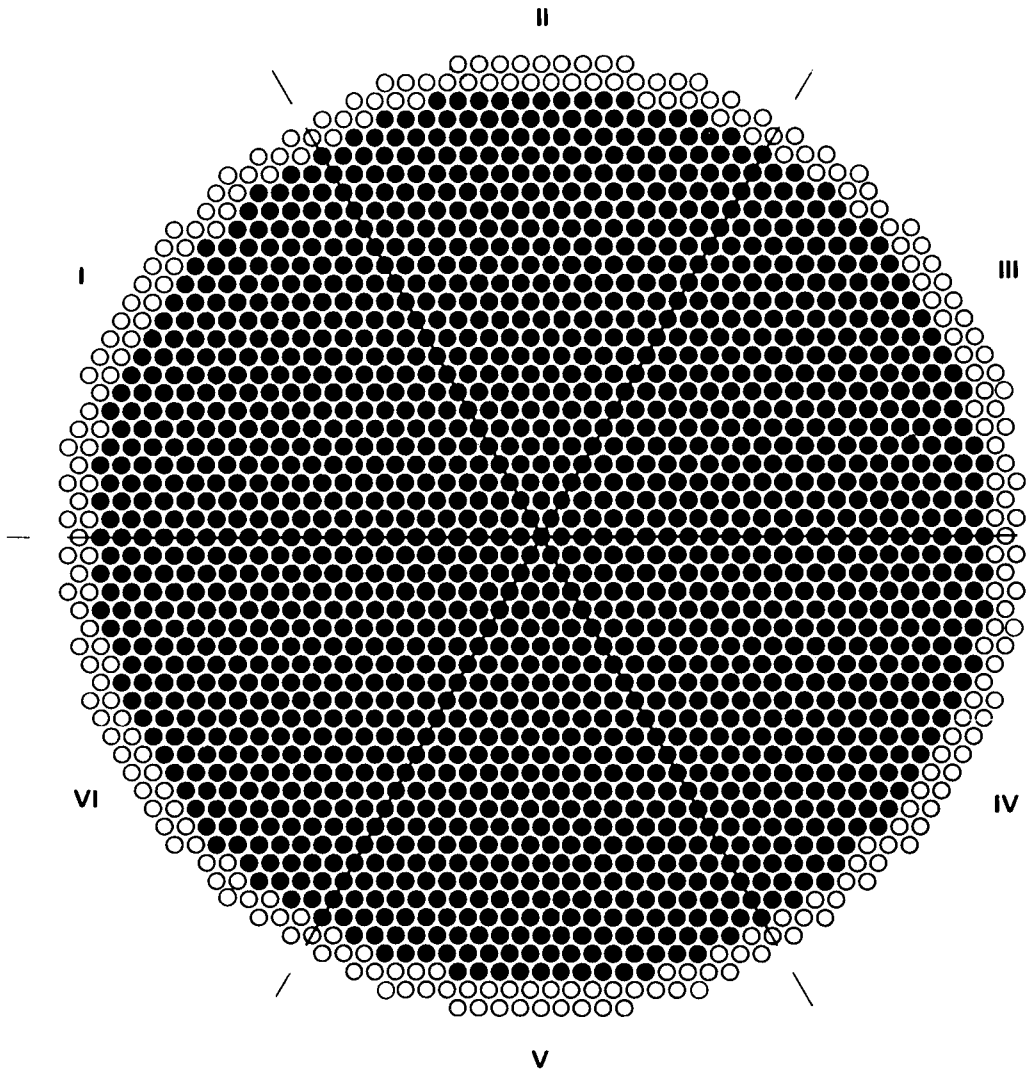

FUEL: 4.31 wt% ^{235}U ENRICHED UO_2 AND PuO_2-NATURAL UO_2 CONTAINING 2.0 wt% PuO_2

EXPERIMENT: 4.3-000-208

LATTICE: 32M

PITCH: 1.598 ± 0.005 cm

GADOLINIUM: 0.566 ± 0.010 g Gd/liter

CONTROL ROD: NONE

SAFETY ROD: NONE

REACTION RATES: NONE

RODS: 256 MO_2 RODS AT ○ PLUS 1657 UO_2 RODS AT ●

k_{eff}: 1.0

COMMENTS: PERIPHERAL UNUSED LATTICE LOCATIONS NOT SHOWN.

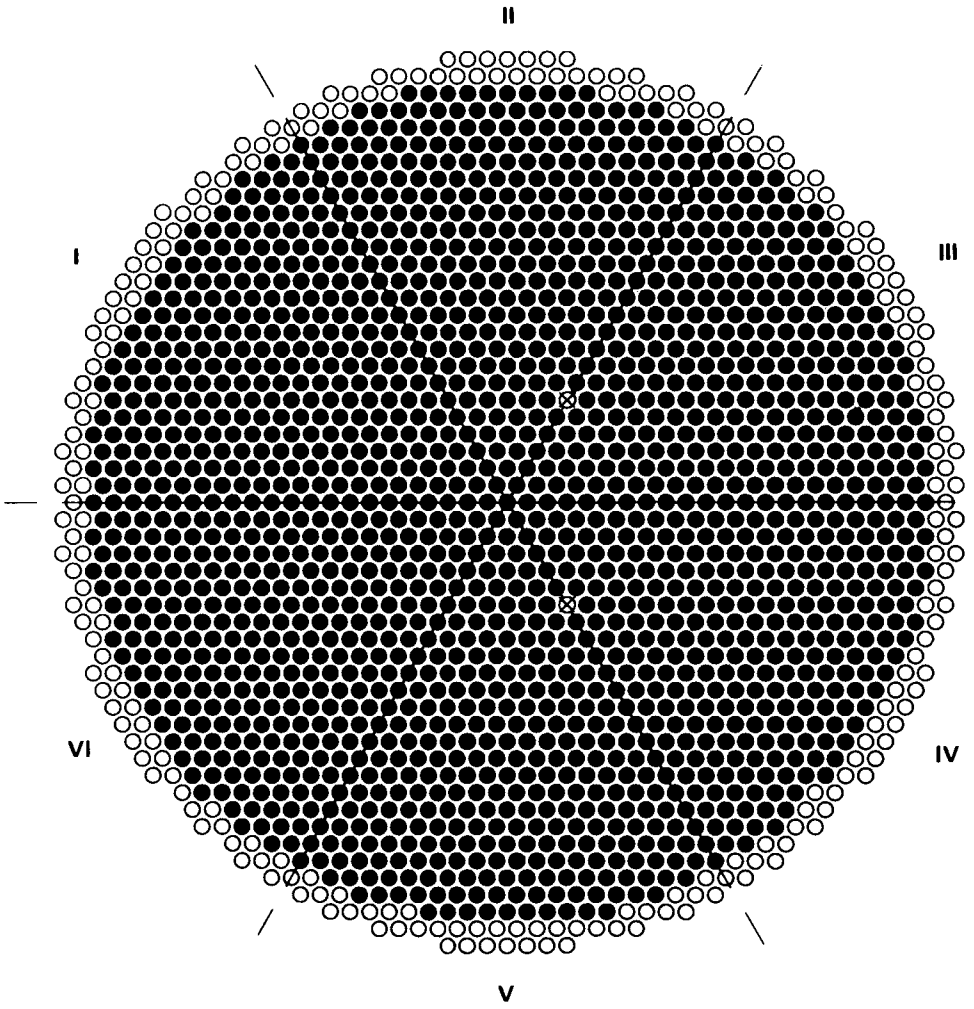

FUEL: 4.31 wt% ^{235}U ENRICHED UO_2 AND PuO_2-NATURAL UO_2 CONTAINING 2.0 wt% PuO_2

EXPERIMENT: 4.3-000-208A

LATTICE: 32M

PITCH: 1.598 ± 0.005 cm

GADOLINIUM: 0.566 ± 0.010 g Gd/liter

CONTROL ROD: OUT

SAFETY ROD: OUT

REACTION RATES: NONE

RODS: 237 MO_2 RODS AT ○ PLUS 1655 UO_2 RODS AT ●

k_{eff}: 1.0

COMMENTS: WATER FILLED ALUMINUM SLEEVE AT ⊠. PERIPHERIAL UNUSED LATTICE LOCATIONS NOT SHOWN.

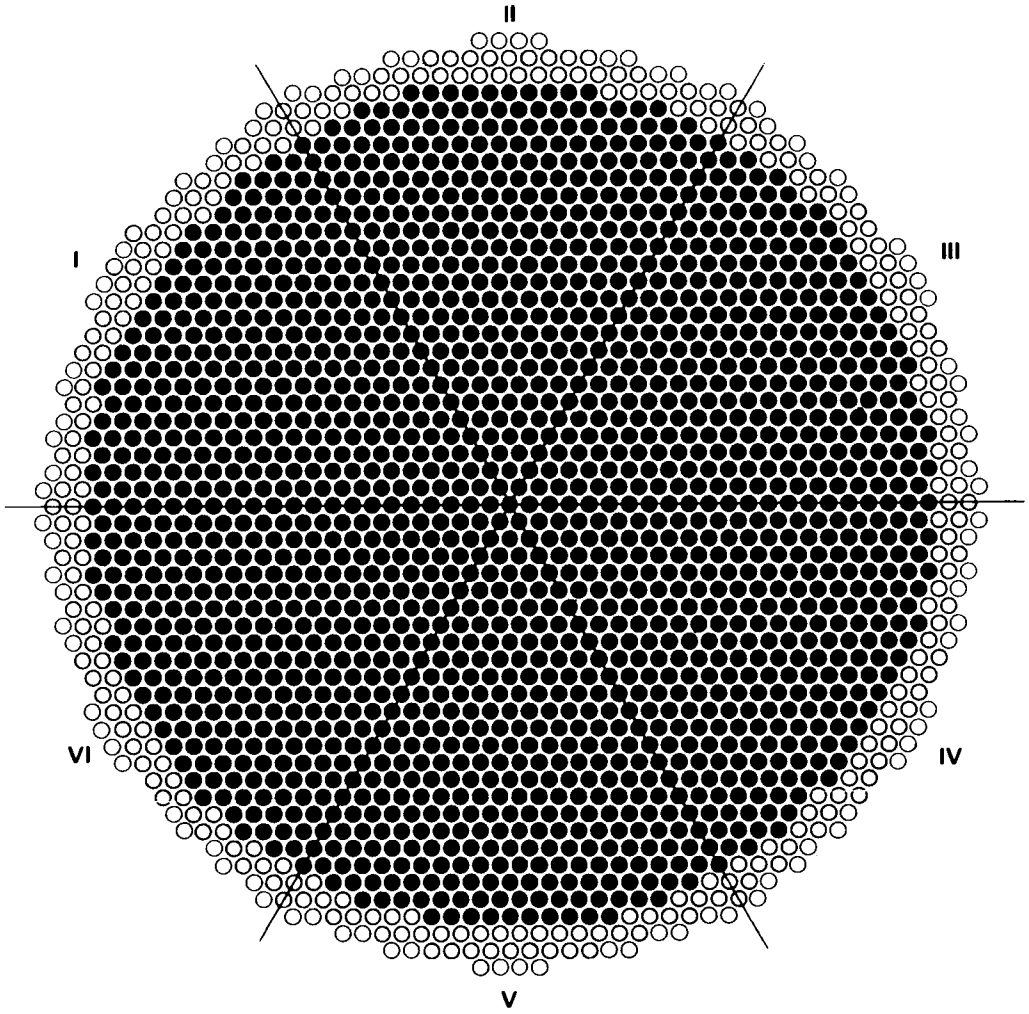

FUEL: 4.31 wt% ^{235}U ENRICHED UO_2 AND PuO_2-NATURAL UO_2 CONTAINING 2.0 wt% PuO_2

EXPERIMENT: 4.3-000-209

LATTICE: 32M

PITCH: 1.598 ± 0.005 cm

GADOLINIUM: SEE COMMENTS

CONTROL ROD: NONE

SAFETY ROD: NONE

REACTION RATES: NONE

RODS: 349 MO_2 RODS AT ○ PLUS 1657 UO_2 RODS AT ●

k_{eff}: SEE COMMENTS

COMMENTS:

$k_{eff} = 1.0$ AT 0.673 ± 0.001
$k_{eff} = 0.996$ AT 0.760 ± 0.001
$k_{eff} = 0.970$ AT 1.371 ± 0.001
$k_{eff} = 0.937$ AT 2.362 ± 0.002

PERIPHERAL UNUSED LATTICE LOCATIONS NOT SHOWN.

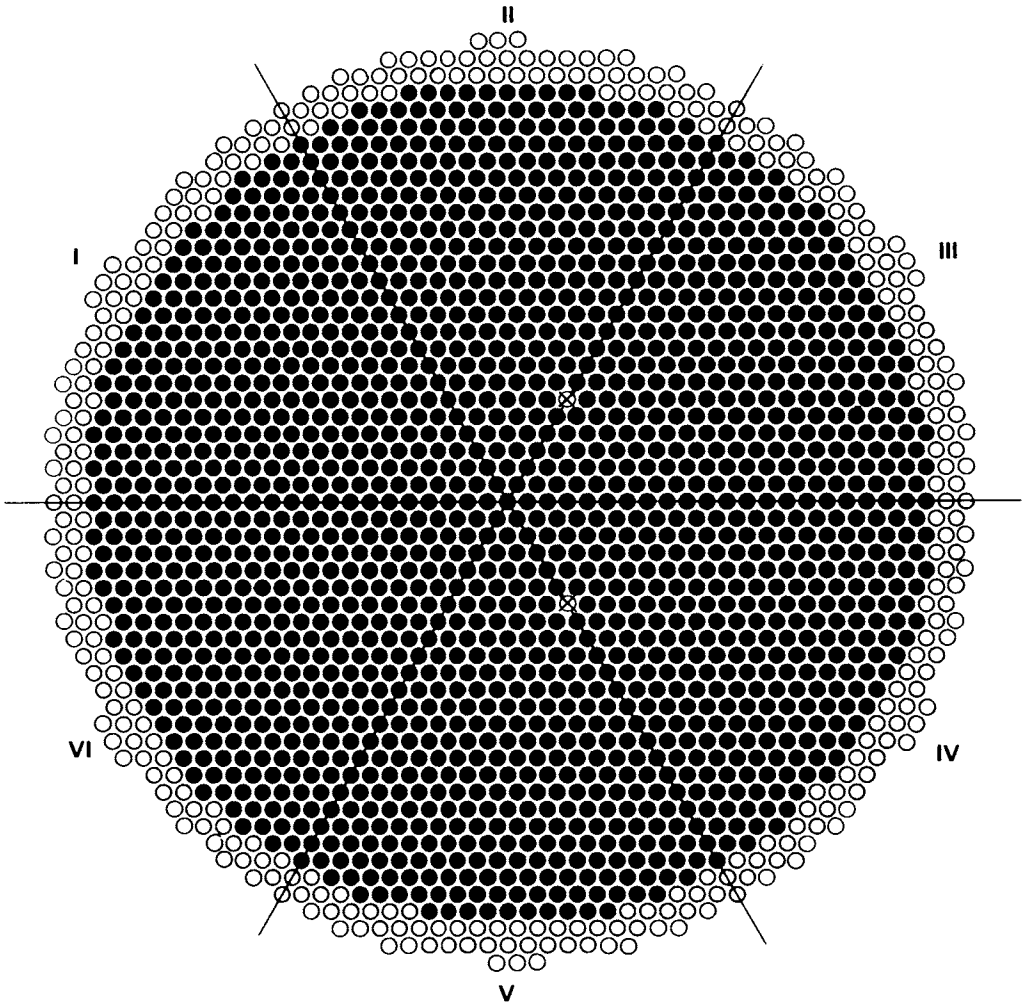

FUEL: 4.31 wt% ^{235}U ENRICHED UO_2 AND PuO_2-NATURAL UO_2 CONTAINING 2.0 wt% PuO_2

EXPERIMENT: 4.3-000-209A

LATTICE: 32M

PITCH: 1.598 ± 0.005 cm

GADOLINIUM: 0.673 ± 0.001 g Gd/liter

CONTROL ROD: OUT

SAFETY ROD: OUT

REACTION RATES: NONE

RODS: 330 MO_2 RODS AT ○ PLUS 1655 UO_2 RODS AT ●

k_{eff}: 1.0

COMMENTS: WATER FILLED ALUMINUM SLEEVE AT ⊠. PERIPHERIAL UNUSED LATTICE LOCATIONS NOT SHOWN.

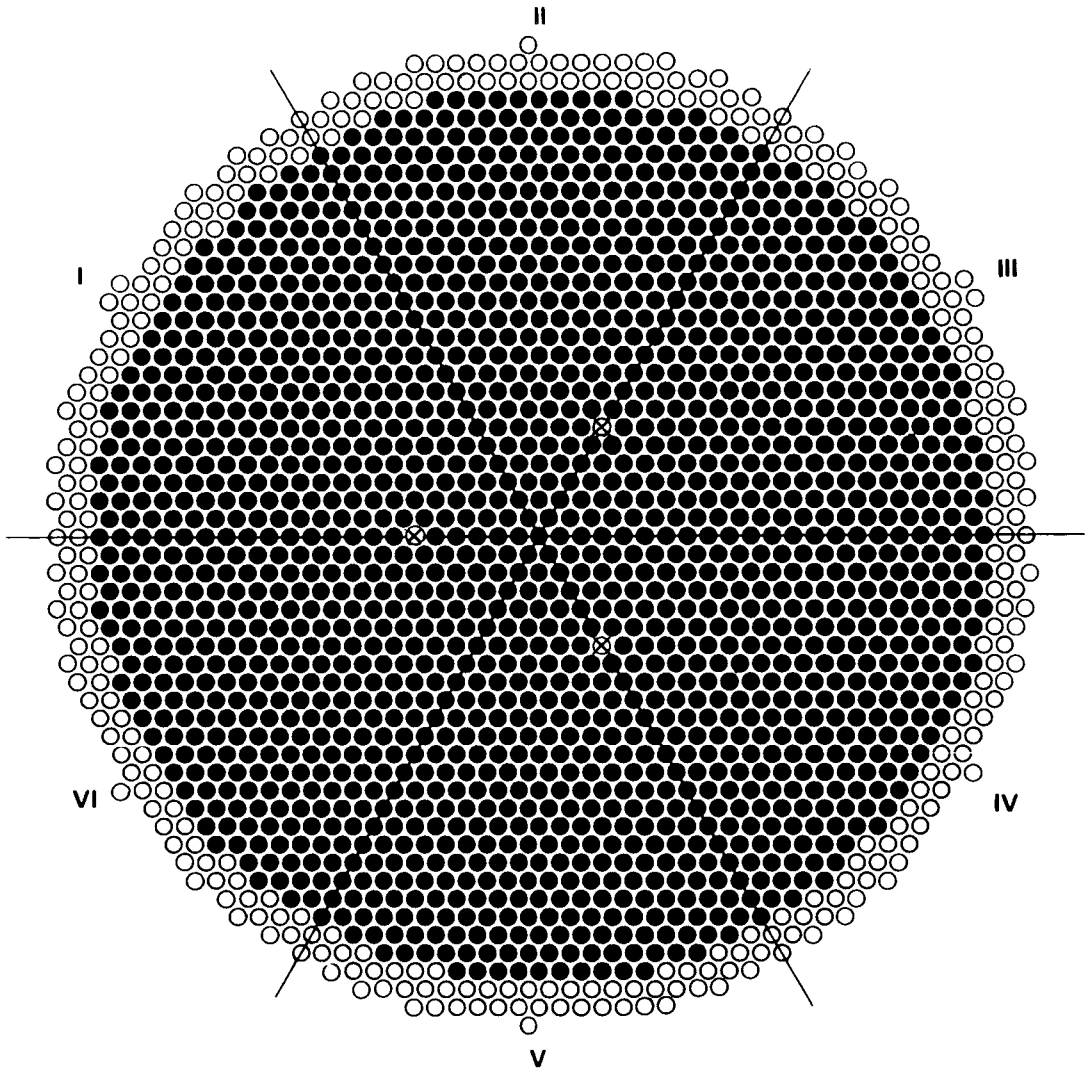

FUEL: 4.31 wt% ^{235}U ENRICHED UO_2 AND PuO_2-NATURAL UO_2 CONTAINING 2.0 wt% PuO_2

EXPERIMENT: 4.3-000-209B

LATTICE: 32M

PITCH: 1.598 ± 0.005 cm

GADOLINIUM: 0.673 ± 0.001 g Gd/liter

CONTROL ROD: OUT

SAFETY ROD: OUT

REACTION RATES: NONE

RODS: 320 MO_2 RODS AT ○ PLUS 1655 UO_2 RODS AT ●

k_{eff}: 1.0

COMMENTS: WATER FILLED ALUMINUM SLEEVE AT ⊠. PERIPHERIAL UNUSED LATTICE LOCATIONS NOT SHOWN.

APPENDIX G

Computerized Plots of Pulse Neutron Source Measurement Data

APPENDIX G

Computerized Plots of Pulse Neutron Source Measurement Data

The observed time behavior of the neutron flux in each of the pulsed neutron source measurements is presented in this Appendix as photo-reproductions of computer plots obtained following data reduction and analysis. In each of the measurements, 511 data channels were used in accumulating and analyzing the time dependent data. Because of limited computer storage capacity, a few of the plots do not reproduce all 511 data points. All of the data have been corrected for coincidence losses. The least-square calculated fit of the data is also shown in each of the plots. The data indicated by an "X" were not considered in the least-squares fitting process; however, these data were included in the (Garelis and Russell 1963) reactivity determinations. The first data channel used in the least-squares fitting is identified as start channel in the legend.

The fundamental mode and the delayed neutron plus background level, as determined by the least-squares fitting of the data, are shown as solid lines in each figure. The slope of the fundamental mode curve is tabulated in the legend of each figure as alpha in $sec.^{-1}$ Also included in the legend of each figure are the (Garelis-Russell (GRRHO) and the Gozani (GOZRHO) determined reactivities in dollars, the neutron background level during each measurement, the delayed neutron level as determined by the least-squares fit, and the data accumulating channel widths in microseconds.

It should be noted that some irregularity exists in the data for measurement number BNFL 11-2. The cause of the irregularity is unknown. Because of its location and the methods of data analyses the presence of the irregularity should have a minimal effect on the results. With respect to reactivity, the value determined by the (Gozani 1965) method would probably be least affected by the irregularity.

MEASUREMENT NUMBER BNFL 11-2

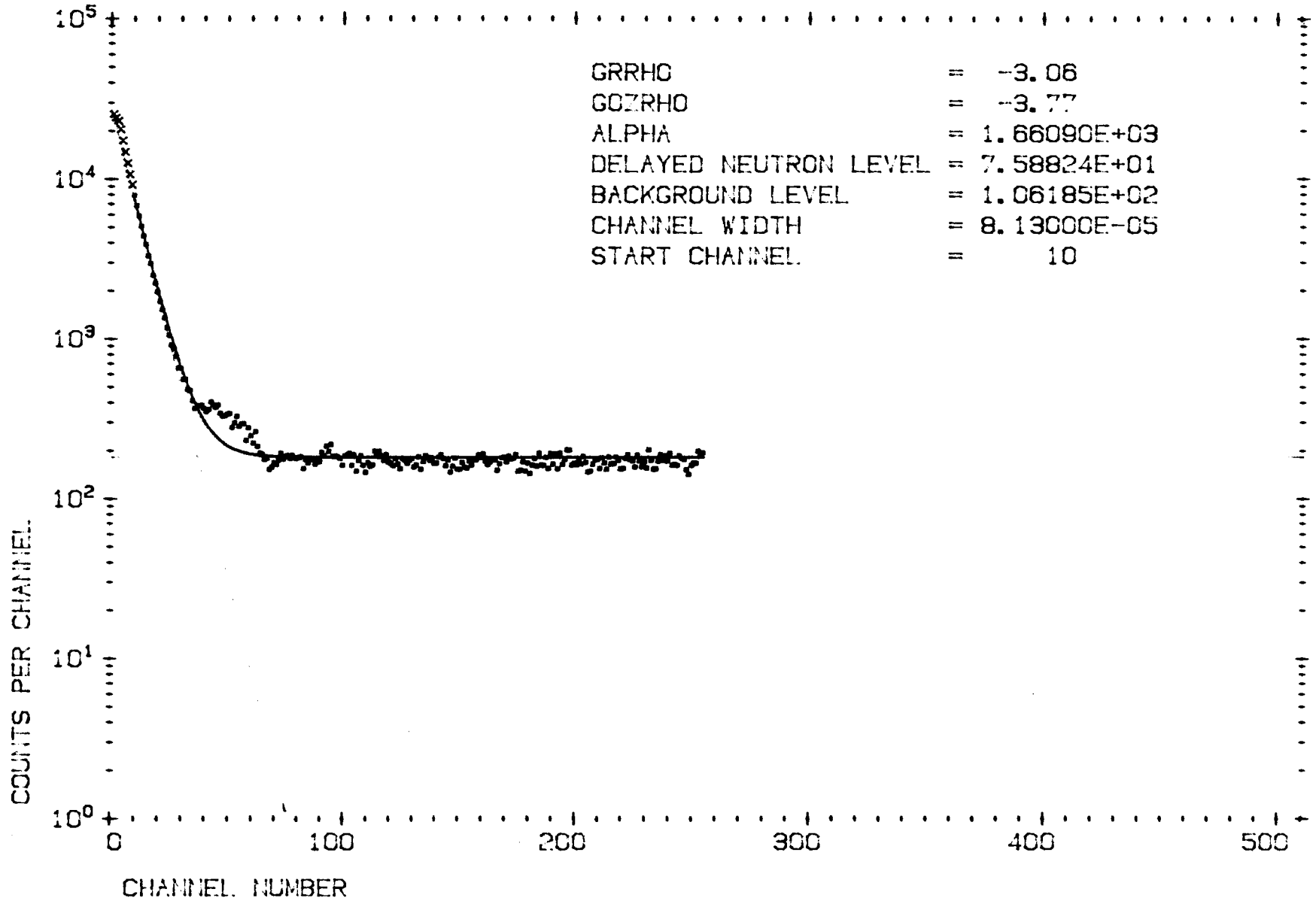

MEASUREMENT NUMBER BNFL 11-3

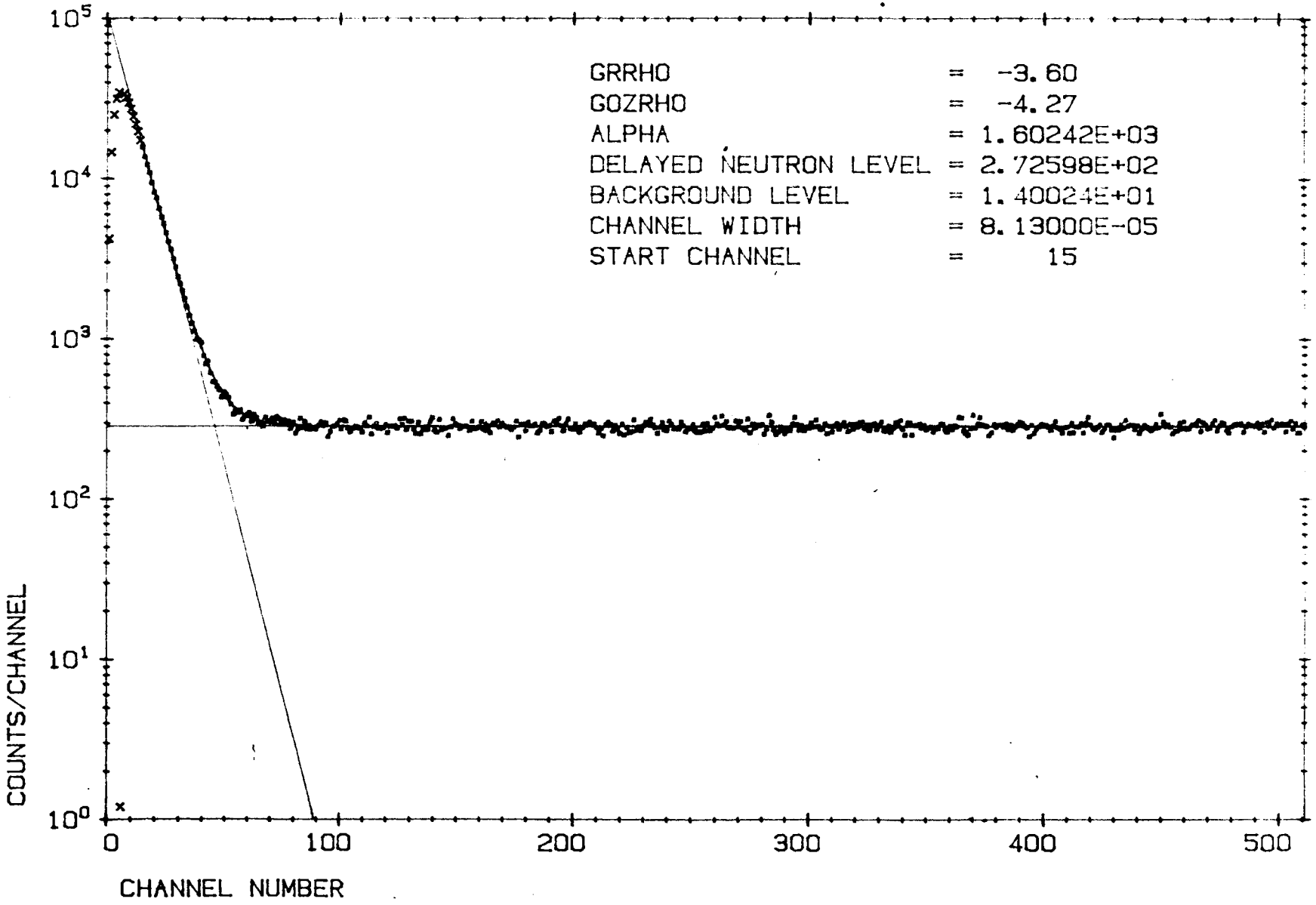

MEASUREMENT NUMBER BNFL 11-4

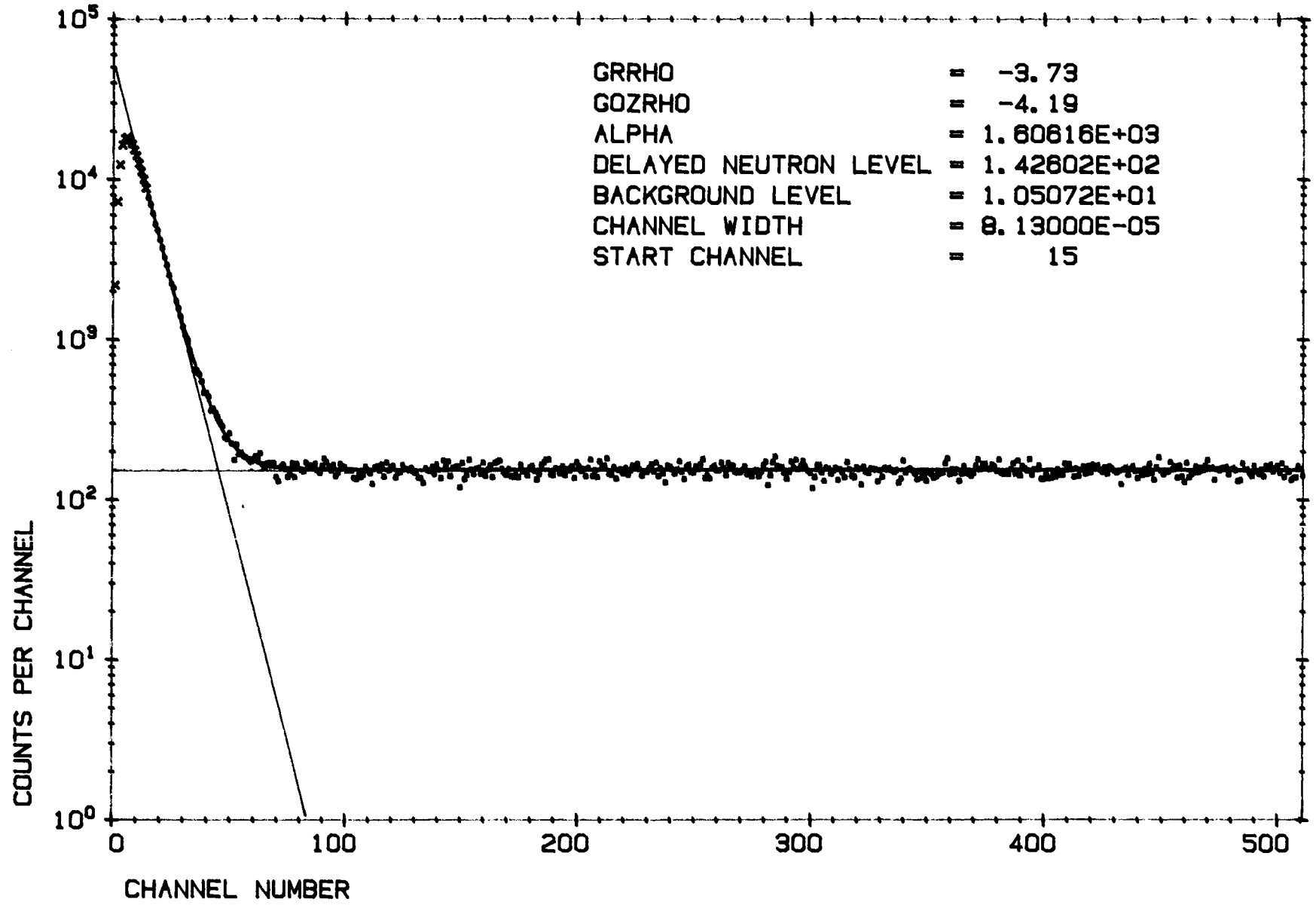

MEASUREMENT NUMBER BNFL 11-5

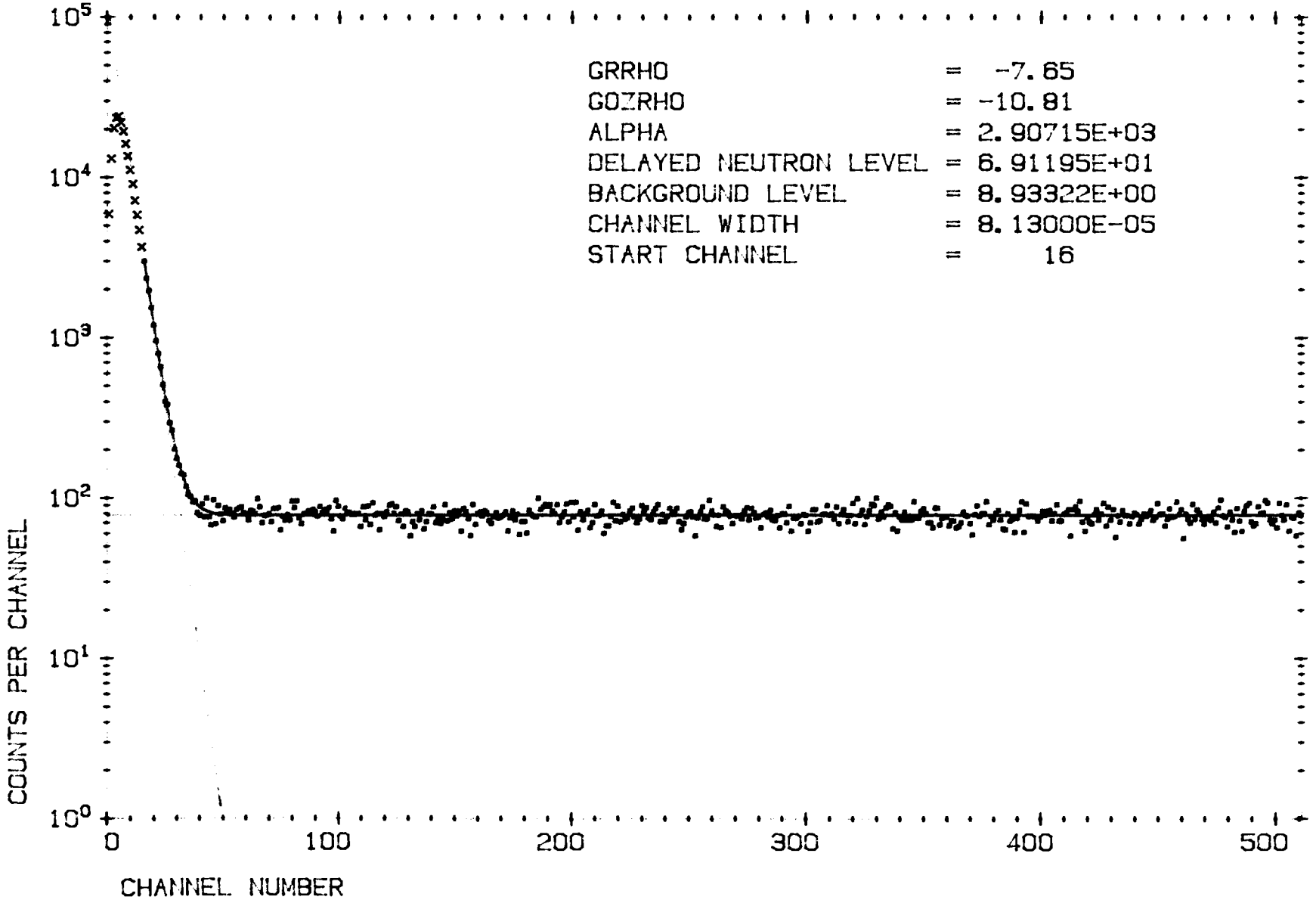

MEASUREMENT NUMBER BNFL 11-6

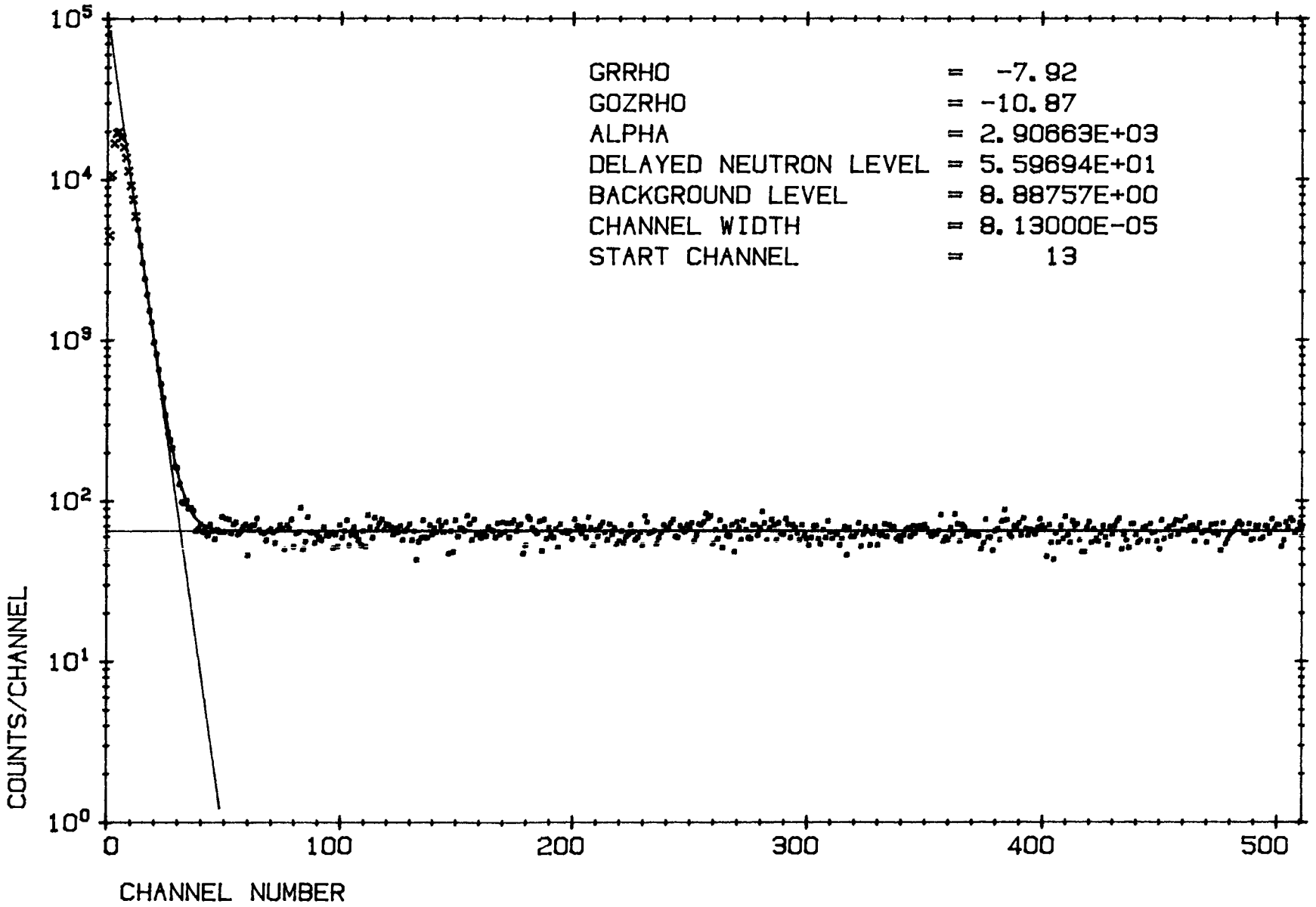

MEASUREMENT NUMBER BNFL 11-7

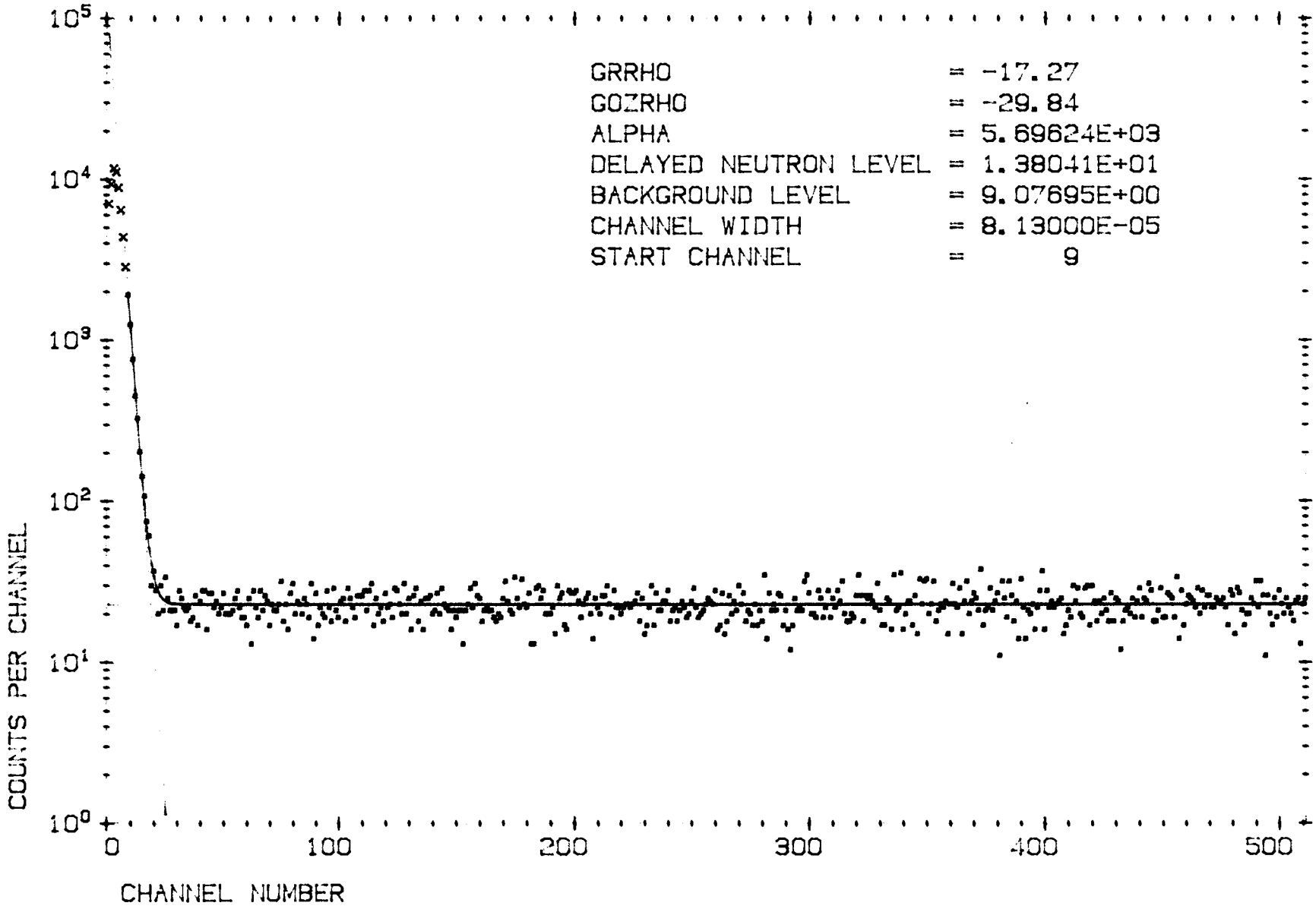

MEASUREMENT NUMBER BNFL 11-8

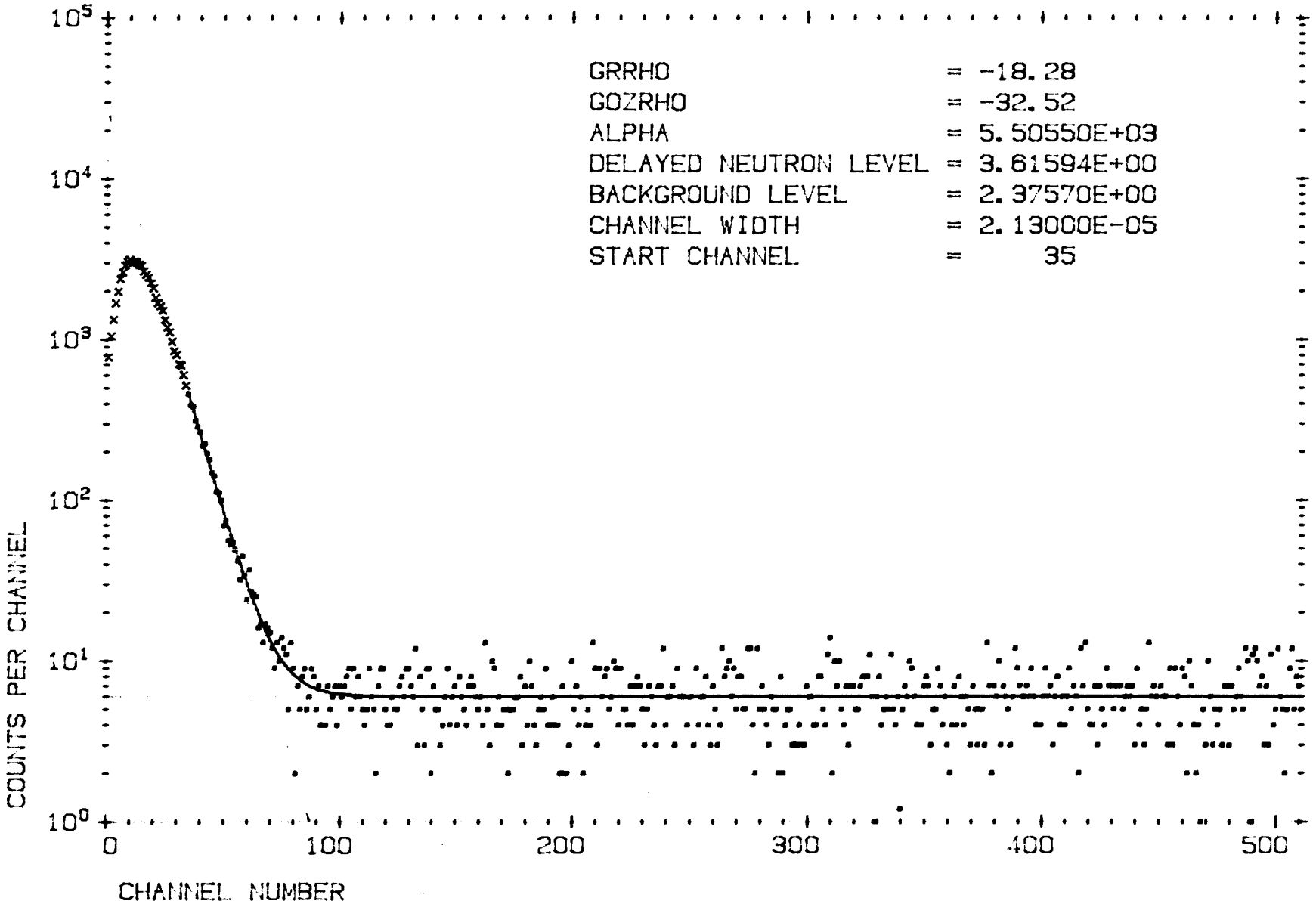

MEASUREMENT NUMBER BNFL 11-9

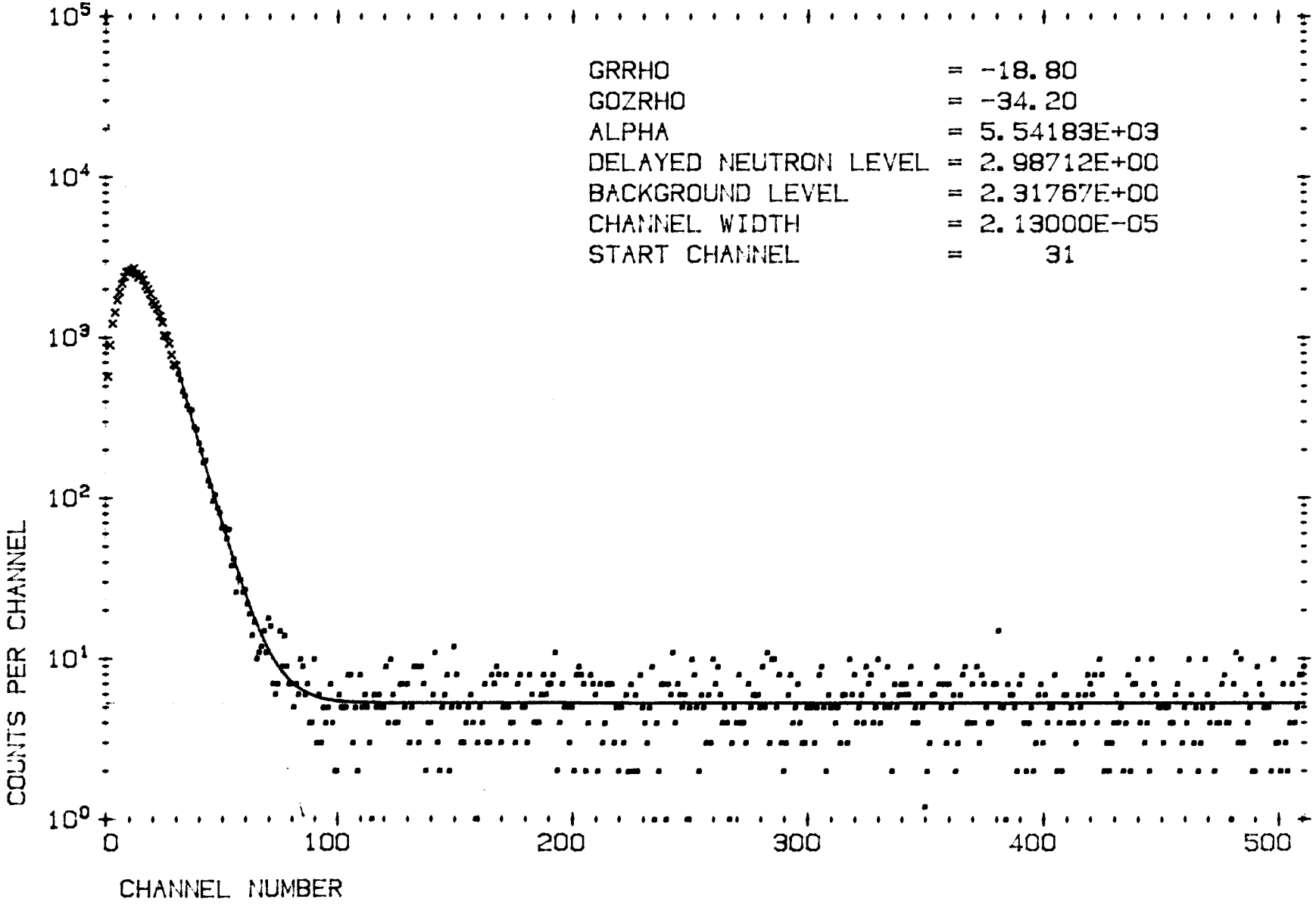

MEASUREMENT NUMBER BNFL 12-1

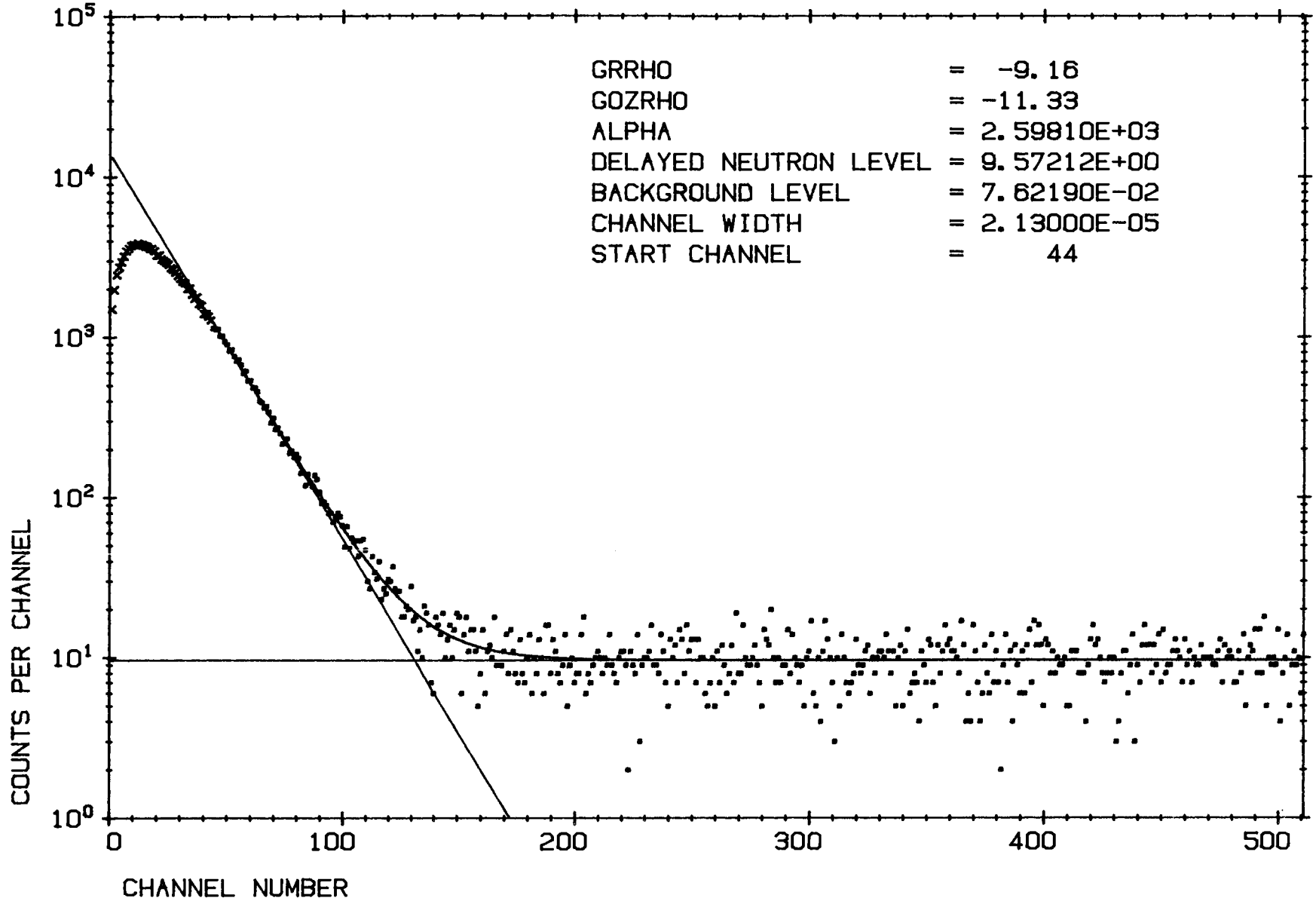

MEASUREMENT NUMBER BNFL 12-3

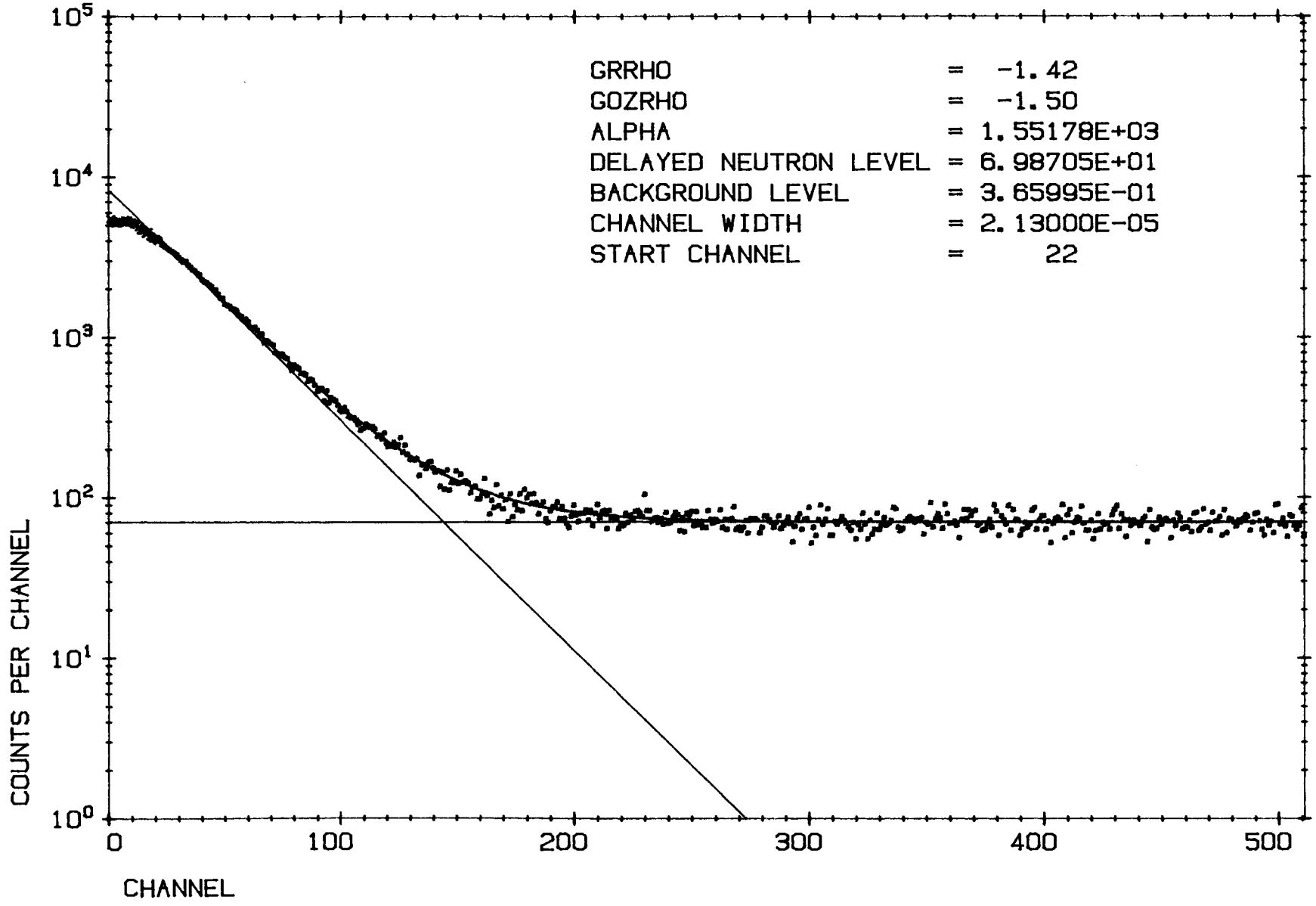

MEASUREMENT NUMBER BNFL 12-4

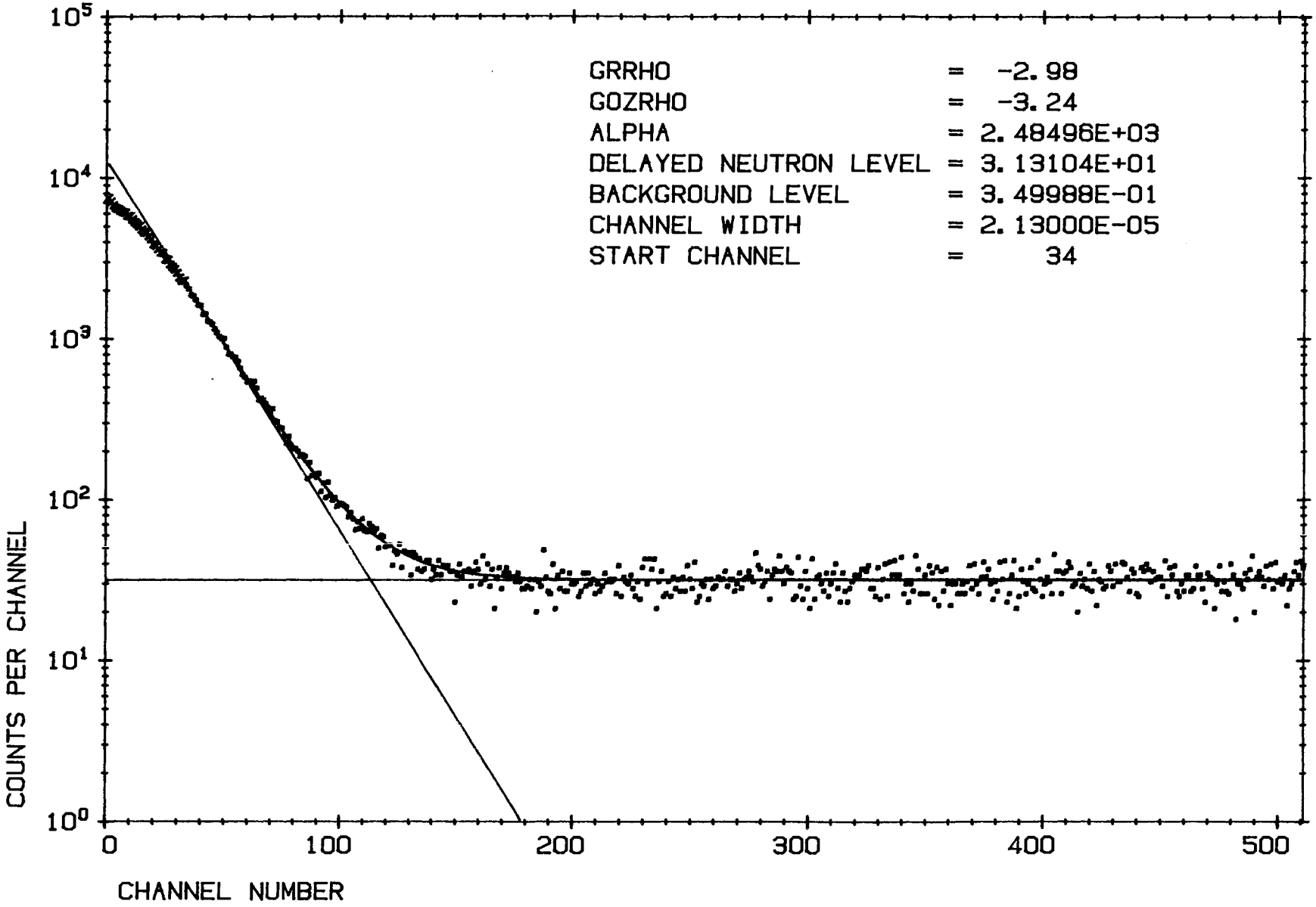

MEASUREMENT NUMBER BNFL 12-5

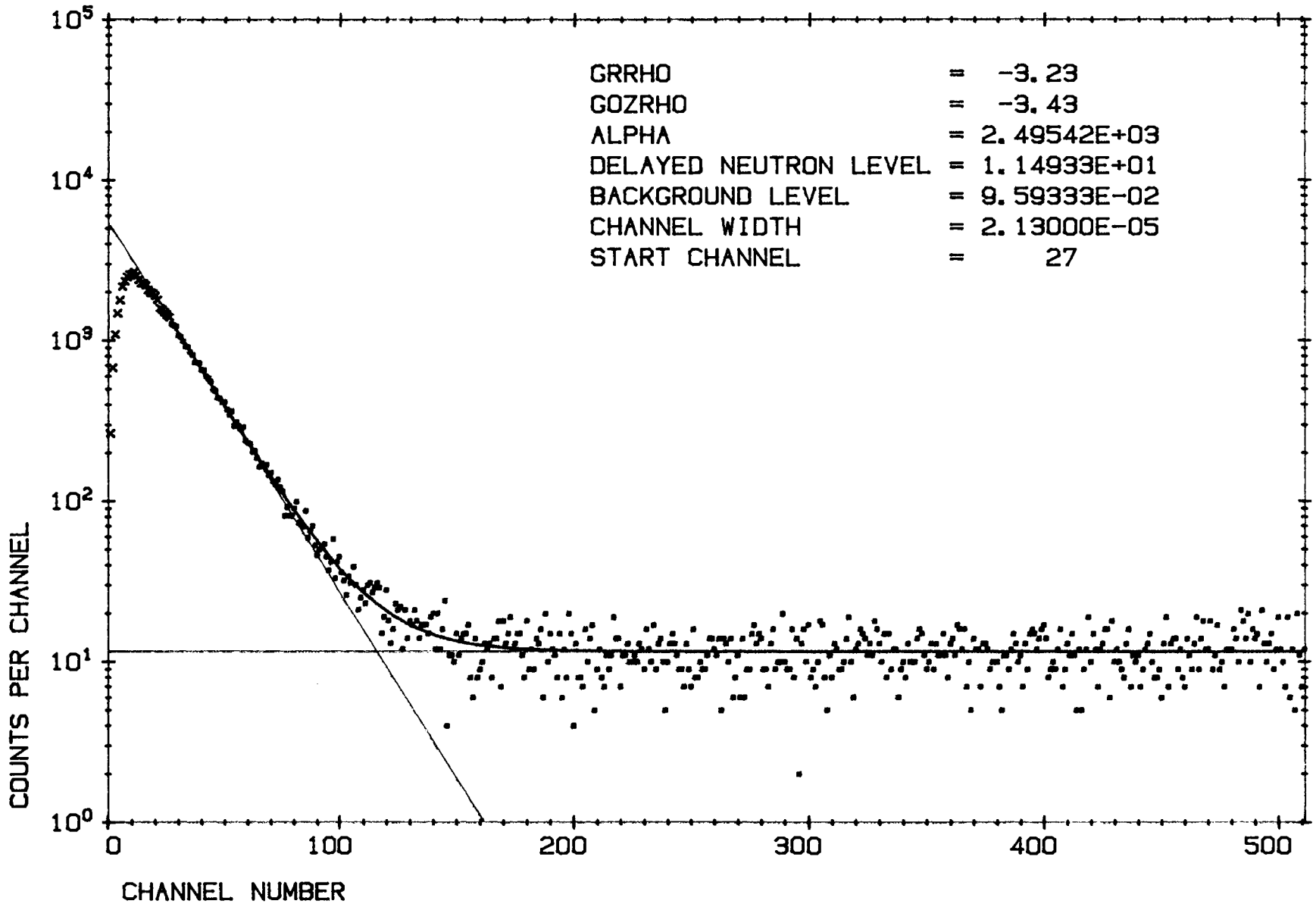

MEASUREMENT NUMBER BNFL 12-6

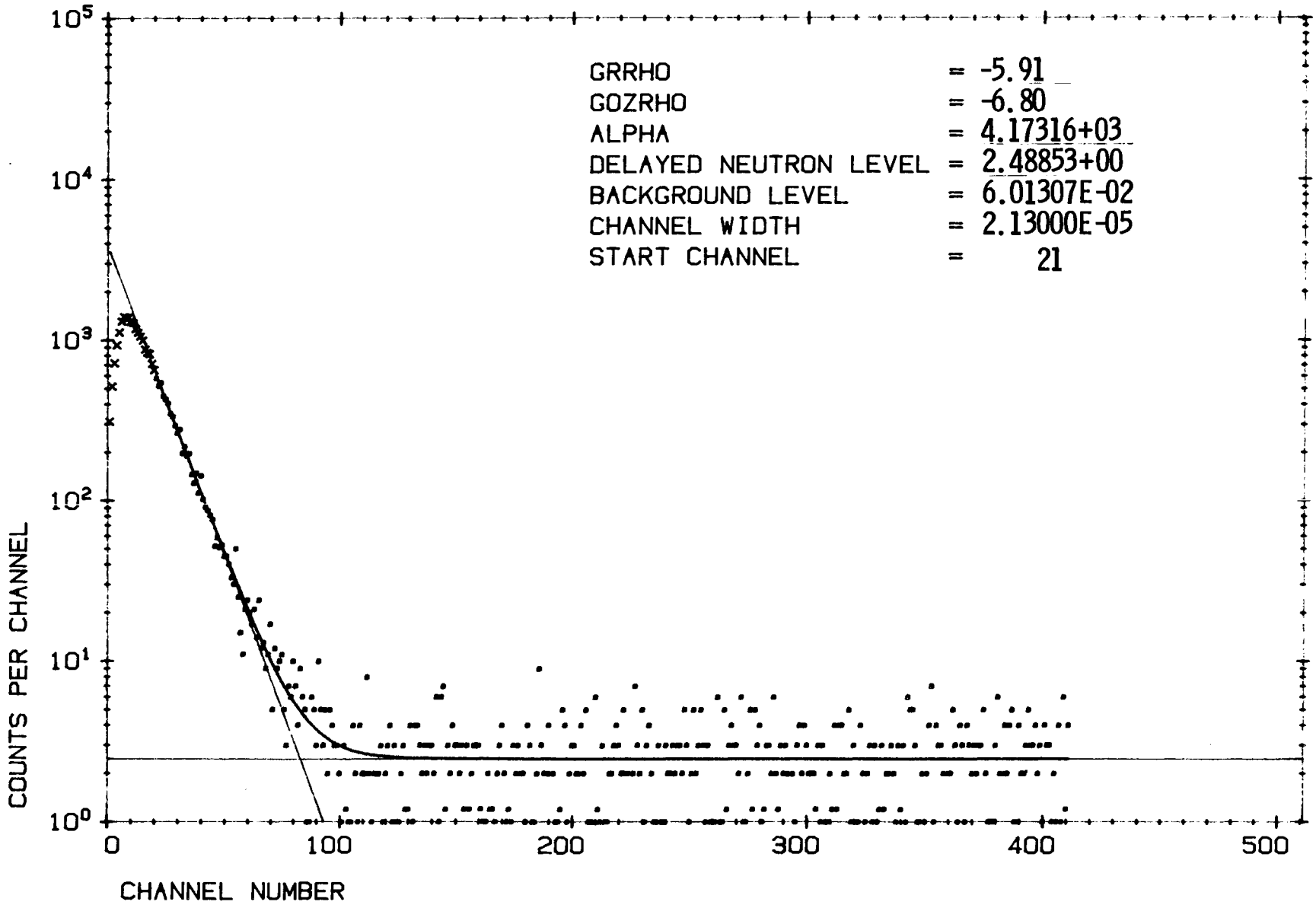

MEASUREMENT NUMBER BNFL 12-7

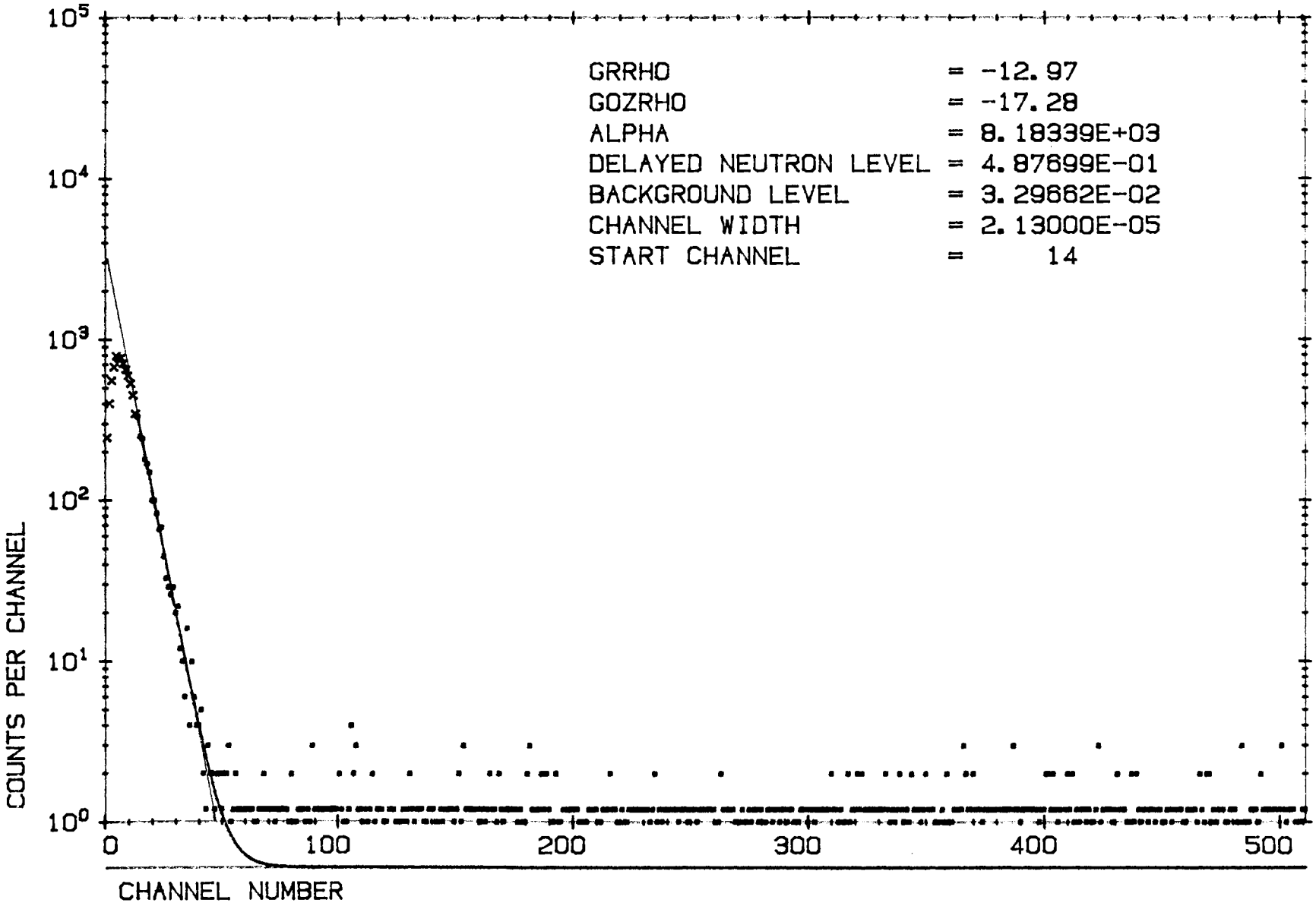

MEASUREMENT NUMBER BNFL 12-8

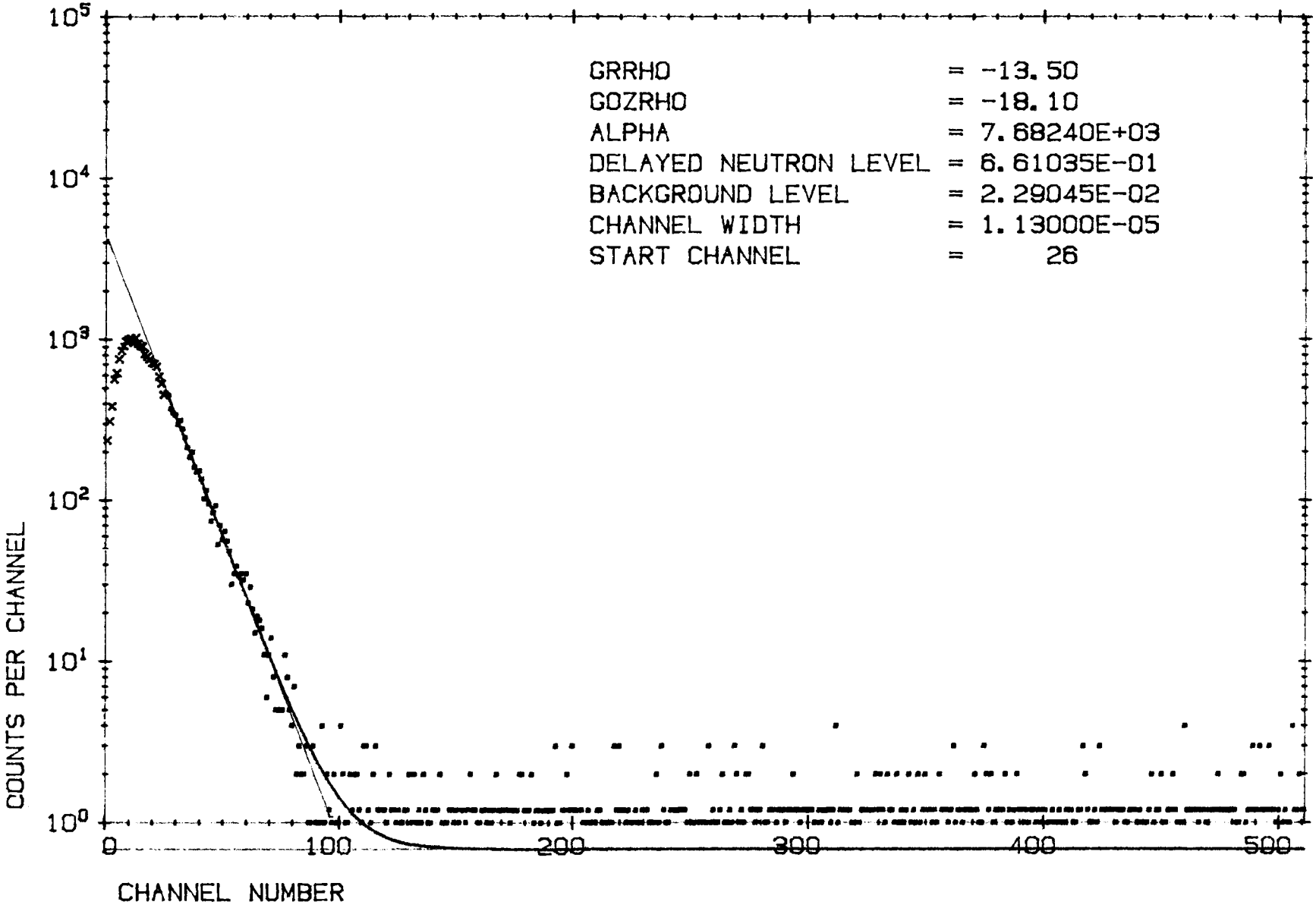

MEASUREMENT NUMBER BNFL 13-6

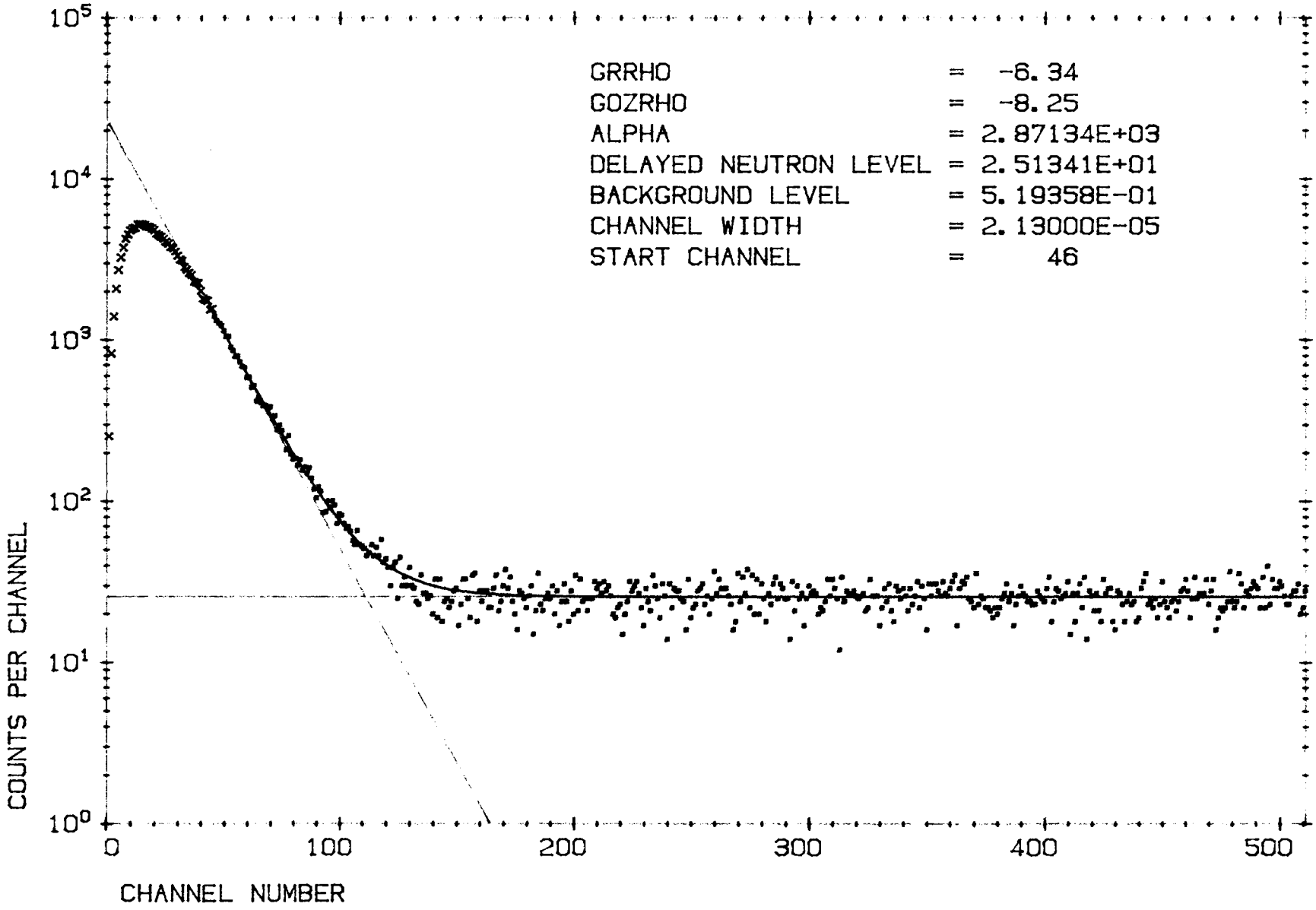

MEASUREMENT NUMBER BNFL 13-5

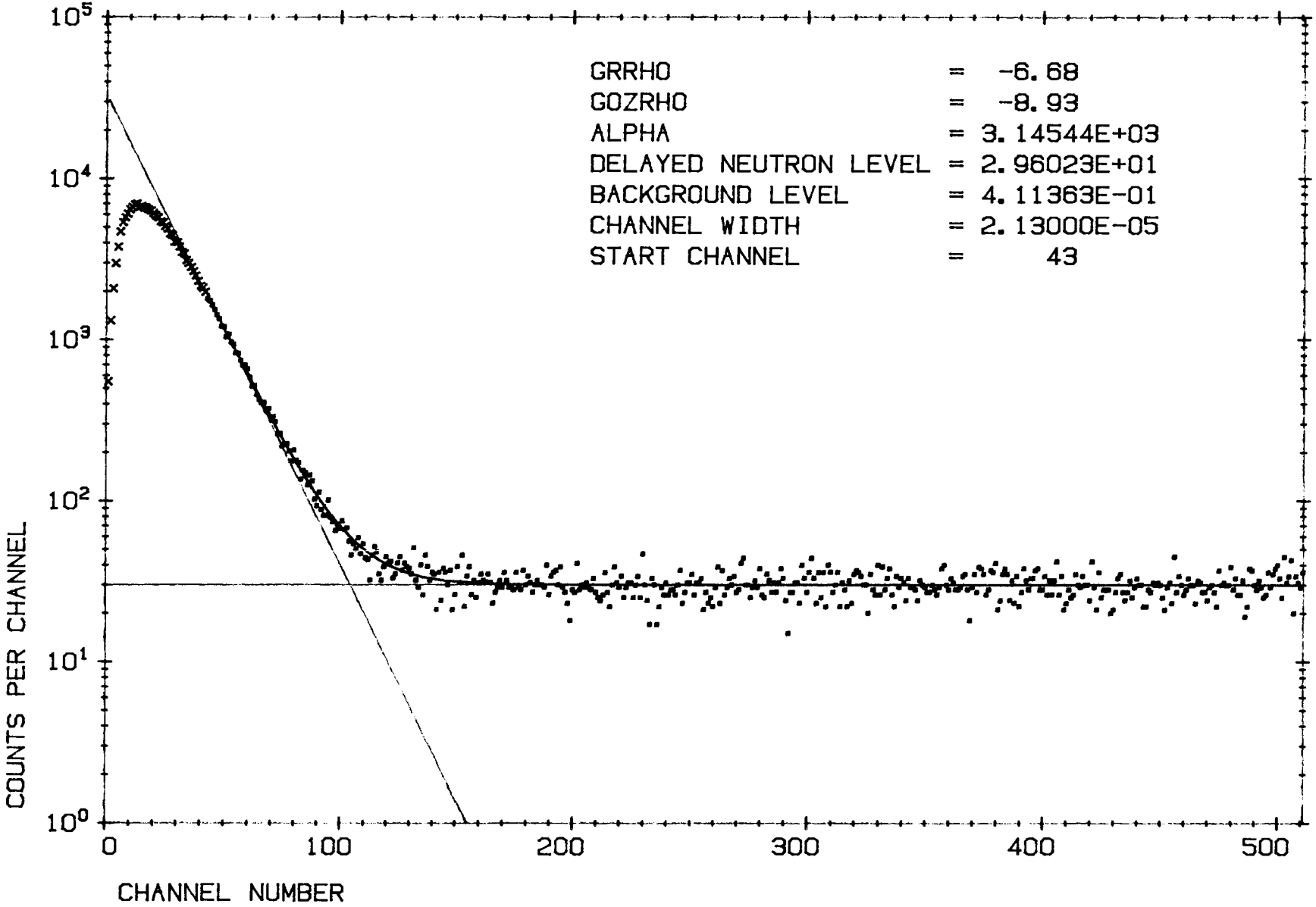

MEASUREMENT NUMBER BNFL 13-4

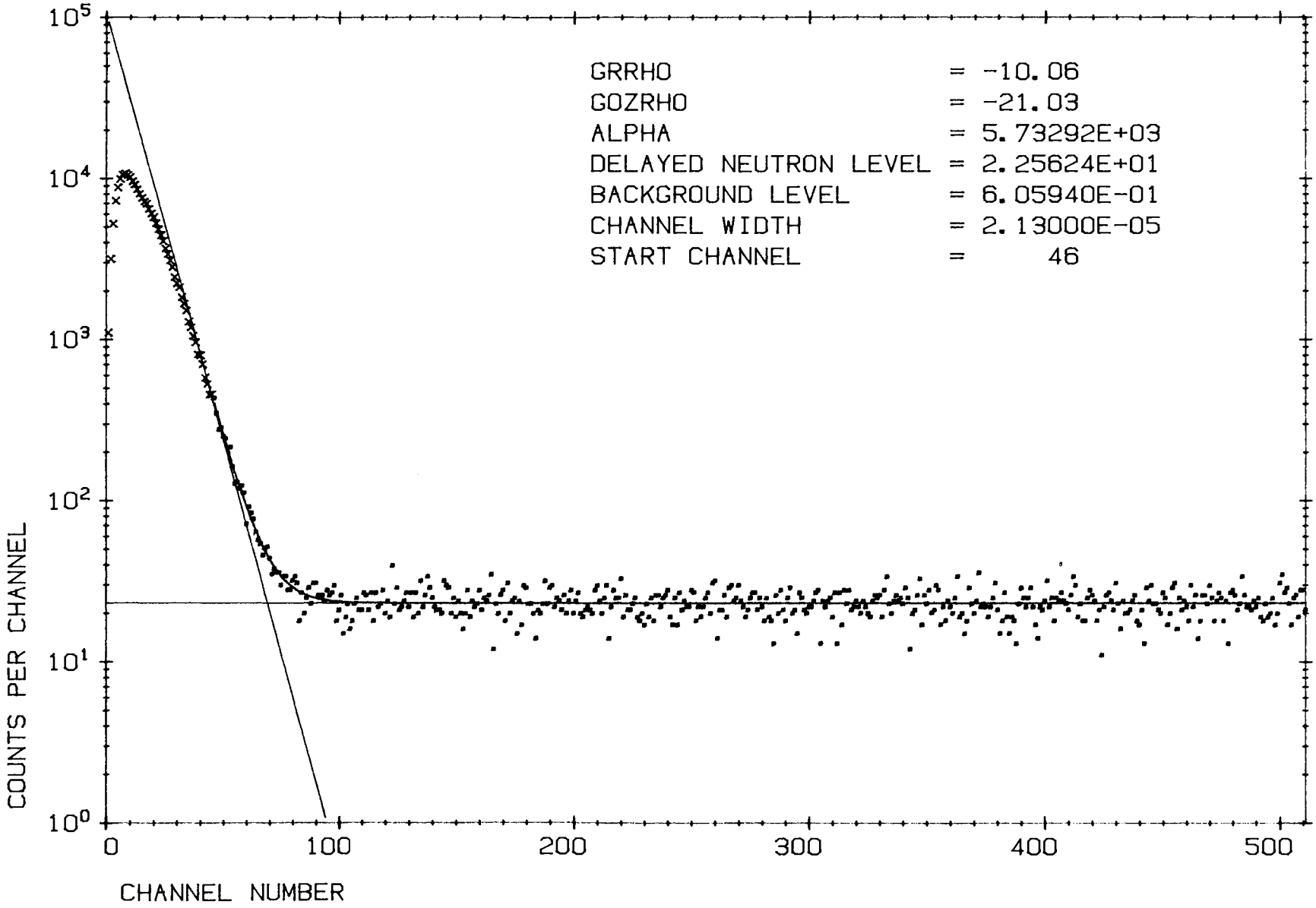

MEASUREMENT NUMBER BNFL 13-3

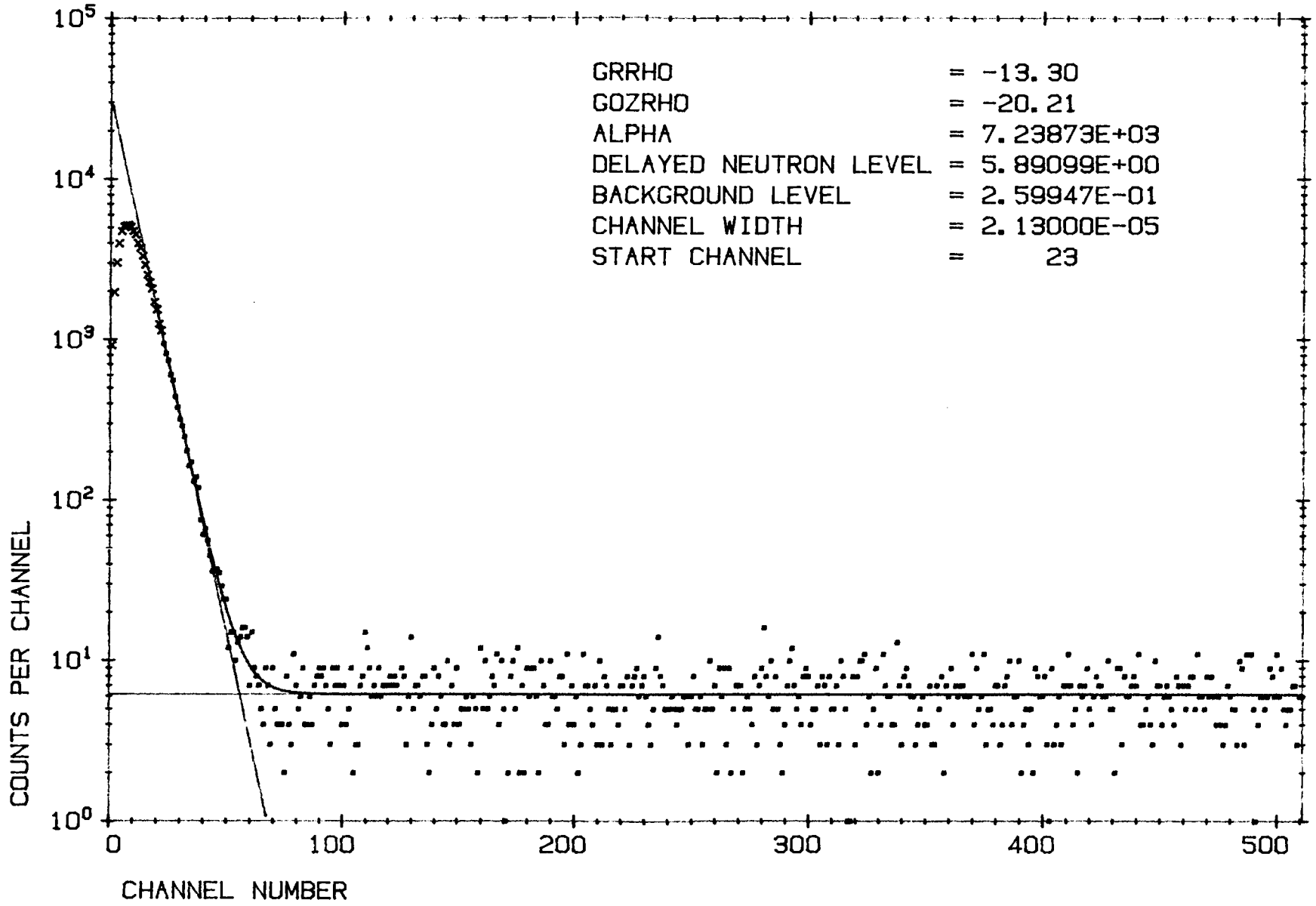

MEASUREMENT NUMBER BNFL 13-2

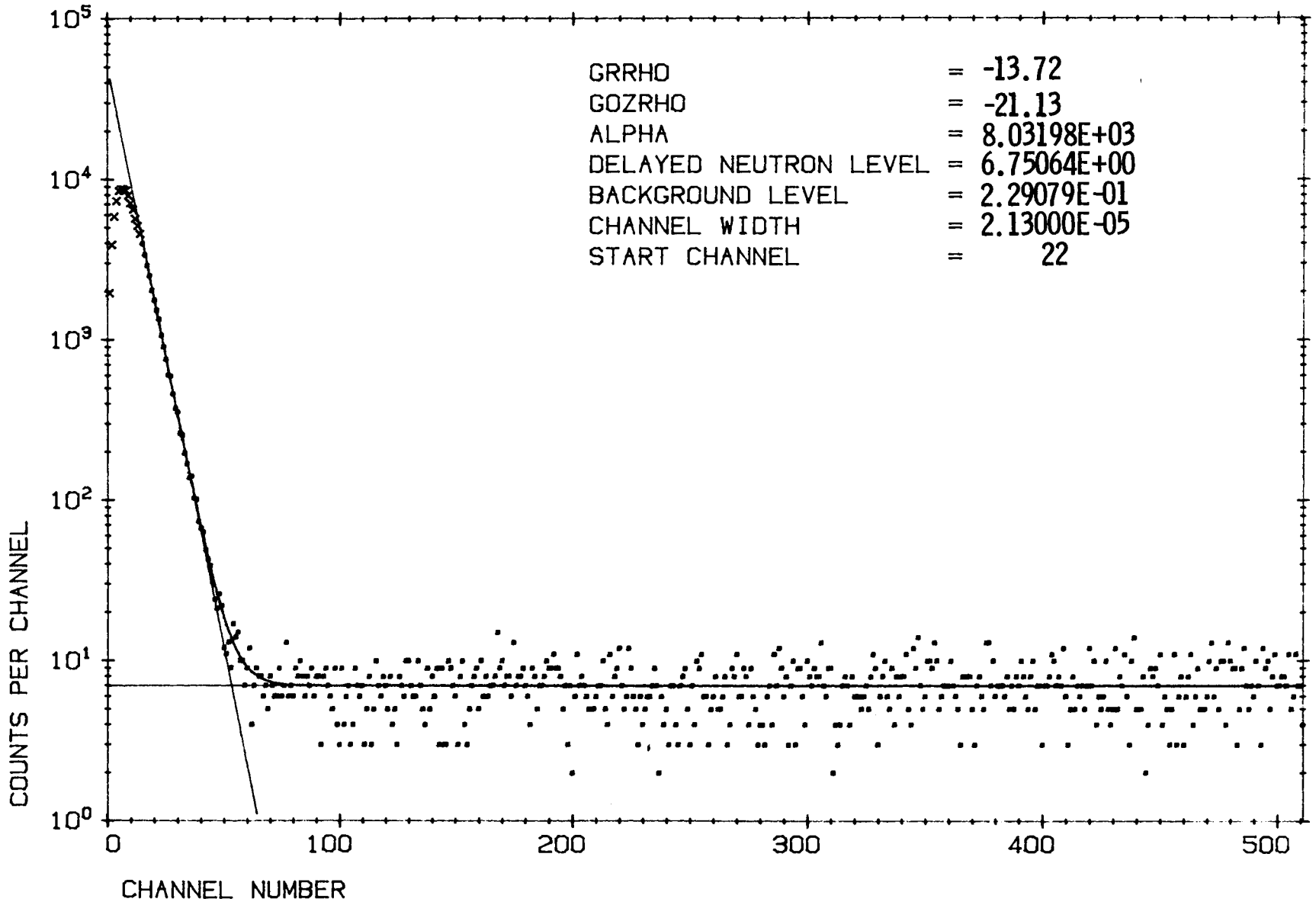

MEASUREMENT NUMBER BNFL 13-1

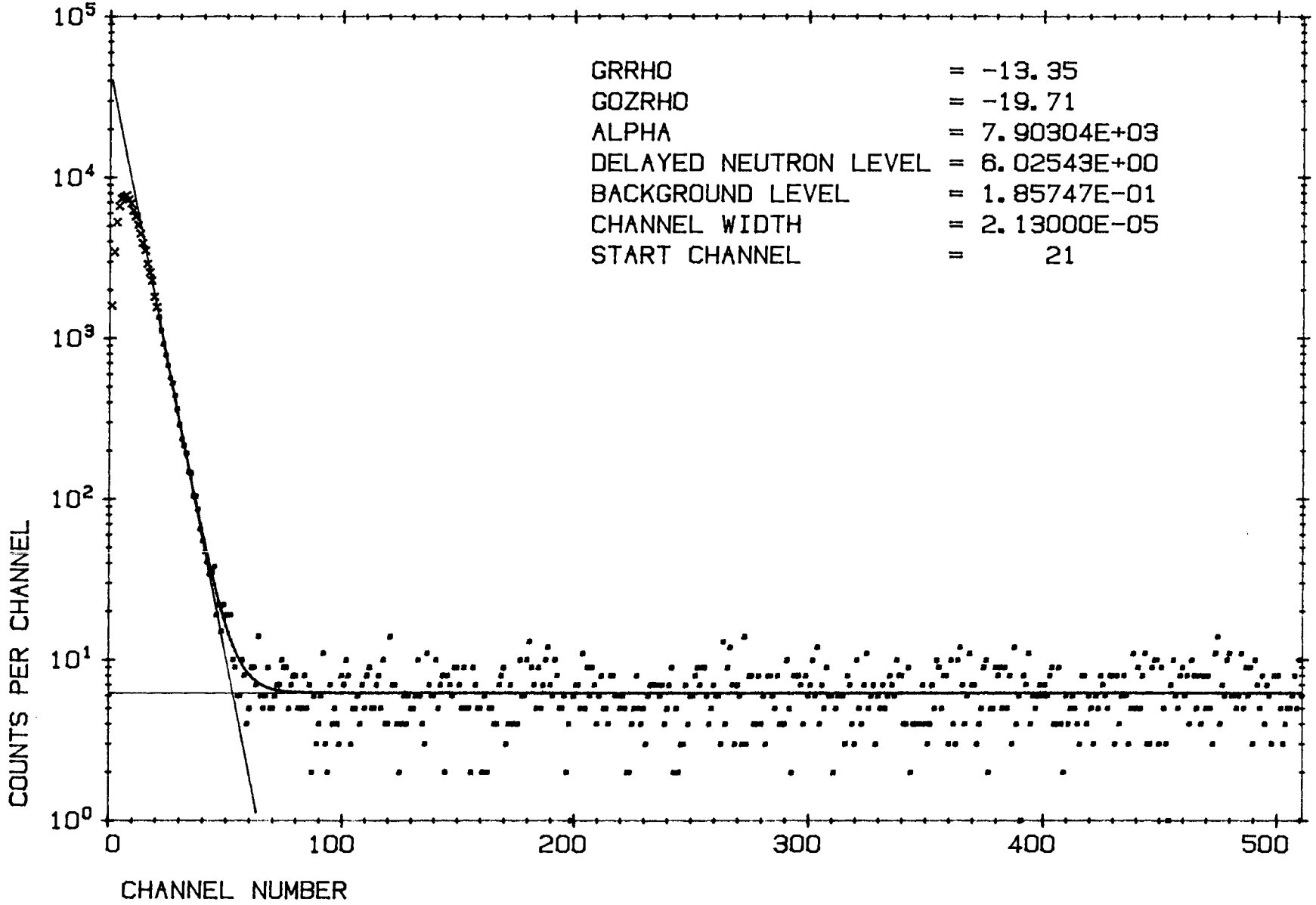

MEASUREMENT NUMBER BNFL 21-2

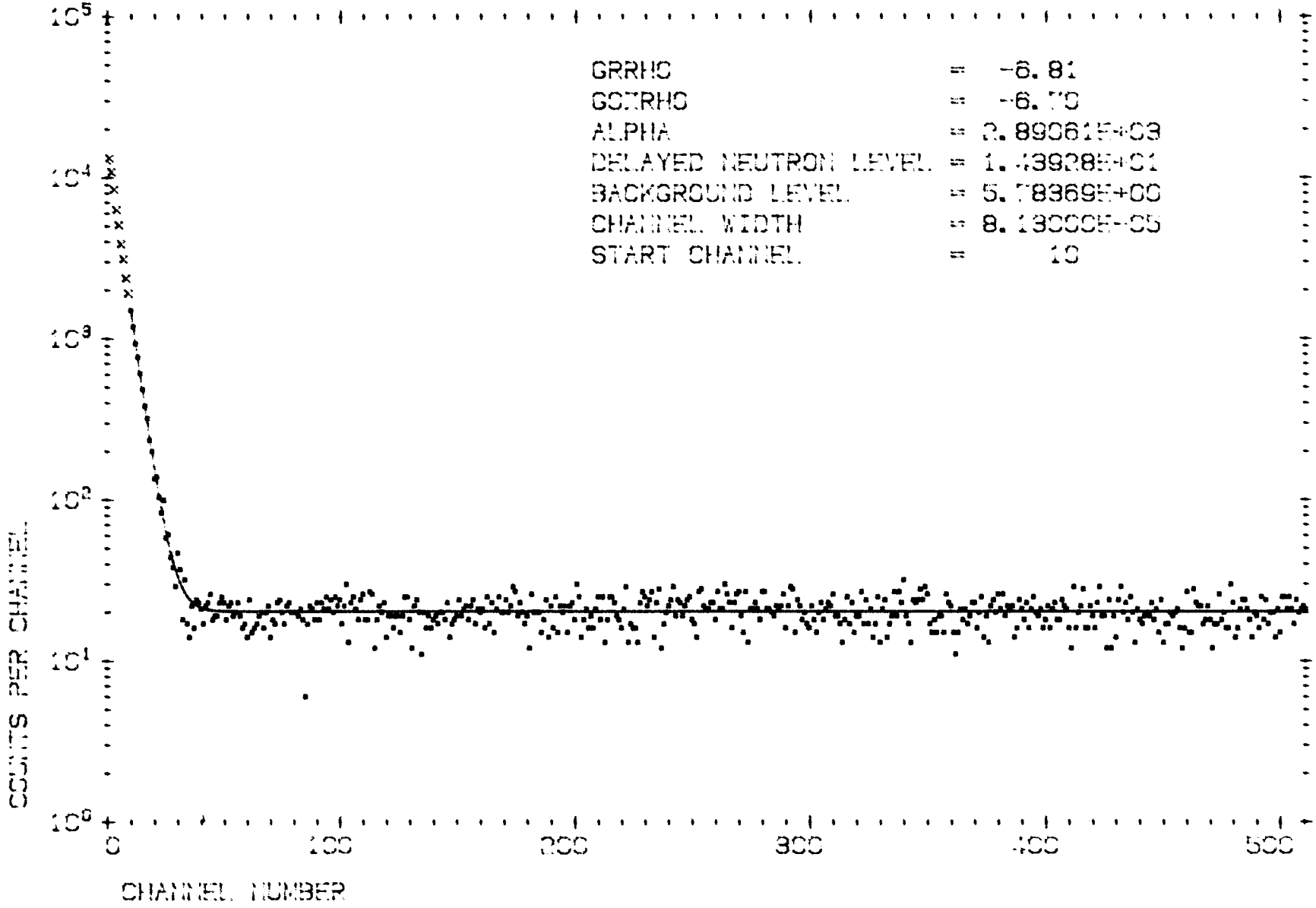

MEASUREMENT NUMBER BNFL 21-4

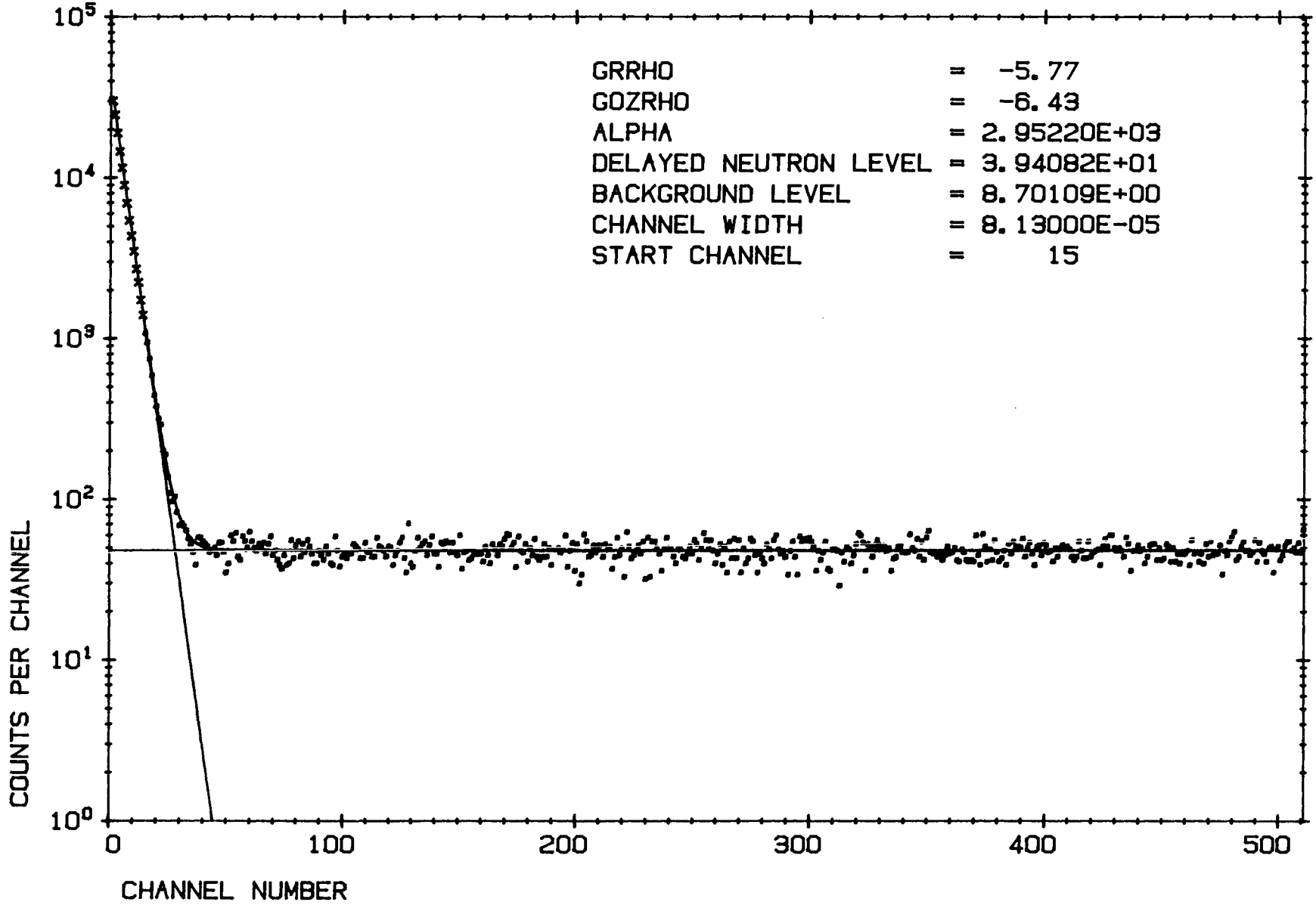

MEASUREMENT NUMBER BNFL 21-11

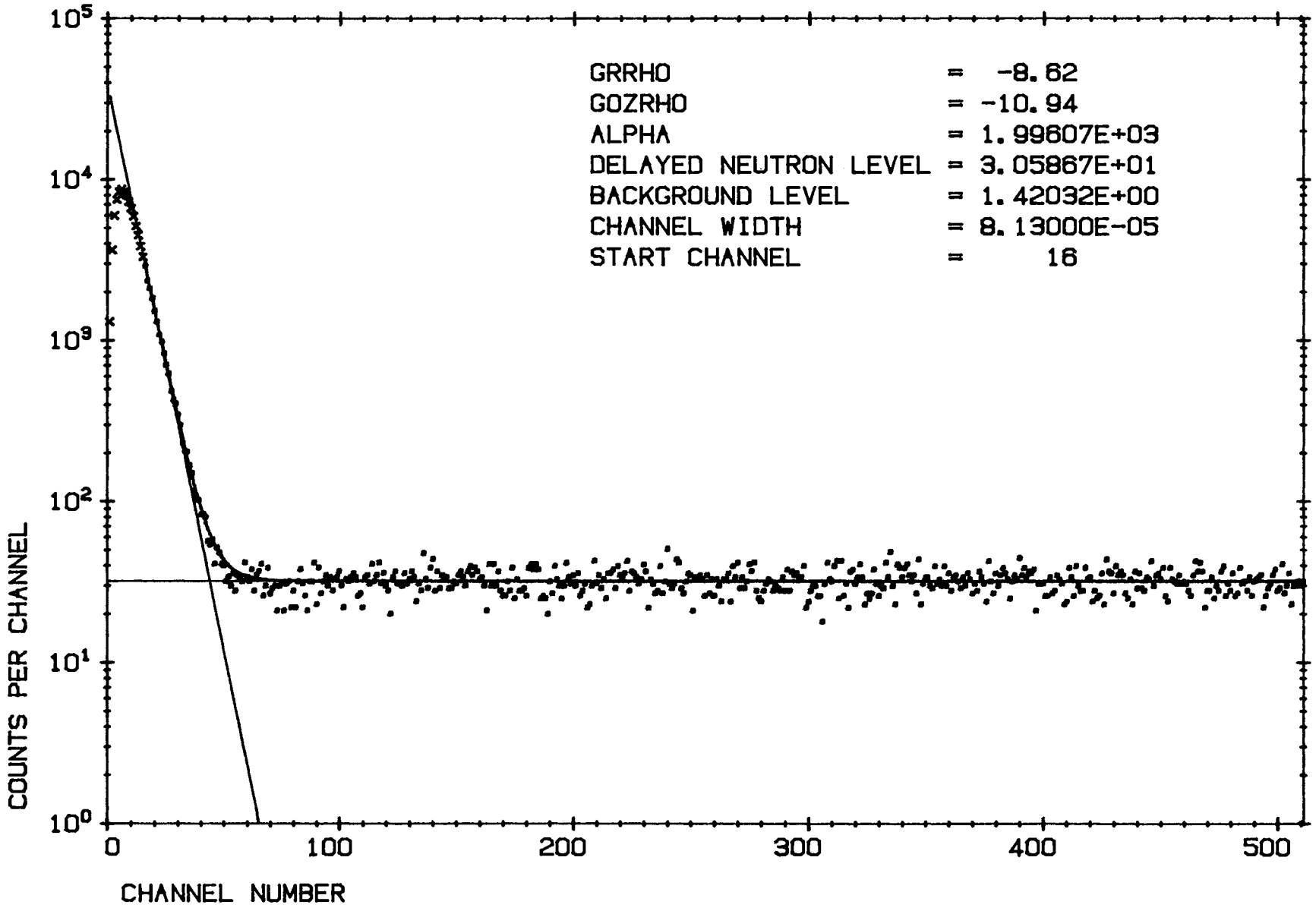

MEASUREMENT NUMBER BNFL 21-12

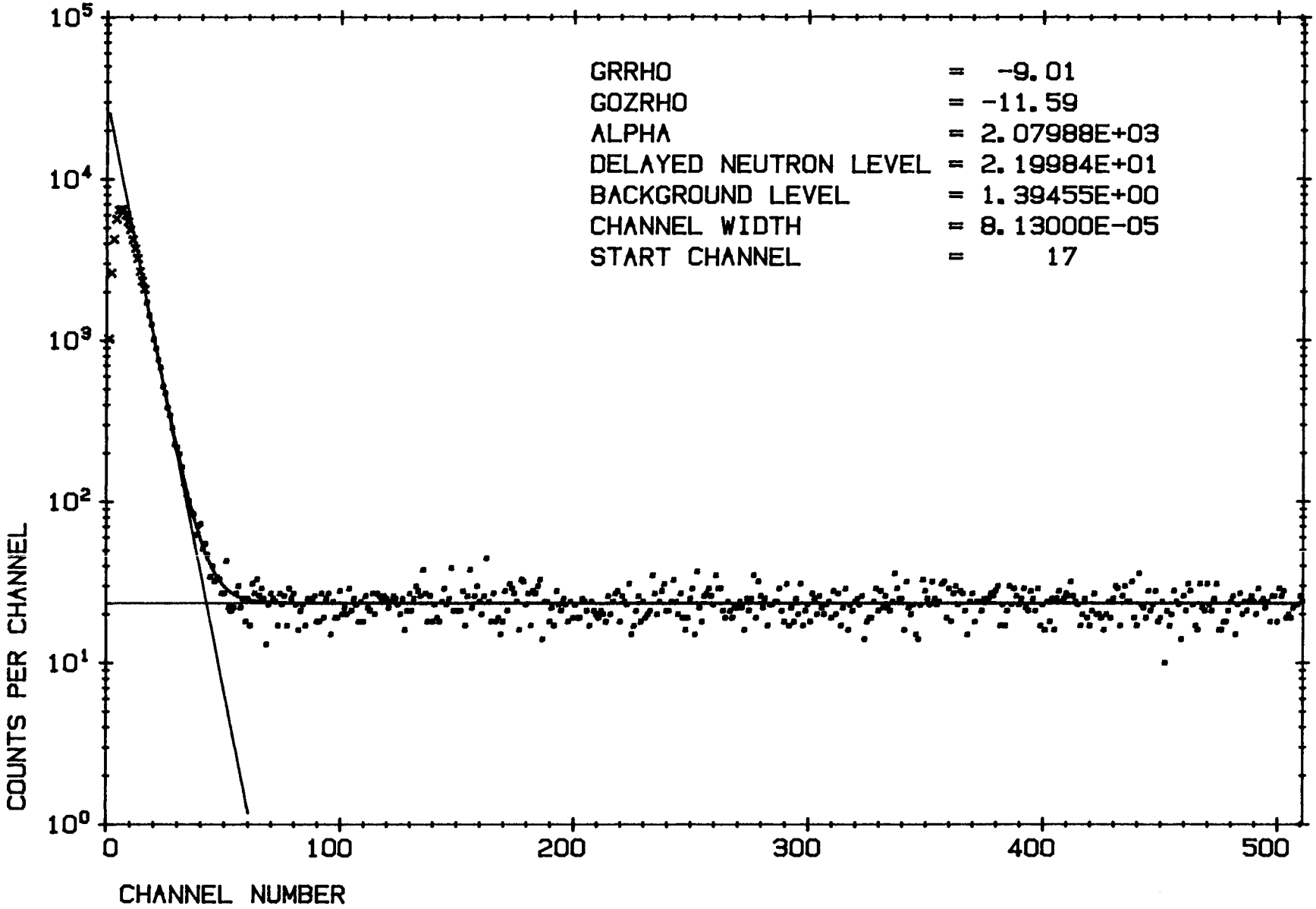

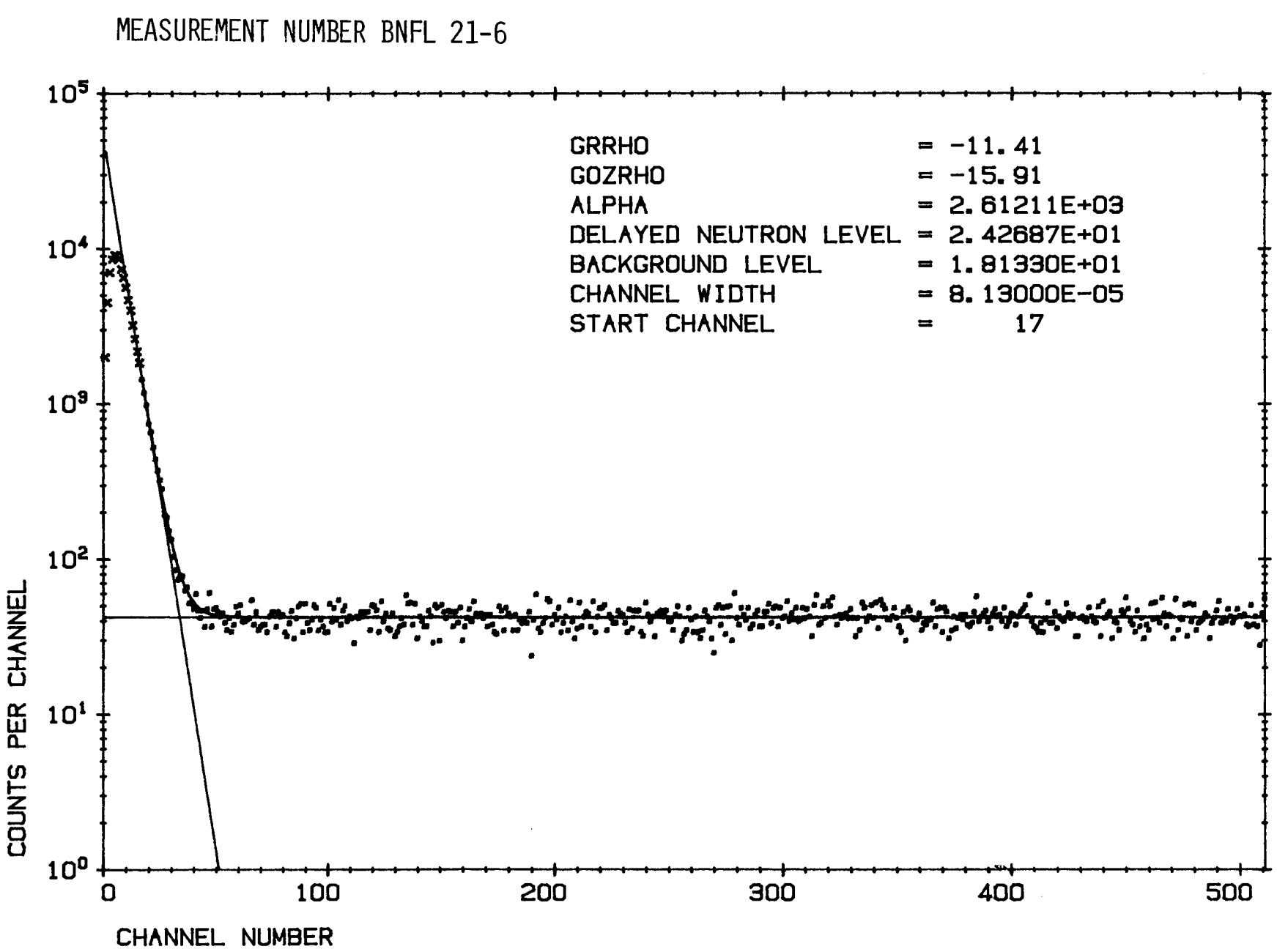
MEASUREMENT NUMBER BNFL 21-6
GRRHO = -11.41
GOZRHO = -15.91
ALPHA = 2.61211E+03
DELAYED NEUTRON LEVEL = 2.42687E+01
BACKGROUND LEVEL = 1.81330E+01
CHANNEL WIDTH = 8.13000E-05
START CHANNEL = 17
COUNTS PER CHANNEL
CHANNEL NUMBER
10^5
10^4
10^3
10^2
10^1
10^0
0
100
200
300
400
500

MEASUREMENT NUMBER BNFL 21-7

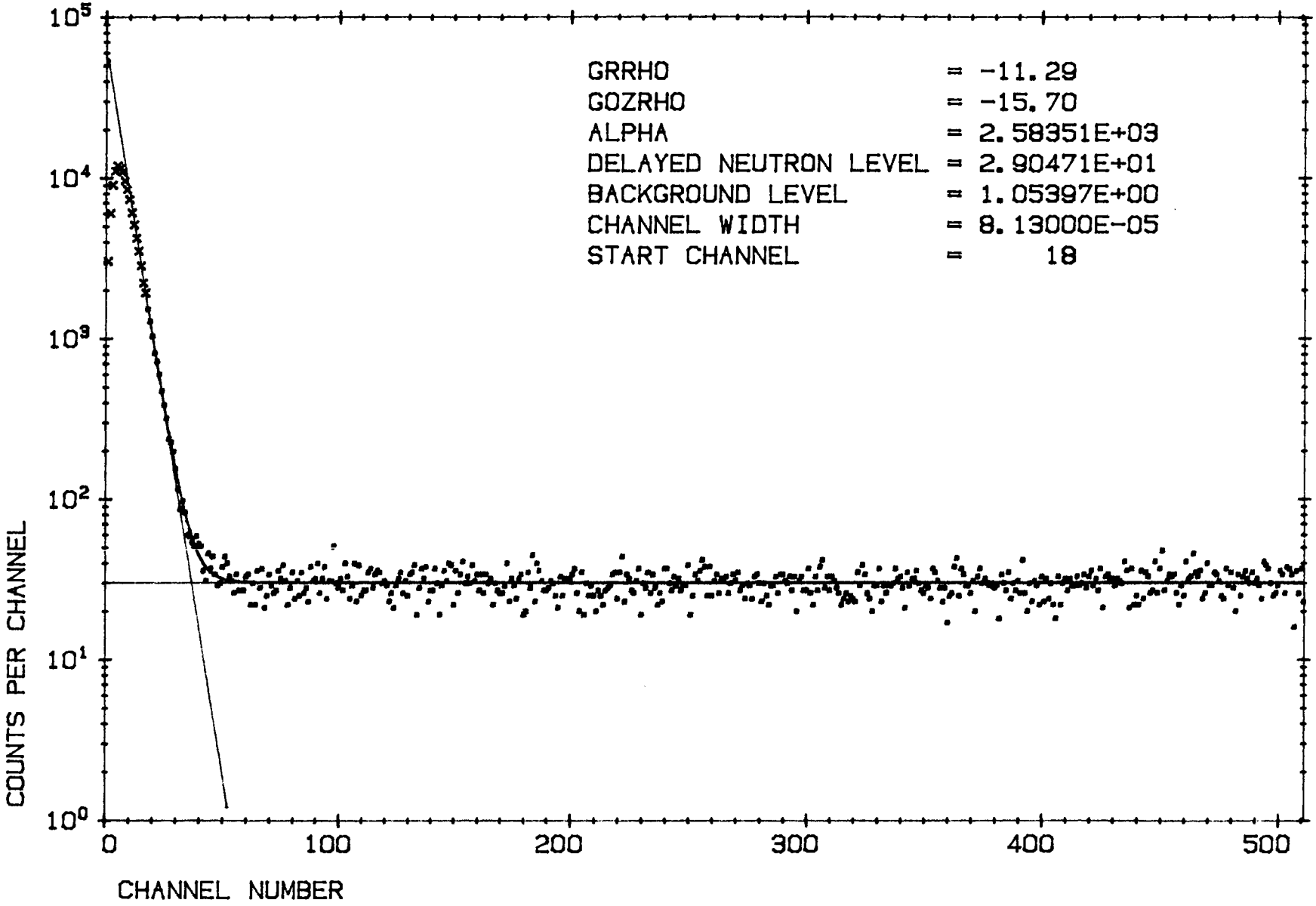

MEASUREMENT NUMBER BNFL 21-8

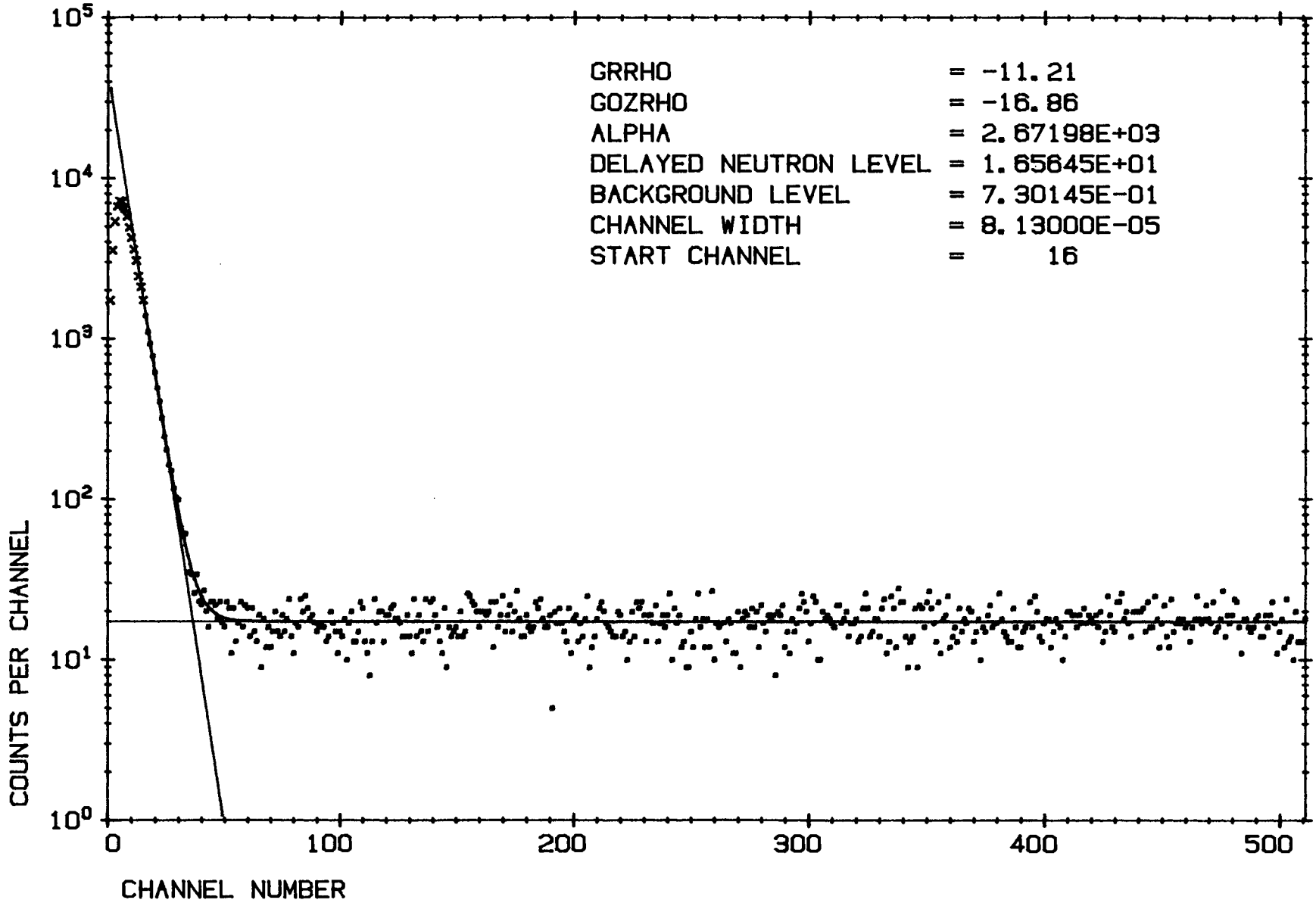

MEASUREMENT NUMBER BNFL 21-9

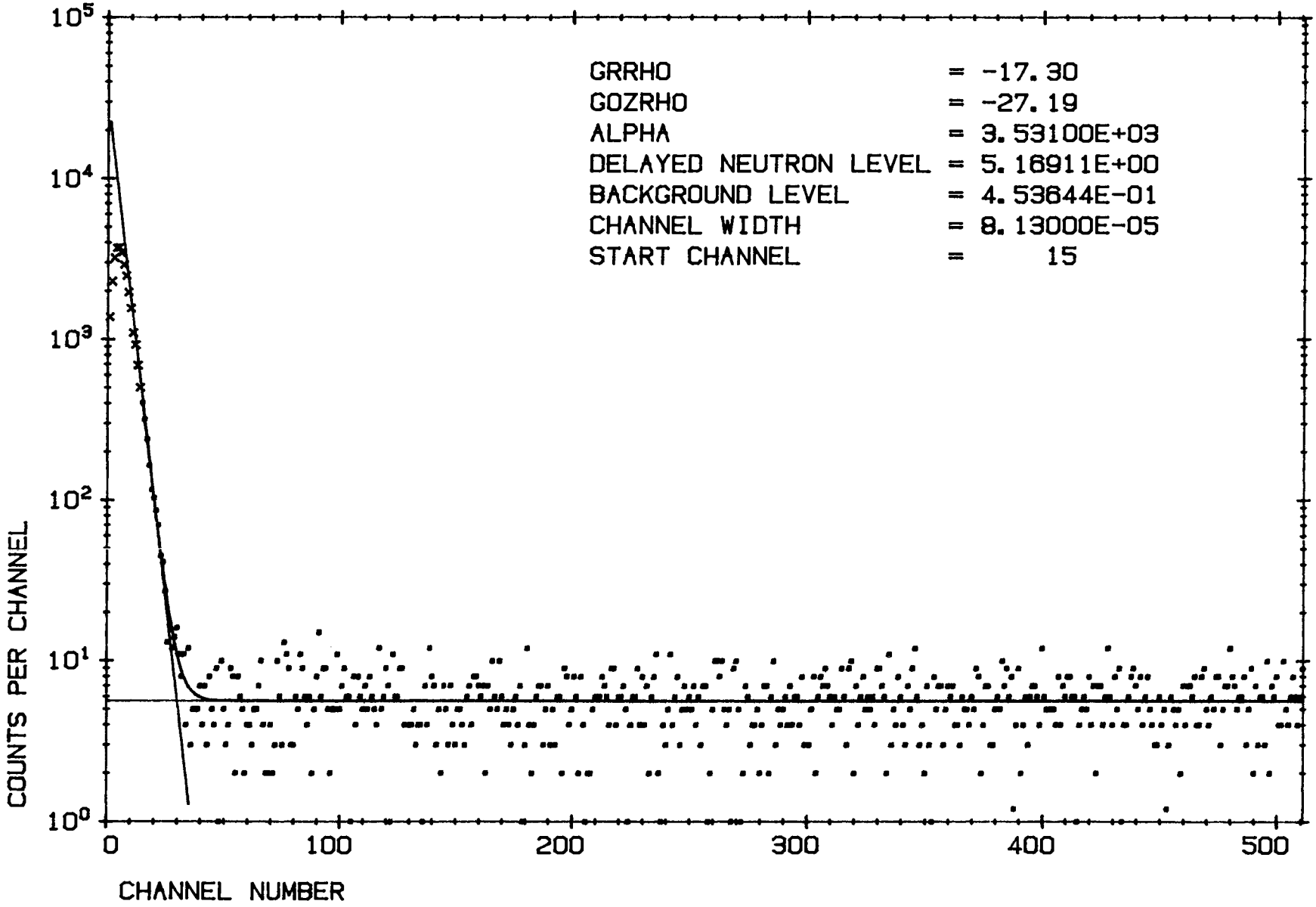

MEASUREMENT NUMBER BNFL 21-10

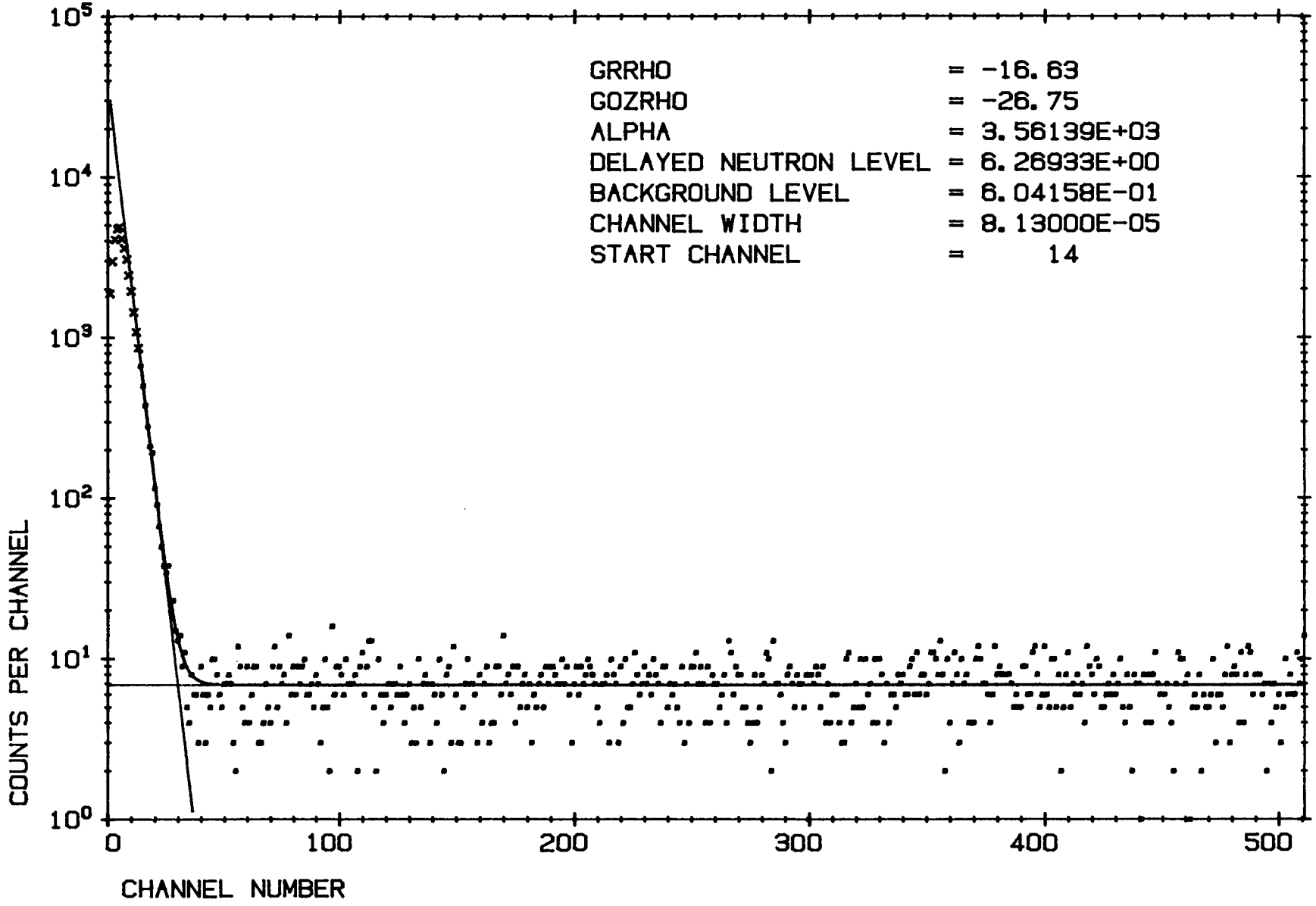

MEASUREMENT NUMBER BNFL 22-2

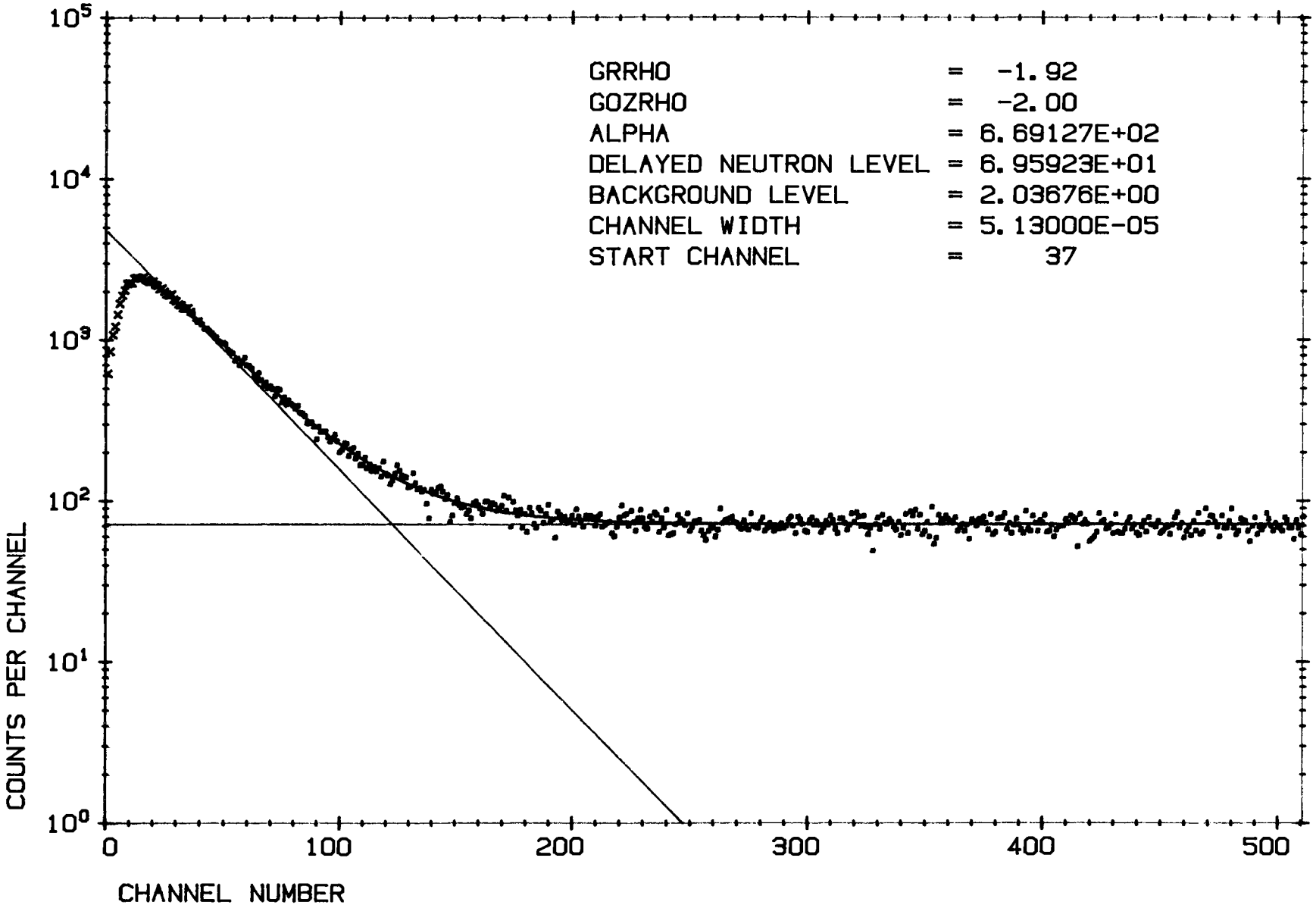

MEASUREMENT NUMBER BNFL 22-1

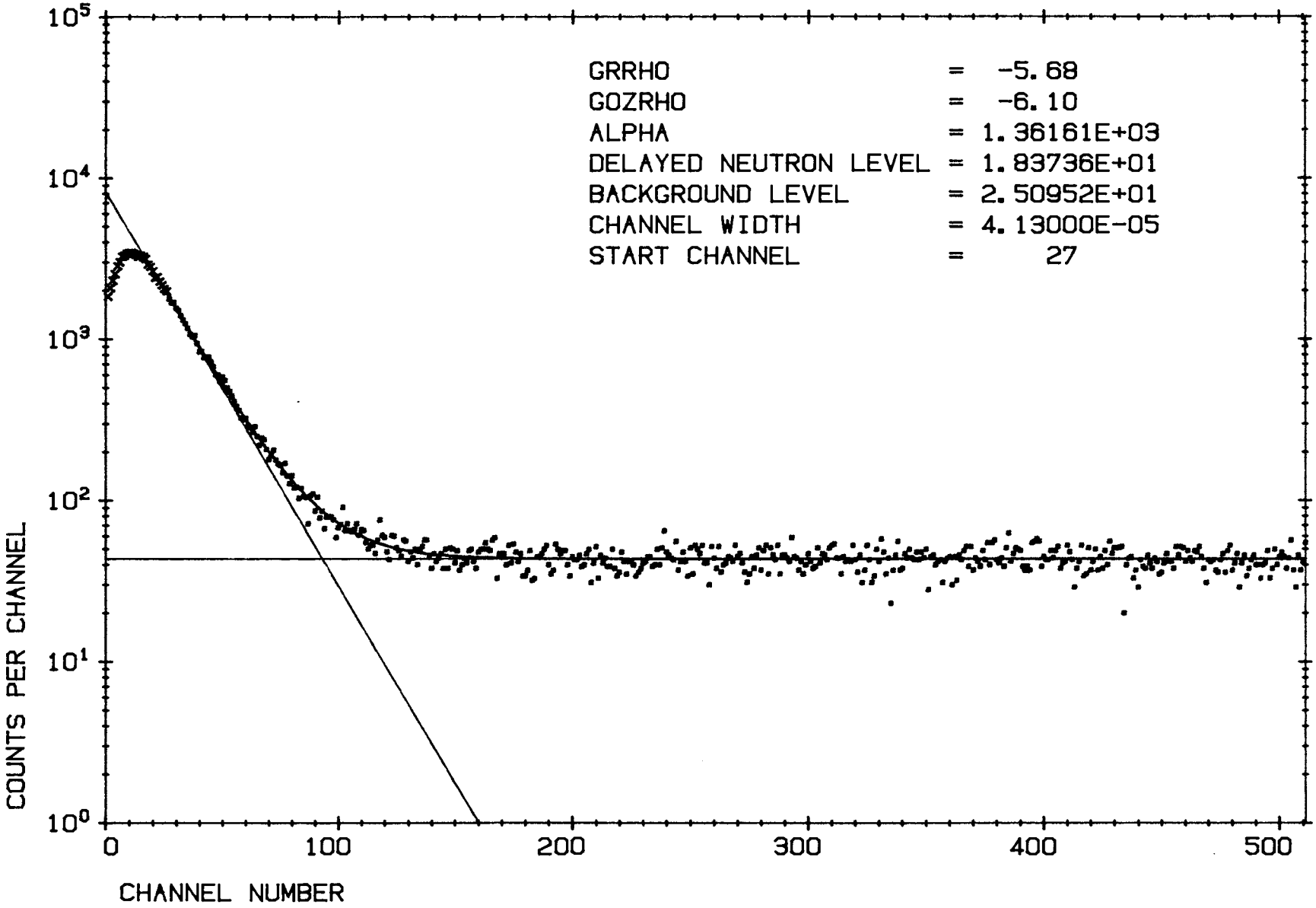

MEASUREMENT NUMBER BNFL 22-4

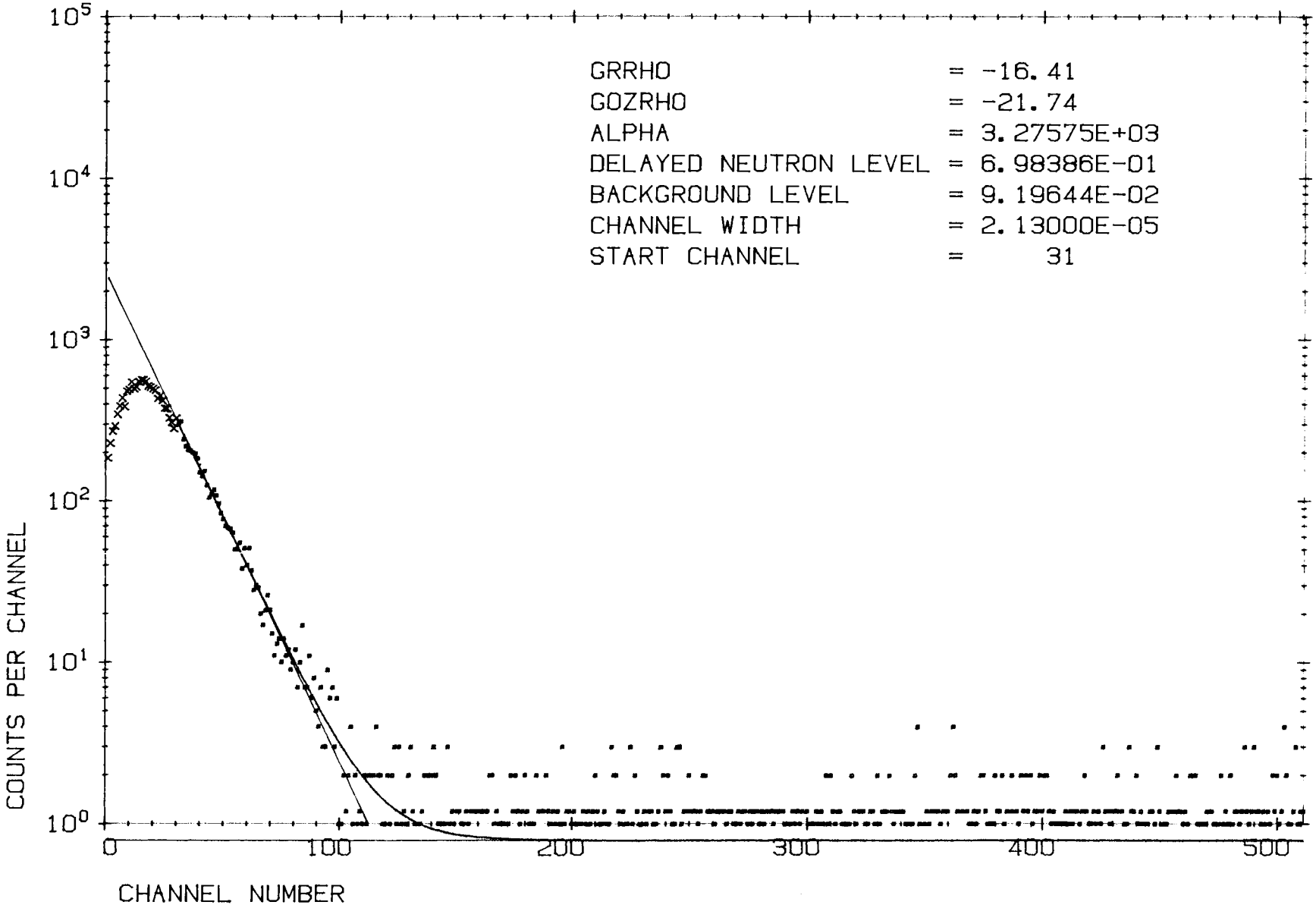

MEASUREMENT NUMBER BNFL 32-5

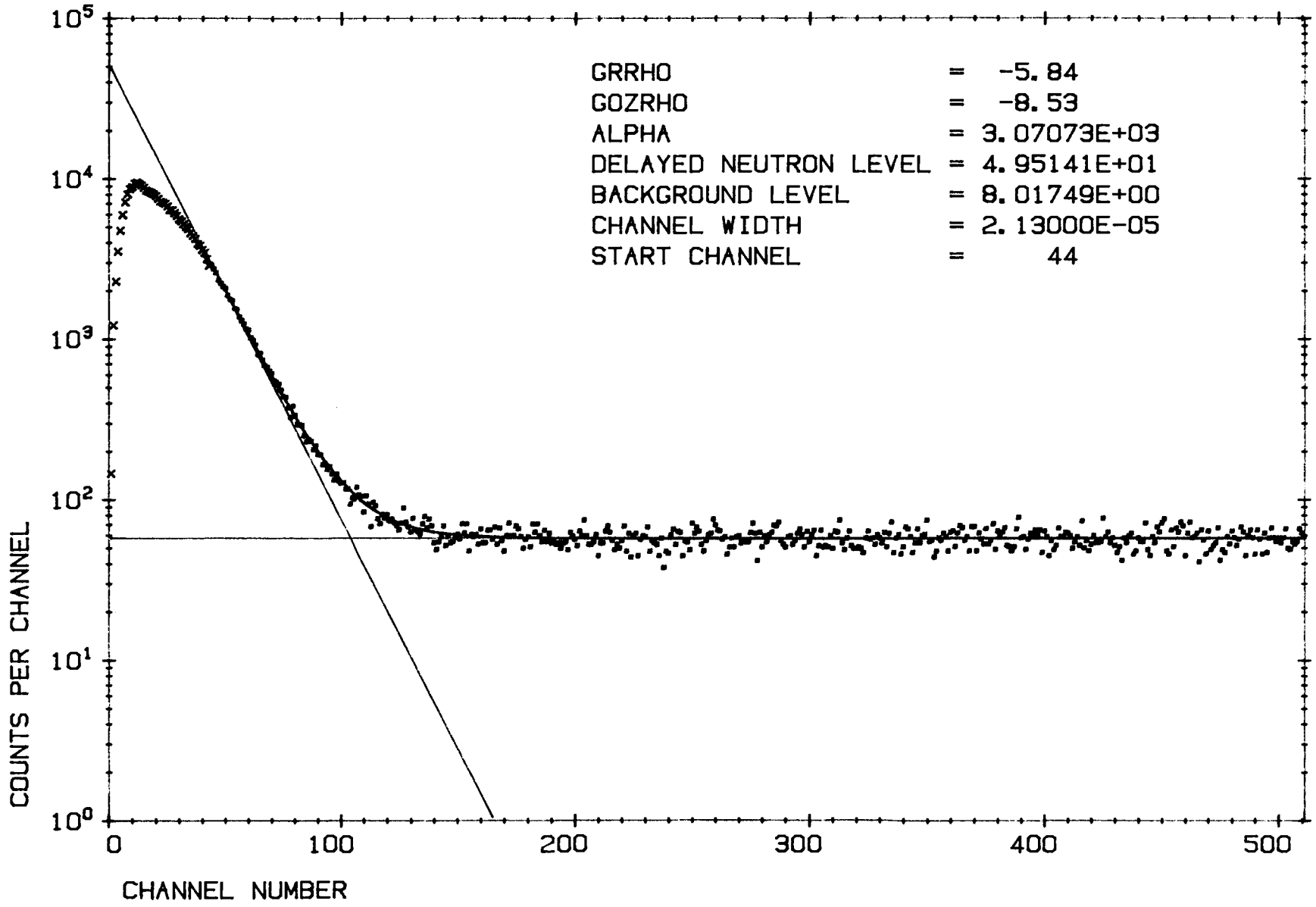

MEASUREMENT NUMBER BNFL 32-4

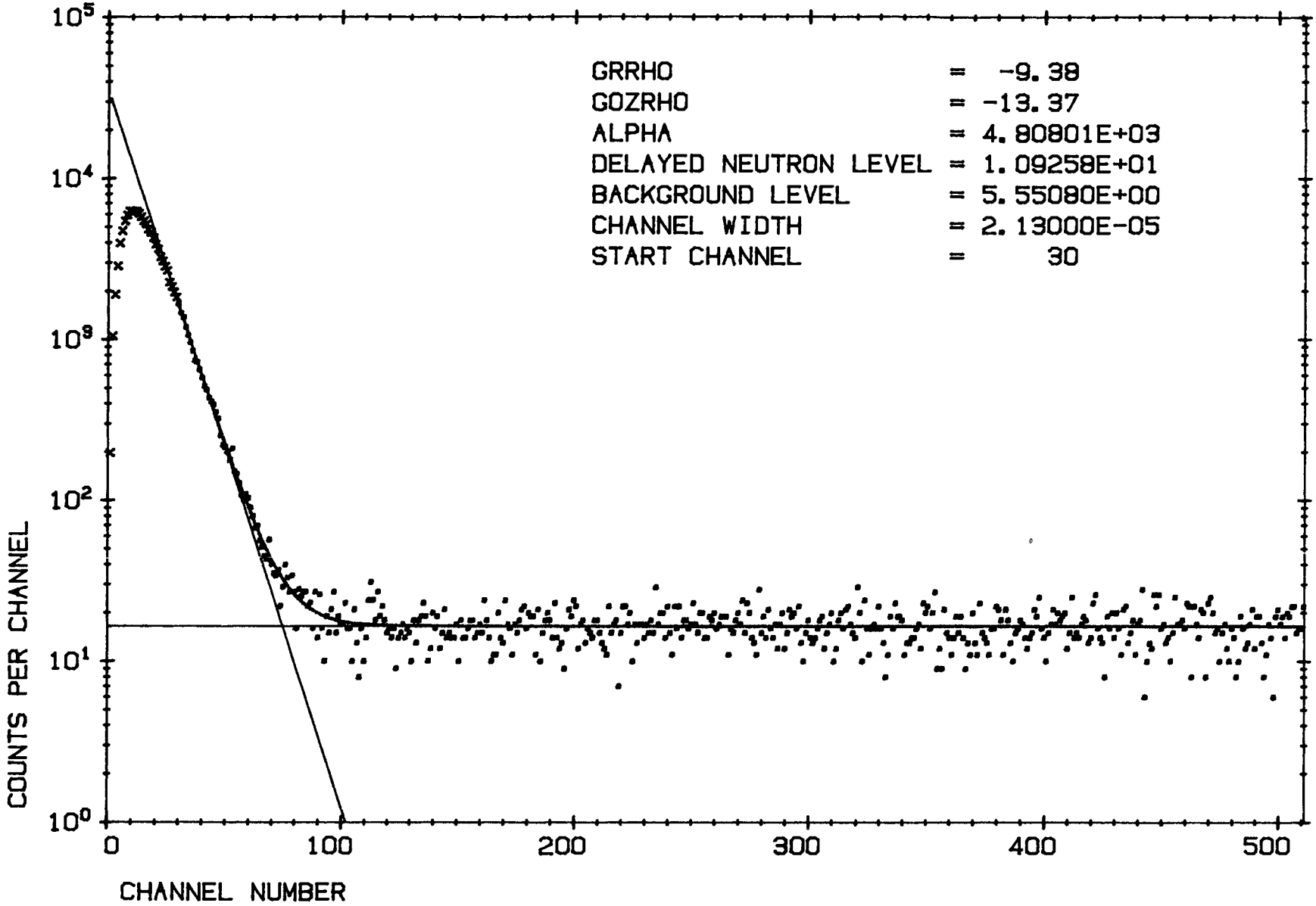

MEASUREMENT NUMBER BNFL 32-2

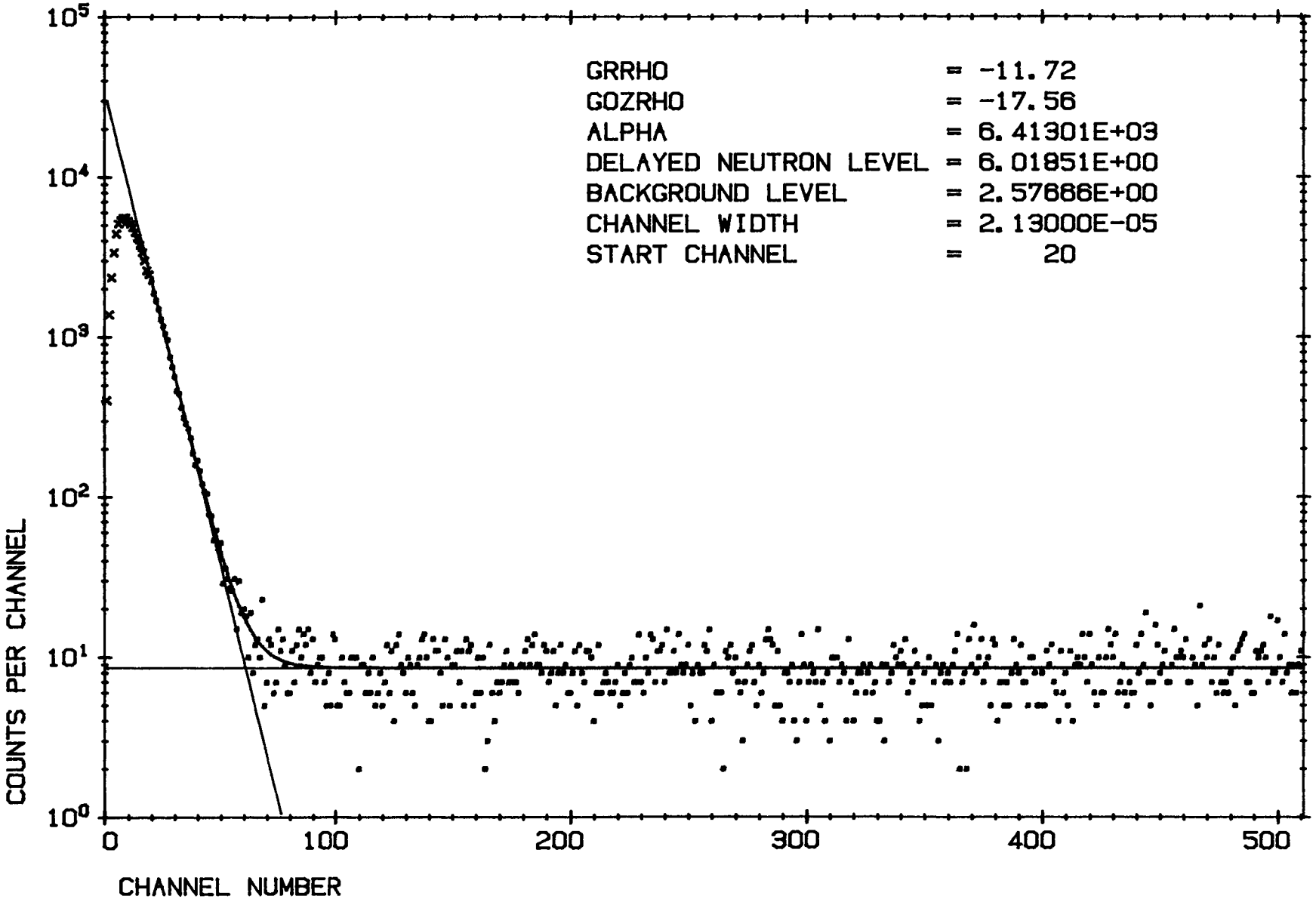

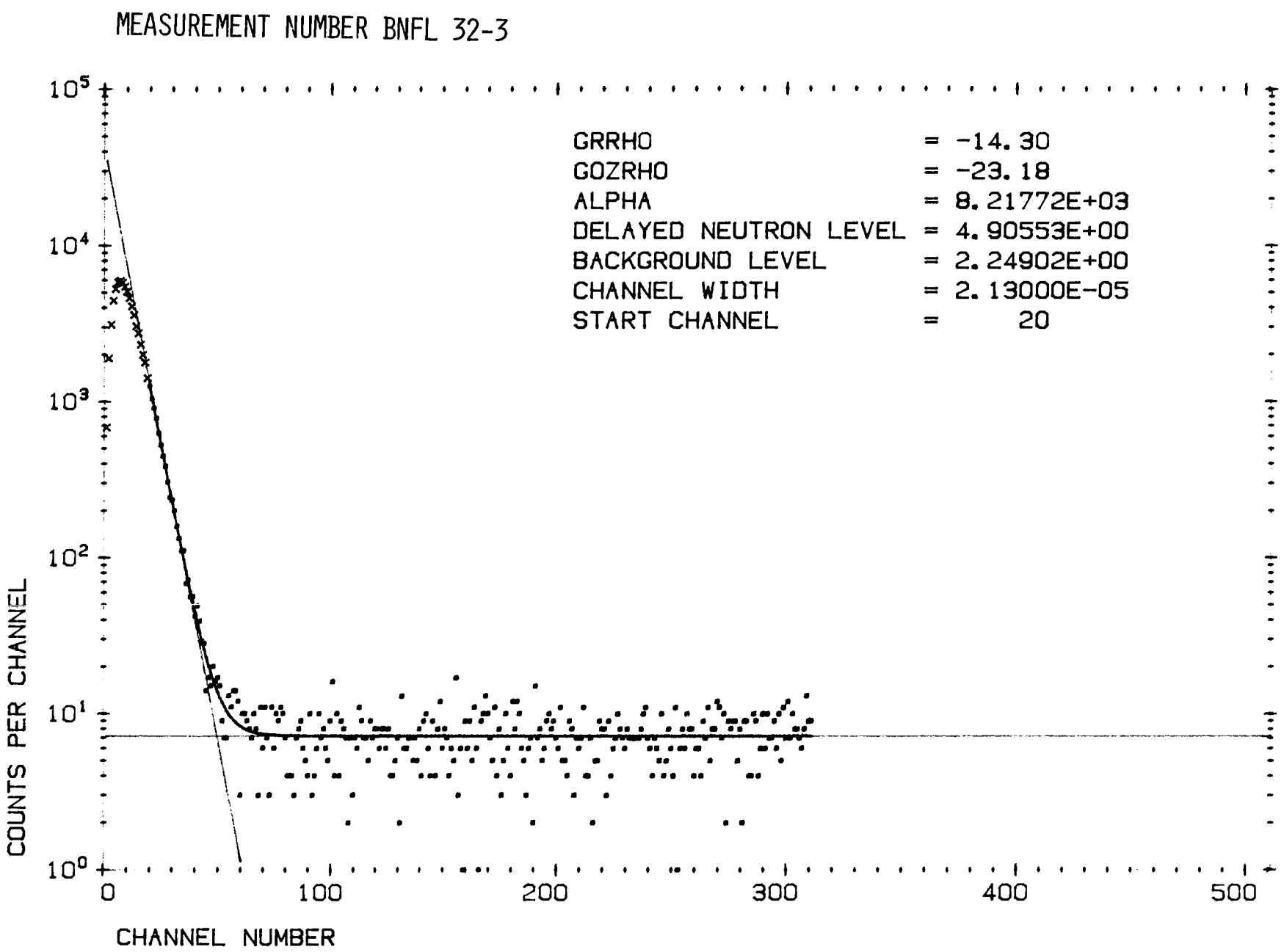
MEASUREMENT NUMBER BNFL 32-3
GRRHO = -14.30
GOZRHO = -23.18
ALPHA = 8.21772E+03
DELAYED NEUTRON LEVEL = 4.90553E+00
BACKGROUND LEVEL = 2.24902E+00
CHANNEL WIDTH = 2.13000E-05
START CHANNEL = 20
COUNTS PER CHANNEL
CHANNEL NUMBER
10^5
10^4
10^3
10^2
10^1
10^0
0
100
200
300
400
500

MEASUREMENT NUMBER BNFL 32M-1

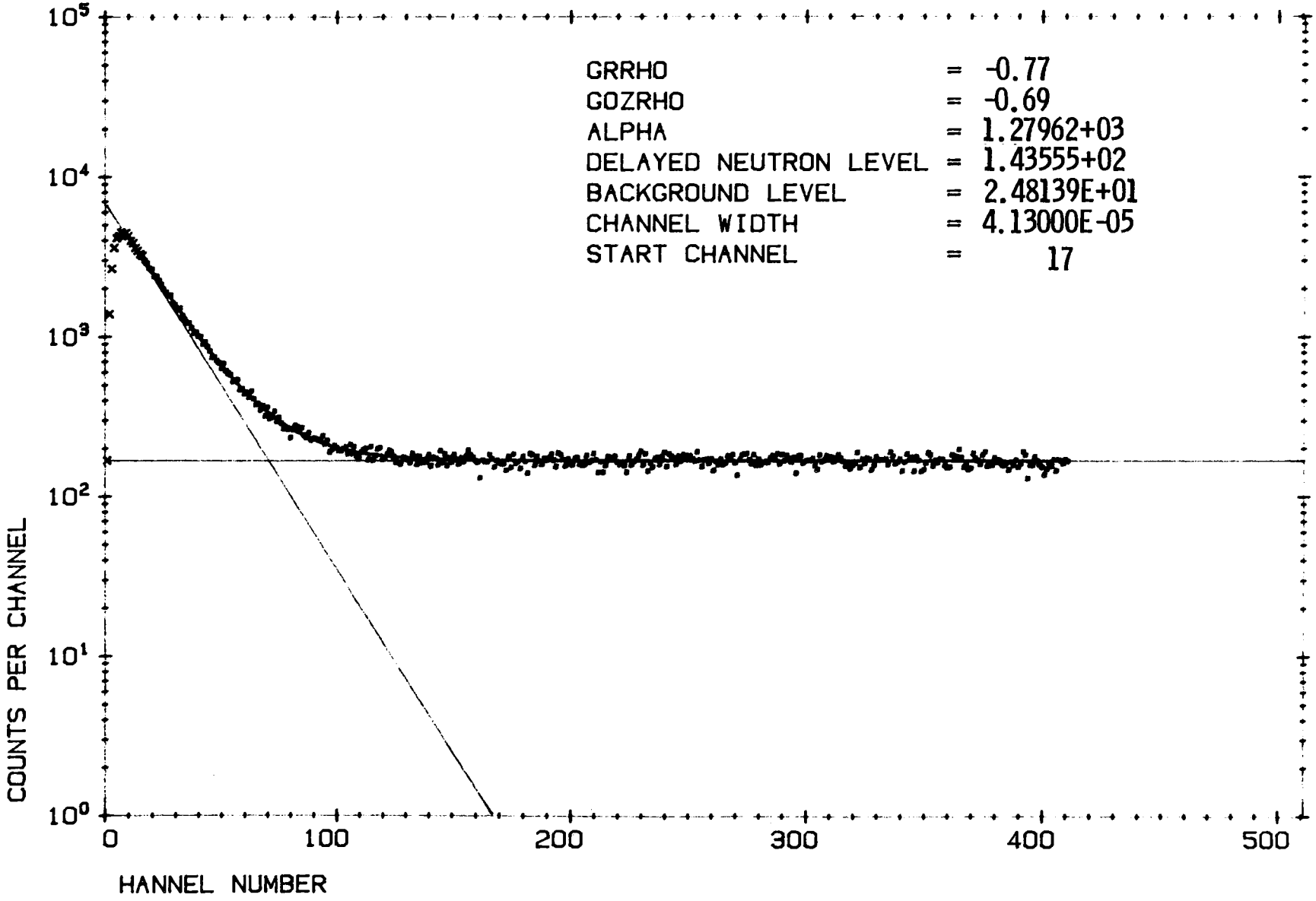

MEASUREMENT NUMBER BNFL 32M-3

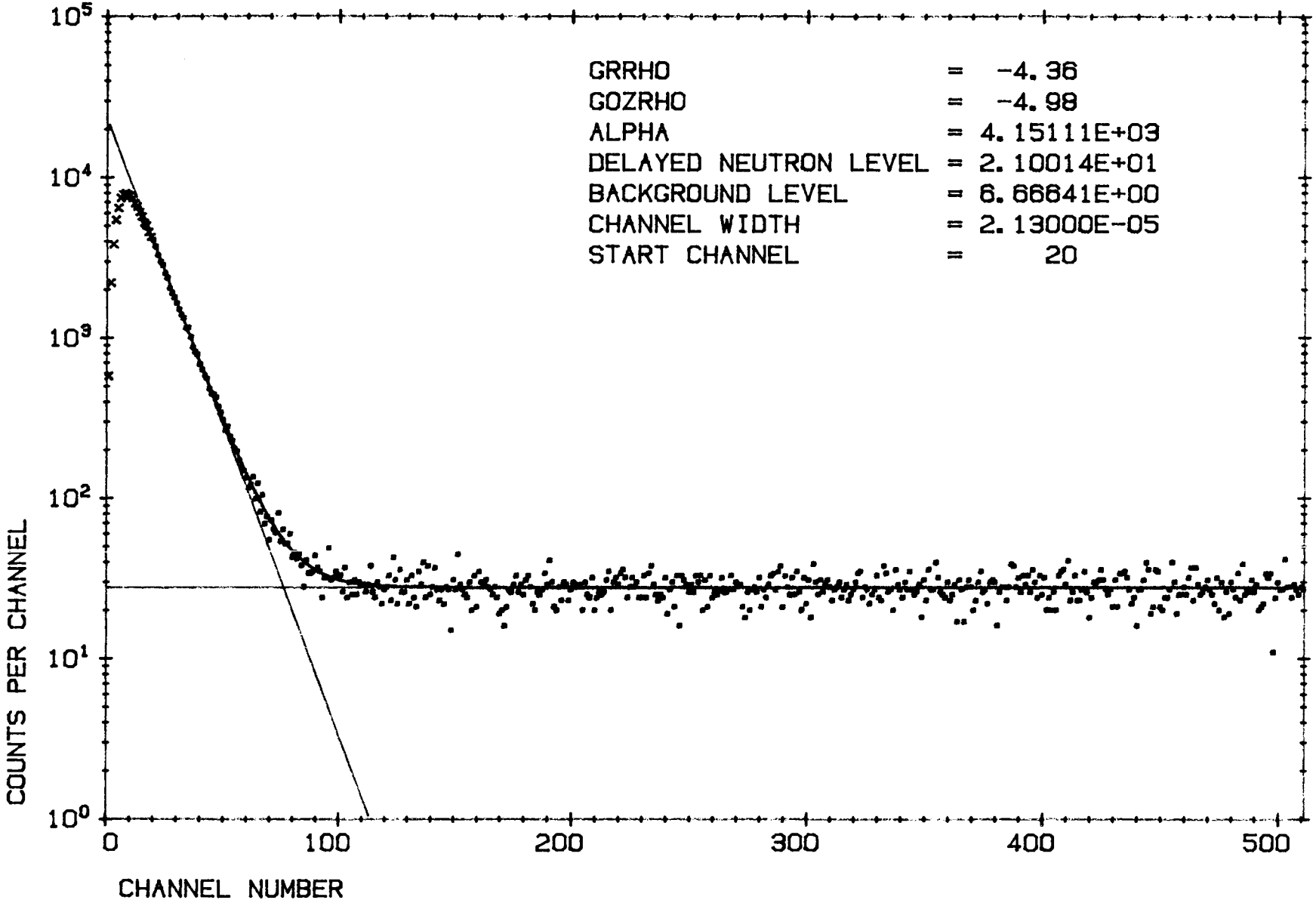

MEASUREMENT NUMBER BNFL 32M-4

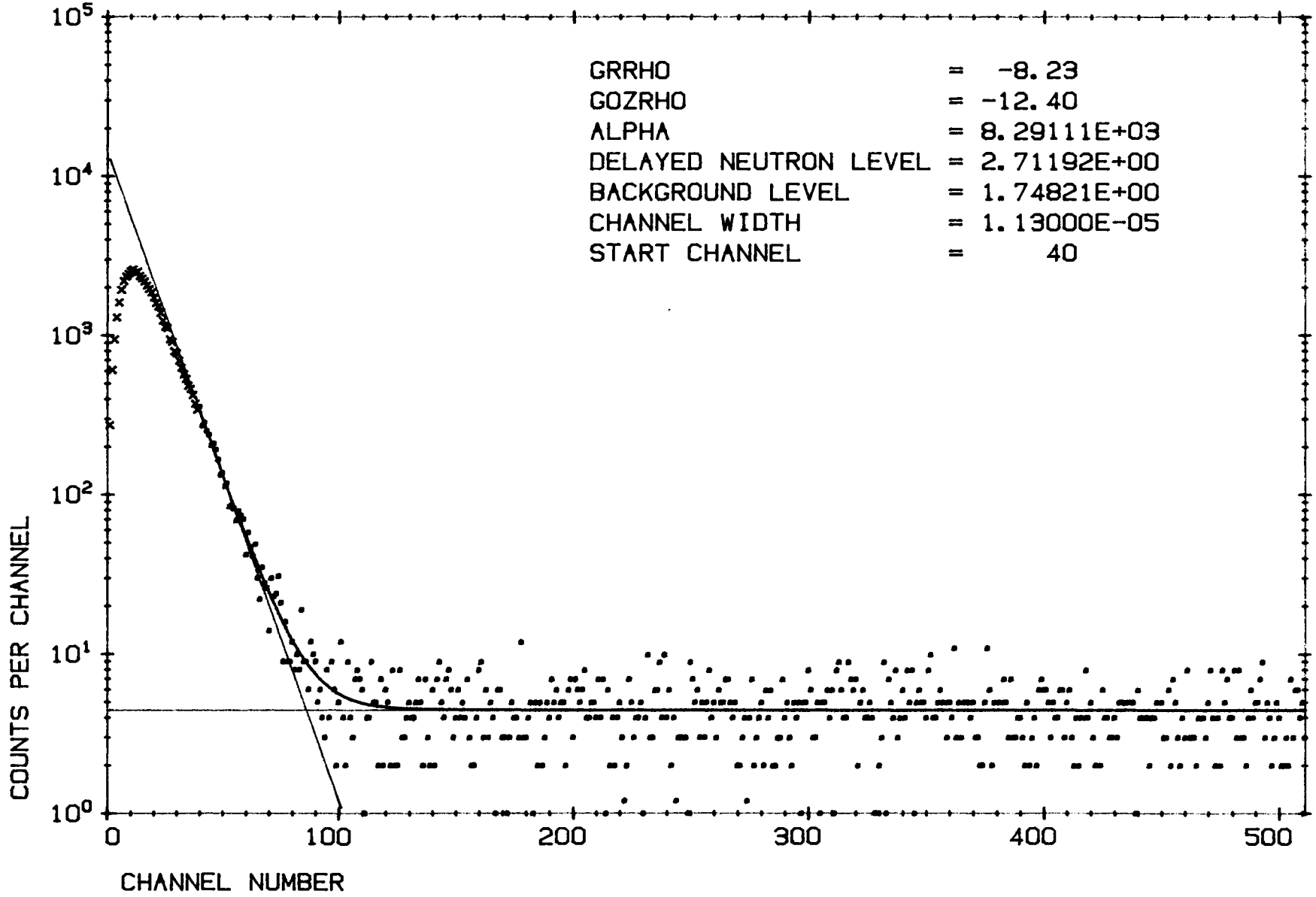

APPENDIX H

Fast Fission Ratio and Relative Conversion Ratio Measurements

The preparation, irradiation, data reduction, and analyses of foil packs to determine $^{238}U/^{235}U$ Fast Fission Ratios in the 4.31 wt% ^{235}U enriched UO_2 fueled lattices is presented in this Appendix along with the results obtained. Also similar details are presented in this Appendix for determining the ^{238}U capture to ^{235}U fission ratio in the 4.31 wt% ^{235}U enriched UO_2 fuel relative to that in a known thermal flux (the Relative Conversion Ratio).

RPD/MFM/830

FAST FISSION RATIO AND RELATIVE CONVERSION RATIO MEASUREMENTS IN WATER MODERATED UO2 LATTICES

M F MURPHY

Reactor Physics Division
AEE Winfrith

21.July 1983

CONTENTS

1 INTRODUCTION

As part of a programme of criticality experiments, reaction rate measurements have been made in a series of water moderated lattices of 12.7 mm diameter 4.3% enriched UO_2 fuel rods. This report deals with the measurements of Fast Fission Ratios and Relative Conversion Ratios in these lattices. The Fast Fission Ratio (FFR) is defined here as the ratio of; fission rate per atom of U238, to fission rate per atom of U235. The Relative Conversion Ratio (RCR) is defined as the ratio of; capture rate per atom of U238, to fission rate per atom of U235, in the reactor fuel, relative to the same ratio in a well thermalised neutron spectrum.

A major aspect of these measurements was that the irradiations took place in the USA and the measurements were made at AEE Winfrith. This resulted in a considerable logistics problem but by good planning and the co-operation and diligence of all concerned this problem was overcome. However, the long distance involved inevitably meant that samples were not available for measurement until about 28 hours after the irradiation. It was therefore necessary to modify the techniques that are normally used in the Reactor Physics Division Counting Laboratory on samples that are available about two hours after shut-down. These modifications will be detailed later in this paper.

FFR and RCR measurements can be made separately. However, to economise on materials and reactor time it was convenient to use components from the same experimental sample pack (Figure 1) to measure both ratios.

2 MEASUREMENT OF FAST FISSION RATIO

2.1 METHOD

The basis of the method used for measuring FFR[1][2] involves the simultaneous irradiation, in a fuel element, of two uranium samples of different enrichments. The fission product γ-ray activity of each sample is then measured and hence, knowing the enrichments, the ratio of U238 to U235 fission product activities can be deduced. A calibration factor to relate fission product activities to true fission rates is determined in a separate experiment.

2.2 ENRICHMENTS

The choice of enrichments for the sample pair is a compromise between; minimising the flux perturbations in the measuring region, and obtaining a well conditioned simultaneous equation. In these measurements the sample pair comprised a 4.3% U235 UO_2 disc and a 0.04% U235 uranium metal foil. The UO_2 disc is effectively a 0.2 mm thick slice of the fuel element and therefore has a negligible perturbation effect, the 0.07 mm depleted foil with its 0.07 mm depleted metal guard foils causes a perturbation of less than 1%[2].

For the lattices studied, the U238 fission rate in the enriched disc was in the range 5% to 12% of the total fission rate, whilst in the depleted foil the U235 fission rate was 10% to 20% of the total fission rate. Thus the simultaneous equations for deducing the FFRs were reasonably well conditioned.

2.3 IRRADIATION

The samples are positioned in the measuring pack as shown in Figure 1. The depleted guard foils protect the depleted foil from fission products from the enriched UO_2 material, and ensure that there is no net loss of fission products from the depleted foil. The 4.3% UO_2 disc is also used to measure the U235 lattice to thermal fission ratio, as part of the RCR measurement, in conjunction with similar UO_2 discs irradiated simultaneously in a thermal spectrum. Also contained in the pack is the UO_2 pellet to be used in the U238 capture rate measurement.

Measurement packs were irradiated in sets of three in each of the lattice arrangements studied. A simultaneous irradiation was made, in each case, in the thermal column of the Winfrith source reactor Nestor. The thermal column is a graphite cube of 1.8m side. The 4.3% UO_2 discs used for the thermal irradiation were mounted in a special graphite holder which was positioned in the column, 1.4m from the face nearest the reactor. These UO_2 discs were guarded on each side by identical discs, to provide the same interchange of fission products as in the lattice packs. Synchronisation of the irradiations was achieved by maintaining a telephone link during the start-up phase. The neutron shutter to the thermal column has opened when the American reactor was at 37% of full power, on a constant doubling time. The irradiations were for exactly two hours, at a constant neutron flux of about $2 \times 10^8 ncm^{-2}s^{-1}$, in both the experimental reactor and the Nestor thermal column.

Following the irradiation the measuring packs were transported by road and air and arrived at AEE Winfrith about 28 hours after the irradiation had finished.

2.4 DETECTOR SYSTEM

The fission product γ-ray activities were measured on a detector system having as its basis two NaI(Tl) detectors 50mm in diameter by 50mm thick. These are installed, in a vertically opposed configuration, in an automatic sample changer mechanism which is housed in a thermostatic enclosure, controlled to $\pm 0.1^{o}C$. Temperature stabilisation is necessary as the detectors have a gain coefficient with temperature of 1% per $1^{o}C$. Control of the detector system is effected by a PDP computer via CAMAC and the activity data are collected by the computer via CAMAC scalers [3].

2.5 COUNTING PROCEDURE

The detector system discriminators were set to accept pulses from γ-rays greater than 0.64 MeV in energy. Normally a discriminator level of 1.28 Mev is used but the lower value was used in these measurements to compensate for the long delay, by including more of the γ-rays from longer lived fission products.

After irradiation and transport to AEE Winfrith the measuring packs were dismantled and the foils and discs were carefully cleaned with a solvent. This was particularly important for the depleted foils as it removed possible contamination by small particles of enriched UO_2. The depleted foils were then mounted in aluminium holders which were inserted into the plastic holders of the automaic detector system. The depleted foils were measured by themselves on the system to avoid interference from the much higher activity UO_2 discs ($\sim$ x25). After sufficent counts had been accumulated from the depleted foils, they were removed and the UO_2 discs from the measuring packs and from the thermal column were loaded on to the system. The measurement then continued until sufficient counts had been accumulated from the UO_2 discs. Another identical detector system was also used but the samples were measured in the reverse order; enriched first and then depleted. So effectively two separate measurements were made on each set of samples.

2.6 ANALYSIS

The data collected from the measurements were transmitted to the main computer at AEE Winfrith (ICL 2976) at the end of the measurement. Analysis of the data was then performed by the FREDA code [a]. which, after correcting for deadtime, background, mass, decay, etc, produces Fast Fission Ratios and U235 lattice to thermal ratios, with their theoretical and rms errors.

Consider: a depleted foil counted at time t, and an enriched foil counted at time t'. Then one may write:

$$C^D(t) = N^D_8 F_8 G_8(t) + N^D_5 F_5 G_5(t) \qquad (1)$$

$$C^E(t') = N^E_8 F_8 G_8(t') + N^E_5 F_5 G_5(t') \qquad (2)$$

where: C = total count-rate
N = number of atoms per sample
F = count-rate at a standard delay time
G = decay factor relative to standard delay time
indices D = depleted
E = enriched
suffices 8 = U238
5 = U235

a) AEEW fission ratio computer programme

Solving (1) and (2) for F8 and F5 one finds:

$$\frac{F_8}{F_5} = \left[\frac{C^D N_5^E G_5(t')}{C^E N_8^D G_5(t)} - \frac{N_5^D}{N_8^D}\right] \cdot \left[1 - \frac{C^D N_8^E G_8(t')}{C^E N_8^D G_8(t)}\right]^{-1} \qquad (3)$$

If the depleted foil is counted n times and the enriched disc is counted m times, then FREDA solves nm equations of form (3) and produces a mean value of F8/F5. This is the ratio of fission product γ-ray activities, which must be converted by a calibration factor to the true fission ratio. The determination of this factor is described in Section 5.1.9. The FFR results are presented in Section 4.1.

2.7 Ba140/La140 METHOD

As a check on possible systematic errors the FFR was also measured by another method. This involved using the same uranium sample pair as for the previous method but measuring only one particular fission product γ-ray. The relative abundances of the Ba140 fission product, produced in the two types of sample, were measured by observing the decay of its daughter La140. This method is largely independent of the previously described detection method but is somewhat less precise.

Ba140 decays by β-emission, with a 12.8 day half life, to La140 which decays by β-emission, with a 40.2 hour half life, to stable Ce140. At short times after irradiation the La140 activity is low, it builds up to a maximum at about 5 days after shut-down, and then decreases until at about 14 days after shut-down it is decaying with the Ba140 half life. The main γ-ray emitted by La140 has an energy of 1.6 Mev; at about 3 days after shut-down this can be clearly resolved from other fission product γ-rays by using a germanium γ-ray detector.

The La140 activities were measured by placing the various samples in turn, in a reproducible position, close to a Ge(Li) detector of 15% relative efficiency. The γ-ray spectra were collected on a multi-channel analyser and were analysed by the GAMANAL code (3); a typical spectrum is shown in Figure 4.

The peak areas obtained were corrected for Ba140 and La140 decay using the code COUNTLA(a), this corrects for the ingrowth of La140 and for decay during counting. An analysis, similar to that described in Section 2.6, was then carried out to give the ratio of La140 activity from U238 relative to that from U235. This ratio was then converted to the true fision rate ratio by applying the Ba140 fission yields for U238 and U235. The yields used were; U235 (6.34±0.06)% and U238 (6.01±0.10)%(4). The results for this method are presented in Section 4.1.

a) AEEW decay computer programme

3 MEASUREMENT OF RELATIVE CONVERSION RATIO

3.1 INTRODUCTION

The measurement of RCR can be conveniently considered in two parts; the U238 lattice to thermal capture ratio and the U235 lattice to thermal fission ratio.

3.2 U238 CAPTURE METHOD

The nuclear transformations involved in the U238 capture measurement are as follows:

$$U238 + n \rightarrow U239 \xrightarrow[23.5\ min]{\beta^-} Np239 \xrightarrow[2.35\ days]{\beta^-} Pu239$$

The rate of U238 capture is determined after irradiation by observing the decay of Np239. This decays by β-emission to excited states of Pu239 which reach the ground state by γ-ray emission, as shown in Figure 4. Some of the higher energy γ-rays are highly internally converted, giving rise to the emission of plutonium X-rays which are in coincidence with the γ-rays. By observing the coincidences between the 104 kev K X-rays and the 106 kev γ-rays, good discrimination can be obtained against fission product γ-rays and natural activity.

The method used for the U238 capture determinations was derived from a dissolution technique, developed initially for measurements in particulate UO_2 fuel(5). It had been necessary, in that case, to dissolve a large number of the particles to produce a solution containing the average activity of a test section. A small aliquot of this solution could then be taken for activity measurements. The same principle can be applied to rod type fuel where it is necessary to examine a representative section of the fuel.

The choice of this method for U238 capture was governed by three factors:

(a) The original technique for rod type lattices(2) required thin UO_2 discs, 0.12mm thick, and matching UO_2 pellets, to be made to tolerances of about ±0.002mm. It was doubtful if these components could have been made on the time scale envisaged for these measurements.

(b) The fabrication of UO_2 components to such fine tolerances is extremely costly.

(c) The dissolution method can use components with larger tolerances, ±0.05mm, and therefore lower cost and easier availability, and yet gives results which are comparable in accuracy(6) to the original method.

To use the relaxed fabrication tolerances, bearing in mind that resonance capture is effectively a surface effect, a UO_2

pellet about 20mm long must be used rather than a thin disc. This ensures that resonance activation of the end surfaces of the pellet, caused by neutron streaming, is small compared to the total activation. The derivation of the required tolerances is given in Section 5.2.3. Suitable measuring pellets were produced from standard fuel pellets by removing a thin slice of material from each end with a high speed diamond saw. Care was taken to ensure that the resulting flat end surfaces were perpendicular to the length of the pellet. The 0.25mm thick UO_2 discs for the thermal column measurements, and those for the fission measurements in the reactor, were prepared by cutting slices of UO_2 of approximately the required thickness from standard pellets. The slices were then lapped with a planetary lapping machine to the specified thickness and flatness.

3.3 SOURCE PREPARATION

The irradiation procedure has been described in Section 2 but it should be noted that about 40 mg of 93% U235 U_3O_8 powder was also included in the thermal column irradiations to provide a fission product correction source. After irradiation and transportation to Winfrith, the UO_2 pellets for the U238 capture rate measurement were weighed and then dissolved in nitric acid. Each solution was made up to a known volume ($\sim$ 250 ml) and a suitable aliquot was taken to give the required activity in the final source. The UO_2 discs and the U_3O_8 powder from the thermal irradiation were also dissolved in the same way. Solutions were also prepared of unirradiated natural uranium and 93% enriched uranium to act as natural activity standards. At this stage a portion of a solution containing a known mass of unirradiated natural uranium was added to each aliquot to give, as closely as possible, the same total mass of uranium in each aliquot. This was to ensure that the γ-ray transmission probabilities from each source were nearly identical, so that the resulting differential corrections from one source to another were very small. Each of the aliquots was reduced to dryness by heating; the resultant residues were then redissolved in nitric acid and made up to volumes of 5 ml. Portions of these solutions were transferred to 2 ml liquid source holders using hypodermic syringes. The quantities of solution transferred were determined gravimetrically.

3.4 Np239 DETECTION SYSTEM

The Np239 activities were measured by a coincidence method using a detection system based on two pairs of NaI(Tl) detectors 75 mm in diameter and 25 mm thick. Each pair of detectors is vertically opposed and the liquid sources are located in turn between the detectors by means of a twelve position horizontal turntable. The two pairs of detectors are diametrically opposite relative to the turntable. Pulses from the detector amplifiers are passed to single channel analysers which select pulses equivalent to an energy range of 95 kev to 115 kev. The selected pulses from each pair of detectors are used to drive a coincidence unit which produces an output pulse if the pulses at the two inputs ocur within 400 ns of each other. Thus the system

preferentially detects coincident Np239 radiations and discriminates against fission product γ-rays and natural activity. The system is housed in a thermostatic enclosure and the sample changer mechanism is computer controlled. Counts are collected, by the computer, from the coincidence units and the single channel analysers.

3.5 Np239 COUNTING PROCEDURE

The liquid sources were loaded onto the twelve position turtable in the order shown below:

Position	Sample
1	Lattice position 1
2	Lattice position 1 duplicate
3	Lattice position 2
4	Lattice position 2 duplicate
5	Lattice position 3
6	Lattice position 3 duplicate
7	Thermal disc 1
8	Thermal disc 2
9	Irradiated U235
10	Unirradiated U235
11	Unirradiated natural U
12	Am243 standard source

Each source was measured for ten minutes at a time and this procedure continued for about three days to accumulate sufficient counts to give the required precisions. The duplicate sources were additional aliquots taken from the same original solution. A comparison of the results from a source and its duplicate gave information on the reproducibility of the method itself, after the dissolution stage, eliminating effects due to variations in the lattice geometry, for example. The thermal sources were made from two separate UO_2 discs.

It was necessary to measure the fission product activities of the sources, relative to the irradiated U235 source, in order to make corrections for fission product interference. These measurements were made on the detection system, previously used to measure the fission ratios, which was described in Section 2. A discriminator level equivalent to 0.64 MeV was used.

3.6 U238 CAPTURE ANALYSIS

After the collected data had been transferred to the main computer, the analysis was carried out using the ANCORA code (a). This makes corrections for; deadtime, decay, mass, background, natural activities, fission products, chance coincidences, γ-ray transmission, etc, and produces lattice to thermal Np239 activity ratios and errors.

Natural activity corrections were made on the basis of the counts recorded from the unirradiated samples of natural and enriched uranium. Knowing the isotopic compositions and masses

a) AEEW coincidence counting analysis computer programme

of these samples, the specific natural activity can be derived for U235 and U238. Then, as the isotopic compositions and masses of all the other sources are known, the individual natural activity for each source may be derived.

Corrections for fission product interference were made by using the coincidence counts from the fission products in the irradiated U235 source as a reference. The counts due to fission products in the other sources were derived via the previously determined ratios of fission product activities. Making corrections for natural activities and fission products as described above has the advantage that the corrections are determined close to the time of counting, rather than in a previous calibration. Therefore small variations in amplifier gain or analyser threshold will have negligible effects on the derived Np239 activity ratios.

As stated previously, the total uranium contents of all the sources were made as closely as possible the same by adding unirradiated uranium during preparation. Nevertheless, there were still corrections to be made for γ-ray transmission from the sources. These corrections were made by first calculating the linear γ-ray absorption coefficient for a source from its chemical composition. The γ-ray escape probability was then obtained, by interpolation, from a table of absorption coefficients versus escape probabilities. This table was produced, using published tabulated functions (7), assuming that each detector crystal has 2Π geometrical efficiency. This is not strictly the case but, as the detectors are 75 mm in diameter and the 15 mm sources are only 10 mm away from them, it is a reasonable approximation. The method has been checked by a Monte-Carlo code, using the specific detector geometry, and was found to be satisfactory.

The results of the U238 capture measurements are given in Section 4.2.

3.7 Np239 MEASUREMENT BY Ge(Li) DETECTOR

As a check on possible systematic errors in the NaI(Tl) coincidence detection system, the Np239 measurement was repeated on selected liquid sources using a high resolution germanium detector. Discrimination against fission products was obtained solely by virtue of the detector's high resolution, as it was not operated in the coincidence mode. It was therefore necessary to measure the 278 kev Np239 γ-ray as this was the only significant Np239 peak clear of fission product γ-rays.

The measurements were made using a Ge(Li) detector installed in an automatic sample changer system and the γ-ray spectra were collected on a multi-channel analyser. These spectra were transmitted to the main computer where they were corrected for Np239 decay and for the sample masses. Lattice to thermal activity ratios were then calculated. The results obtained are given in Section 4.2.

3.8 U235 LATTICE TO THERMAL FISSION RATICS

The ratio of the U235 fission rate in the reactor lattice relative to the U235 fission rate in a thermal spectrum was determined, in conjunction with the Fast Fission Ratio measurement, using the two 0.25 mm thick UO_2 discs from each lattice pack and similar discs from the thermal column. UO_2 discs were positioned at each end of the UO_2 pellet to be used for the U238 capture measurements, as shown in Figure 1. A mean U235 fission rate for the pellet region could then be obtained. Also a comparison of the rates measured by the two discs gives an indication of possible flux gradients through the pack. The irradiation and counting procedure was described in Section 2; the analysis of the data was carried out by the FREDA code.

Consider: a lattice disc counted at time t after shut-down, and a thermal disc counted at time t' after shut-down. Then one may write:

$$C^L(t) = N_5^L F_5^L G_5(t) + N_8^L F_8^L G_8(t) \qquad (4)$$

$$C^T(t') = N_5^T F_5^T G_5(t') \qquad (5)$$

where: C = total count-rate
N = number of atoms per sample
F = count-rate at a standard delay time
G = decay factor relative to the standard delay time
indices L = lattice (reactor)
T = thermal column
suffices 8 = U238
5 = U235

Solving (4) and (5) for F_5^L and F_5^T one finds:

$$\frac{F_5^L}{F_5^T} = \frac{C^L(t) N_5^T G_5(t')}{C^T(t') N_5^L G_5(t)} \left[1 + \frac{N_8^L F_8^L G_8(t)}{N_5^L F_5^L G_5(t)} \right]^{-1} \qquad (6)$$

where the term in brackets is effectively the correction to the lattice sample count for U238 fissions. The F_8^L/F_5^L ratio is, in fact, the FFR that was obtained from the depleted and enriched samples, as described previously in Section 2.

Lattice to thermal U235 fission ratios were obtained for each pair of UO_2 discs from each measurement pack. These ratios were then combined with the U238 capture lattice to thermal ratios to give the Relative Conversion Ratios. The results obtained are given in Section 4.2.

4 RESULTS

4.1 FAST FISSION RATIO RESULTS

The results for the FFR measurements are presented in Table 1. Errors quoted on the individual values of FFRγ are based on those produced by the FREDA code but also take account of any differences between the results from the two detector systems. The error quoted on each mean value is the standard error derived in the usual way from the deviations of the individual values from the mean. This error reflects all the random processes in the measurement, including any effects of the reactor environment, and is less than 1% for all five irradiations.

To convert FFRγ to true FFR the FFRγ values are multiplied by a calibration factor of 1.031 ± 2%. The error on the factor is the major systematic error in the measurement of FFR. Corrections and errors in the determination of FFR are discussed in Section 5.1 and are summarised in Table 3. A comparison of the results from the gross γ-ray method with those from the La-140 method is given in Table 6. The mean ratio, for all the irradiations, of gross γ-ray to La-140 is 1.025 ± 1.2% random, ± 2.5% systematic.

4.2 RELATIVE CONVERSION RATIO RESULTS

The results of the Relative Conversion Ratio measurements are presented in Table 2. The RCR is derived by dividing the lattice to thermal ratio of U238 capture by the lattice to thermal ratio of U235 fission. Errors quoted on the U235 fission ratios and the U238 capture ratios are based on those produced by the FREDA and ANCORA codes respectively. A contribution from other causes is included as indicated in Tables 4 and 5. The errors on the mean RCR values are derived from the deviations of the values from the mean. As for FFR this error on the mean may include effects due to small variations in the reactor environment. The quoted errors on the mean RCR are 0.5%, or less, for every irradiation. A comparison between the coincidence counting method and the Ge(Li) detector method is given in Table 6. The mean ratio of coincidence to Ge(Li) is 0.996 ± 0.8%. Corrections and errors in the measurement of RCR are discussed in Section 5.2 and are summarised in Tables 4 and 5.

5 CORRECTIONS AND ERRORS

5.1 CORRECTIONS AND ERRORS FOR FAST FISSION RATIO

5.1.1 Deadtime

A correction was applied by FREDA assuming a deadtime of 1 μsecond. For the count-rates encountered in these experiments the maximum corection was about 0.15% and the error on the correction produced a negligible effect on the results.

5.1.2 Detector Background

A separate detector was used specifically to measure γ-ray background activity. Prior to each measurement the ratio was determined of the background activity from the measuring detectors to that from the background detector. This ratio was then applied to the counts collected from the background detector during the measurement to derive the background counts from the measuring detectors. The error on the final result due to background is estimated at 0.1%.

5.1.3 Natural Activity

The natural activities of the samples were determined by measuring them on the automatic γ-ray detection system prior to the preparation of the sample packs. The contribution of the natural activity was about 8% for the depleted foils and less than 1% for the UO_2 discs. As the natural activties were determined to ±2% this gave a ±0.16% error on the FFR result.

5.1.4 Feedthrough

Samples that are being measured on the automatic detector system are subject to interference or "feedthrough" from samples in the magazine. Approximately 0.1% of the activity from a sample in the magazine is detected at the measuring position. The depleted and UO_2 samples are separated for measurement to minimise this problem but even so there is a correction of about 0.3% to be made. The effect on the result is an additional error of about 0.03%.

5.1.5 Perturbation

Putting a depleted uranium foil into the 4.31% UO_2 measuring pack inevitably causes a flux perturbation. Previous measurements with varying thicknesses of depleted foils have shown that the perturbation is less than 1% but with an uncertainty of ±1%.

5.1.6 γ-Ray Attenuation

Small corrections were made for the effects of γ-ray attenuation in the depleted and UO_2 samples. Initial calculations were made using a Monte-Carlo code. This showed that the attenuation in a typical depleted foil was 1.0% and in a typical UO_2 disc was 1.7%. Corrections to the individual foils were then made by FREDA using the algorithm $1 + (C.M/D^2)$, where M is the sample mass, D is its diameter and C is a constant derived by comparison with the Monte-Carlo result. The effect on FFR was estimated to be an additional error of less than 0.1%.

5.1.7 Sample Holders

As the depleted and UO_2 samples are measured separately on the automatic detector system, the depleted and UO_2 samples from a particular experimental pack are measured in the same sample holder. Any positioning or attenuation effects due to the sample holder therefore cancel out in the calculation of FFR.

5.1.8 Sample Enrichments

It can be shown from a consideration of the equation for FFR in Section 2.7 that a variation in the U235 content of the depleted foil gives rise to an effect many times smaller in FFR. The increased error varies from 0.3% for the first irradiation to 0.1% for the last irradiation. Any variation in the enrichment of the enriched discs has an almost direct effect on FFR. The enrichments of both materials have been measured by comparison with natural uraniun samples. The 185 kev γ-ray from U235 was observed using a Ge(Li) detector. The depleted enrichment was measured to be (0.0417 ± 0.0006)% and the UO_2 enrichment was measured to be (4.31 ± 0.03)%, compared to the quoted value of (4.31 ± 0.01)%.

5.1.9 Conversion Factor for FFR_γ to FFR

As stated previously the measured FFR is derived in terms of γ-ray activities rather than true fission rates. The relationship is given by $FFR_\gamma . P = FFR$, where FFR_γ is the γ activity ratio derived by FREDA, P is the calibration factor and FFR is the true fission rate ratio. A brief description of the method used to deduce the calibration factor is given below.

The true FFR was measured close to the peripheral reflector of the source reactor Nestor using Zebra type (8) U235 and U238 absolute fission chambers (ZEB48 and ZEB57) operated under cadmium shields. Then the FFR_γ was measured using depleted and natural uranium foils placed in demountable dummy fission chambers. The dummy chambers were positioned in the cadmium shields in the same location as real fission chambers had been. An irradiation of exactly 2 hours was made, then about 24 hours later the foils were measured on the γ- detector system in the same way as described in Section 2. After the gross γ- ray FFR had been determined the La-140 activities were also measured by the method described in Section 2.7.

The true FFR measured by fission chambers was 0.00150 ± 2% and by the La-140 method was 0.00151 ± 2%, the FFR_γ was 0.00145 ± 1%. This gives a calibration factor of P = 1.03 ± 2.2%. Previous work in the Zebra reactor has yielded similar values of P for experiments using a γ-ray discrimination level of 0.65 MeV.

5.1.10 Decay Correction

Decay corrections were made by using a previously determined decay table incorporated in the FREDA code. The error due to this correction was estimated to be 0.5%.

5.2 CORRECTIONS AND ERRORS FOR U238 CAPTURE

5.2.1 Deadtime and Chance Coincidences

Corrections were made by ANCORA for deadtime and for chance coincidences. The magnitudes of the corrections were about 0.2% in both cases and were of opposite sign. The effect of errors on the corrections on the final results was negligible.

5.2.2 Natural Activity

The method of correction for natural activity was described in Section 3.6. The magnitude of the correction was between 1% and 6%, depending on the sample activity. Uncertainties on the corrections had the effect of an additional error of about 0.15% on the final result.

5.2.3 Calculation of Tolerances on Dimensions of Measuring Pellet in RCR Determinations

Tolerance on Pellet Diameter

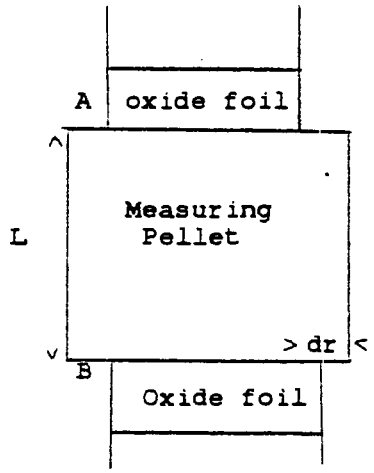

Consider measuring pellet with oversize diameter = r+dr exposing additional surface area of $4\Pi r dr$. (The additional cylindrical surface would be accommodated in the calculations). This constitutes a fractional increase in surface area of

$$\frac{4\Pi r\ dr}{2\Pi r\ L} = \frac{2\ dr}{L}$$

This will cause a fractional increase in resonance activation of dr/L since the solid angle for neutrons able to strike A or B is half that to strike the cylindrical surface. Since resonance activation accounts for 50% of the total U238 capture rate in the rcd a limit of 0.1% on an increase in total capture rate requires a limit of an increase of 0.2% in resonance capture i.e. dr/L = 0.002 since L = 15.49 mm dr = 0.03 mm.

Thus the tolerance on the pellet diameter = 2 dr = 0.06 mm or 0.002".

Tolerance on Surface Flatness

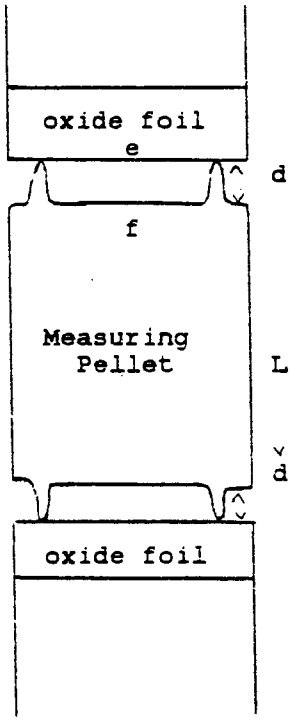

Assuming that neutrons entering the gap d will be absorbed (since the gap is very small compared with the diameter) and absorbed equally on surfaces e and f, each gap is therefore equivalent to an extra surface of $2\pi r \cdot d$.

This will be a fractional increase in area of

$$\frac{2\pi r\ d}{2\pi r\ L} = \frac{d}{L}$$

Since an increase in resonance capture must be limited to 0.2% (to limit increases in the total capture to 0.1%).

$$\frac{d}{L} = 0.002 \quad d = 0.002 \times 15.5 \text{ mm} = 0.031 \text{ mm or } 0.0012"$$

Thus the ends of the measuring pellet and the oxide foil must be flat to within 0.031 mm.

5.2.4 γ-Ray Attenuation

The method of correction for γ-ray attenuation in the liquid sources was described in Section 3.6. Although there was about a 23% loss of γ-rays due to absorption, the differential effects were very small. The effects of errors in the corrections were less than 0.1%.

5.2.5 Holder Calibration

The liquid source holders are made with as near the same dimensions as is practicable. Calibrations of the holders using standard solutions of Np-239 have shown that the efficiencies of the holders do not vary beyond ± 0.2%.

5.2.6 Fission Product Correction

The method of correction for fission product interference was described in Section 3.6. The correction varies from about 1% for the latice samples to about 7% for the thermal samples. The effect of errors in the fision product corrections resulted in an additional error of about 0.15% on the final result.

5.2.7 Decay Correction

Due to the method of measurement and analysis it was only necessary to make corrections over a period of about 2 hours. The size of the correction was about 2.5% and the error on the correction resulted in a negligible error on the final results.

5.2.8 Sample Dispensing

Liquid sample preparation was carried out by an experienced Chemist and great care was taken to minimise errors by careful weighing during the various stages of preparation. An analysis(10) of the method has indicated that an error of ± 0.2% is possible in the quoted mass of a sample.

5.2.9 U235 Fission Lattice to Thermal Ratio

The corrections and errors in the determination of the U235 fission ratio are broadly the same as has been discussed for the FFR measurement in Section 5.1. The components are summarised in Table 5.

6 SUMMARY

Measurements have been made of Fast Fission Ratios and Relative Conversion Ratios in five different water moderated UO_2 lattices. The measurements were out of the ordinary in that the irradiations took palce in the USA and the activity determinations were made at AEE Winfrith. In spite of the transportation problems involved, successful measurements have been achieved for all five experiments.

The Fast Fission Ratios have been measured with an accuracy of 2.3% and the Relative Conversion Ratios with an accuracy of 0.5% or better. The results have been checked for systematic errors by using alternative methods where possible and no significant errors have been found.

7 ACKNOWLEDGEMENTS

I wish to record my thanks to Dr W H Taylor for his help and advice in the initial planning of these experiments. I thank; Dr S Bierman and his team at Battelle PNL in the USA for the care taken in providing carefully controlled irradiation conditions, and Mr M March and Mr R Stout and his team at AEEW for organising the Nestor irradiations. I thank; Mr W Cox for preparing the liquid sources, Mr A Gregory and Mr R Keay for organising the transportation of the samples, and Mr F Eltham for running the analysis codes.

8 REFERENCES

(1) W A V BROWN et al. Measurements of Fast Fission Ratio. AEEW-R 341.

(2) G A Barnett et al. Measurement of Relative Conversion Ratio and Fast Fission Ratio in Low Enrichment Oxide Lattices. AEEW - R 648.

(3) W H Taylor et al. Control of the Counting Laboratory at AEE Winfrith by a Small Computer. AEEW - R 830.

(4) J B Niday, R Gunnink. Computerised Quantitative Analysis by Gamma-Ray Spectrometry. UCRL-51061.

(5) J G Cunninghame. The Status of Fission Product Yield Data in 1977. AERE - R 8753.

(6) W H Taylor et al. Measurement of Fast Fission Ratio and Relative Conversion Ratio in Particulate Fuel. AEEW - R 712.

(7) M F Murphy et al. RCR Measurements in the Natural Uranium Metal/ H_2O Cores in JUNO Using the Liquid Source Method. International Publication. ETM/P161.

(8) S Chandrasekav. Tabulated Functions. Astrophysics. Jul Vol 108, No. 1, P92 (1948).

(9) J M Stevenson, A M Broomfield. Measurements and Calculations of Ratios of Effective Fission Cross-Sections in the Zero-Power Fast Reactor Zebra. AEEW - R 526.

(10) J'Grattan. An Assessment of Errors in the Preparation of Liquid Sources of Natural UO_2 Foils and Plates. AEEW-CSR(78)16.

TABLE 1

FAST FISSION RATIO RESULTS

Expt	Pack	FFR_γ	% Random Error	Mean FFR_γ	% Random Error	FFR	% Error
1	1	0.001901	0.6				
1	2	0.001914	0.6	0.00190	0.4	0.00196	2.3
1	3	0.001901	0.6				
2	1	0.002161	0.6				
2	2	0.002215	0.6	0.00218	0.8	0.00225	2.4
2	3	0.002171	0.6				
3	1	0.003785	0.8				
3	2	0.003866	0.8	0.00385	0.8	0.00396	2.4
3	3	0.003886	0.8				
4	1	0.00564	0.9				
4	2	0.00557	0.9	0.00559	0.5	0.00571	2.3
4	3	0.00556	0.9				
5	1	0.00552	0.8				
5	2	0.00548	0.8	0.00553	0.5	0.00568	3.3
5	3	0.00558	0.8				

TABLE 2

RELATIVE CONVERSION RATIO RESULTS

Expt	Pack	F5 L/T	% Random Error	C8 L/T	% Random Error	RCR	% Random Error	Mean RCR	% Random Error
1	1	6.43	0.5	17.47	0.8	2.72	0.9		
1	2	6.44	0.5	17.43	0.8	2.70	0.9	2.70	0.5
1	3	6.46	0.5	17.38	0.8	2.69	0.9		
2	1	0.934	0.25	2.96	0.5	3.17	0.6		
2	2	0.940	0.25	3.01	0.5	3.20	0.6	3.18	0.3
2	3	0.922	0.25	2.94	0.5	3.18	0.68		
3	1	0.877	0.25	4.42	0.5	5.04	0.6		
3	2	0.859	0.25	4.37	0.5	5.09	0.6	5.08	0.4
3	3	0.855	0.25	4.37	0.5	5.11	0.6		
4	1	0.355	0.25	2.72	0.5	7.58	0.6		
4	2	0.359	0.25	2.74	0.5	7.62	0.6	7.64	0.3
4	3	0.357	0.25	2.72	0.5	7.64	0.6		
5	1	1.210	0.25	9.10	0.5	7.52	0.6		
5	2	1.223	0.25	9.16	0.5	7.49	0.6	7.50	0.3
5	3	1.212	0.25	9.09	0.5	7.50	0.6		

TABLE 3

CORRECTIONS TO FFR

Correction	Size	Error on Correction	Effect
Dead time	0.15%	10%	0.015%
Background	5%	2%	0.1%
Depleted natural activity	8%	2%	0.16%
UO_2 natural activity	1%	2%	0.02%
Feedthrough	0.3%	10%	0.03%
Perturbation	1%	100%	1%
γ-ray attenuation	1.7%	10%	0.07%
Depleted enrichment	0.00417%	1.5%	0.2%
UO_2 enrichment	4.31%	0.25%	0.25%
Factor FFR_γ to FFR	1.031	2.2%	2.2%
Decay	x2	0.5%	0.5%
Detector stability	-	-	0.1%

TABLE 4

CORRECTIONS TO U238 CAPTURE RATIO

Correction	Size	Error on Correction	Effect
Deadtime and chance coincidences	0.2%	10%	0.02%
Natural Activity	1%-6%	2.5%	0.15%
Perturbation - pellet size mismatch	0.15%	100%	0.15%
γ-ray attenuation	23%	10%	0.1%
Holder calibration	0.2%	100%	0.2%
Fission product correction	1%-7%	2%	0.15%
Fission product corrections ratio	1	1%	0.07%
Decay correction	2.5%	0.5%	0.01%
Sample dispensing	-	0.2%	0.2%
Detector stability	-	-	[illegible]

TABLE 5

CORRECTIONS TO U235 FISSION RATIO

Correction	Size	Error on Correction	Effect
Deadtime	0.15%	10%	0.015%
Background	0.3%	2%	0.006%
Natural activity	1%	1.5%	0.015%
Feedthrough	1%	10%	0.1%
γ-ray attenuation	1.7%	10%	0.01%
Holder calibration	0.1%	1.0%	0.1%

TABLE 6

CHECK MEASUREMENTS

Expt	Co/Ge(Li)	% Error	FFR_γ/La	% Error	U235 FREDA/Ge(Li)	% Error
1	-	-	1.042	2.6	1.030	0.8
2	1.029	3	1.027	2.7	-	
3	0.990	1.5	1.020	2.8	1.015	1.0
4	1.011	1.2	1.027	2.9	-	
5	0.986	0.9	1.009	2.9	1.015	1.0
Mean	0.996	0.8	1.025	2.5	1.020	0.8

Notes:

1. Co/Ge(Li indicates coincidence counting for U238 capture compared to Ge(Li) counting for U238 capture
2. FFR_γ/La indicates the gross γ-ray method for FFR compared to the La140 method
3. U235 FREDA/Ge(Li) indicates the gross γ-ray method for U235 lattice to thermal ratio compared to the La140 method
4. The error on FFR_γ/La contains a large systematic component from the calibration factor P and from the uncertainties on the Ba140 fission yields

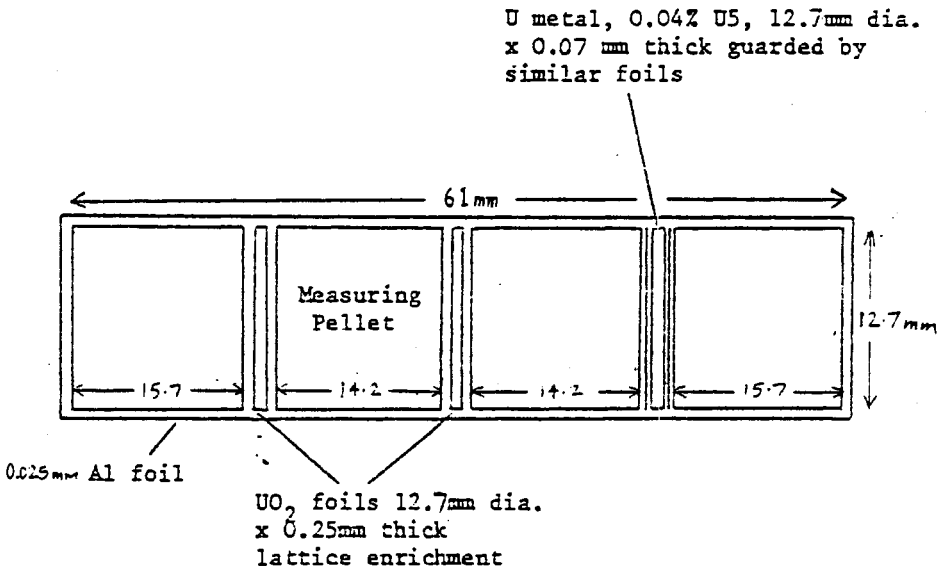

FIGURE 1 RCR Pack

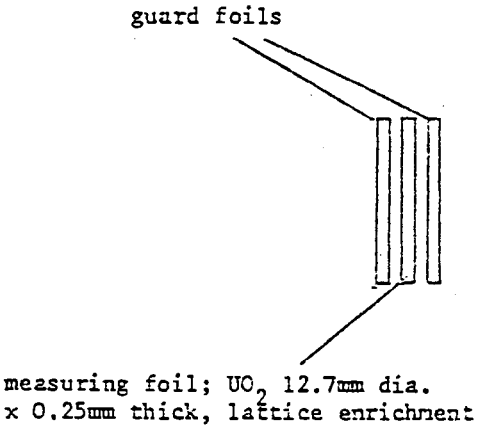

FIGURE 2 Thermal Foil Pack

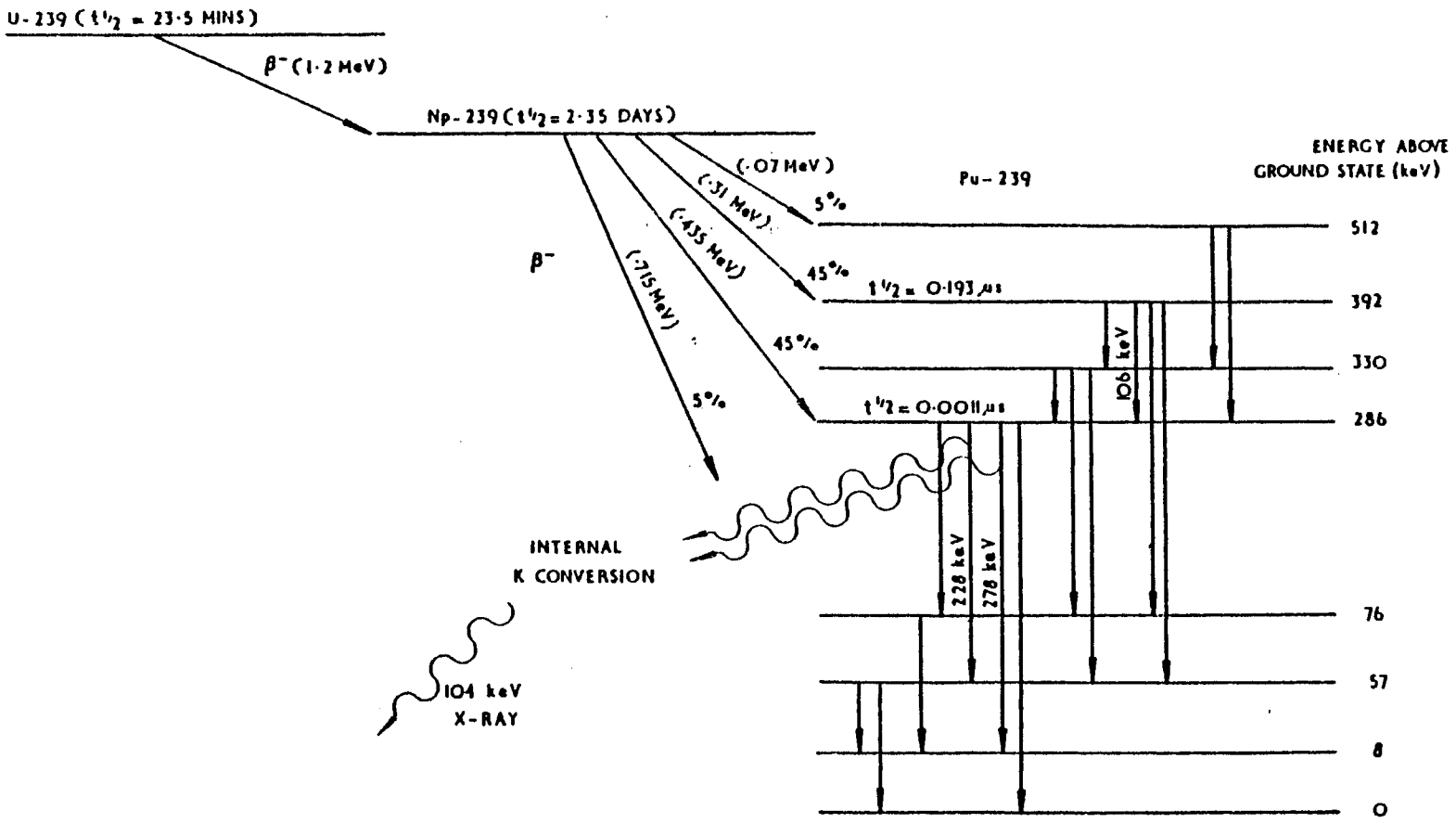

FIG. 3. U-239 DECAY SCHEME

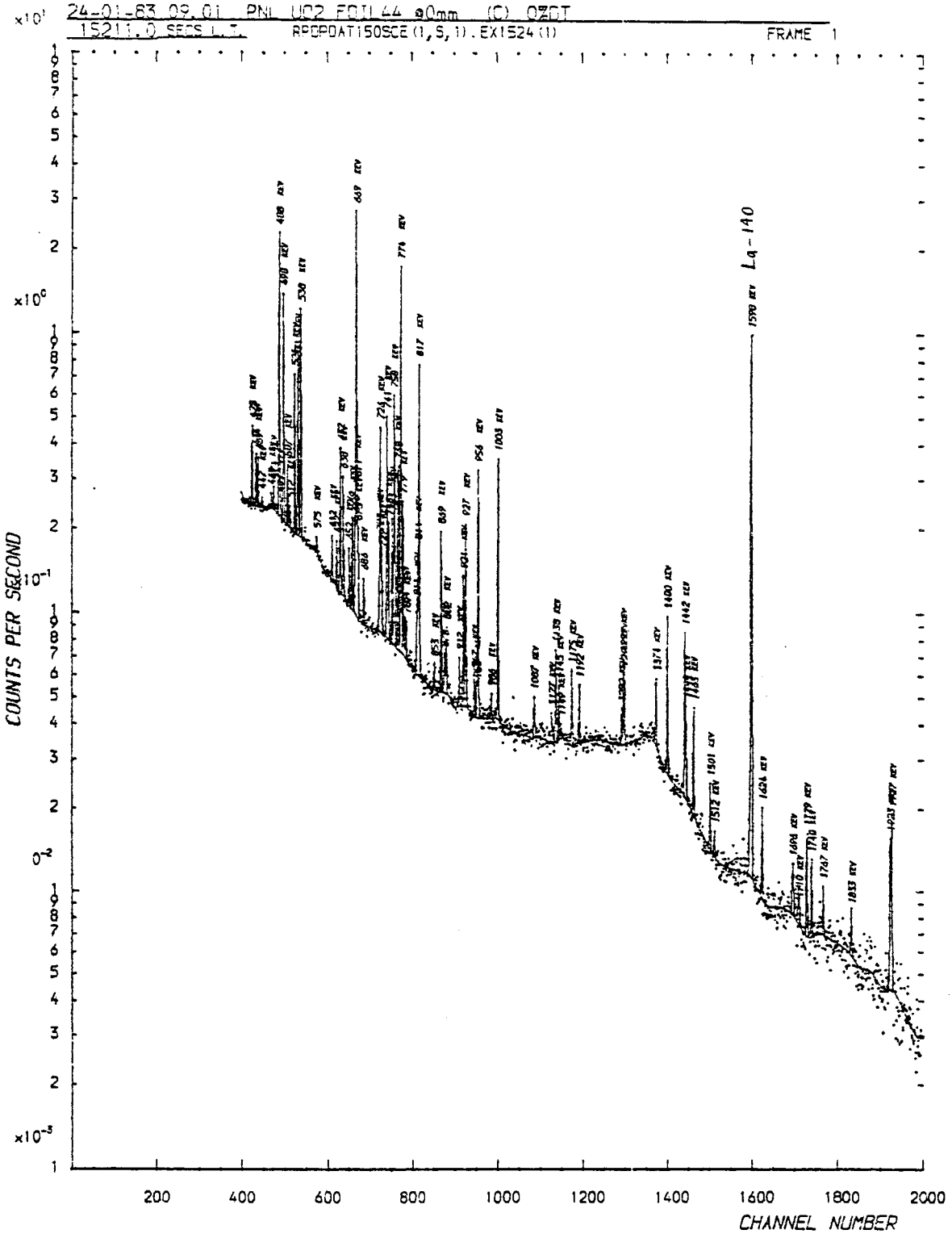
24-01-83 09.01 PNL UO2 FOIL 44 @0mm (C) 0%DT
15211.0 SECS L.T.
RPDPDAT150SCE(1,S,1).EX1524(1)
FRAME 1
COUNTS PER SECOND
CHANNEL NUMBER
La-140
1596 KEV

APPENDIX I

Photo Reductions of Control Channel 4 Recorder Charts During Reaction Rate Measurements

APPENDIX I

Photo Reductions of Control Channel 4 Recorder Charts During Reaction Rate Measurements

Copies of the recorder chart displaying the thermal neutron flux level immediately preceding and during each irradiation associated with the reaction rate measurements are presented in this Appendix for information only. No attempt has been made to define or modify the notations made on the chart recordings at the time of irradiations. The constancy of the flux level achieved during the irradiations can be noted.

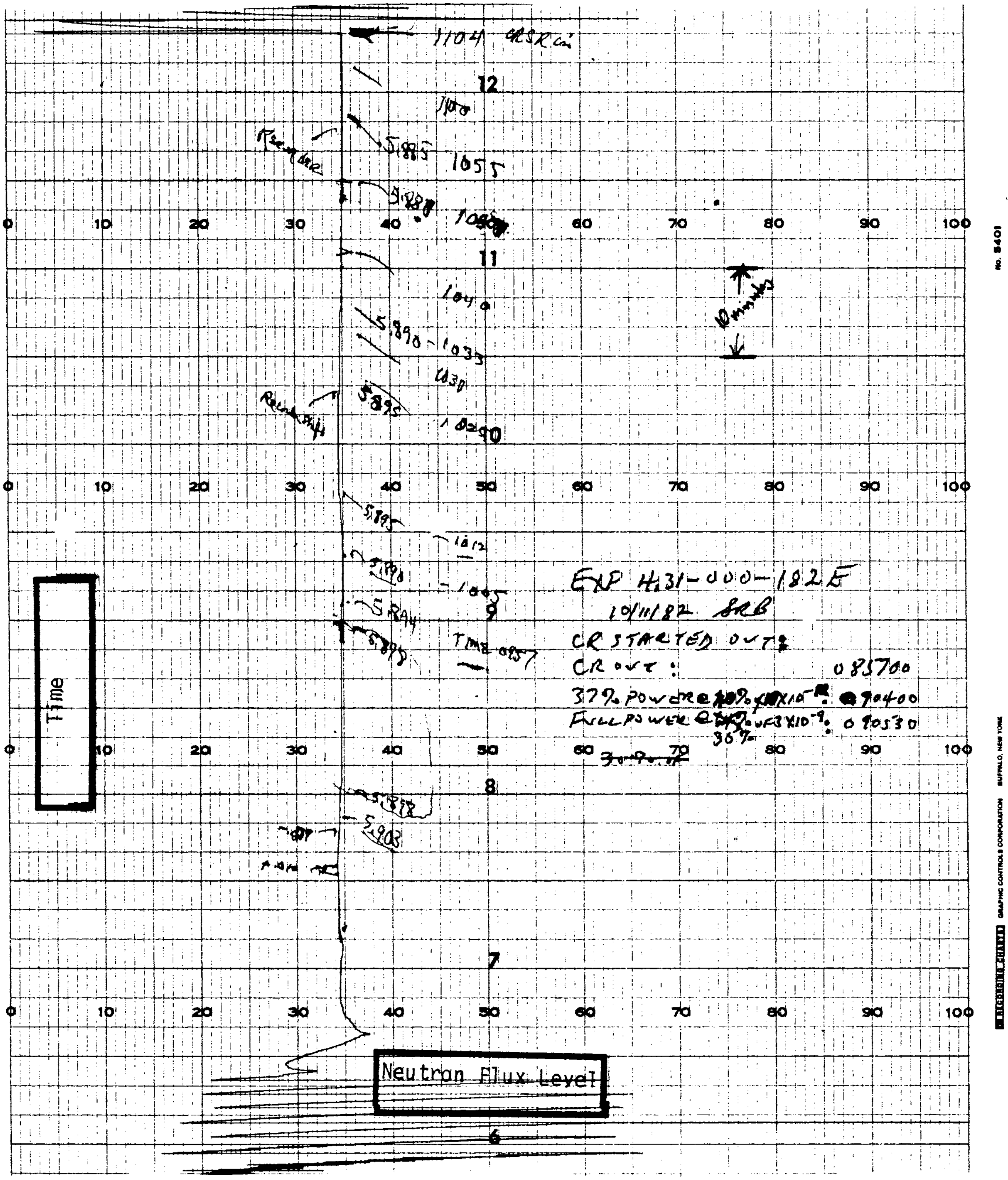
Time
Neutron Flux Level
EXP 431-000-182E
10/11/82
CR STARTED OUT
CR OUT : 083700
37% POWER
FULL POWER
No. 5401
GRAPHIC CONTROLS CORPORATION BUFFALO, NEW YORK

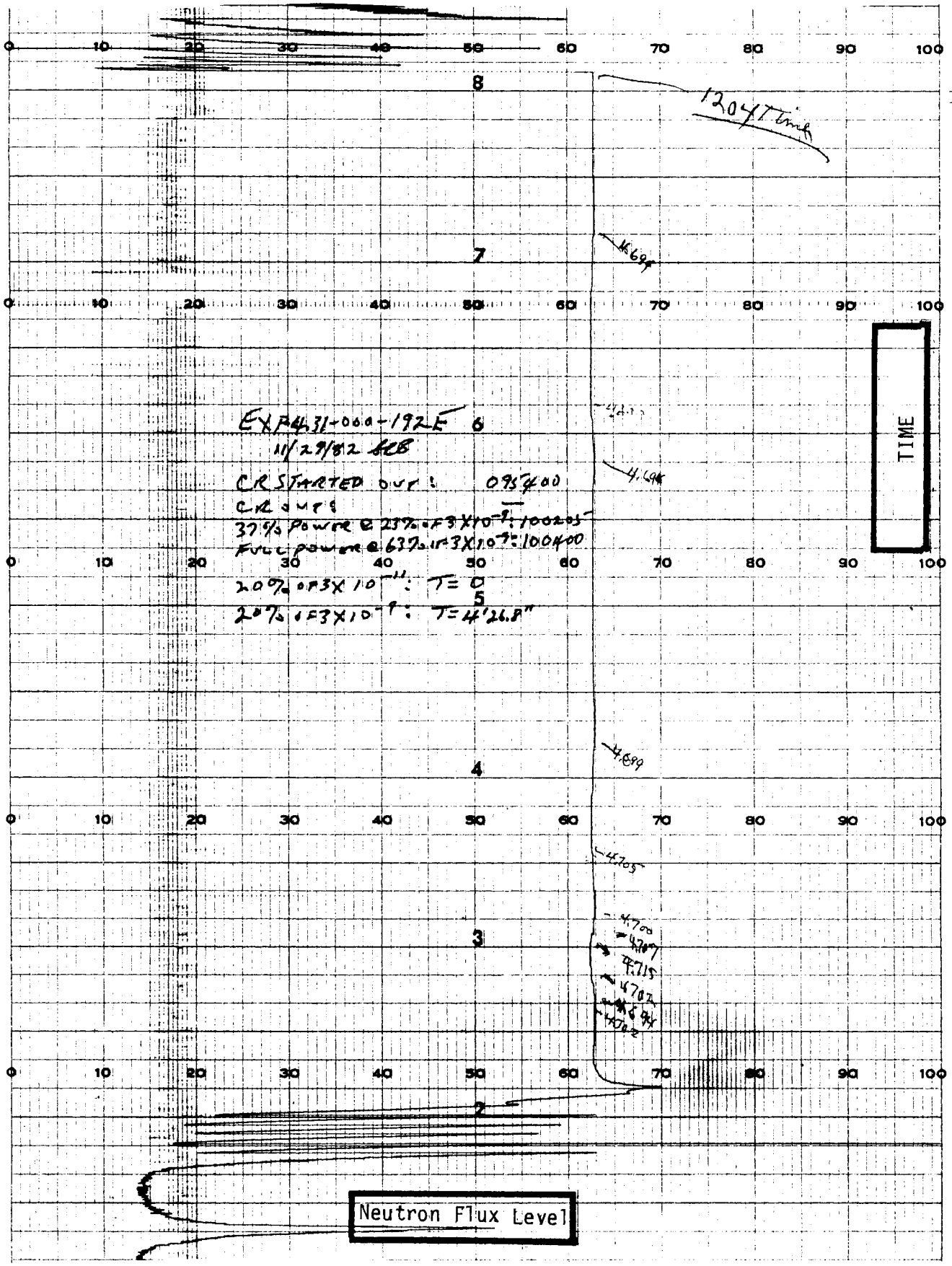
0 10 20 30 40 50 60 70 80 90 100
8
7
6
5
4
3
2
1
TIME
Neutron Flux Level
EXP 431-000-192E
11/29/82 HEB
CR STARTED OUT: 095400
CR DUMP:
37% POWER @ 23% 1E3X10⁻⁹: 100205
FULL POWER @ 63% 1E3X10⁻⁹: 100400
20% 0E3X10⁻¹¹: T=0
20% 1E3X10⁻⁹: T=4'26.8"
1204 Time
4.699
4.694
4.699
4.705
4.700
4.707
4.715
4.707
4.698
4.702

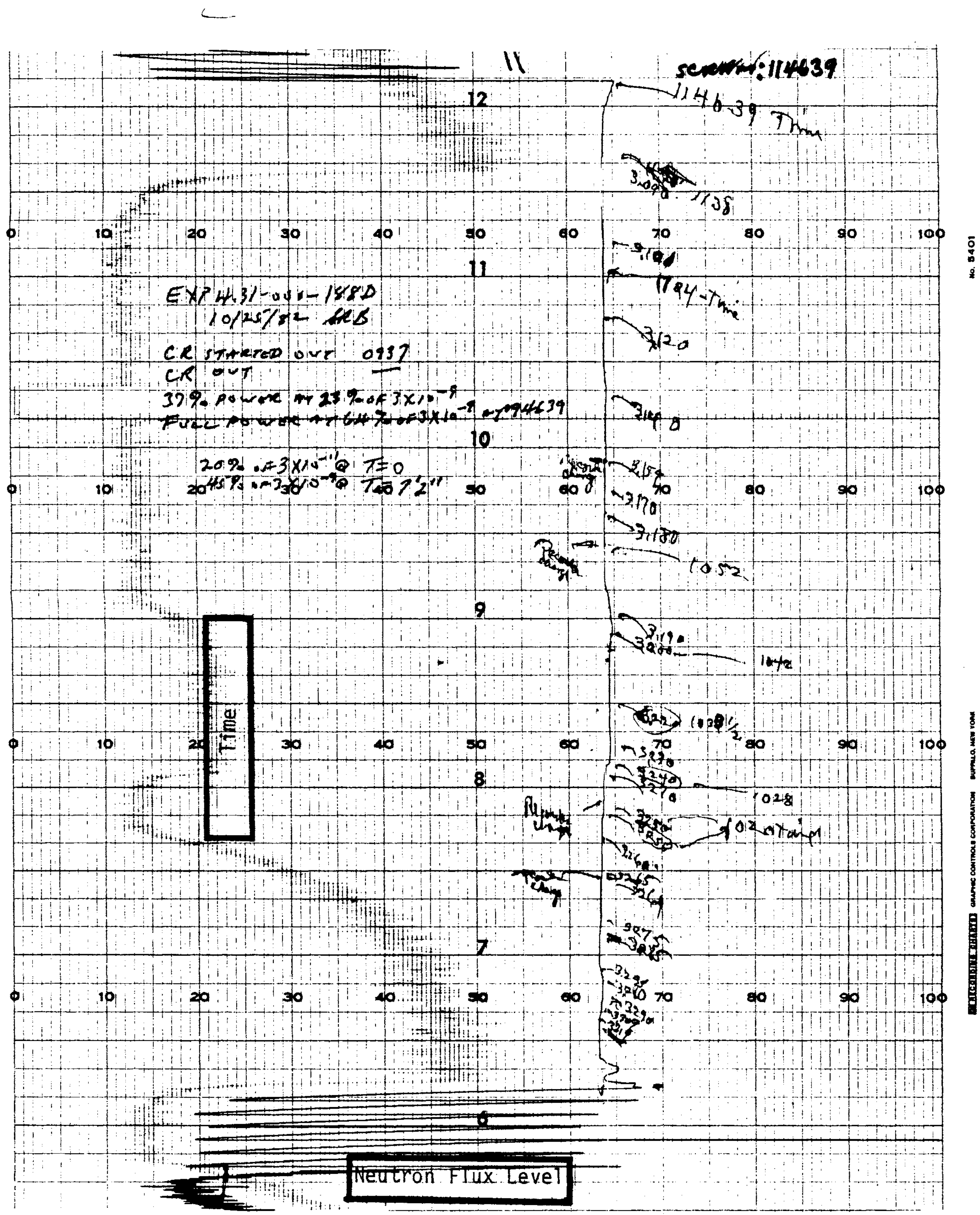
Time
Neutron Flux Level

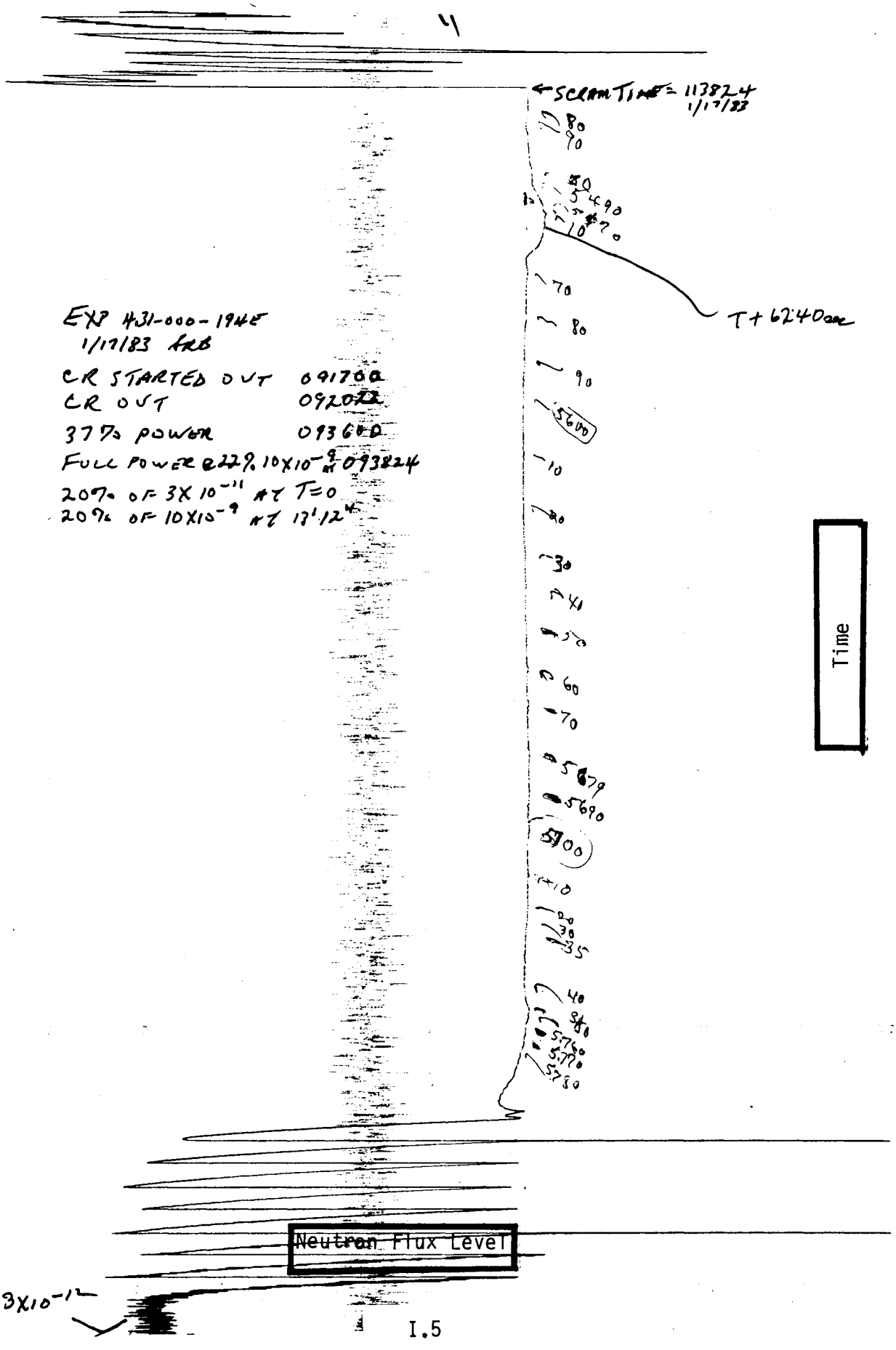
4
SCRAM TIME = 113824
1/17/83
T+6240sec
EXP 431-000-194E
1/17/83 ARB
CR STARTED OUT 091700
CR OUT 092022
37% POWER 093600
FULL POWER @ 229 10X10⁻⁹ @ 093824
20% OF 3X10⁻¹¹ AT T=0
20% OF 10X10⁻⁹ AT 13'12"
Time
Neutron Flux Level
3X10⁻¹¹

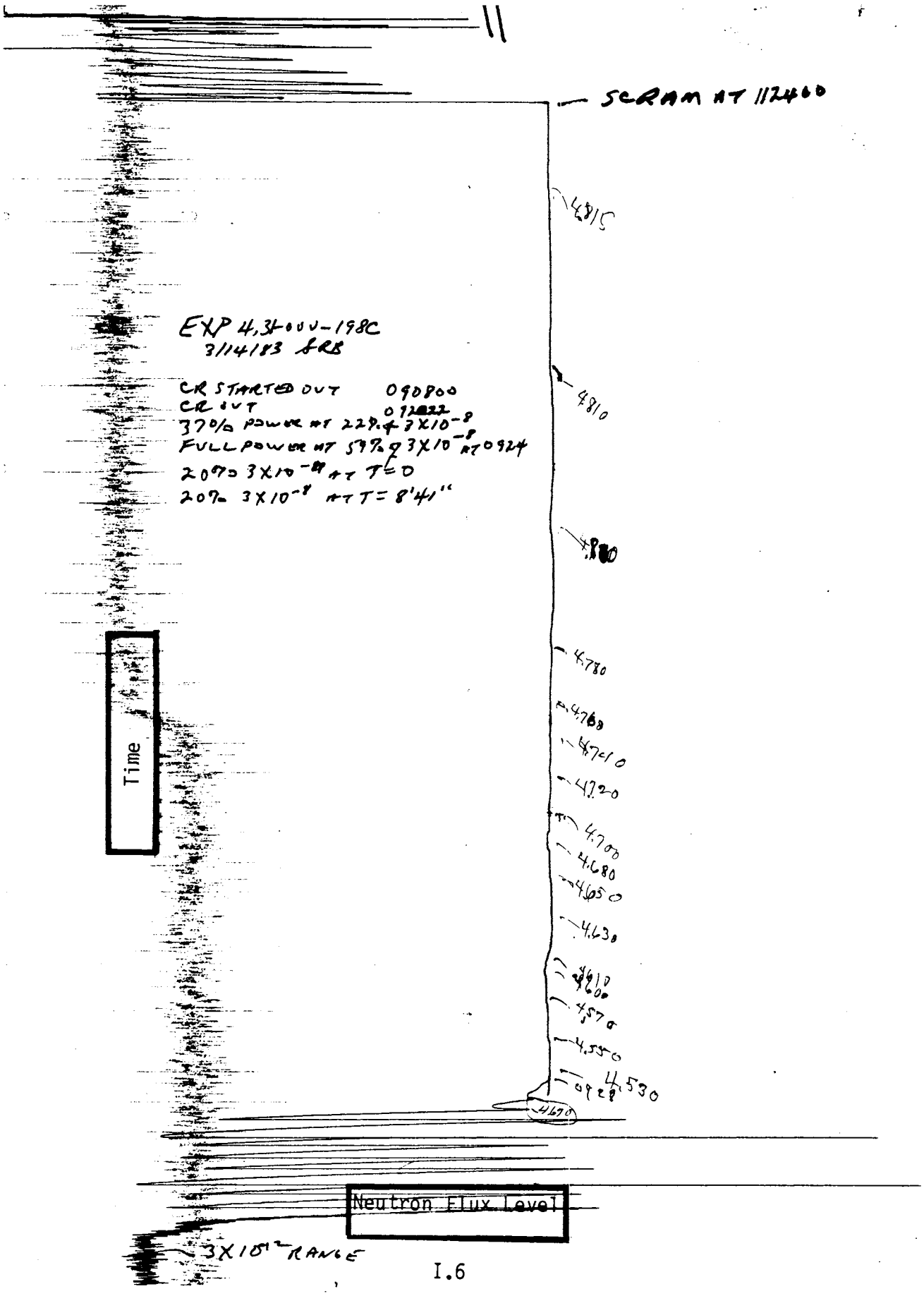
SCRAM AT 112400
4815
EXP 4,340V-198C
3/14/83 SRB
CR STARTED OUT 090800
CR OUT 092822
37% POWER AT 229.4 3X10-8
FULL POWER AT 59% 3X10-8 AT 0924
20% 3X10-8 AT T=0
20% 3X10-8 AT T=8'41"
4810
4780
4760
4740
4720
4700
4680
4650
4630
4610
4600
4570
4550
4530
4690
Time
Neutron Flux Level
3X10-2 RANGE

Time
Neutron Flux Level

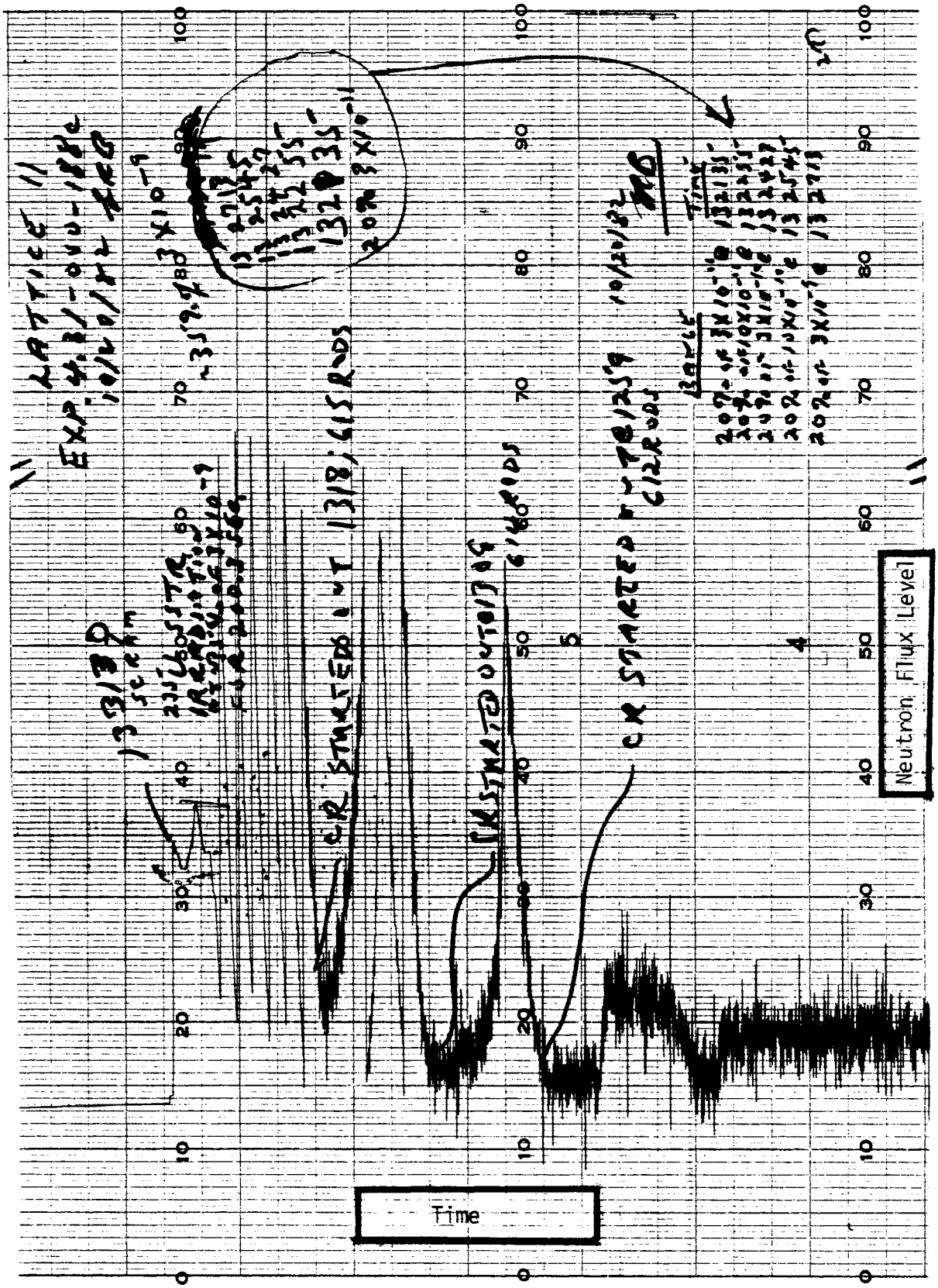
Time
Neutron Flux Level

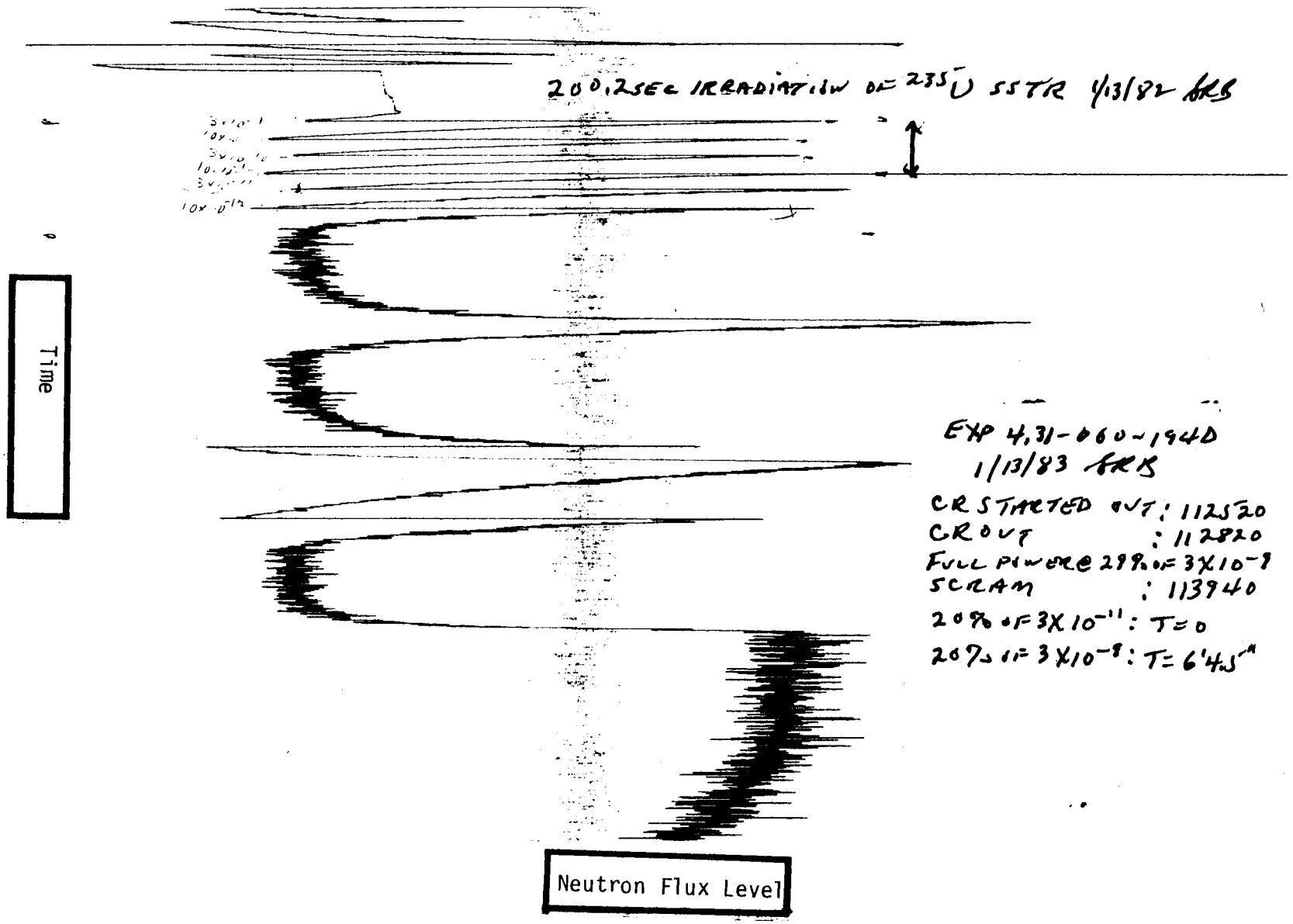
200.2SEC IRRADIATION OF 235U SSTR 1/13/82 BRB
Time
Neutron Flux Level
EXP 4.31-060-194D
1/13/83 BRB
CR STARTED OUT: 112520
CR OUT : 112820
FULL POWER @ 29% OF = 3X10-9
SCRAM : 113940
20% OF = 3X10-11 : T=0
20% OF = 3X10-9 : T= 6'4.5"

Time
Neutron Flux Level

PNL-4967
UC-46

DISTRIBUTION

No. of
Copies

OFFSITE

Richard B. Chitwood
Office of Nuclear Fuel Cycle
U. S. Department of Energy
NE 340
Mail Stop B-107
Washington, DC 20545

Clint Bastin
Office of Nuclear Fuel Cycle
U. S. Department of Energy
NE 340
Mail Stop B-107
Washington, DC 20545

10 Richard T. Keay
British Nuclear Fuels, Ltd.
Technical Services
R101 Rutherford House
Risley, Warrington, Cheshire
WA3 6AS
England

27 DOE Technical Information Center

ONSITE

DOE Richland Operations Office

H. E. Ransom
M. J. Plahuta

22 Pacific Northwest Laboratory

S. R. Bierman (10)
E. D. Clayton
D. A. Dingee
R. M. Fleischman
E. S. Murphy
L. D. Williams
Publishing Coordination (2)
Technical Information (5)